Title
Investigating the relationship between individual differences in the brain and social network structure

Author
Hyon, Ryan

Publication Date
2022

Peer reviewed|Thesis/dissertation

UNIVERSITY OF CALIFORNIA

Los Angeles

Investigating the relationship between individual differences in the brain and social network structure

A dissertation submitted in partial satisfaction of the requirements for degree of Doctor of Philosophy in Psychology

by

Ryan Hoon Hyon

2022

ABSTRACT OF THE DISSERTATION

Investigating the relationship between individual differences in the brain and social network structure

by

Ryan Hoon Hyon

Doctor of Philosophy in Psychology

University of California, Los Angeles, 2022

Professor Carolyn M. Parkinson, Chair

Little is known about the individual differences in sociobehavioral tendencies that uniquely characterize individuals occupying social network positions (e.g., eigenvector centrality), which are associated with a disproportionate amount of influence, popularity, and leverage. Furthermore, although it has been well-established that people closer together in their social network often share similarities in demographic attributes, much less is known about the types of inter-individual similarities shared by friends that run deeper than such "surface-level" characteristics. This dissertation integrates tools from social network analysis, neuroimaging, and machine learning to address these gaps in the literature and advance our understanding of how the brain shapes and is shaped by real-world social networks.

The dissertation of Ryan Hoon Hyon is approved.

Martin M. Monti

Matthew D. Lieberman

Naomi I. Eisenberger

Carolyn M. Parkinson, Committee Chair

2022

Table of Contents

LIST OF FIGURES

LIST OF TABLES

ACKNOWLEDGMENTS

I want to first thank my advisor, Dr. Carolyn Parkinson. You've been an extremely generous and supportive mentor, and you've gone out of your way to provide me with countless opportunities that have helped me grow and learn new things. Thank you for your openness to feedback and your willingness to grow as a mentor, too. I really look up those qualities and hope to embody them, wherever I end up in the future.

I want to also thank Drs. Matt Lieberman, Naomi Eisenberger, and Martin Monti, who sit on my dissertation committee - thank you for your support over the years. Matt and Naomi, you were so welcoming when I first arrived to UCLA as a staff researcher; and suffice to say, your advice and insights since then have been invaluable. Martin, thank you for your very thoughtful feedback on my dissertation and for bringing your methodological expertise to the table.

Special thanks to my family. Words cannot describe my gratitude towards your support. And shout out to my friends!

VITA

Education

2022	Candidate in Philosophy in Psychology, University of California, Los Angeles
2021	Master of Arts in Psychology, University of California, Los Angeles
2017	Bachelor of Arts in Neuroscience, Dartmouth College

Fellowships and Honors

2021	Honorable Mention, National Science Foundation Graduate Research Fellowship
2020	UCLA Graduate Research Mentorship Program
2020	UCLA Graduate Summer Research Mentorship Program
2020	Duke Summer School in Social Neuroscience and Neuroeconomics
2019	UCLA Summer Institute in Computational Social Science
2019	Honorable Mention, National Science Foundation Graduate Research Fellowship
2019	Poster Award, Social and Affective Neuroscience Society Meeting

Publications

Hyon, R., Wheatley, T., Kleinbaum, A.M., Welker, C.L., Parkinson, C. (in review). Pre-existing neural similarity predicts future increases in social closeness.

Hyon, R., Chavez, R., Chwe, J.A., Wheatley, T., Kleinbaum, A.M., Parkinson, C. (in press). White matter connectivity in brain networks supporting social and affective processing predicts real-world social network characteristics. *Communications Biology.*

Baek, E.C., **Hyon, R.,** López, K., Finn, E.S., Porter, M.A., Parkinson, C. (2022). In-degree centrality in a social network is linked to coordinated neural activity. *Nature Communications*.

Matz, S.C., **Hyon, R.,** Baek, E.C., Parkinson, C., Cerf, M. (in review). Personality similarity predicts synchronous neural responses in fMRI and EEG data.

Hyon, R., Youm, Y., Chey, J., Kwak, S., Parkinson, C. (2020). Similarity in functional brain connectivity at rest predicts interpersonal closeness in the social network of an entire village. *Proceedings of the National Academy of Sciences of the United States of America.* https://doi.org/10.1073/pnas.2013606117.

Hyon, R., Kleinbaum, A.M., Parkinson, C. (2020). Social network proximity predicts similar trajectories of psychological states: Evidence from multi-voxel spatiotemporal dynamics. *Neuroimage*. https://doi.org/10.1016/j.neuroimage.2019.116492.

Baek, E.C., **Hyon, R.,** Porter, M.A., & Parkinson, C. (2020). How do our brains support our real-life friendships? *SocArXiv.* https://doi.org/10.31235/osf.io/vy2jr.

Presentations

Hyon, R., Lopéz, K., Baek, E.C., Porter, M.A., Parkinson, C., Inter-subject similarity in multi-voxel response pattern trajectories reflects similarities in preferences and personality. Social and Affective Neuroscience Society Meeting (virtual due to COVID-19). May 2021.

Hyon, R., Youm, Y., Chey, J., Parkinson, C., Functional connectomes predict friendship and centrality in the social network of an entire village. UCLA Brain Research Institute Annual Neuroscience Poster Session, Los Angeles CA. November 2019.

Hyon, R., Youm, Y., Chey, J., Parkinson, C., Functional connectomes predict friendship and centrality in the social network of an entire village. Social and Affective Neuroscience Society Meeting, Miami FL. May 2019.

Hyon, R., Wheatley, T., Kleinbaum, A.M., Parkinson, C., Individual differences in white matter microstructure patterns predict social network centrality. Social and Affective Neuroscience Society Meeting, Brooklyn NY. May 2018.

Relevant Professional Experience

2021 Computational Social Neuroscientist PhD Intern, Apple, Inc.

General Introduction

Human social structures - ranging from dyadic pairings, family units, small communities, to large-scale societies - have given rise to the civilizations and cultures that are uniquely characteristic of our species. Being embedded in large social structures can confer many advantages to humans. However, successful living in complex social networks requires that an individual has the capacity to employ a wide range of sociocognitive skills, such as remembering and individuating many conspecifics, tracking the reputations of others and of one's self, managing a multitude of diverse relationships, and recognizing others' traits and the relationships between others and using this knowledge to predict others' behavior in order to avoid conflict (Dunbar, 1993, 2003). Consequently, humans' exceptional sociocognitive skills may have been selected for over the course of human brain evolution, and this skillset may have facilitated the human capacity to not only forge affiliative ties with many others but also successfully survive in the resulting complex social structures. These relationships across individuals comprise a complex web of affiliative ties that can be characterized as a social network. Within a given social network, individuals systematically vary in their social network position characteristics, such as their number of social ties and the extent to which they may be connected to other well-connected individuals or to other groups that might otherwise be unconnected (Figure 1). This inter-individual variability in social network position characteristics is likely, in part, a consequence of the inter-individual variability in how people construct and manage their social environment. Yet, very little is known about the sociobehavioral tendencies that are associated with individual differences in social network position characteristics, much less how these tendencies may interact to yield the direct and indirect relationships that give rise to the broader structure of human social networks.

This introduction seeks to synthesize the emerging literature characterizing how individual differences in brain structure and function relate to individuals' social network position characteristics. To this end, we first provide an overview of social network positions and their real-world consequences. We then discuss the literature that has characterized social network position characteristics as trait-like individual difference variables. We then review how neuroimaging has proven to be a promising tool to investigate the neurocognitive mechanisms underlying individual differences that are characteristics of particular social network position characteristics. We then review how one's direct and indirect social relationships can shape one's cognitive, emotional, and behavioral tendencies. We end the review by discussing the potential of future work to tease apart the causal relationship between an individual's sociobehavioral tendencies and their real-world social network position and to investigate the extent to which neural homophily and social influence processes are involved in the relationship between inter-individual neural similarity and social network proximity.

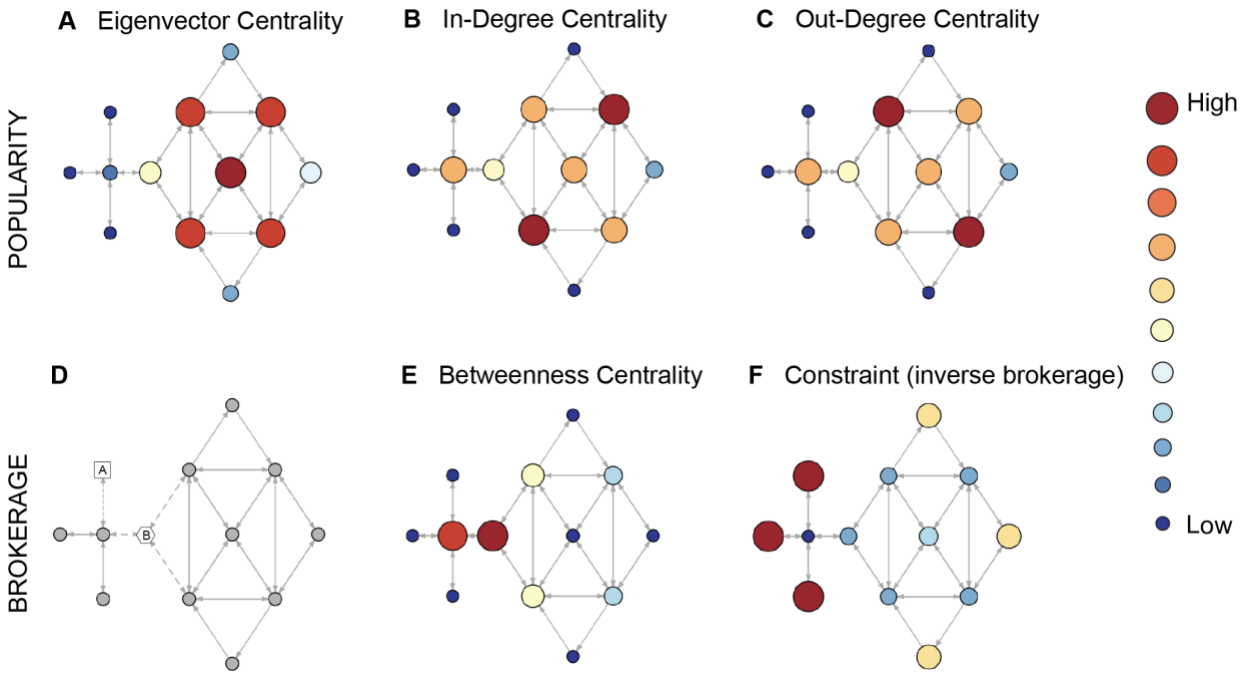

Figure 1. (A) In a social network, an individual's popularity or status can be defined by their eigenvector centrality, which reflects how well-connected they are to well-connected others. **(B, C)** In-degree and out-degree centrality are also measures of connectedness that take into account an individual's direct social ties. Whereas **(B)** in-degree centrality captures the number of directed edges toward an individual, **(C)** out-degree centrality captures the number of directed edges away from an individual. **(D)** Brokers connect otherwise unconnected individuals. If person A were removed, everyone else in the network would still be connected to each other. Thus, person A occupies a position that is low in brokerage. In contrast, if person B were removed, there would be two groups of people that would be unconnected. Thus, person B occupies a position that is high in brokerage. Two common methods of calculating brokerage are **(E)** betweenness centrality and **(F)** constraint (i.e., inverse brokerage). Whereas **(F)** betweenness centrality measures the extent to which an individual lies on the shortest path between two given people, **(F)** constraint is a relatively more local measure of brokerage that accounts for the extent to which an individual has access to non-redundant social partners. Figure adapted from Weaverdyck & Parkinson (2018).

Social network position characteristics and their real-world consequences

In a social network, individuals can be represented by nodes (i.e., "actors"), and connections between individuals that correspond to a relationship can be represented by edges (i.e., "ties"). A social network can be defined within a given boundary, such as geographic boundaries that physically constrain a community (an island community) or social boundaries that can make it difficult to socialize with out-of-network actors (e.g., academic programs, clubs). Edges between individuals can be weighted to represent the strength of a given relationship. For instance, an edge can be weighted by the number interactions in a given window of time in order to encode interaction frequency between two actors. On the other hand, edges can also be unweighted such that they simply encode the existence of a relationship or can be unweighted to characterize relationships that meet a certain threshold (e.g., if the number of interactions exceeds a given threshold). Furthermore, edges can represent any type of relationship, such as monetary exchanges, connections on social media, shared attributes, or friendship. The current review focuses on networks in which edges capture friendships given the centrality of friendship to human life (Dunbar, 2021) and due to the focus of past relevant work on this topic. The relative importance of an individual in the context of their social network can

be characterized by their centrality (see Baek et al. (2021) for a review of social network analysis).

The simplest variant of centrality, degree centrality, is the measure of the number of edges attached to an individual or the number of actors with whom the individual shares a social tie. In directed networks, both out-degree and in-degree centrality can be calculated. Out-degree centrality, which is the measure of an individual's outgoing social ties, is calculated by summing the number of actors with whom an individual identifies having a social tie. On the other hand, in-degree centrality is the measure of an individual's incoming social ties, calculated by summing the number of other actors that identify having a social tie with a given individual. Thus, whereas out-degree centrality captures an individual's consideration of their own social ties (i.e., their perception of their social ties), in-degree centrality captures an individual's popularity or the extent to which they are well-liked. Out-degree centrality, which is synonymous with social network size when calculated from ego-centric network data (Baek et al., 2021), has been linked to reduced psychological distress (A. Courtney et al., 2021) and is predictive of future well-being (Huxhold et al., 2013; Pinquart & Sörensen, 2000; Rafnsson et al., 2015; X. Wang, 2016). On the other hand, in-degree centrality has been linked to the capacity to influence social norms and shape the behavior of others (Osgood et al., 2013; Zingora et al., 2020) and is also related to being perceived as kind and trustworthy (Parkhurst & Hopmeyer, 2016).

Eigenvector centrality is a prestige-based measure of centrality that takes into account how well-connected one is to other well-connected actors (Bonacich, 1972; Masuda et al., 2017). Consider a townsperson with few social ties, one of which is with the mayor of the town. Although this townsperson has a relatively low degree centrality, they would have relatively high

eigenvector centrality, given that they are connected to the mayor, a highly influential individual who themself presumably has high eigenvector centrality (assuming that the mayor would need to cultivate and maintain social relationships with many other people). By virtue of this connection with a well-connected individual, the townsperson may wield relatively more influence than other actors that have many social ties with relatively non-influential actors (Baek et al., 2021). Holding a position of high eigenvector centrality has been shown to have several social- and health-related benefits. Eigenvector centrality is associated with happiness (Fowler & Christakis, 2009), job retention (Ballinger et al., 2016), and reproductive success in animals (Brent, 2015). Furthermore, individuals with low eigenvector centrality may be more prone to bullying (Salmivalli et al., 1996) and negative gossip (Ellwardt et al., 2012), suggesting that an individual holding a position of high eigenvector centrality may be shielded from social mistreatment by virtue of being well-connected to other well-connected actors that may come to their defense.

Another variant of centrality, betweenness centrality, measures the extent to which an individual lies on the shortest path between two given people and has been conceptualized as a measure of brokerage (Wasserman & Faust, 1994). In a social network, an individual has the capacity to act as a broker to the extent that they fill gaps or network holes in the social structure, thereby connecting otherwise unconnected individuals to one another (Burt, 1994). Thus, an individual in a position of high betweenness centrality may have the capacity to function as a broker if other people must interact with them in order to interact with each other. However, betweenness centrality may not always reflect an individual's capacity for brokerage and can be impacted by other aspects of network structure. For example, an individual may be characterized by high betweenness centrality by virtue of lying on the shortest path between others due to

being close to a true broker but may not function as a true broker (Baek et al., 2021; Everett & Valente, 2016). Alternatively, constraint is a relatively more local measure of brokerage that accounts for the extent to which an individual has access to non-redundant social partners and thus may be less prone to influence from global network characteristics (Burt, 1994, 2004). Although betweenness centrality and constraint are two common methods to characterize brokerage, brokerage can also be formalized in different ways (Gould & Fernandez, 1989).

Brokers have the capacity to control the flow of resources (e.g., information) and are in a privileged position to coordinate behavior across local ties (Burt, 2015; Burt et al., 2013; Hahl et al., 2016). Consequently, they reap immense personal benefits - brokers tend to receive high performance ratings in organizational contexts (Mehra et al., 2001), come up with useful ideas (Burt, 2004; Leonardi & Bailey, 2016), foster innovation (Obstfeld, 2005), attain faster promotions (Brass, 1984), and achieve more professional success (Burt, 1997). These benefits are likely due to the fact that brokers have access to, control over, and can integrate diverse information and resources that would otherwise be "stuck" within segregated groups (Burt et al., 2013; Cvitanovic et al., 2017). Taken together, an individual's social network position characteristics have widespread, substantial consequences with respect to their social status, health and well-being, and professional success.

Social network position characteristics as individual differences

A recent collection of neuroimaging studies have demonstrated that humans spontaneously track the social network position characteristics of familiar others when either passively viewing their faces or performing an unrelated task while undergoing functional magnetic resonance imaging (fMRI; Basyouni & Parkinson, 2022; Morelli et al., 2018;

Parkinson et al., 2017; Peer et al., 2021; Weaverdyck & Parkinson, 2018; Zerubavel et al., 2015), a phenomenon that bears resemblance to how people engage in "split-second social perception" whereby they spontaneously process information about the apparent intentions, traits, and emotions of others when merely viewing their faces (Freeman & Johnson, 2016; Todorov et al., 2007). More recent work has demonstrated that people can relatively accurately infer aspects of strangers' social network position characteristics from "thin slices" of their behavior or appearance, such as brief videos or facial photographs (Alt et al., 2021; Mobasseri et al., 2022). Thus, humans may perceive social network position characteristics as stable, trait-like individual differences, the knowledge of which can be used to inform a perceiver's cognition and behavior and therefore promote favorable social interactions. Indeed, social network position characteristics have been shown to be partially heritable, stable across contexts, and resemble trait-level individual difference variables (Falk & Bassett, 2017; Fowler et al., 2009; Jackson, 2009).

The systematic variance in social network positions characteristics across individuals may be due to "passive characteristics" (Jackson, 2009) such as attractiveness, that can affect other actors' behavior towards them. In support of this hypothesis, past work has shown that physical attractiveness is predictive of social status, popularity, and social acceptance (Kleck et al., 1974; Lerner & Lerner, 1977; Salvia et al., 1975; Webster & Driskell, 1983), and people are able to infer aspects of strangers' social network position characteristics simply based on their appearance with relative accuracy (Alt et al., 2021; Mobasseri et al., 2022). On the other hand, individuals may come to occupy particular kinds of social network positions because they exhibit particular cognitive styles, personality traits, and/or sociobehavioral tendencies. For instance, an individual that tends to be attracted to and bonds with highly gregarious people that are prone to

forging and maintaining many social ties may come to occupy a position of high eigenvector centrality, or an individual that enjoys engaging with socially diverse groups of people may occupy a position of high brokerage. On the other hand, an individual that prefers to construct and maintain a particularly cohesive, tightly-knit social environment may occupy a position of low brokerage. Prior work has shown that brokers tend to be characteristically high in self-monitoring (Feiler & Kleinbaum, 2015; Mehra et al., 2001; Sasovova et al., 2010), which is associated with an intuitive sensitivity to social cues, allowing an individual to engage in chameleon-like behavior, adapting their own behavior to their social circumstances (Lennox & Wolfe, 1984; Snyder, 1974). Self-monitoring has been shown to be associated with closely monitoring the thoughts, actions and feelings of others (Funder & Harris, 1986; Ickes et al., 1990), and individuals high in self-monitoring also tend to exert a disproportionate amount of effort in providing emotional help (Toegel et al., 2007) and advice (Flynn et al., 2006) to their social ties. Self-monitoring may be advantageous for individuals characteristically high in brokerage, given that brokers may excel at adjusting their behavior to blend into different social groups and contexts, thereby enabling them to form social ties with individuals that would otherwise be unconnected.

Despite past work linking measures of centrality to personality traits (e.g., self-monitoring, extraversion), inter-individual variability in social network position characteristics is not well-explained by common measures of individual differences, such as personality measures that are typically collected in self-report surveys and questionnaires. Although a small handful of research has demonstrated modest relationships between personality traits and measures of social network centrality (Asendorpf & Wilpers, 1998; Casciaro, 1998; Feiler & Kleinbaum, 2015; Klein et al., 2004; Y. H. Lee et al., 2010; Y. Liu & Ipe, 2010; Pollet et al., 2011; Selfhout et al.,

2009; Totterdell et al., 2008; Venkataramani et al., 2010), these are, at best, weakly correlated relationships. Furthermore, research has also yielded null results when testing if self-reported personality measures are linked to social network position characteristics, (Fang et al., 2015; Klein et al., 2004; Landis, 2016; Neubert & Taggar, 2004; Roberts et al., 2008), particularly when using a large, demographically representative sample that is not comprised solely of undergraduate students (Roberts et al., 2008). Taken together, researchers still lack a comprehensive understanding of the sociobehavioral tendencies that may determine individuals' social network position characteristics.

The traditional approach in psychology of using self-report surveys and questionnaires has yielded some success in characterizing latent constructs (e.g., personality traits) that are predictive of individual differences in traits and behaviors (Paunonen, 2003). However, introspection about one's own mental processes is often inaccurate (Dijksterhuis, 2004; Wilson, 2002; Wilson & Nisbett, 1978), and an individual's self-representation can also be confounded in a laboratory context by their inclination to appear socially desirable to researchers (King & Bruner, 2000). These limitations of self-report surveys and questionnaires may, in part, explain why such measures do not reliably capture variance in social network position characteristics. However, neuroimaging can complement traditional survey-based approaches by elucidating individual differences in neurocognitive functioning that are linked to individual differences in social network position characteristics. Such inter-individual variability in neurocognitive function can shed light on, and shape testable hypotheses about, the sociobehavioral tendencies that are characteristic of individuals occupying certain social network positions.

Using neuroimaging to study individual differences in social network position characteristics

The study of individual differences has long been acknowledged as an important focus of psychology and neuroscience, as treating inter-individual variability as meaningful signal can help advance theory and improve prediction of individual cognition and behavior (Corr & Mobbs, 2018; Kosslyn et al., 2002; Underwood, 1975). Recent technological and methodological advances have facilitated the investigation of individual differences with neuroimaging (Dubois & Adolphs, 2016), an approach that can allow researchers to look "under the hood" to examine the neurocognitive functions underlying individual differences.

This rapidly growing area of research has demonstrated that individual differences in brain structure and neural responding are predictive of individual differences in self-reported personality traits (DeYoung et al., 2010) and individual differences in a wide range of neurocognitive processes, such as low-level perception (Haberman et al., 2015; Reeder, 2017), metacognition (Rouault et al., 2018), memory and learning (Cetron et al., 2019; Hampson et al., 2006; Miller & Van Horn, 2007; Tan et al., 2011), economic decision making (Kable & Levy, 2015; Ma et al., 2011; Talukdar et al., 2018), emotion regulation (H. Lee et al., 2012; Paschke et al., 2016), and social cognition (Banissy et al., 2012; Bukowski et al., 2020; Chavez & Heatherton, 2015; Eres et al., 2015; Hildebrandt et al., 2021; Kliemann et al., 2018; Parkinson & Wheatley, 2014; Richardson et al., 2018; van Buuren et al., 2021; van den Brink et al., 2012). Importantly, individual differences in brain structure and neural responding are also predictive of individual differences in real-world outcomes, such as consumer choices (Tusche et al., 2010), sun-screen use (Falk et al., 2010), smoking behavior (Falk et al., 2011), substance abuse vulnerability (Rapuano, Rosenberg, et al., 2020), drinking behavior (A. L. Courtney et al., 2018),

and weight gain (Rapuano, Laurent, et al., 2020). Such research has found, for example, that neural responses to ads discouraging smoking behavior in the ventromedial prefrontal cortex later predicted reductions in smoking behavior (Falk et al., 2011). Given the role of ventromedial prefrontal cortex in self-related processing and implicit valuation, the researchers conclude that the resulting tendency to smoke less was driven by neural processing that integrated the message content and the self, thereby motivating future cessation of smoking behavior (Falk et al., 2011). Taken together, neuroimaging has proven to be a fruitful approach in elucidating the neurocognitive mechanisms that underlie individual differences in how individuals tend to think and behave.

Individual differences in neuroanatomy linked to individual differences in social network position characteristics

A growing body of work in the past decade has begun to use structural magnetic resonance imaging (sMRI) to examine the relationship between inter-individual variability in brain structure and individual differences in social network characteristics. A relatively early study investigating this relationship demonstrated that macaques that were pseudo-randomized into social groups of varying sizes exhibited individual differences in gray matter density in the mid superior temporal sulcus, inferior temporal gyrus, rostral superior temporal gyrus, and amygdala approximately one year later (Sallet et al., 2011). More specifically, living in a larger social group caused future increases in gray matter density in these brain regions, which are implicated in face and body processing, object recognition, vocalization encoding, and emotion processes, respectively. Thus, even in the span of only one year, macaques remarkably developed increases in gray matter density in brain regions implicated in social cognition in

response to increased cognitive demands of living in larger social groups. These findings provided striking evidence that characteristics of an individual's social network can cause differences in neuroanatomy, which were likely a result of the sociocognitive demands of living in large social groups. On the other hand, individual differences in neurocognitive function may drive individual differences in how individuals build and maintain their social relationships, which may give rise to inter-individual variability in social network position characteristics.

A subsequent collection of cross-sectional sMRI studies on humans have yielded convergent findings. Out-degree centrality (defined as social network size in the following studies) has been shown to be positively correlated with the volume of orbitofrontal cortex (P. A. Lewis et al., 2011; Powell et al., 2012), and this relationship was mediated by individual differences in mentalizing ability (Powell et al., 2012). Out-degree centrality has also been shown to be positively correlated with gray matter density in orbitofrontal cortex (Von der Heide et al., 2014) and with volume and gray matter density in the amygdala (Bickart et al., 2011, 2012; Von der Heide et al., 2014). Furthermore, research using diffusion tensor imaging (DTI) demonstrated that the microstructural integrity of white matter tracts connecting the amygdala and orbitofrontal cortex was significantly associated with out-degree centrality (Hampton et al., 2016). Separate work has shown that the orbitofrontal cortex is implicated in value-based decision making in social contexts (Báez-Mendoza et al., 2021; Padoa-Schioppa & Cai, 2011) and that the amygdala is involved in tracking social dominance of others (Watanabe & Yamamoto, 2015) and social hierarchies (Ligneul et al., 2016). Furthermore, structural connectivity between the amygdala and orbitofrontal cortex is crucial to support the orbitofrontal cortex in encoding value representations (Rushworth et al., 2013). This body of work suggests that having more social ties is associated with a heightened ability to engage in evaluating the

social value of others and integrating this information with decision-making processes. Degree centrality in an online social network has also been shown to be significantly associated with gray matter density in superior temporal sulcus and entorhinal cortex (Kanai et al., 2012), which have been implicated in social perception and associative memory processes, respectively.

Overall, this collection of sMRI studies have identified several regions of the brain whose anatomical properties bear statistical dependencies with individuals' real-world social network position characteristics. The localization of these relationships in the brain shed light on the neurocognitive mechanisms that may drive certain aspects of sociobehavioral tendencies associated with individual differences in social network position characteristics.

Individual differences in neural responding linked to individual differences in social network position characteristics

fMRI can complement sMRI in investigating the relationship between individual differences in sociobehavioral tendencies and social network position characteristics. More specifically, it can provide researchers an opportunity to examine neural responding in real-time, whether it is in response to constrained tasks probing particular facets of mental processing, or in response to rich, naturalistic stimuli that mimic everyday perceptual experiences. fMRI can also be used to characterize functional brain networks by assessing the extent to which different brain regions couple with one another at rest (resting-state functional connectivity). In so doing, fMRI can provide a window into the neurocognitive functions associated with localized neural responses, in which inter-individual variability may be linked to individual differences in social network position characteristics.

The aforementioned study in which macaques were pseudo-randomized into social groups of varying sizes also demonstrated that the macaques living in larger social groups later exhibited increased resting-state functional connectivity between the superior temporal sulcus and anterior cingulate cortex and between the superior temporal sulcus and rostral prefrontal cortex (Sallet et al., 2011). Given the established role of superior temporal cortex in social perception (Lahnakoski et al., 2012) and the role of anterior cingulate cortex in the tracking of motivation of others using social cues (e.g., emotional expressions) in both humans and monkeys (Apps et al., 2016), heightened functional connectivity between these two regions may be associated with an increased capacity to engage in social perceptual processes that are used to understand the motivations of others' behavior. Furthermore, in humans, rostral prefrontal cortex and superior temporal cortex have been shown to be recruited when individuals make predictions about the intentions of others and when individuals are updated about the intentions of others (Behrens et al., 2008). Although it is unclear if macaques exhibit theory of mind capabilities, heightened functional connectivity between the rostral prefrontal cortex and superior temporal cortex may be indicative of an increased capacity to understand and infer the intentions of other individuals. Taken together, these longitudinal changes in functional connectivity may suggest that living in larger social groups necessitates an increased capacity to engage in socio-affective processing, particularly in tracking the social cues of others and using these social cues to inform internal representations of others' intentions and mental states. A subsequent study on humans demonstrated that resting-state functional connectivity between the amygdala and brain regions supporting social perceptual processes, such as fusiform gyrus, temporal pole, rostral superior temporal sulcus, and orbitofrontal cortex, was positively correlated with individuals' out-degree centrality (Bickart et al., 2012). A similar relationship was found between out-degree centrality

and functional connectivity between the amygdala and brain regions supporting social affiliative processes, such as the ventromedial prefrontal cortex, subgenual and rostral anterior cingulate cortex, and nucleus accumbens (Bickart et al., 2012). This body of resting-state fMRI work has produced results that are convergent with the aforementioned sMRI research, such that heightened structural and functional connectivity between brain regions implicated in socio-affective processing are associated with occupying positions of relatively high centrality in the real-world.

More recent work has also shown that individuals characterized by high in-degree centrality in their real-world social network exhibited more similar neural responses to each other (and to their peers in general) relative to individuals characterized by low in-degree centrality in response to watching naturalistic audiovisual stimuli (i.e., movie clips) in regions of the default mode network, such as the dorsomedial prefrontal cortex, precuneus, posterior cingulate cortex, and inferior parietal lobule (Baek et al., 2022). Neural similarity in these brain regions are associated with inter-individual similarities in the understanding and interpretation of narratives (Finn et al., 2018; Nguyen et al., 2019; Yeshurun et al., 2017). Furthermore, recent work has suggested that the default mode network integrates external contextual information with internal experiences and schemas to generate predictive models of situations as they unfold over time and thus neural similarity observed in the default mode network may reflect the generation of shared meaning across individuals (Yeshurun et al., 2021). Thus, individuals characterized by high in-degree centrality (i.e., highly popular individuals) may process and interpret the world around them in a fashion that is similar to that of their peers. This tendency to engage in normative processing may help them form social ties with many people and solidify their position of in-degree centrality, thereby granting them the capacity to influence the social

norms and shaping the behaviors of individuals in their social network (Osgood et al., 2013; Zingora et al., 2020).

Research using task-based fMRI has shown that functional connectivity between left and right temporoparietal junctions in response to a social exclusion paradigm was negatively correlated with individual differences in the density of online social networks (Schmälzle et al., 2017). Given that these brain regions are implicated in mentalizing, individuals with more sparse social networks may be more likely to engage in mentalizing when faced with social exclusion relative to individuals with more dense social networks. Thus, it is possible that individuals that lack the social safety of dense social networks (Hurlbert et al., 2000) may engage in more mentalizing when faced with social exclusion as a coping mechanism (Schmälzle et al., 2017). In other words, individuals in highly dense social networks may afford to conserve mentalizing resources when faced with social exclusion, as their relatively higher position of centrality affords them with a social safety net. Furthermore, individuals high in betweenness centrality in their online social networks recruited the dorsomedial prefrontal cortex, temporoparietal junction, medial prefrontal cortex, and posterior cingulate cortex more than did individuals low in betweenness centrality when receiving divergent peer feedback and providing their recommendation in an fMRI task that involved reviewing mobile game apps and sharing these reviews (O'Donnell & Falk, 2015). These brain regions have been implicated in inferring the mental states of others (Schurz et al., 2014), and preceding work demonstrated that individuals with heightened responses in the temporoparietal junction were more successful in convincing other people to adopt their viewpoints (Falk et al., 2013). Moreover, a separate study showed that salespeople with heightened responses in the temporoparietal junction and medial prefrontal cortex were more effective in communicating information to their clients (Dietvorst et al., 2009).

Thus, the heightened responses in mentalizing regions in the brains of individuals that are characteristically high in brokerage may suggest that brokers are particularly adept at inferring the mental states of others and communicating persuasively. This increased effectiveness in mentalizing and capacity to engage in theory of mind may comprise, in part, the neurocognitive mechanism underlying a broker's ability to skillfully manage the flow of information between disparate individuals and coordinate behavior across neighboring social ties to their liking (Burt et al., 2013).

Taken together, these findings demonstrate that neuroimaging can be leveraged to provide a window into the individual differences in neurocognitive processing that are characteristic of, and may lead to, certain social network position characteristics. Such an approach can shed light on the sociobehavioral tendencies that are linked to the occupation of particular social network positions. However, an individual's neurocognitive processes and sociobehavioral tendencies may also be related to those of surrounding actors. Although it is important to investigate the individual differences associated with social network position characteristics, it is also critical to investigate how individual differences in neurocognitive processes and sociobehavioral tendencies are related to one's immediate social ties and to broader social network structure.

Interpersonal similarity and proximity in real-world social networks

In a given social network, two individuals may share similarities in their number of social ties, the extent to which they are central, or the extent to which they bridge disparate groups, but the people to whom they are connected can be different, which can have meaningful consequences. The way with which an individual thinks, feels, and behaves is shaped by how

their friends think, feel, and behave. Crucially, an individual's cognitive, emotional, and behavioral tendencies can also be shaped by those of individuals with whom they are indirectly connected (e.g., friends-of-friends, friends-of-friends-of-friends). Thus, despite never meeting or interacting with more distant people in one's social network, an individual can nevertheless be meaningfully influenced by their cognitive, emotional, and behavioral tendencies. Indeed, a growing body of research has documented a phenomenon whereby various behaviors, emotions, attitudes, and health conditions appear to spread across individuals and their social ties in their social network over time. More specifically, research has demonstrated that obesity (Christakis & Fowler, 2007), smoking (Christakis & Fowler, 2008), alcohol consumption (J. Niels Rosenquist et al., 2010), loneliness (Cacioppo et al., 2009), depression (J. N. Rosenquist et al., 2011), sleep behavior and drug use (Mednick et al., 2010), divorce (McDermott et al., 2009), food consumption (Pachucki et al., 2011), cooperative and altruistic behavior (Fowler & Christakis, 2010), sexual activity (Brakefield et al., 2014), tastes in entertainment (Christakis & Fowler, 2009), political mobilization (Bond et al., 2012), and even happiness (Fowler & Christakis, 2009) can spread across individuals.

Whereas social influence can mediate the spread of such behaviors, emotions, attitudes, and health conditions across individuals, humans also tend to cluster in their social networks based on similarities in their age, gender, ethnicity, and in other demographic attributes and behaviors, such as drug use, religious beliefs, political orientations, and taste in music (Kandel, 1978; Knoke, 1990; Mark, 1998; Marsden, 1988; McPherson et al., 2001). This tendency to be surrounded by familiar others, known as "homophily" or "assortativity," appears to be a ubiquitous property of human social networks and has been observed across various contexts, such as modern industrialized societies, online communities, and hunter-gatherer communities

(Apicella et al., 2012; Fu et al., 2012; K. Lewis et al., 2012; McPherson et al., 2001). These inter-individual similarities in demographic characteristics and behavior may reflect similarities in how people closer together in their social networks attend to, interpret, and react to the world around them. To probe the nature of these inter-individual similarities in cognitive and behavioral tendencies, traditional approaches have used personality surveys and questionnaires to measure inter-individual similarities in personality traits and dispositions. However, these investigations of assortativity based on self-reported personality traits have yielded negative or inconsistent results (Feiler & Kleinbaum, 2015; Selfhout et al., 2009, 2010). This is at odds with the widespread intuition that friends' similarities transcend "surface-level" characteristics, such as demographic attributes. Empirical work supporting this intuition has shown that a sense of inter-individual similarity in thoughts, feelings, and beliefs (a "generalized shared reality") is indeed predictive of social connection between individuals (Rossignac-Milon et al., 2020). Furthermore, recent work has shown that this intuition acts as a social prior, such that people expected that friends in a fictive online community would exhibit similar behavior in an economic decision-making game (Schwyck et al., 2022).

It is possible that similarities in self-reported personality traits may not be sensitive to the types of psychologically meaningful similarities that are observed among friends. On the other hand, recent research has demonstrated that friends share exceptional similarities in their linguistic styles (Kovacs & Kleinbaum, 2020), suggesting that perhaps alternative approaches to measure inter-individual similarities in cognition and behavior may yield some success in uncovering the inter-individual similarities observed among people close together in their social networks.

Inter-individual neural similarity and proximity in real-world social networks

A growing body of recent research using neuroimaging has shown that individuals' proximity in their real-world social networks are associated with inter-individual similarities in neural responding. In one study, researchers characterized the full social network of a cohort of students in a graduate program, a subset of whom underwent fMRI while passively watching naturalistic audiovisual stimuli (i.e., movie clips; Parkinson et al., 2018). Individuals that were closer together in their social network, as measured by their geodesic distance (i.e., "degrees of separation"; see Baek et al. (2021) for a review of relevant social network analysis terminology), exhibited greater similarity in neural responding in several cortical regions, such as the superior parietal cortex, which has been implicated in attentional allocation (Kastner et al., 2000; Shomstein, 2012), and in the inferior parietal cortex, which has been implicated in bottom-up attentional control, mentalizing, and processing the narrative content of stories (Corbetta & Shulman, 2002; Mar, 2011; Yeshurun et al., 2017, 2021). Importantly, this relationship was statistically significant even when controlling for inter-individual similarities in demographic characteristics, suggesting that the observed neural similarities captured similarities in how individuals attended to, interpreted, and emotionally reacted to the stimuli above and beyond what could be explained by inter-individual similarities in age, gender, and ethnicity.

Follow-up work also demonstrated that similarities in temporal trajectories of multivoxel pattern responses to naturalistic stimuli are also associated with individuals' proximity in their real-world social network, suggesting that people closer together in their social network experience similar patterns of recurrence in brain activity over time when viewing movie clips (Hyon, Kleinbaum, et al., 2020), particularly in a dorsal aspect of the posterior parietal cortex, which is associated with the dorsal attention network. Given the role of this brain region in

endogenously-driven shifts in attention (Cabeza et al., 2008), people closer together in their social network may experience similar temporal fluctuations in their attention states that may be directed towards internal states and memories when watching movie clips. Strikingly, in both studies carried out by Parkinson et al. (2018) and Hyon et al. (2020), the relationship between neural similarity and social network proximity was strongest among pairs of individuals that shared a direct social tie (i.e., a social distance of 1) and grew weaker as social distance increased. The apparent decay in inter-individual similarity across greater social distances suggests that even individuals that are not directly connected (i.e., a social distance of 2) share more similar patterns in neural responding relative to individuals that are farther apart (i.e., a social distance of 3+). Overall, these studies suggest that task-based fMRI is a promising tool to identify inter-individual neural similarities among people closer together in their social network. Such neural similarities can help elucidate the similarities in how people tend to think, feel, and behave that characterize people closer together in real-world social networks. However, inter-individual similarities that are associated with how close people are in their social network may vary across different social contexts and life stages. In line with this notion, one study yielded null results when assessing the relationship between inter-individual similarities in resting-state functional connectivity and how close schoolchildren were in the social network of their school (McNabb et al., 2020). Thus, further research is needed to investigate if the relationship between neural similarity and social network proximity generalizes to other communities, such as those that are characterized by different cultures, age groups, or organizational structures. Expanding this research to include different samples of individuals can also shed light on the extent to which inter-individual neural similarities associated with social network proximity may vary as a function of the social context.

One recent study demonstrated that inter-individual similarities in neuroanatomy are predictive of social network proximity. More specifically, schoolchildren closer together in their real-world social network exhibited greater inter-individual similarity in the gray matter volume of "social brain" regions associated with the default mode network, above and beyond the effects of inter-individual similarity in demographic characteristics (D'Onofrio et al., 2021). This effect was not found in other brain regions in this study. A handful of prior work has linked individual differences in gray matter volume and thickness within "social brain" regions to individual differences in social cognitive abilities, such as mentalizing (P. A. Lewis et al., 2011; Rice et al., 2014; Rice & Redcay, 2015; Wiesmann et al., 2020) and empathic tendencies (Banissy et al., 2012; Eres et al., 2015). Thus, inter-individual anatomical similarities in brain regions associated with social cognition may facilitate mutual understanding, predictability, and communication among people that are closer together in their social network, given that these factors are important for forming social ties (Cutting & Dunn, 1999; Erdley & Day, 2017).

Taken together, the research discussed in this section points toward the utility of functional and structural neuroimaging in identifying the neural predictors of how close people are in their real-world social networks, and the localization of these neural predictors can shed light on the types of cognitive, emotional, and behavioral similarities exhibited by people closer together in their social networks.

Does the brain shape social networks or do social networks shape the brain?

Investigating the relationship between the brain and the social networks in which it is embedded is critical considering that real-world social network structure likely shapes an individual's social interactions and that an individuals' tendency to use their brain in certain

ways likely shapes their real-world social network structure. With few exceptions, the research discussed in the current article is unable to address these causal relationships. Although one study in particular found that macaques' social group size was associated with future increases in gray matter density in brain regions associated with social cognition, there have been no comparable studies on humans that have leveraged longitudinal study designs. This may be due to the fact that ethical and practical considerations can preclude certain longitudinal designs, as it is not trivial to force individuals to form certain social ties, and random assignment to different social networks structures is not always possible or feasible. However, future work would benefit from using longitudinal study designs to test if pre-existing individual differences in the brain predict individuals' future social network position characteristics. Such longitudinal research can also test if the occupation of certain social network positions predicts future individual differences in neuroanatomy or neural responding (e.g., the extent of recruitment of brain regions associated with mentalizing during a theory of mind task). Future work using longitudinal designs can also investigate the extent to which pre-existing neural similarities causally predict future friendship formation (i.e., homophily) and/or the extent to which social influence processes cause individuals to develop similarities in their neural characteristics over time. In the former case, pre-existing neural similarities may reflect similarities in how people attend to, interpret, and emotionally respond to the world around them, which can foster less effortful interpersonal communication, more interpersonal predictability, and affiliative tie formation (Berger & Calabrese, 1975; Clore & Byrne, 1974; Redcay & Schilbach, 2019). Moreover, individuals may have a pre-existing generalized shared reality, which reflects similarities in internal states (e.g., feelings, beliefs, concerns) about the world in general and has been shown to be predictive of the extent to which people feel connected with each other (Rossignac-Milon et

al., 2020). Alternatively, social influence processes may mediate relationships between inter-individual similarities and social network proximity, whereby sustained and intensive interactions can lead individuals to become more similar to each other over time. In essence, individuals' ways of thinking, feeling, or behaving may "rub off" on each other, such that they may develop similarities in their thoughts about the world (Rossignac-Milon et al., 2020), convergent emotional experiences (Anderson et al., 2003; Butler, 2015; Gonzaga et al., 2007), and alignments in attitudes (Davis & Rusbult, 2001). It is likely that both homophily and social influences processes at play, such that individuals that are connected via an indirect tie (i.e., characterized by a social distance of two) may be subjected to relatively local social influences, thereby becoming more similar over time. In turn, such convergence over time may facilitate affiliative tie formation between these individuals.

Concluding remarks

Humans are embedded in social networks, and an individual's relative position in their social network can have substantial ramifications with respect to meaningful outcomes, such as their health, sociality, professional success, and happiness. Yet, little is known about the cognitive, affective, and behavioral traits that are linked to occupation of particular kinds of social network positions, such as those characterized by centrality and/or brokerage. Although traditional approaches of using self-report surveys and questionnaires to capture latent constructs have been relatively successful in identifying traits that are related to real-world behavior, such constructs have not been met with much success in characterizing individual differences in real-world social network position characteristics. This lack of relative success may be due to the fact that social network position characteristics depend not only on an individual's immediate

relationships but also on third-party relationships in their communities of which an individual may not always be aware. Furthermore, this approach has also yielded limited success in characterizing the similarities shared among individuals that are closer together in their social networks, beyond similarities in demographic attributes. However, the integration of neuroimaging and social network analysis in a growing body of recent work has demonstrated that individual differences in neuroanatomy and neurocognitive processes are linked to social network position characteristics and that people closer together in their social network also share similarities in neuroanatomy and neural responding. Thus, this research has begun to elucidate the sociobehavioral tendencies that characterize individuals occupying particular social network positions and the interpersonal similarities that are exhibited by people closer together in their social networks. However, many questions remain, particularly with respect to the extent to which the brain shapes social networks and the extent to which social networks shape the brain. Taken together, the research described here and future work building on such findings can advance our understanding of the organizational principles of real-world social network structures and of the neurocognitive mechanisms that give rise to them.

The current research

The aforementioned research has provided preliminary evidence that neuroimaging can elucidate the neurocognitive mechanisms that are characteristic of individuals that occupy certain social network positions. A separate line of research has begun to demonstrate that individual differences in the microstructural integrity of white matter connectivity supporting social cognition are predictive of an array of socio-cognitive and behavioral traits (Baumgartner et al., 2015; Chavez & Heatherton, 2015; S. S. Wang et al., 2014; Y. Wang et al., 2017; Y. Wang &

Olson, 2018; Xu & Potenza, 2012). The majority of this work has examined the relationship between microstructural integrity of single white matter tracts and individual differences in cognition and behavior. However, data-driven machine learning models have shown promise in robustly predicting individual differences based on distributed patterns of white matter microstructural integrity (Y. Wang et al., 2020). Study 1 in this dissertation aims use machine learning to predict individuals' real-world social network position characteristics based on their patterns of white matter microstructural integrity distributed across brain networks that support social cognition.

As reviewed in the previous section, not only does an individual's social network position characteristics have meaningful consequences but also the people to whom an individual is connected directly and indirectly can also influence how an individual thinks, feels, and behaves. Moreover, individuals that share similarities in demographic attributes and behaviors tend to cluster closely together in their social network. A handful of neuroimaging studies have demonstrated that people closer together in their social network exhibit similarities in neural responding when watching naturalistic stimuli (Hyon, Kleinbaum, et al., 2020; Parkinson et al., 2018), suggesting that people closer together in their social network may think about and respond to the world around them in a similar fashion. A separate line of research has shown that patterns of resting-state functional connectivity ("functional connectomes") are predictive of individual differences in a variety of socio-cognitive and behavioral traits and self-reported personality (Beaty et al., 2018; Christov-Moore et al., 2020; Dubois et al., 2018; Finn et al., 2015; Meskaldji et al., 2016; Miranda-Dominguez et al., 2014; Rosenberg et al., 2015, 2018). Thus, inter-individual similarities in functional connectomes may capture inter-individual similarities in how individuals may think about and respond to the world around them. Study 2 in

this dissertation tests if inter-individual similarities in resting-state functional connectomes are predictive of how close people are in their real-world social network.

Prior work demonstrating a relationship between a relationship between neural similarity and social network proximity has been cross-sectional (D'Onofrio et al., 2021; Hyon, Kleinbaum, et al., 2020; Parkinson et al., 2018). Thus, this research is unable to address the extent to which pre-existing neural similarities may lead to friendship formation or the extent to which friends undergo a convergence in neural characteristics over time. Study 3 in this dissertation aims to test if pre-existing similarities in neural responses to naturalistic stimuli are predictive of friendship eight months later and if individuals with pre-existing neural similarities grow closer together in their social network over time.

Little is known about the individual differences in sociobehavioral tendencies that uniquely characterize individuals occupying social network positions (e.g., eigenvector centrality), which are associated with a disproportionate amount of influence, popularity, and leverage. Furthermore, although it has been well-established that people closer together in their social network often share similarities in demographic attributes, much less is known about the types of inter-individual similarities shared by friends that run deeper than such "surface-level" characteristics. This dissertation integrates tools from social network analysis, neuroimaging, and machine learning to address these gaps in the literature and advance our understanding of how the brain shapes and is shaped by real-world social networks.

Chapter 1: White matter connectivity in brain networks supporting social and affective processing predicts real-world social network characteristics

[Note: This is a copy of the in press manuscript: Hyon, R., Chavez, R., Chwe, J.A., Wheatley, T., Kleinbaum, A.M., Parkinson, C. (in press). White matter connectivity in brain networks supporting social and affective processing predicts real-world social network characteristics. *Communications Biology.*]

Introduction

All human cognition and behavior are embedded within the context of real-world social networks. In any social network, people vary systematically with respect to the number of friends that they have, the extent to which they are well-connected to well-connected others, and the extent to which they connect people who would otherwise be unconnected to each other. Although these social network position characteristics have meaningful consequences for individuals and their communities (Brass, 1984; Burt, 1994, 1997, 2004; Jackson & Matthew O. Jackson, 2008; Krackhardt, 1990; Morelli et al., 2017; Seibert et al., 2001; Smith et al., 2020), they are not well captured by measures typically used to assess individual differences in personality, such as self-report surveys administered to individuals in isolation (Feiler & Kleinbaum, 2015; Selfhout et al., 2009). However, recent work has shown that social network position characteristics constitute significantly heritable individual difference variables that are stable across contexts (Fowler et al., 2009; Jackson, 2009). The heritability of social network position characteristics may be driven, at least in part, by the heritability of social, affective, and behavioral tendencies, which may be reflected in individual differences in the networks of brain regions that support relevant aspects of social perception, cognition, and affective processing.

Here, we sought to investigate this possibility by integrating structural neuroimaging data with characterizations of participants' positions in their real-world social networks.

A growing body of research has begun to highlight the critical role of white matter connectivity in supporting social cognition (Y. Wang & Olson, 2018), and the structural integrity of white matter tracts has been linked to a variety of individual differences in social, cognitive, and behavioral traits (Baumgartner et al., 2015; Chavez & Heatherton, 2015; Metoki et al., 2017; S. S. Wang et al., 2014; Y. Wang et al., 2018; Xu & Potenza, 2012). Although past work has largely focused on how the structural integrity of single white matter tracts relate to sociobehavioral tendencies, using data-driven machine learning models to map relationships between distributed patterns of white matter microstructural integrity and sociobehavioral tendencies can provide an informative window into the complex web of connectivity between brain regions that supports social cognition (Y. Wang et al., 2020).

Here, we used diffusion magnetic resonance imaging (dMRI) to test whether individual differences in distributed patterns of white matter microstructural integrity are predictive of individual differences in social network position characteristics. To this end, we characterized the complete social networks of three different bounded communities of individuals, a subset of whom underwent dMRI. We then used probabilistic tractography to delineate groups of white matter tracts associated with three key facets of social processing: face perception, mentalizing, and mirroring, as well as affective processing. Finally, we used a machine learning algorithm to predict characteristics of individuals' social network positions based on patterns of white matter microstructural integrity across tracts in these brain networks. Rather than only examining univariate relationships between single tracts and social network position characteristics, leveraging a data-driven, multivariate approach can improve predictive performance by taking

into account distributed connectivity signatures (i.e., multi-tract patterns of white matter microstructural integrity).

Patterns of microstructural integrity distributed across white matter tracts in the affective processing, mirroring, and face perception brain networks were predictive of structural characteristics of individuals' positions in their real-world social networks, such as the extent to which they bridge between disparate people or groups (brokerage), and the extent to which they are well-connected to well-connected others (eigenvector centrality). However, we found no significant relationship between social network position characteristics and patterns of white matter microstructural integrity in the mentalizing brain network. In addition, while distributed patterns of white matter microstructural integrity were predictive of social network position characteristics, no single white matter tract appeared to be necessary or sufficient for predicting social network position characteristics. These findings suggest that individual differences in brain networks that support social perception, affective processing, and understanding others' actions may be particularly important in determining the structural positions that individuals occupy in their real-world social networks.

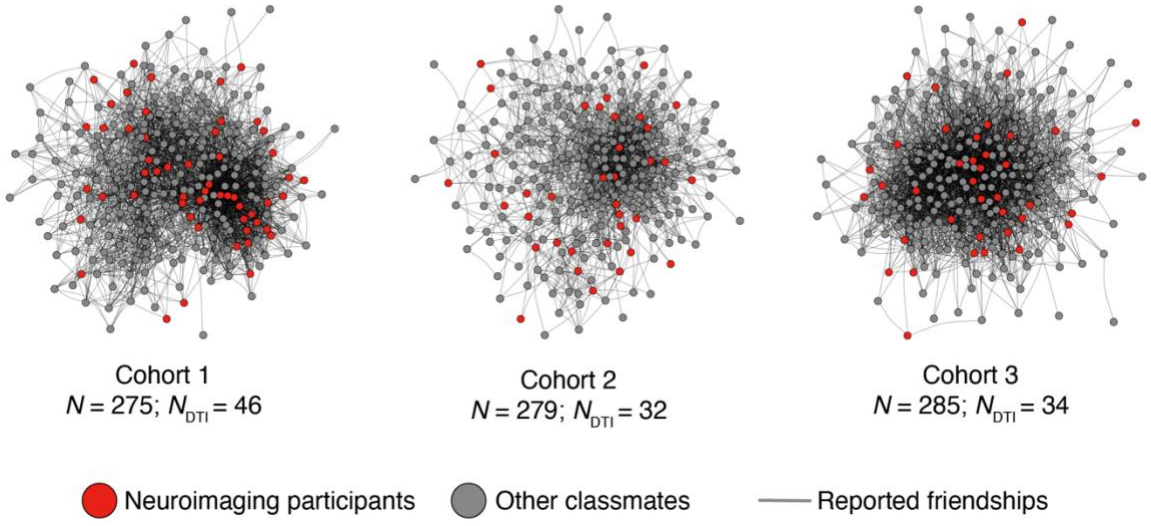

Figure 1. Social network characterization. Three cohorts of first-year graduate students completed a survey in which they indicated their social ties with other students. These three social networks were reconstructed using this data. Nodes indicate students, and lines reflect mutually reported ties between students. Across all three cohorts, a subset of students (red nodes; $N = 112$ after exclusions; see Methods) participated in the dMRI study. The Fruchterman-Reingold layout algorithm, as implemented in the igraph package, was used to position the nodes.

Results

We first characterized the complete social networks of three cohorts of a graduate program. Members of each cohort ($N_{cohort\text{-}1} = 275$; $N_{cohort\text{-}2} = 279$; $N_{cohort\text{-}3} = 285$) completed an online survey (see Methods); data from this survey was used to characterize each cohort's social network (Fig. 1). A subset of the individuals who participated in the social network survey also participated in the dMRI study ($N_{cohort\text{-}1} = 46$; $N_{cohort\text{-}2} = 32$; $N_{cohort\text{-}3} = 34$ after exclusions based on participant movement; see Methods), in which diffusion-weighted images were collected (see Methods for more details).

For each dMRI participant, we characterized their position in the social network of their cohort in terms of five social network position characteristics: out-degree centrality (the number of people whom the participant names as a friend), in-degree centrality (the number of people who name the participant as a friend), eigenvector centrality (the extent to which the participant is well-connected to other well-connected individuals), betweenness centrality (a global measure of brokerage measuring the fraction of shortest paths between other members of the social network that pass through the participant), and constraint (a local measure of brokerage accounting for the extent to which someone has access to non-redundant social partners; see Methods for details on social network position characteristics). Thus, two measures of brokerage were considered: constraint and betweenness centrality. We examined betweenness centrality to be consistent with prior work that used betweenness centrality as a measure of brokerage in establishing the heritability of this aspect of social network position (Fowler et al., 2009). We

included constraint following our own prior work integrating neuroimaging and social network data (Parkinson et al., 2017), and given that constraint is a more local measure of brokerage that may be more impacted by individuals' own sociobehavioral tendencies, rather than those of other nearby individuals in the network (Baek et al., 2021). In contrast, betweenness centrality captures how often an individual lies on the shortest path between other people in the social network, and thus can be dramatically impacted by factors beyond an individual's own sociobehavioral tendencies (Baek et al., 2021). For example, individuals with high betweenness centrality may not function as true brokers, as they may lie on the shortest path between others because they are merely in close proximity to a true broker (Baek et al., 2021). Thus, relative to betweenness centrality, constraint may bear a stronger relationship to the sociobehavioral tendencies that are characteristic of brokers, which in turn are reflected in patterns of white matter microstructural integrity in the brain.

Regions of interest (ROIs) in four *a priori* defined brain networks associated with different aspects of socio-affective processing (i.e., affective processing, face perception, mentalizing, and mirroring networks) were functionally defined using the meta-analysis tool Neurosynth (Yarkoni et al., 2011) (Fig. 2). This method provides an approximation of the location of a given ROI if it had been mapped with fMRI in each individual. The three social brain networks examined here were selected based on recent reviews on white matter and social cognition that have emphasized their role in social interactions and processing[20]: Successful social interactions require (1) recognizing and extracting information from others' faces (via regions in the face perception network), (2) quickly understanding their actions, emotions, and intentions through brain regions involved in both producing and observing actions (via regions in the putative mirroring network), and (3) representing and reasoning about their mental states (via

regions of the mentalizing network). Probabilistic tractography was then conducted to trace the white matter tracts connecting every possible pair of ROIs in each brain network (see Methods). Ultimately, the affective processing network consisted of 33 white matter tracts, the face perception network consisted of 50 white matter tracts, the mentalizing network consisted of 41 white matter tracts, and the mirroring network consisted of 49 white matter tracts. To characterize the microstructural integrity of each white matter tract, average fractional anisotropy (FA) values were extracted such that each white matter tract had a corresponding single FA value. FA captures the directional coherence of water in white matter tracts and has been shown to be highly sensitive to factors such as myelination, axonal packing density, and axonal diameter (Beaulieu, 2002).

Using a leave-one-subject-out cross-validation scheme, we used a machine learning algorithm based on ridge regression (see Methods) to test whether patterns of microstructural integrity of white matter tracts within each of the four aforementioned brain networks were predictive of out-degree centrality, in-degree centrality, eigenvector centrality, betweenness centrality, and constraint (Fig. 3). Model performances were measured using the correlation between actual and predicted values of social network position characteristics, and *p*-values were corrected for multiple comparisons using false discovery rate (FDR) thresholding (see Methods).

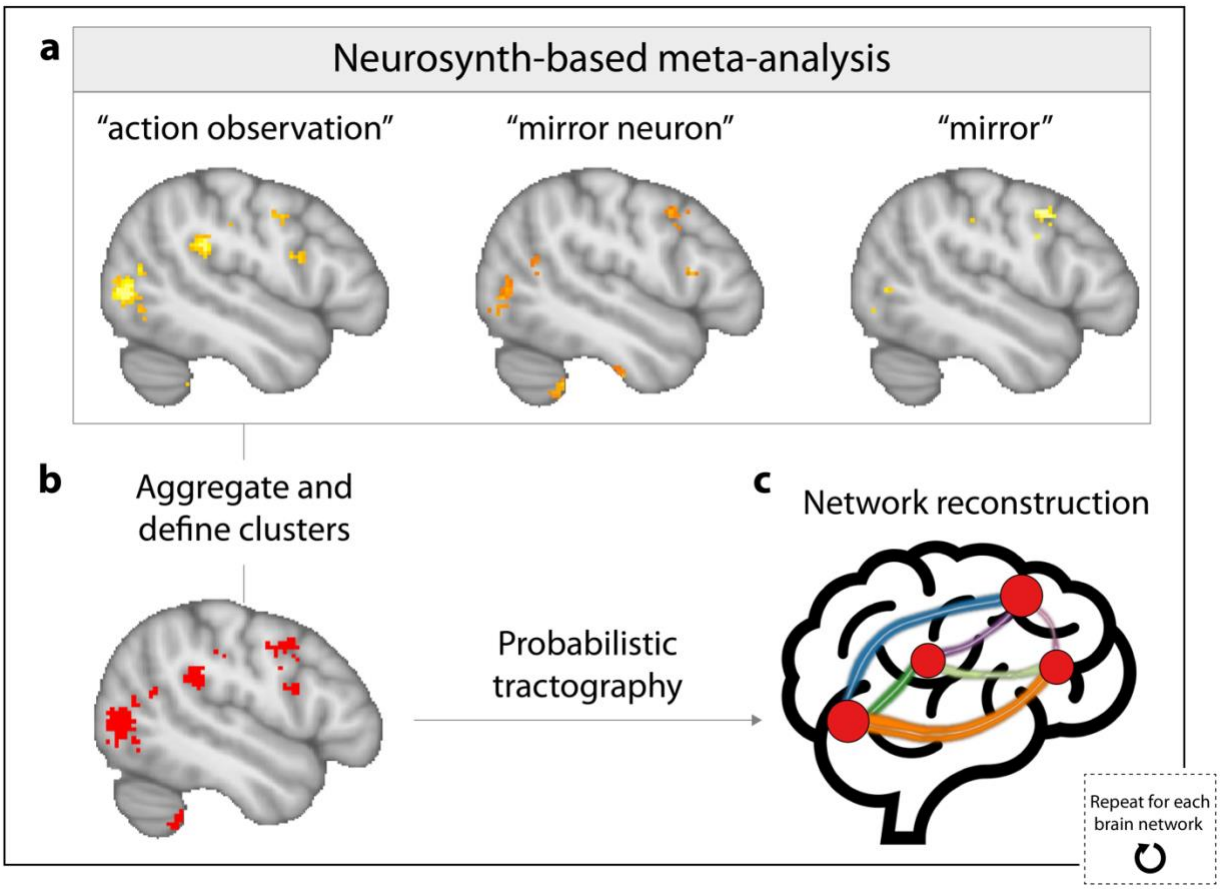

Figure 2. Schematic illustrating the process of reconstructing white matter tracts between regions involved in particular facets of socio-affective processing. (a) Meta-analysis-based images of brain regions associated with a particular facet of socio-affective processing (e.g., mirroring) were generated by submitting sets of keywords (e.g., action observation, mirror neuron, mirror) to Neurosynth[22]. (b) These images were aggregated across terms in a set, and discrete regions of interest were identified. (c) For each subject, probabilistic tractography was then conducted to trace white matter tracts (colored lines in this schematic image) connecting each pair of brain regions (red nodes). This procedure was repeated to construct the affective processing, mentalizing, and face perception networks (see Methods for further details).

Patterns of white matter microstructure within the affective, mirroring, and face perception networks are predictive of social network position characteristics

Patterns of microstructural integrity across white matter tracts in the affective processing network significantly predicted individuals' constraint ($r = 0.263$, $p = 0.002$, $p_{FDR\text{-}corrected} = 0.010$), betweenness centrality ($r = 0.240$, $p = 0.006$, $p_{FDR\text{-}corrected} = 0.015$), and eigenvector centrality ($r = 0.211$, $p = 0.013$, $p_{FDR\text{-}corrected} = 0.026$). Patterns of microstructural integrity across

white matter tracts in the mirroring network significantly predicted individuals' constraint (r = 0.210, p = 0.013, $p_{FDR\text{-}corrected}$ = 0.026), eigenvector centrality (r = 0.244, p = 0.005, $p_{FDR\text{-}corrected}$ = 0.019), and out-degree centrality (r = 0.239, p = 0.006, $p_{FDR\text{-}corrected}$ = 0.022). Patterns of microstructural integrity across white matter tracts in the mentalizing network significantly predicted individuals' eigenvector centrality (r = 0.186, p = 0.025, $p_{FDR\text{-}corrected}$ = 0.033) and betweenness centrality (r = 0.172, p = 0.034, $p_{FDR\text{-}corrected}$ = 0.046). Patterns of microstructural integrity across white matter tracts in the face perception network significantly predicted individuals' betweenness centrality (r = 0.229, p = 0.008, $p_{FDR\text{-}corrected}$ = 0.015).

We repeated the above analytic procedure in our primary analyses to test if patterns of microstructural integrity distributed across white matter tracts in each brain network were significantly predictive of social network position characteristics while controlling for demographic variables (i.e., age, gender), as well as handedness and academic cohort. We also controlled for self-reported extraversion, given that extraversion has been associated with social network position characteristics, such as eigenvector centrality[10] (associations between control variables and social network characteristics are reported in Appendix - Note 1). Patterns of microstructural integrity across white matter tracts in the affective processing network were significantly predictive of constraint (r = 0.240, p = 0.005, $p_{FDR\text{-}corrected}$ = 0.014) while controlling for these variables. Furthermore, patterns of microstructural integrity across white matter tracts in the mirroring network were significantly predictive of eigenvector centrality (r = 0.265, p = 0.002, $p_{FDR\text{-}corrected}$ = 0.010) and constraint (r = 0.232, p = 0.007, $p_{FDR\text{-}corrected}$ = 0.014) when controlling for these variables (Fig. 4).

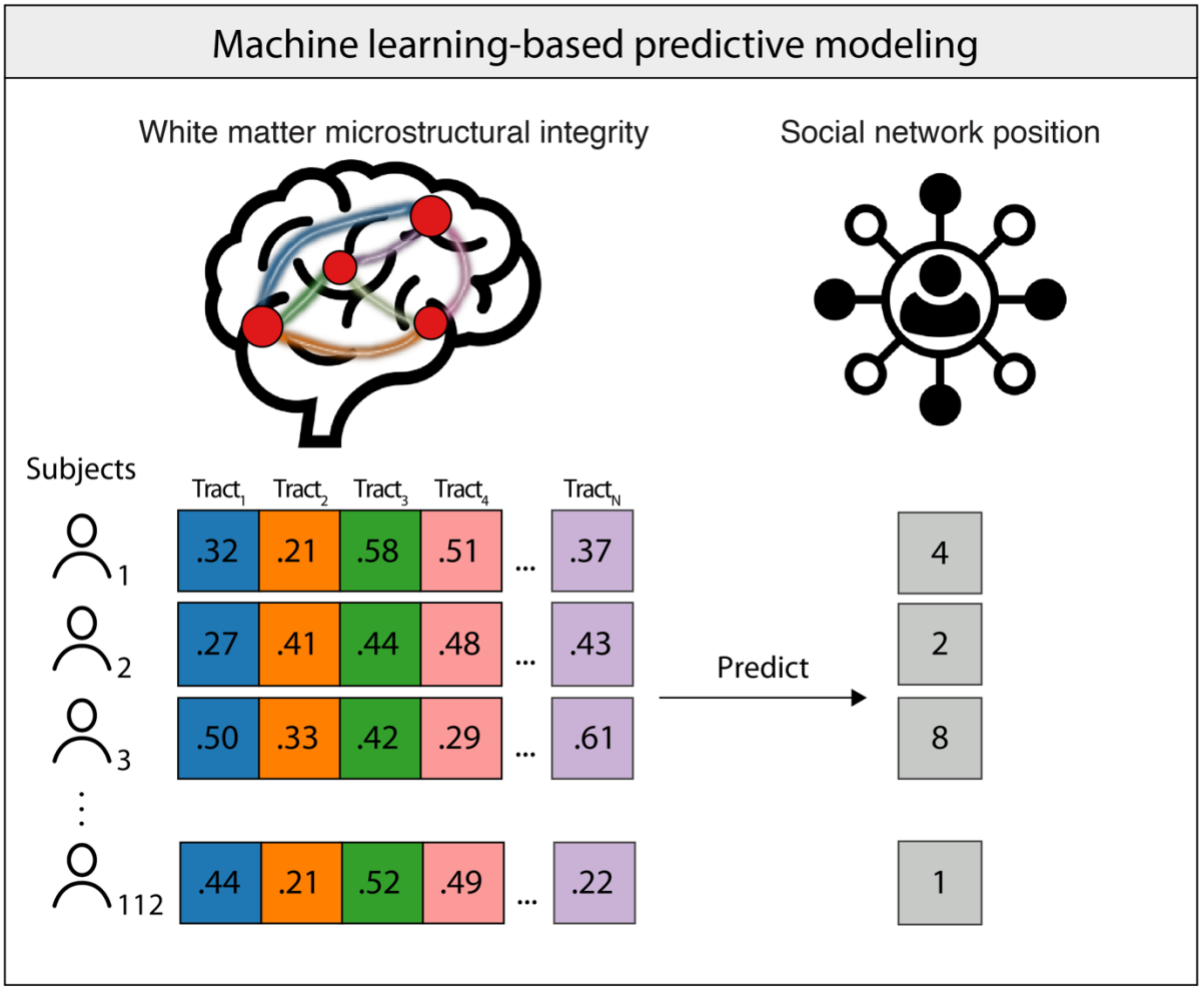

Figure 3. Multivariate prediction of social network position characteristics based on patterns of white matter microstructural integrity. For each subject, average FA was extracted from each white matter tract in a given brain network, and the resulting set of FA values were used as predictors (as shown in different colors) in a ridge regression-based algorithm to predict individuals' social network position characteristics (see Methods for further details). This procedure was performed for the mirroring, affective processing, mentalizing, and face perception brain networks.

Patterns of white matter structure across major white matter tracts are predictive of social network position characteristics

In an exploratory analysis, we used Freesurfer's TRACULA (TRActs Constrained by UnderLying Anatomy) tool (Yendiki et al., 2011), an algorithm for automated global

probabilistic tractography, to reconstruct 18 major white matter tracts for each subject. We then used the same analytic procedure to test if patterns of microstructural integrity across these major, well-established white matter tracts can predict social network position characteristics. We observed results similar to those in the primary analysis (see Appendix - Note 2), such that patterns of microstructural integrity were predictive of eigenvector centrality and betweenness centrality, and were also predictive of in-degree centrality and eigenvector centrality when controlling for demographic characteristics (age, gender), extraversion, handedness, and cohort. These results corroborate our primary findings that distributed patterns of white matter microstructural integrity are predictive of social network position characteristics. They also demonstrate that these findings are robust to the use of markedly different data analytic procedures.

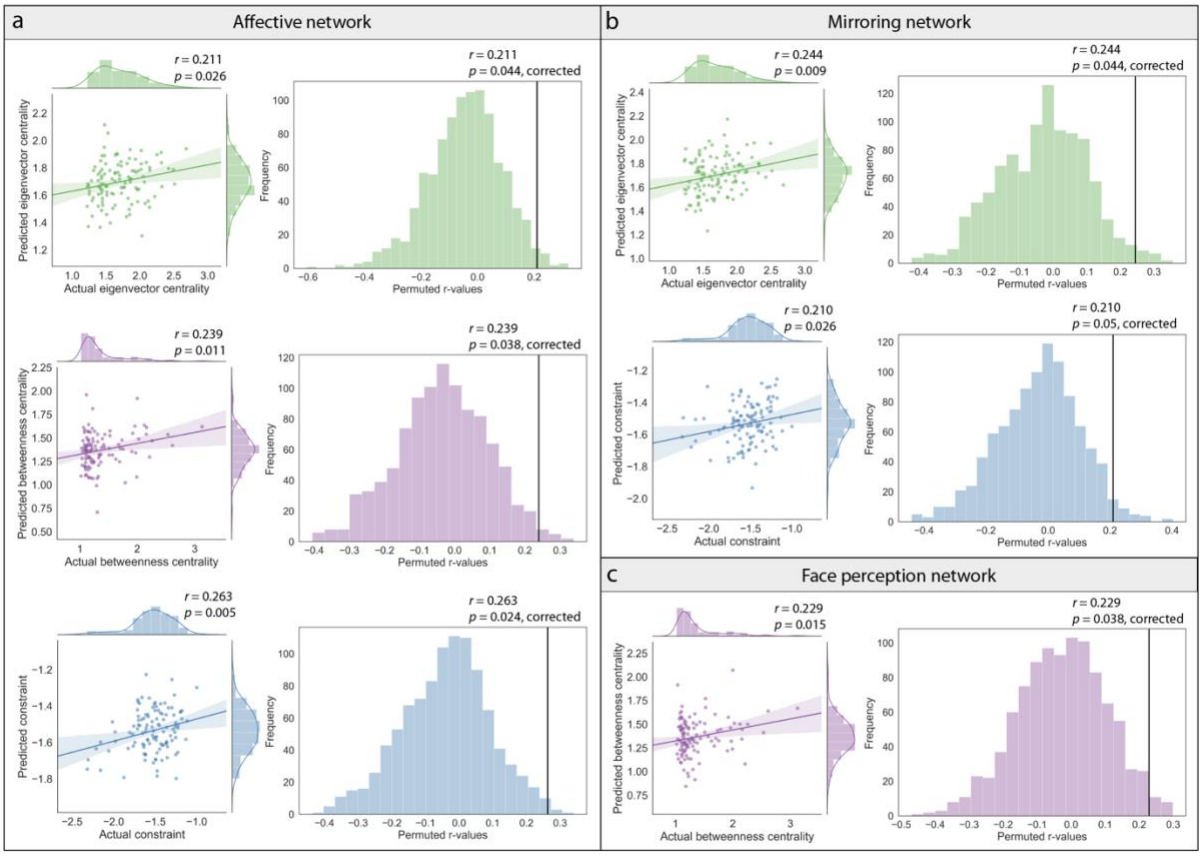

Figure 4. Multivariate patterns of white matter microstructural integrity predicted real-world social network position characteristics. (a) Whereas patterns of white matter microstructural integrity in the affective processing network were predictive of constraint, (b) patterns of white matter microstructural integrity in the mirroring network were predictive of constraint and eigenvector centrality. (c) Patterns of white matter microstructural integrity in the face perception network were predictive of betweenness centrality. For each model, the predictive performance was measured using the Pearson correlation between the actual and predicted values of the social network variable of interest (N=112); p-values are FDR-corrected; shaded regions indicate 95% CIs. Social network position values were normalized within cohort and square-root transformed prior to analysis.

No single white matter tracts are necessary to predict social network position characteristics

Our primary results suggest that patterns of microstructural integrity distributed across white matter tracts in the mirroring network are predictive of eigenvector centrality, and that patterns of microstructural integrity distributed across white matter tracts in the affective

processing and mirroring networks are predictive of constraint, when controlling for covariates. We then sought to conduct exploratory analyses to investigate whether certain white matter tracts were disproportionately contributing to the predictive performance of these models. To this end, we tested whether the exclusion of any single white matter tract would significantly diminish the predictive performance of each full model (i.e., using all *P* predictors, where *P* is the number of tracts in a given brain network). We first calculated the true difference in predictive performance between the full model and a model leaving one tract out (i.e., using *P* - 1 predictors). This true difference value was then compared against a null distribution of 1,000 difference values in predictive performance generated by permutation testing. This procedure was repeated *P* times (i.e., for each tract) for each of these three models, such that the relative contribution of each predictor to each model's predictive performance was evaluated (see Methods).

There were no single tracts that, when omitted, significantly compromised the models' ability to predict eigenvector centrality or constraint from patterns of white matter microstructural integrity in the mirroring network. A similar pattern of null results was observed when testing if the omission of single tracts compromised the models' ability to predict constraint from patterns of white matter microstructural integrity in the affective network. These results suggest that the exclusion of single white matter tracts from the set of predictors in the affective processing or mirroring networks does not significantly diminish the respective full models' performance in predicting social network position characteristics. Thus, within the brain networks in which patterns of white matter microstructural integrity were significantly predictive of social network position characteristics, no single tract was *necessary* for making such predictions. This procedure was also repeated using the set of predictors derived from the TRACULA analysis, and this analysis also returned null results.

Single white matter tracts alone are not sufficient to predict social network position characteristics

We next sought to test whether any single white matter tract in the affective processing, mirroring, face perception, or mentalizing networks would be *sufficient* to predict the social network position characteristics, while controlling for extraversion and our other control variables (e.g., demographic variables). For each of the 173 white matter tracts, we used ordinary least squares regression to test whether its microstructural integrity was predictive of any of the five social network position characteristics (out-degree centrality, in-degree centrality, eigenvector centrality, betweenness centrality, and constraint; see Methods). The microstructural integrity of single tracts was not predictive of any of the five social network position characteristics, even when a relaxed threshold for determining significance was used (see Methods). This procedure was also repeated using the set of predictors derived from the TRACULA analysis, and this analysis also returned null results.

The results of our primary analysis demonstrate that distributed patterns of white matter microstructural integrity across tracts in brain networks supporting social and affective processes are predictive of structural characteristics of people's positions in their real-world social networks. Specifically, patterns of white matter microstructural integrity amongst white matter tracts between brain regions associated with affective processing and mirroring were predictive of the extent to which individuals connect otherwise unconnected people and the extent to which individuals are well-connected to other well-connected people in their real-world social networks, above and beyond the effects of demographic variables and extraversion (Fig. 4).

Discussion

Patterns of white matter microstructure may shape sociobehavioral tendencies linked to social network position characteristics

These findings expand on past work demonstrating that various social network position characteristics are heritable individual difference variables that are stable across contexts (Burt, 2012; Fowler et al., 2009). The genetic basis of social network position characteristics may operate in part via individuals' passive characteristics, which influence how others behave toward them (e.g., their appearance). Consistent with this possibility, physical attractiveness has been shown to be predictive of social status, popularity, and social acceptance (Kleck et al., 1974; Lerner & Lerner, 1977; Salvia et al., 1975; Webster & Driskell, 1983), and people can somewhat accurately infer aspects of strangers' social network position characteristics (i.e., in-degree centrality and constraint) based on their physical appearance (Alt et al., 2021). On the other hand, the genetic basis of social network position characteristics may also manifest through active characteristics–e.g., sociobehavioral tendencies that facilitate the occupation of certain social network position characteristics (Jackson, 2009). For example, such active characteristics might include an individual's sociability, their tendency to introduce their friends to one another, the extent to which they express empathy toward others, their propensity to engage in behavioral mimicry in social interactions, or some combination of these factors. Individual differences in such sociobehavioral tendencies are likely driven by individual differences in brain structure, but little is known about the relationship between neuroanatomy and social network position characteristics.

Past research has demonstrated that out-degree centrality is linked to individual differences in structural properties of brain regions and white matter connectivity (Bickart et al., 2011; Hampton et al., 2016; Kanai et al., 2012; Noonan et al., 2018; Von der Heide et al., 2014). The studies referred to here linked individual differences in neural predictors to social network size, which was measured in a variety of ways. However, these different measures of social network size all correspond to out-degree centrality. Thus, we use the more precise term out-degree centrality here (since the term network size would imply something different, for example, in sociocentric networks, such as those characterized here, than in egocentric networks). To characterize out-degree centrality, these studies used an egocentric network approach, in which participants enumerate their contacts via free recall or the number of friends that participants have in online communities. This work has yielded important insights into the relationship between brain structure and sociality. At the same time, such approaches have important limitations. For example, it is difficult to disentangle variability in out-degree centrality (self-reported network size) from individual differences in social perception or memory (when self-report is used) or from individual differences in engagement with a particular online platform (when number of friends on social media websites is used) (Baek et al., 2021; Beaulieu, 2002; Brewer, 2000; Brewer & Garrett, 2001; Burt, 1984; Marsden, 1990, 2003). In contrast, the sociocentric network approach used here incorporates data on social ties provided by each individual in the network and can be used to calculate characteristics of individuals' social network position that take into account broader patterns of social ties (e.g., third party relationships). Thus, the sociocentric network approach can complement the egocentric network approach by capturing a more complete picture of a social network, thereby

expanding the types of inferences that can be drawn about people's relative social network position characteristics.

Research in sociology and ecology has demonstrated that social network position characteristics whose calculation often depends on sociocentric network data (e.g., in-degree centrality, eigenvector centrality, constraint, betweenness centrality) have particularly impactful consequences in real-world social networks. These include measures of evolutionary fitness and likelihood of survival across a variety of social species (Brent et al., 2013; Stanton & Mann, 2012), as well as social influence (Brass, 1984), professional success (Brass, 1984; Burt, 1994, 1997), others' perceptions of one's competence and leadership (Burt, 2004; Mehra et al., 2006), and the likelihood of becoming the target of negative gossip and scapegoating (Ellwardt et al., 2012). Furthermore, whereas out-degree centrality has not been found to be heritable, other, often sociocentrically-derived, social network position characteristics have been shown to be heritable individual difference variables (Fowler et al., 2009). Thus, the latter may constitute stable traits that are relatively invariant across contexts (Burt, 2012). Indeed, a growing body of research has integrated sociocentric network analysis and neuroimaging to demonstrate that people spontaneously encode and track the extent to which others hold positions of in-degree centrality (Morelli et al., 2018; Zerubavel et al., 2015), eigenvector centrality, and brokerage (Parkinson et al., 2017) in real-world social networks. These findings suggest that individuals spontaneously retrieve complex knowledge about people's relative social network position characteristics that may be crucial for informing cognition and behavior. However, the neural predictors and sociobehavioral tendencies associated with such social network position characteristics are not well understood in social neuroscience and psychology, given that the data necessary to calculate these characteristics (i.e., sociocentric network data) is seldom collected.

Patterns of white matter microstructural integrity in brain networks supporting socio-affective processing predict social network position characteristics

The localization of the current results can shed light on the types of active characteristics, or sociobehavioral tendencies, that may be associated with particular social network position characteristics. In particular, patterns of microstructural integrity of white matter tracts in the affective processing and mirroring networks were predictive of constraint (an inverse measure of brokerage), beyond the effects of demographics (age, gender), handedness, cohort, and extraversion. Brokers connect people who would not otherwise be connected and thus wield leverage in controlling the flow of resources (e.g., information) and in coordinating behavior across local social ties (Burt et al., 2013). Given that occupying positions of brokerage involves interacting with different groups of people, brokers may be exceptionally skilled in adapting their thoughts and behavior to meet the variable demands of their diverse social environment. Indeed, past work has shown that across different contexts, people occupying positions of brokerage are characteristically high in self-monitoring (Kleinbaum et al., 2015; Mehra et al., 2001; Oh & Kilduff, 2008; Sasovova et al., 2010), which is associated with an intuitive sensitivity to subtle social cues and with the ability to modify one's behavior to adapt to social circumstances (Lennox & Wolfe, 1984; Snyder, 1974). Individuals high in self-monitoring have been shown to closely monitor the thoughts, actions, and feelings of people around them (Funder & Harris, 1986; Ickes et al., 1990) and also invest considerable effort in providing emotional help (Toegel et al., 2007) and advice (Flynn et al., 2006) to their contacts. Such sociobehavioral tendencies may be driven by individual differences in patterns of white matter microstructural integrity across the affective processing and mirroring networks. The affective processing network may

support the monitoring and interpretation of emotions and the regulation of one's own emotions (Gross, 2015; Parkinson & Wheatley, 2014; Zaki et al., 2009), and the mirroring network may mediate the representation, understanding, and mimicry of the actions of others (Friston et al., 2011; Iacoboni et al., 1999; Rizzolatti & Craighero, 2004). Given that brokers are highly attuned to cues of situational appropriateness, they are likely exceptionally skilled at accurately perceiving and interpreting the emotions and actions of others. Brokers may also be particularly likely to exhibit social chameleon-like behavior such that they engage in nonconscious mimicry and imitate the behaviors of their social contacts. Such behavior has been shown to be associated with increased mutual feelings of affiliation, rapport, and liking (Lakin et al., 2003) and would be conducive to bridging disparate groups of people that may behave in different ways.

Additionally, patterns of microstructural integrity of white matter tracts in the mirroring network were predictive of eigenvector centrality, a prestige-based measure of centrality that takes into account not only an individual's own centrality but also the centralities of their contacts (Bonacich, 1987). Given the relative dearth of previous research investigating cognitive and behavioral traits associated with eigenvector centrality, the link between eigenvector centrality and the cognitive and behavioral tendencies associated with the mirroring network is unclear. However, being highly attuned to social cues and having the ability to effectively understand and imitate the actions of others may be particularly characteristic of individuals occupying positions of high eigenvector centrality, as such tendencies are conducive to being well-liked (Lakin et al., 2003) and may also lead to the formation and maintenance of social ties with other well-connected individuals.

Patterns of white matter microstructure were not significantly predictive of out-degree centrality, in-degree centrality, and betweenness centrality beyond the effects of covariates.

While it is difficult to interpret null findings, we note that this may be attributable to a variety of factors. For example, given that a sociocentric network approach was used here, participants only enumerated contacts within their bounded social network; thus, the measure of out-degree centrality used here was limited to capturing nominations of friends within the social network. While the bounded social networks characterized here were composed of people in a rural, isolated location who largely live, eat, socialize, and study with one another (see Methods), participants may have had friends outside of their academic cohorts that were not characterized. It is possible that patterns of white matter microstructure in social processing networks would be predictive of out-degree centrality if friendships with people outside of participants' academic cohorts were taken into account. Alternatively, more targeted analyses in tracts defined *a priori* may yield significant predictions of out-degree centrality, whereas the current study corrected for multiple comparisons across multiple sets of analyses.

Patterns of white matter microstructural integrity were also not predictive of in-degree centrality, but they were significantly predictive of eigenvector centrality. This suggests that individual differences in patterns of white matter microstructural integrity are related to individual differences in characteristics of the social network position that take into account indirect relationships and broader patterns of social ties (i.e., being well-connected to well-connected others) that go beyond more local characteristics (i.e., the number of direct nominations one receives from others).

At the same time, consistent with the possibility that constraint, as a more local measure of brokerage, is more strongly related to individuals' sociobehavioral tendencies (in contrast to betweenness centrality, a measure of brokerage that can be impacted by more distal factors, such as lying on the shortest path between others due to being close to a true broker[41]), patterns of

white matter microstructural integrity were not predictive of betweenness centrality, but were predictive of constraint.

Patterns of white matter microstructural integrity in the mentalizing network did not predict social network position characteristics

While patterns of white matter microstructural integrity within the affective processing and mirroring networks were predictive of social network position characteristics when controlling for covariates, those in the mentalizing network were not. Thus, structural characteristics of individuals' positions in their social networks appear to be linked to connectivity in brain networks involved in rapid, automatic processes involved in understanding and relating to others and their emotional states (e.g., mirroring and affective processing), but not in those supporting more cognitive facets of interpersonal understanding. Understanding cues to the internal states of others – i.e., the construct of empathy – may be broken down into emotional and cognitive empathy, which are distinct processes with distinct neural mechanisms (Barrett et al., 2016; Decety & Jackson, 2004; Shamay-Tsoory, 2011; Yu & Chou, 2018; Zaki & Ochsner, 2012). On the one hand, regions in the putative human mirror neuron network support emotional empathy, which is an automatic, rapid process that mediates one's emotional, sensorimotor, and visceral response to the affective state of another person. On the other hand, a different set of brain regions supports cognitive empathy, which is a comparatively slow, effortful process that mediates one's conscious ability to understand or explicitly recognize the mental states (e.g., perspectives, intentions) of others (Barrett et al., 2016; Lin et al., 2010; Neumann & Strack, 2000; Yu & Chou, 2018).

Here, empathy was one of the terms used to define brain regions in the mentalizing network (see Methods). Whereas this term may have yielded brain regions associated with *both* cognitive and emotional empathy, terms such as mirror neuron and mirror that were used to define regions in the mirroring network are aligned with emotional, but not cognitive, empathy. Thus, it is possible that individual differences in patterns of white matter microstructural integrity in the mirroring network reflect individual differences in emotional empathy (and not cognitive empathy) and that these individual differences are linked to individuals' social network position characteristics. Indeed, past work has shown that individual differences in the microstructural integrity of white matter tracts connecting perception and action-related regions (i.e., regions in the mirroring network) and regions involved in affective processing are predictive of emotional, but not cognitive, empathy[62]. In contrast, individual differences in patterns of white matter microstructural integrity in the mentalizing network likely at least partially reflect individual differences in cognitive empathy. It is possible that cognitive empathy is not linked to people's social network position characteristics. It is also possible that cognitive empathy relies on more domain-general neural mechanisms (Decety & Lamm, 2007; Schneider et al., 2012), whereas emotional empathy relies on more domain-specific neural circuitry (Decety, 2011), which could make associations between cognitive empathy and its structural correlates less robust than those between emotional empathy and its structural correlates. Furthermore, a limitation of the current study is that a group-level meta-analytic map was used to define regions of interest associated with the mentalizing network. However, recent work has demonstrated that the spatial specificity of the mentalizing network is highly heterogeneous across individuals (Y. Wang et al., 2021). This finding may explain the current study's null results when using patterns of white matter microstructural integrity within the mentalizing

network to predict social network position characteristics, and future work may benefit from using functional localizers to identify mentalizing regions of interest that would be used as seed regions in probabilistic tractography.

Conclusions and future directions

We suggest that future work build on the current findings by examining the extent to which individual differences in the processes supported by the aforementioned brain networks (e.g., emotional empathy, facets of affective processing, such as empathic accuracy) mediate the relationship between brain structure and social network position characteristics. Future work should also examine the extent to which individual differences in brain structure precede or result from individual differences in social network position characteristics. It is possible that brokers attain their advantageous social network position characteristics through distinctive capacities for interpersonal understanding, which are reflected in structural characteristics of brain networks involved in mirroring and affective processing. It is also possible that occupying a high-brokerage position in one's social network places more demands on one's capacity for social and affective information processing (e.g., due to the need to be sensitive to differing social and emotional cues in different social groups and to flexibly modulate one's behavior to suit different contexts). Over time, this may lead to structural differences in the brain networks that support such processing.

In addition, while the current study pooled data from three different bounded communities, all participants were graduate students at a university in the United States. Future work could extend these findings by examining the relationship between white matter microstructure and social network position characteristics in different cultural settings and at

different stages of development. Furthermore, given a large enough sample size, future work would also benefit from training and testing models on different samples of individuals, as this would shed light on whether relationships between white matter microstructural integrity and social network position characteristics are consistent across contexts and communities. Additionally, while the current study used FA as a measure of microstructural integrity, future work may benefit from testing if other measures of white matter microstructure, such as axial diffusivity, mean diffusivity, radial diffusivity, or the number of probabilistic tractography streamlines are predictive of social network position characteristics.

Future work may also benefit from using functional localizers to identify seed regions of interest, as the location of functionally defined brain regions may vary from person to person (Fedorenko et al., 2010). In particular, aspects of the mentalizing network have recently been shown to vary substantially across individuals (Y. Wang et al., 2021). Thus, using functional localizers to define subject-specific seed regions of interest would likely confer greater sensitivity for detecting systematic links between patterns of white matter microstructural integrity and traits such as social network position characteristics. Furthermore, with functionally localized subject-specific ROIs, it is also possible to test if the size of ROIs may systematically affect FA-based prediction of social network position characteristics.

Additionally, the current work focused on patterns of white matter microstructure across tracts *within* brain networks, as it was motivated by an interest in linking individuals' social network position characteristics to anatomical connectivity among brain regions involved in particular mental functions (e.g., linking characteristics of tracts connecting brain regions involved in affective processing to measures of social network centrality). We did not test whether patterns of white matter microstructure across functionally defined tracts *between* brain

networks were predictive of social network position characteristics. It is conceivable that patterns of white matter microstructure across between-network tracts and, correspondingly, interactions between different mental functions (to the extent that tracts between such networks support interactions between the corresponding mental functions), also play an important role in shaping social behavioral tendencies and therefore an individual's social network position characteristics. We did, however, find that patterns of white matter microstructure across TRACULA-defined major white matter tracts were predictive of social network position characteristics. Future work could benefit from specifically considering tracts between different functionally defined brain networks.

Our exploratory analyses indicated that no single white matter tract in particular was necessary for predicting social network position characteristics. Furthermore, no single white matter tract was sufficient for predicting social network position characteristics on its own. Rather, our results suggest that patterns of microstructural integrity values derived from a multivariate set of white matter tracts were necessary for predicting social network position characteristics. These findings expand on recent neuroimaging research demonstrating the utility of data-driven machine learning models in mapping relationships between multivariate sets of neural predictors and person-level outcomes. Such data-driven predictive modeling frameworks have been adopted to link functional neuroimaging data to a wide range of social, cognitive, and behavioral traits (Beaty et al., 2018; Christov-Moore et al., 2020; Finn et al., 2015; Meskaldji et al., 2016; Miranda-Dominguez et al., 2014; Rosenberg et al., 2015). In particular, recent work has demonstrated that whole-brain patterns of resting-state functional connectivity are predictive of one's location in a real-world social network (Hyon, Youm, et al., 2020). Taken together with the current results, these findings suggest that applying machine learning to high-dimensional

neuroimaging data is a fruitful approach for gaining insight into how brain structure and function relate to individuals' positions in their real-world social networks.

Methods

Social network characterization

Subjects in Part 1 of the study were from three different cohorts of first-year students in a graduate program at a private university in the United States who participated as part of their coursework on leadership. The total size of all three cohorts was 842 students, and 839 students participated in the social network survey, resulting in an overall response rate of 99.6% ($N_{Cohort\text{-}1}$ = 275, 91 females, response rate = 99.3%; $N_{Cohort\text{-}2}$ = 279, 89 females, response rate = 100%; $N_{Cohort\text{-}3}$ = 285, 120 females, response rate = 99.7%). For each cohort, an online social network survey was administered 3-4 months after the subjects had arrived on campus. Subjects followed an e-mailed link to the study website where they responded to a survey designed to assess their position in the social network of students in their cohort of the academic program. The survey was adapted from prior work (Burt, 1994; Hyon, Kleinbaum, et al., 2020; Parkinson et al., 2017, 2018). It read, "*Consider the people with whom you like to spend your free time. Since you arrived at [institution name], who are the classmates you have been with most often for informal social activities, such as going out to lunch, dinner, drinks, films, visiting one another's homes, and so on?*" A roster-based name generator was used to avoid inadequate or biased recall. Subjects indicated the presence of a social tie with an individual by placing a checkmark next to their name. Subjects could indicate any number of social ties and were not constrained by a time limit. The bounded social networks characterized here were composed of people in a rural,

isolated location who predominantly lived, ate, socialized, and studied with one another. However, the social network survey used here inquired only about students' interactions with other members of their academic cohort. Thus, the current approach does not capture the students' social ties that exist outside of their cohort of classmates (e.g., relationships with family members, friends outside of the program). That being said, the current study was conducted at a relatively insular and remotely located institution where subjects' contacts outside of campus likely play a smaller role in their daily lives relative to their everyday, in-person interactions with their classmates. All data collection procedures were performed in accordance with the standards of the Dartmouth College Institutional Review Board.

Each cohort's social network data was analyzed using igraph in R (Csárdi & Nepusz, 2014). The social networks of the three cohorts are depicted in Fig. 1. Five social-network-derived metrics were calculated for each subject who participated in the neuroimaging study (see *Part 2: Neuroimaging study)*: out-degree centrality, in-degree centrality, eigenvector centrality, betweenness centrality, and constraint. An unweighted graph was used to calculate each of these social network position characteristics for each subject, as described in greater detail below. For descriptive purposes, for each cohort's social network, we then calculated the mean and median numbers of social ties across individuals (i.e., average total degree centrality, summing incoming and outgoing ties for each individual) and the reciprocity of the graph, which refers to the probability that person *i* nominated person *j* as a friend if person *j* nominated person *i* as a friend (mean social ties$_{Cohort\text{-}1}$ = 91, median social ties$_{Cohort\text{-}1}$ = 77, reciprocity$_{Cohort\text{-}1}$ = 0.53; mean social ties$_{Cohort\text{-}1}$ = 78, median social ties$_{Cohort\text{-}1}$ = 70, reciprocity$_{Cohort\text{-}1}$ = 0.49; mean social ties$_{Cohort\text{-}1}$ = 55, median social ties$_{Cohort\text{-}1}$ = 46, reciprocity$_{Cohort\text{-}1}$ = 0.48).

Social network position characteristics

Out-degree centrality. The out-degree centrality of an individual was calculated as the sum of the individual's outgoing social ties (i.e., the number of people whom the individual nominated).

In-degree centrality. The in-degree centrality of individual was calculated as the sum of individual's incoming social ties (i.e., the number of times the individual was nominated by others).

Eigenvector centrality. A graph consisting of nodes connected by edges can be characterized by an adjacency matrix **A**, populated by elements such that $a_{ij} = 1$ if nodes *i* and *j* are directly connected, and $a_{ij} = 0$ if these nodes are not connected. The eigenvector centrality of each node is given by the eigenvector of **A** in which all elements are positive. The requirement that all elements of the eigenvector must be positive yields a unique eigenvector solution (that is, that corresponding to the greatest eigenvalue). Here, when computing eigenvector centrality, the directionality of the graph was preserved; in the event of asymmetric relationships, only incoming, rather than outgoing, ties were used to compute eigenvector centrality.

Betweenness centrality. The betweenness centrality of an individual was calculated as the proportion of shortest paths between two given nodes that pass through the individual. An unweighted, undirected graph was used to estimate betweenness centrality.

Constraint. The constraint of actor *i* is given by the following equation, where P_{ij} corresponds to the proportion of *i*'s direct social ties accounted for by their tie to actor *j.* The inner summation approximates the indirect constraint imposed on *i* by other actors, *q,* who are socially connected to both *i* and *j* (mutual friends of *i* and *j*):

$$\text{Constraint}_i = \sum_{j=1}^{n}\left(P_{ij} + \sum_{q=1}^{n} P_{iq}P_{qj}\right)^2 \qquad (1)$$

An unweighted, undirected graph was used to estimate constraint; that is, the presence of any social tie, irrespective of its direction or if it was reciprocated, was used to compute the constraint of each node. Constraint was then negated to yield a measure of network brokerage.

All social network position characteristic data were normalized (z-scored) within-cohort. These data were then concatenated across all three cohorts. For each of the social network position characteristics, we then applied the square-root transformation, given that the distributions for each of the social network position characteristics were positively skewed. Correlations between social network characteristics are reported in Appendix - Table 1.

Neuroimaging subjects

A subset of 130 individuals who had completed Part 1 of the study completed a subsequent dMRI study ($n_{Cohort\text{-}1}$ = 54; $n_{Cohort\text{-}2}$ = 36; $n_{Cohort\text{-}3}$ = 40). Subjects in cohort 1 were scanned 6-7 months after their arrival on campus, subjects in cohort 2 were scanned 7-8 months after their arrival on campus, and subjects in cohort 3 were scanned within the first month of their arrival on campus. Subjects provided informed consent in accordance with the policies of the institution's ethical review board. Of the 130 subjects, data from 18 subjects were excluded from analysis due to excess movement. Data from the resulting 112 subjects (40 female) aged 24-35 (M = 27.78, SD = 2.01) were used for analysis. The neuroimaging study was advertised to all students in each cohort via email. All students who were interested in participating and who passed a standard MRI safety screening participated in the DTI scan.

dMRI acquisition

Magnetic resonance imaging was conducted with a Philips Achieva 3.0 Tesla scanner using a 32-channel phased array head coil. Diffusion-weighted images were collected using 70 contiguous 2 mm thick axial slices with 32 diffusion directions (91 ms TE, 8845 TR, 1000 s/mm^2 b-value, 240 mm FOV, 90° flip angle, 1.875 mm x 1.875 mm x 2 mm voxel size). Thirty-three diffusion-weighted volumes were collected per subject. High-resolution anatomical images were also acquired using a T1-weighted MPRAGE protocol (8.2 s TR; 3.7 ms TE; 240 x 187 FOV; 0.938 mm x 0.938 mm x 1.0 mm).

Diffusion tensor imaging

We performed standard preprocessing steps using the Diffusion toolbox in FSL 5.0.10 (Behrens et al., 2003), which included brain extraction, eddy current correction, and motion correction. We then used FSL's *dtifit* to fit a diffusion tensor model at each voxel to generate an FA map for each subject (FA serves as a general marker of white matter microstructural integrity) (Beaulieu, 2002). We also used FSL's *BEDPOSTX* (Behrens et al., 2003, 2007) to model crossing fibers and white matter fiber orientations in each voxel. Both linear and non-linear methods were used to align subjects' fractional anisotropy images in native space to MNI152 standard space. FSL FLIRT (12 degrees of freedom, corratio cost function) was used to generate an affine transformation matrix to align fractional anisotropy images to T1 anatomical images. FSL FLIRT was used to generate an affine transformation matrix to align T1 space to MNI152 standard space, and FSL FNIRT used this "affine guess" to generate a non-linear warpfield to align T1 space to MNI152 standard space. FSL FNIRT was then used to apply the

first affine FLIRT matrix (i.e., native space to T1 space transform) and the FNIRT warpfield in one step to transform fractional anisotropy images to MNI152 standard space.

Defining social processing networks: ROI definition and probabilistic tractography

Probabilistic tractography was conducted to reconstruct white matter tracts between ROIs associated with each of four facets of social processing: affective processing, mirroring, mentalizing, and face perception. This process was used to define the affective processing, mirroring, mentalizing, and face perception networks (i.e., each of the four sets of ROIs, and the tracts connecting its constituent regions). A schematic of this procedure is visualized in Fig. 2.

Keywords were submitted to Neurosynth (Yarkoni et al., 2011) to generate whole-brain meta-analysis-based images of networks of brain regions involved in affective processing (emotion, valence, affective, mood, arousal), mirroring (action observation, mirror neuron, mirror), mentalizing (theory of mind, mentalizing, empathy), and face perception (faces, face recognition, face). For each brain network, the meta-analysis-based images associated with each keyword were aggregated, and the FSL *cluster* command was used to identify the discrete ROIs in each of the aggregated meta-analysis images. The FSL *FLIRT* and *FNIRT* commands were used to transform ROIs from standard space to each subject's native diffusion space. This method provides an approximation of the location of a given ROI if it had been mapped with fMRI in each individual. Each ROI was then dilated by a single voxel and was masked using a brain mask in order to create more liberal ROI masks to ensure that ROIs would extend into neighboring white matter. Due to being exceptionally large and/or spanning multiple regions, a small subset of ROIs were then masked using subject-specific anatomical masks generated using the Freesurfer anatomical parcellation algorithm (Desikan et al., 2006; Fischl, 2012; Fischl et al.,

2002) in order to split the ROI into smaller constituent ROIs, which were subsequently used for analysis. Details regarding the size of each ROI, the anatomical regions associated with each ROI, and whether the ROI was masked using subject-specific anatomical masks are provided in Appendix - Tables 2-5.

For each brain network, the FSL *probtrackx2* command was then used to perform probabilistic tractography between every possible pair of ROIs within each of the left and right hemispheres (i.e., tractography was not performed to trace inter-hemispheric tracts), with a contralateral hemisphere exclusion mask and a brainstem exclusion mask. Two-mask seeding was used, and 1,000 probabilistic tract streamlines were taken at each voxel within each mask, which allows resulting tractography maps to include streamlines originating from and terminating in each ROI. For each proposed white matter tract, if more than half of the subjects yielded zero fiber tracts (i.e., if more than half of the subjects did not have a valid tracing), the corresponding white matter tract was excluded from further analysis. The remaining output connectivity distribution maps were divided by the corresponding total number of existing streamlines to normalize and convert the images into probabilistic maps. These probabilistic maps were then thresholded such that all voxels with a probability below 1% were zeroed in order to reduce false-positive fiber tracts. The resulting probabilistic maps were then binarized within each subject and summed across all subjects in standard space to create group-level tractography images. The group-level tractography images were manually inspected to determine thresholds that minimized spurious connections. Tracts that were identified as spurious upon manual inspection were excluded from further analysis. The resulting group-level images were then transformed back into each subject's native diffusion space. For each subject, we then masked the resulting images using subject-specific white matter tissue masks, which were

generated by FSL's FMRIB, conservatively thresholded at 50% in order to eliminate spurious white matter, and binarized. For each subject, FA values were extracted from each voxel from each white matter tract image using subject-specific FA maps thresholded at 0.2, which is a standard practice to create conservative FA maps. The resulting FA values were averaged across voxels within each tract to yield a single FA value reflecting the microstructural integrity of a given white matter tract.

Structural connectome-based predictive modeling of social network position characteristics

We tested if inter-individual variability in patterns of white matter microstructural integrity would be predictive of individuals' positions in their real-world social network (Fig. 3). That is, the independent variables consisted of a multivariate set of predictors measuring white matter microstructural integrity, and the outcome variable consisted of a given social network position characteristic. We used Scikit-learn (Pedregosa et al., 2011) to implement the predictive modeling analysis. Using Scikit-learn's Pipeline function, we created an algorithm that performed two steps in sequence on the training data for each fold (models fit to each fold's training data were used to predict social network position characteristics based on white matter microstructural integrity values in the corresponding testing data): (1) normalize the predictors using Scikit-learn's StandardScaler function (which subtracts the mean and scales to unit variance) and (2) implement ridge regression. Given the multicollinearity among the predictors, regularized ridge regression was used. We used a nested cross-validation scheme to perform hyperparameter tuning using a grid search procedure (i.e., optimizing the lambda (λ) regularization hyperparameter from a grid/range of values logarithmically spaced between 10^{-5} and 10), such that the training data of each of the 10 outer data folds was further subdivided into

10 inner folds consisting of sub-training and validation datasets. Within each of these inner folds, for each hyperparameter value provided in the hyperparameter grid, the algorithm was trained on the sub-training data and tested on the validation data. The hyperparameter value used in the model with the best performance across all validation sets was identified as the optimal hyperparameter for the corresponding outer training fold. Using this optimal hyperparameter, the algorithm was trained on the outer fold's training data and tested on the outer fold's testing data. This process was repeated independently for each of the ten outer data folds. This procedure yielded a predicted social network position characteristic value for each subject in the sample. Out-of-sample performance was evaluated by calculating the Pearson *r*-value between predicted and actual social network position characteristic values. All reported *p*-values reflect one-sided tests of if participants' actual social network position characteristics were positively associated with the social network position characteristics predicted by the tra

ined models, based on participants' dMRI data (negative associations would not be interpreted in this context). Given that we tested if patterns of white matter microstructural integrity associated with brain networks were predictive of five different social network position characteristics, we corrected for multiple comparisons across these five sets of statistical tests using FDR thresholding.

To test whether inter-individual variability in patterns of white matter microstructural integrity would be predictive of social network position characteristics above and beyond the effects of demographics and extraversion, we repeated the analysis described above while controlling for age, gender, handedness, cohort, and self-reported extraversion. Extraversion was assessed using the relevant items of the Big Five 44-item inventory (O. P. John et al., 2008b).

Testing whether any single white matter tracts were necessary for predicting social network position characteristics

The primary results demonstrate that patterns of microstructural integrity distributed across white matter tracts in the affective processing network are predictive of constraint, and that patterns of microstructural integrity distributed across white matter tracts in the mirroring network are predictive of constraint and eigenvector centrality, even while controlling for variables including age, gender, handedness, cohort, and extraversion. Thus, in these three models (two models predicting constraint; one model predicting eigenvector centrality), we tested if any predictors (i.e., where a predictor corresponds to the microstructural integrity of a given white matter tract) in particular were disproportionately contributing to significant predictions of social network position characteristics.

For each of the three models mentioned above, the following procedure was implemented. We created *P* additional 'leave-one-tract-out' models where *P* reflects the number of predictors (tracts) in the corresponding full model. Each of these additional models excluded one of the *P* predictors that had been included in the corresponding full model such that the number of predictors in the resulting leave-one-tract-out model was equal to *P* - 1. The permutation testing procedure used in the primary analysis was then used to calculate the performance of each of the *P* leave-one-tract-out models in predicting the relevant social network position characteristic. For each of the *P* leave-one-tract-out models, the difference in the model's predictive performance (i.e., the *r*-value measuring the correlation between predicted and actual values) and that of the full model was calculated. We then tested the statistical significance of this difference in predictive performance (i.e., tested if excluding a given predictor significantly diminished the full model's performance). To this end, we used a

permutation testing procedure where social network position characteristics were randomly shuffled across subjects in each of 1,000 permuted datasets. Here, in each permuted dataset, *r*-values were obtained for the full model and for each of the *P* leave-one-tract-out models. For each of the leave-one-tract-out models, we then calculated the difference between its *r*-value and that of the full model within each permuted dataset; this produced a null distribution of 1,000 difference values for each of the leave-one-tract-out models. We then calculated a *p*-value measuring the frequency with which the true difference value was greater than the permuted difference values in this null distribution.

Testing whether any single white matter tracts alone were sufficient for predicting social network position characteristics

We next tested if the microstructural integrity of any single white matter tract in the social processing brain networks defined above was alone *sufficient* to predict social network position characteristics while controlling for extraversion and demographics. To do so, we used Scikit-learn (Pedregosa et al., 2011) to implement ordinary least squares regression in a predictive modeling framework. There were 173 white matter tracts in total across the four examined brain networks. Thus, to test if microstructural integrity of each of these 173 white matter tracts were predictive of the five social network position characteristics (out-degree centrality, in-degree centrality, eigenvector centrality, betweenness centrality, and constraint), we conducted 865 statistical tests.

For each statistical test, we used Scikit-learn's Pipeline function to create an algorithm that performed two steps in sequence on the training data for each fold (models fit to each data fold's training data were used to predict social network position characteristics based on the

white matter microstructural integrity value in the corresponding testing data; see "Structural connectome-based predictive modeling of social network position characteristics*"* for details of the data-folding procedure): (1) normalize the predictors using Scikit-learn's StandardScaler function and (2) implement linear regression. Out-of-sample performance was evaluated by calculating the Pearson *r*-value between predicted and actual social network position characteristic values. All reported *p*-values reflect one-sided tests of if participants' actual social network position characteristics were positively associated with those predicted by each trained single-tract model (negative associations would not be interpreted in this context). To correct for multiple comparisons across all 865 statistical tests, we used FDR thresholding. This procedure corrects for the total number of models tested and corresponding results indicated that data from single tracts could not predict social network position characteristics, unlike the data from distributed patterns of tracts used in our main analyses. At the same time, we note that the threshold used in these exploratory single-tract analyses (correcting for multiple comparisons across 865 statistical tests) was much more conservative than that used in our main analyses, where predictors from each brain network were combined into a single model to predict each examined social network position characteristic. Therefore, as an additional point of comparison, we also examined results of single-tract analyses using a less conservative threshold for determining statistical significance: Given that we tested if microstructural integrity associated with single tracts was predictive of five different social network position characteristics, we corrected for multiple comparisons across these five sets of statistical tests. This relaxed threshold yielded identical results to the results obtained using a more conservative threshold (see Results and Discussion sections).

Appendix

Appendix - Note 1. Assessing relationships between covariates and social network position characteristics

Statistical tests were performed to investigate if covariates used in the current study were significantly associated with social network position characteristics. Associations between each social network position characteristic and continuous covariates were tested with Pearson correlations; associations between each social network position characteristic and categorical variables were assessed with *t*-tests.

Age. Age was not significantly associated with out-degree centrality (r = -0.017, p = 0.855), in-degree centrality (r = -0.106, p = 0.267), eigenvector centrality (r = -0.105, p = 0.271), betweenness centrality (r = 0.057, p = 0.551), or constraint (r = -0.089, p = 0.348).

Gender. Male and female subjects did not significantly differ in their out-degree centrality ($t(110) = 1.20$, p = 0.232), in-degree centrality ($t(110) = 1.45$, p = 0.783), eigenvector centrality ($t(110) = 1.45$, p = 0.391), betweenness centrality ($t(110) = 1.45$, p = 0.160), or constraint ($t(110) = 1.45$, p = 0.151).

Handedness. Left-handed and right-handed subjects did not significantly differ in their out-degree centrality ($t(110) = 1.60$, p = 0.874), in-degree centrality ($t(110) = -0.216$ p = 0.830), eigenvector centrality ($t(110) = -0.226$, p = 0.822), betweenness centrality ($t(110) = 0.765$, p = 0.446), or constraint ($t(110) = -0.371$, p = 0.711).

Cohort. Subjects in cohort 1 and subjects in cohort 2 did not significantly differ in their out-degree centrality ($t(110) = -0.848$, p = 0.400), in-degree centrality ($t(110) = -0.994$, p = 0.323), eigenvector centrality ($t(110) = -0.906$, p = 0.368), betweenness centrality ($t(110) = -1.124$, p = 0.265), or constraint ($t(110) = -0.526$, p = 0.600). Subjects in cohort 1 and subjects in

cohort 3 did not significantly differ in their out-degree centrality ($t(110) = -0.316$, $p = 0.753$), in-degree centrality ($t(110) = -0.282$, $p = 0.779$), eigenvector centrality ($t(110) = -0.055$, $p = 0.957$), betweenness centrality ($t(110) = -0.754$, $p = 0.454$), or constraint ($t(110) = -0.971$, $p = 0.335$). Subjects in cohort 2 and subjects in cohort 3 did not significantly differ in their out-degree centrality ($t(110) = 0.507$, $p = 0.614$), in-degree centrality ($t(110) = 0.691$, $p = 0.492$), eigenvector centrality ($t(110) = 0.895$, $p = 0.373$), betweenness centrality ($t(110) = 0.310$, $p = 0.757$), or constraint ($t(110) = -0.604$, $p = 0.547$). The lack of significant differences in social network position characteristics across cohorts is to be expected given, for example, that we normalized data within cohort prior to aggregating data across cohorts for subsequent analyses.

Extraversion. Extraversion was significantly associated with out-degree centrality ($r = 0.264$, $p = 0.005$), in-degree centrality ($r = 0.481$, $p = 8.00 \times 10^{-8}$), eigenvector centrality ($r = 0.373$, $p = 5.16 \times 10^{-5}$), betweenness centrality ($r = 0.330$, $p = 3.73 \times 10^{-4}$), and constraint ($r = 0.316$, $p = 6.95 \times 10^{-4}$).

Appendix - Note 2. Testing if patterns of white matter microstructure across major white matter tracts are predictive of social network position characteristics

We complemented our main analyses, which were specifically focused on tracts between regions implicated in social and affective processing, by conducting an exploratory analysis of major, well-established white matter tracts. To do so, we used Freesurfer's TRActs Constrained by UnderLying Anatomy (TRACULA) tool (Yendiki et al., 2011), an algorithm for automated global probabilistic tractography, which reconstructs 18 major white matter tracts for each subject. We then performed the following procedure to characterize the predictors used in the predictive modeling analysis. Each subject's FA map was thresholded at 0.20. For each subject,

each tract was thresholded at 20% of the maximum value, binarized, and used as a mask to extract the mean FA from the corresponding subject's FA image. This procedure yielded 18 predictors that captured a pattern of white matter microstructural integrity distributed across major white matter tracts in each subject's brain.

Similar to our main analyses, we first implemented a data-driven, machine learning approach to predict individuals' social network position characteristics based on their patterns of microstructural integrity distributed across these 18 well-established white matter tracts using a ridge regression-based algorithm (see Methods in the main text). Using a leave-one-subject-out cross-validation scheme, the algorithm significantly predicted individuals' eigenvector centrality ($r = 0.215$, $p = 0.011$) and betweenness centrality ($r = 0.186$, $p = 0.025$) based on patterns of white matter microstructural integrity distributed across all 18 white matter tracts (see Methods). Each reported correlation value reflects the relationship between the actual social network position characteristic values and the values predicted by a given model. This analytical procedure was then repeated while controlling for demographic characteristics (age, gender), extraversion, handedness, and cohort. Patterns of microstructural integrity across the 18 major white matter tracts were significantly predictive of in-degree centrality ($r = 0.233$, $p = 0.007$) and eigenvector centrality ($r = 0.291$, $p = 0.001$) when controlling for these variables.

Assessing relations between social network position characteristics

Statistical tests were performed to investigate the relationships between the social network characteristics. Associations between each social network position were tested with Pearson correlations (Appendix -Table 1).

Appendix - Table 1. Correlations between social network characteristics.

	Out-degree centrality	In-degree centrality	Eigenvector centrality	Betweenness centrality	Constraint
Out-degree centrality					
In-degree centrality	0.51***				
Eigenvector centrality	0.87***	0.80***			
Betweenness centrality	0.89***	0.59***	0.76***		
Constraint	0.73***	0.72***	0.81***	0.68***	

Note: Constraint was negated to yield a measure of brokerage. ***$p < .001$

Appendix - Table 2. Functionally defined ROIs in the affective processing network.

ROI Label	Hemisphere	Voxel count	Region(s)	Notes
Aff-1	left	99	rostral anterior cingulate cortex	
Aff-2	left	273	ventromedial prefrontal cortex	
Aff-3	left	502	dorsomedial prefrontal cortex	
Aff-4	left	134	insula	
Aff-5	left	729	orbitofrontal cortex	
Aff-6	left	224	amygdala	Masked using anatomical amygdala mask
Aff-7	left	261	temporal pole	Masked using anatomical temporal pole mask
Aff-8	left	332	superior frontal gyrus	
Aff-9	left	209	dorsal-rostral anterior cingulate cortex	
Aff-10	right	243	amygdala	Masked using anatomical amygdala mask
Aff-11	right	86	caudal anterior cingulate cortex	
Aff-12	right	304	dorsomedial prefrontal cortex	
Aff-13	right	147	dorsal-rostral anterior cingulate cortex	
Aff-14	right	981	inferior frontal gyrus	
Aff-15	right	198	insula	
Aff-16	right	106	rostral anterior cingulate cortex	
Aff-17	right	498	temporal pole	Masked using anatomical

				temporal pole mask
Aff-18	right	262	ventromedial prefrontal cortex	

Note: Where noted, cortical ROIs that were additionally masked using anatomical masks based on the Desikan-Killiany atlas as implemented in FreeSurfer and subcortical ROIs that were additionally masked based on anatomical masks based on automatic subcortical segmentation in FreeSurfer (see Methods for more details) (Desikan et al., 2006; Fischl, 2012; Fischl et al., 2002). These masks were generated for each participant using FreeSurfer's recon-all command.

Appendix - Table 3. Functionally defined ROIs in the face processing network.

ROI Label	Hemisphere	Voxel count	Region(s)	Notes
Face-1	left	224	amygdala	Masked using anatomical amygdala mask
Face-2	left	803	inferior temporal gyrus	
Face-3	left	386	posterior superior temporal sulcus	
Face-4	left	459	occipital pole	
Face-5	left	90	lingual cortex	Masked using anatomical lingual cortex mask
Face-6	left	798	lateral occipital cortex	Masked using anatomical lateral occipital cortex mask
Face-7	left	892	fusiform cortex	Masked using anatomical fusiform cortex mask
Face-8	left	337	inferior temporal cortex	Masked using anatomical inferior temporal cortex mask
Face-9	right	243	amygdala	Masked using anatomical amygdala mask
Face-10	right	424	inferior frontal gyrus	
Face-11	right	104	lingual cortex	Masked using anatomical lingual cortex mask
Face-12	right	980	lateral occipital cortex	Masked using anatomical lateral occipital cortex mask
Face-13	right	808	fusiform cortex	Masked using anatomical fusiform cortex mask

Face-14	right	282	middle temporal cortex	Masked using anatomical middle temporal cortex mask
Face-15	right	484	inferior temporal cortex	Masked using anatomical inferior temporal cortex mask
Face-16	right	230	posterior superior temporal sulcus	Masked using anatomical superior temporal sulcus mask
Face-17	right	160	temporal pole	Masked using anatomical temporal pole mask
Face-18	right	354	anterior inferior temporal cortex	Masked using anatomical anterior inferior temporal cortex mask

Note: Where noted, cortical ROIs that were additionally masked using anatomical masks based on the Desikan-Killiany atlas as implemented in FreeSurfer and subcortical ROIs that were additionally masked based on anatomical masks based on automatic subcortical segmentation in FreeSurfer (see Methods for more details) (Desikan et al., 2006; Fischl, 2012; Fischl et al., 2002). These masks were generated for each participant using FreeSurfer's recon-all command.

Appendix - Table 4. Functionally defined ROIs in the mentalizing network.

ROI Label	Hemisphere	Voxel count	Region(s)	Notes
Ment-1	left	1013	precuneus	
Ment-2	left	586	dorsomedial prefrontal cortex	
Ment-3	left	341	ventromedial prefrontal cortex	
Ment-4	left	77	insula	
Ment-5	left	1661	angular gyrus	

Ment-6	left	733	supramaginal gyrus	
Ment-7	left	459	posterior superior temporal sulcus	
Ment-8	left	154	middle temporal gyrus	
Ment-9	left	676	temporal pole	
Ment-10	right	221	ventromedial prefrontal cortex	
Ment-11	right	820	dorsomedial prefrontal cortex	
Ment-12	right	1024	precuneus	
Ment-13	right	2127	inferior frontal gyrus, dorsal prefrontal cortex	
Ment-14	right	1169	temporal pole, anterior temporal cortex	
Ment-15	right	3374	occipitotemporal cortex	
Ment-16	right	1003	supramaginal gyrus	
Ment-17	right	282	posterior superior temporal sulcus	
Ment-18	right	388	supplementary motor cortex	

Note: Where noted, cortical ROIs that were additionally masked using anatomical masks based on the Desikan-Killiany atlas as implemented in FreeSurfer and subcortical ROIs that were additionally masked based on anatomical masks based on automatic subcortical segmentation in FreeSurfer (see Methods for more details) (Desikan et al., 2006; Fischl, 2012; Fischl et al., 2002). These masks were generated for each participant using FreeSurfer's recon-all command.

Appendix - Table 5. Functionally defined ROIs in the mirroring network.

ROI Label	Hemisphere	Voxel count	Region(s)	Notes
Mirr-1	left	1576	lateral occipital cortex	
Mirr-2	left	529	temporoparietal junction	
Mirr-3	left	1439	precentral gyrus, inferior frontal gyrus	
Mirr-4	left	2608	superior parietal lobule	
Mirr-5	left	956	supramarginal gyrus, postcentral gyrus	
Mirr-6	left	703	premotor cortex	
Mirr-7	right	291	supplementary motor cortex	
Mirr-8	right	347	precuneus	
Mirr-9	right	743	premotor cortex	
Mirr-10	right	1123	supramarginal gyrus	
Mirr-11	right	378	temporoparietal junction	
Mirr-12	right	390	lateral occipital cortex	
Mirr-13	right	330	lingual cortex	
Mirr-14	right	1053	precentral gyrus, inferior frontal gyrus	
Mirr-15	right	2766	occipitotemporal cortex	
Mirr-16	right	472	occipital pole	
Mirr-17	right	2872	superior parietal lobule	

Mirr-18	right	36	posterior cingulate cortex	
Mirr-19	right	542	supramarginal gyrus, postcentral gyrus	

Note: Where noted, cortical ROIs that were additionally masked using anatomical masks based on the Desikan-Killiany atlas as implemented in FreeSurfer and subcortical ROIs that were additionally masked based on anatomical masks based on automatic subcortical segmentation in FreeSurfer (see Methods for more details) (Desikan et al., 2006; Fischl, 2012; Fischl et al., 2002). These masks were generated for each participant using FreeSurfer's recon-all command.

Chapter 2: Similarity in functional brain connectivity at rest predicts interpersonal closeness in the social network of an entire village

[Note: This is a copy of the published manuscript: Hyon, R., Youm, Y., Chey, J., Kwak, S., Parkinson, C. (2020). Similarity in functional brain connectivity at rest predicts interpersonal closeness in the social network of an entire village. *Proceedings of the National Academy of Sciences of the United States of America.* https://doi.org/10.1073/pnas.2013606117.]

Introduction

Human social networks exhibit a high degree of homophily, such that individuals who are close together in their social network (i.e., friends or friends-of-friends, rather than people further removed from one another in social ties) tend to be exceptionally similar to one another with respect to physical and demographic traits, such as age, gender, and ethnicity (McPherson et al., 2001). Yet, a common intuition is that friends are similar to each other in ways that go beyond readily observable and relatively coarse characteristics, such as demographics. The most common method to assess such similarities is the administration of self-report surveys measuring how people tend to think and behave (i.e., personality). However, past research has found no evidence, or only relatively weak evidence, for a relationship between similarity in personality and social network proximity (Feiler & Kleinbaum, 2015; Selfhout et al., 2009).

A separate body of research using functional magnetic resonance imaging (fMRI) has shown that patterns of functional brain connectivity at rest comprise person-specific "fingerprints" that capture inter-individual variability in a wide range of social, cognitive, and behavioral tendencies and capacities (Beaty et al., 2018; Christov-Moore et al., 2020; Finn et al., 2015; Meskaldji et al., 2016; Miranda-Dominguez et al., 2014; Rosenberg et al., 2015, 2018). These resting-state "functional connectomes" have also been shown to be predictive of

individual differences in self-reported personality (Dubois et al., 2018). Given that functional connectomes are predictive of an array of cognitive and behavioral phenotypes, inter-individual similarities in functional connectomes may reflect similarities in how friends, and more generally, people close to one another in their social network, think and behave. Such similarities may include those that are not sufficiently captured by widely used self-report surveys, such as measures of personality. Thus, fMRI can provide a window into the types of latent similarities that are associated with friendship. This approach is particularly promising given recent research integrating task-based fMRI and social network analysis, which has shown, for example, that when viewing videos, friends, and more generally, people closer together in their real-world social network, have exceptionally similar neural responses, which could be indicative of similarities in how friends attend to (Lahnakoski et al., 2014), understand (Cantlon & Li, 2013), and interpret (Yeshurun et al., 2017) the world (Hyon, Youm, et al., 2020; Parkinson et al., 2018). Taken together with other recent work (Falk & Bassett, 2017), these findings highlight the promise of integrating social network analysis and tools from cognitive neuroscience to improve our understanding of how individuals shape and are shaped by the real-world social networks in which they are embedded.

Here, we tested if patterns of neural responding at rest (e.g., individuals' functional connectomes) are associated with proximity between individuals in the social network of an entire village (Fig. 1). Specifically, we tested the hypothesis that greater similarity in individuals' functional connectomes would be associated with greater proximity between those individuals in the social network. Given the large body of research demonstrating that links between interpersonal similarity in a number of cognitive, affective, and behavioral outcomes and social network proximity disappear beyond three or four "degrees of separation" (Cacioppo et al.,

2009; Christakis & Fowler, 2007, 2008; Cole et al., 2012; Fowler & Christakis, 2009, 2010; Moussaïd et al., 2015, 2017; J. N. Rosenquist et al., 2011), we focused our analyses on people four or fewer "degrees of separation" from one another in the village's social network (see Methods). We also tested if such relationships would persist after controlling not only for similarities in demographic characteristics, but also for similarities in self-reported personality (i.e., the Big Five personality traits: extraversion, neuroticism, agreeableness, conscientiousness, and openness/intellect), which are thought to capture stable individual differences in people's cognitive, affective, and behavioral tendencies (O. P. John et al., 2008a). Although self-report personality questionnaires capture much variation in how people tend to think and behave, there is considerable variance in such tendencies that is unaccounted for by such questionnaires (Paunonen, 2003) and that may be encoded in individuals' functional connectomes. Here, we tested if similarity in such latent traits is associated with proximity in a friendship network. Additionally, we examined which brain networks were particularly strongly associated with social network proximity to inform interpretations of the psychological significance of these results, as well as predictions for future research. Finally, given the well-established relationship between the physical distance between people and their distance from one another in social ties, we tested if geographic distance moderates the relationship between neural similarity and social network proximity.

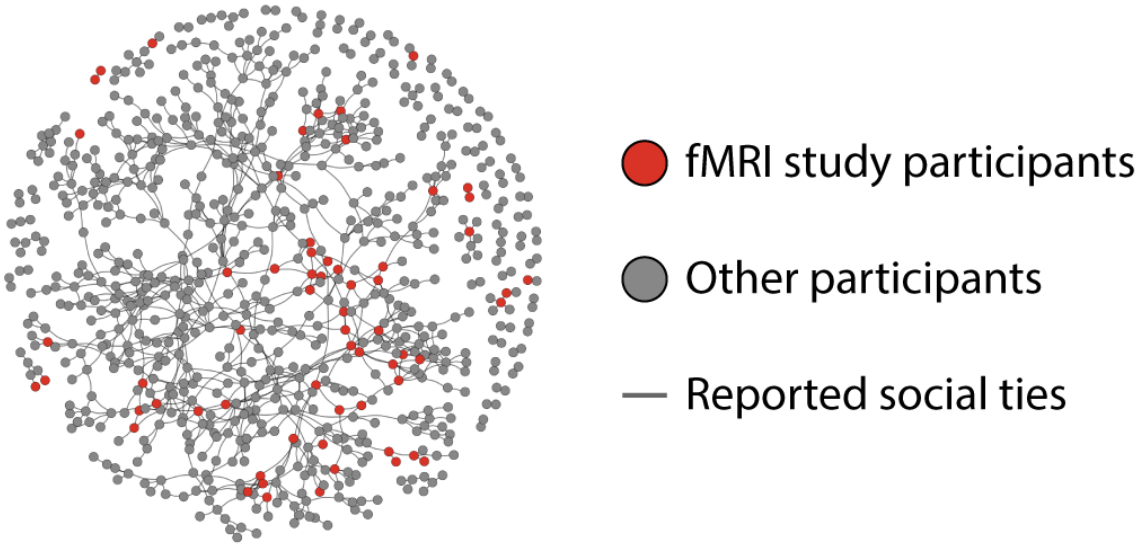

Figure 1. Social network characterization. Residents of a rural village located on a small island completed a survey in which they indicated their social ties with other individuals in their community. The complete social network (N = 798) of the village was reconstructed using this data, and a subset of residents (red nodes; N = 64) participated in the fMRI study. Lines ("edges") indicate the existence of a reciprocated or unreciprocated social tie between individuals. For visualization purposes, unweighted edges were used to depict social ties. However, in our analyses, edges were weighted by individuals' ratings of emotional closeness with one another (see Methods).

Results

The complete social network of individuals living in a rural village community (J. J.-M. Lee et al., 2014; Youm et al., 2014) located on a South Korean island consisting primarily of older adults was characterized (Fig. 1). The relative homogeneity of this sample with respect to demographic characteristics, such as age and race (see Methods), facilitates testing hypotheses regarding relationships between neural similarity and social network proximity, above and beyond inter-individual similarity in demographic variables (which were further accounted for in all statistical analyses). A subset of individuals who participated in the social network survey also participated in the fMRI study, in which they underwent resting-state fMRI. Within each connected component of the social network, the social network proximity between every unique

pair of fMRI participants was calculated; data from pairs of participants within all connected components was combined for statistical analyses (Fig. 1; see Methods for further details). We then characterized each fMRI subject's whole-brain resting-state functional connectome (Fig 2a; Methods). Inter-subject similarities in functional connectomes were then calculated, and the resulting dyadic connectome similarity vectors were subsequently used to predict individuals' social network proximity (Fig 2b; Methods). We also tested for relationships between social network proximity and similarity in connectivity within and between functional brain networks (see Methods).

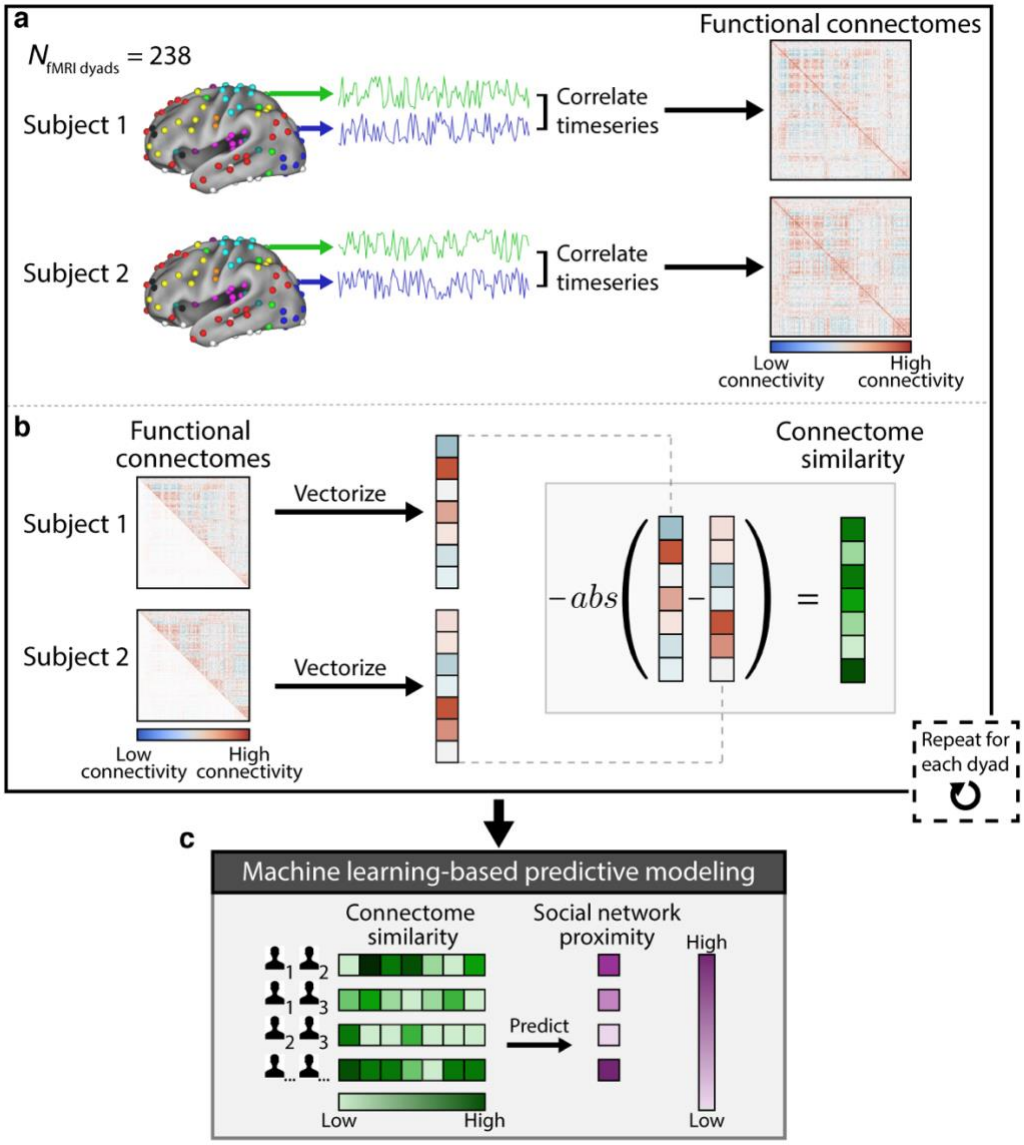

Figure 2. Functional connectome-based predictive modeling of social network proximity. (a) Subjects' data were resampled to standard space, and the Power et al. (Power et al., 2011) atlas was used to define regions of interest (ROIs). Each ROI is associated with one of thirteen functionally defined brain networks, signified by different colors. For each fMRI subject, we then calculated pairwise Pearson correlations between neural time series extracted from a 15-mm-radius sphere centered on each ROI to form a functional connectivity matrix (i.e., a functional connectome). **(b)** The off-diagonal elements in the upper triangular half of each subject's functional connectome were then flattened into a vector. For each unique pair of fMRI subjects, inter-subject similarity in their connectome vectors was measured by calculating pairwise Euclidean distances between corresponding functional connectivity values in subjects' respective connectome vectors. **(c)** We used a partial least squares regression-based algorithm to predict individuals' social network proximity based on the similarity in their functional connectomes (see Methods for further details).

Inter-subject similarity in neural activity predicts social network proximity in the absence of a stimulus

We first implemented a data-driven, machine learning approach to predict social network proximity based on inter-subject similarities in multivariate patterns of resting-state functional connectivity distributed across the entire brain using a partial least squares regression (PLSR)-based algorithm (see Methods for further details). Using a 10-fold cross-validation scheme, the algorithm significantly predicted individuals' social network proximity based on the similarity in their functional connectomes, such that the actual proximity between individuals in the social network was significantly correlated with what was predicted by the model ($r = 0.502$, $p = 1.322 \times 10^{-15}$), while controlling for their similarities in demographic variables, such as age and gender (Fig 3a). Given the dependency structure of the data (i.e., the same individual participates in multiple dyads), we conducted permutation testing to more conservatively estimate the significance of the correlation between real and predicted social network proximity values across dyads (see Methods for further details). As shown in Fig. 3b, the true *r*-value was significantly greater than the majority of the 5,000 permuted *r*-values ($p = 0.036$).

Through the algorithm's dimension reduction procedure (see Methods), 293 unique neural similarity predictors were consistently selected across all 10 cross-validation data folds to be used in predicting social network proximity (see Methods for further details). As shown in Fig. 3c, these predictors measured inter-subject similarity in functional connectivity within and between several networks, and predictors associated with the default-mode network (DMN) were most frequently selected by the algorithm. The consistently-selected predictors, as well as the locations of the most frequently-implicated nodes (e.g., in left ventrolateral prefrontal cortex, the left inferior parietal lobule, and left medial prefrontal cortex), are also visualized on "glass brain" models in Appendix – Fig. 1. However, given the large number of consistently-selected predictors, chord diagrams are provided to convey information about the implicated brain

networks (Fig. 3). Similar results were observed when repeating this analytic procedure excluding dyads that live in the same residences ($p_{permutation}$ = .039; Appendix – Fig. 2), such that similarity in functional connectomes significantly predicted social network proximity, and predictors associated with the DMN were most frequently selected by the algorithm. Similar results were also observed when weighting edges by the frequency with which individuals communicate with each other ($p_{permutation}$ = .013; Appendix – Fig. 3) or the frequency with which they meet with each other ($p_{permutation}$ = .002; Appendix – Fig. 4), rather than weighting edges by emotional closeness ratings. Functional connectome similarity was not, however, predictive of social network proximity when computing social distance in the social network without incorporating edge weights that encode relative interpersonal closeness for directly connected dyads (i.e., emotional closeness, communication frequency, meeting frequency), as shown in Appendix – Fig. 5.

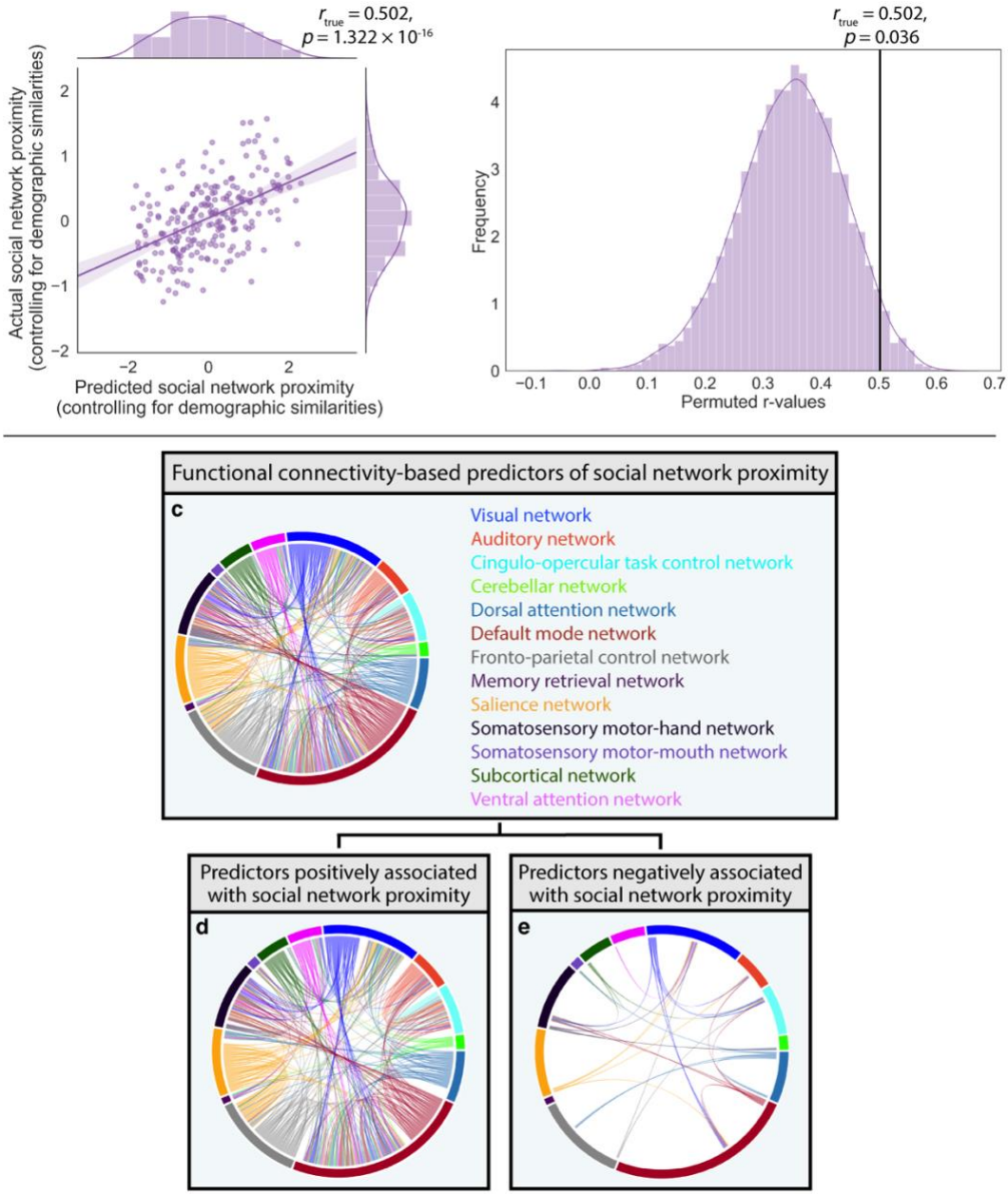

Figure 3. Inter-subject similarity in functional connectomes predicts social network proximity. (a) The PLSR-based algorithm successfully predicted social network proximity from left-out data while controlling for inter-subject similarities in demographic variables. The algorithm's predicted social network proximity was significantly associated with actual social network proximity. **(b)** This relationship was significant after conducting permutation testing to account for the dependency structure of the data (see Methods for further details). **(c)** The algorithm consistently selected a multivariate pattern that included 293 neural similarity predictors across all ten cross-validation data folds for predicting social network proximity. These predictors spanned all thirteen functional brain networks defined in the Power et al. atlas (Power et al., 2011). **(d)** A positive relationship between 261 of these 293 predictors and social network proximity was observed. **(e)** In contrast, only 32 predictors were negatively associated with social network proximity. Note: Colors used for connections between two different brain networks were arbitrarily assigned to one of the two implicated networks.

Individuals who are close together in their social network share similar functional connectomes

In an exploratory analysis, we assessed the direction of the linear relationship between social network proximity and each of the neural similarity predictors selected across all cross-validation data folds to determine if social network proximity was positively associated with similarity in functional connectivity (see Methods for further details). Indeed, 261 of the 293 predictors (89%) were positively associated with social network proximity (Fig. 3d); the remaining 32 predictors were negatively associated with social network proximity (Fig. 3e).

Table 1. Results of linear mixed-effects models testing for associations between functional connectivity within and between brain networks and social network proximity.

Brain network(s)	***ß***	***SE***	***p***	***p* (FDR-corrected)**
DMN-VAN	0.183	0.068	1.803×10^{-4}	0.016
DMN-CN	0.165	0.067	0.001	0.017
SMHN-SMMN	0.165	0.066	4.807×10^{-4}	0.017
DMN-DAN	0.164	0.068	0.001	0.018
COCN	0.160	0.068	0.001	0.018
FPCN-SAN	0.164	0.071	0.001	0.018
AN-SMHN	0.150	0.067	0.002	0.022
DMN-FPCN	0.147	0.067	0.002	0.026
COCN-AN	0.151	0.071	0.003	0.029

Each model included crossed random effects for participants and a fixed effect for neural similarity, with social network proximity as the outcome variable. *P*-values and standard errors were adjusted to account for data redundancy (see Methods). Only significant associations are shown. AN, Auditory network; CN, Cerebellar network; COCN, Cingulo-opercular task control network; DMN, Default mode network; DAN, Dorsal attention

network; FPCN, Fronto-parietal task control network; SAN, Salience network; SMHN, Somatosensory motor-hand network; SMMN, Somatosensory motor-hand network; VAN, Ventral attention network.

Individuals who are close together in their social network share similar functional connectivity within and between brain networks

To complement our data-driven predictive modeling analysis and better inform interpretation of the types of neural similarity associated with social network proximity, we tested if social network proximity was associated with inter-subject similarity in functional connectivity within and between each of the 13 functional brain networks defined in the Power et al. 2011 atlas. For each of the 91 statistical tests (13 tests based on within-network connectivity similarity; 78 tests based on between-network connectivity similarity), we adapted the method outlined by Chen et al. (G. Chen et al., 2017) to fit linear mixed-effects models with crossed random effects to account for the dependency structure of the data (see Methods).

Similarity in functional connectivity was significantly associated with social network proximity when controlling for demographic similarities in nine of these models (Table 1). In all nine models, we observed a positive relationship between functional connectivity and social network proximity, indicating that in cases where the relationship between social network proximity and neural similarity was significant, greater neural similarity was associated with greater proximity in the social network. These effects remained statistically significant after correcting for multiple comparisons across 91 statistical tests using false discovery rate (FDR) thresholding, as shown in Table 1. Consistent with the results of the predictive modeling analyses, the connectivity of areas in the DMN was particularly frequently linked to social network proximity; three of the nine models in which social network proximity was significantly

linked to neural similarity involved the DMN (see Table 1). Similar results were observed when repeating this analytic procedure excluding cohabitating dyads (Appendix – Table 1) and when weighting social ties by inter-individual communication frequency (Appendix – Table 2) or by meeting frequency (Appendix – Table 3) rather than by interpersonal closeness, as well as when social ties were unweighted (Appendix – Table 4).

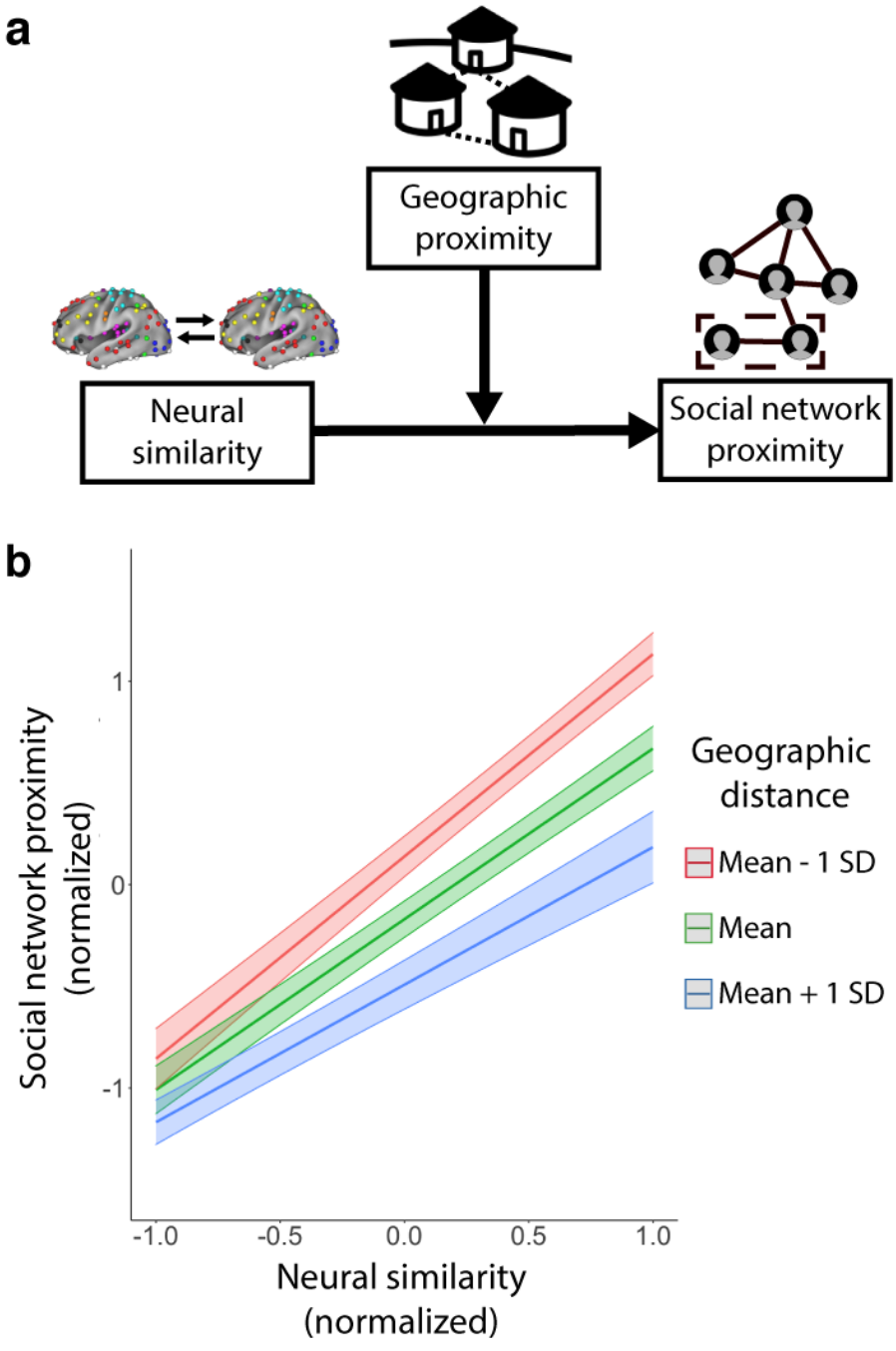

Figure 4. Geographic proximity moderates the relationship between connectome similarity and social network proximity. (a) We tested if geographic distance moderates the relationship between neural similarity and social network proximity. **(b)** A linear mixed-effects model was used to test for an interaction between the effects of connectome similarity and geographic distance on social network proximity (see Methods). We observed a significant interaction between geographic distance and connectome similarity, such that the relationship between neural similarity and social network proximity was especially pronounced among individuals who lived closest to one another in the village (see Results). Shaded areas represent 95% confidence intervals.

Inter-subject similarity in functional connectomes was associated with social network proximity while controlling for personality similarity

In additional exploratory analyses, the same data analytic procedures described above were repeated to test if social network proximity is associated with similarity in functional brain connectivity while controlling not only for demographic similarities, but also for similarities in self-reported personality traits.

In the predictive modeling analysis, the algorithm successfully predicted individuals' proximity to one another in the social network based on the similarity of their functional connectomes while controlling for similarities in the Big Five personality traits and demographic variables ($r = 0.477$, $p = 6.795 \times 10^{-15}$). This significant relationship between actual and predicted social network proximity remained significant after implementing permutation testing to account for the dependency structure of the data ($p = 0.048$). The algorithm's dimension reduction procedure yielded a set of neural similarity predictors that were remarkably similar to those reported in the primary predictive modeling analysis, which controlled only for inter-subject similarities in demographic variables. Similarly, there was an overwhelmingly positive relationship between these predictors and social network proximity (Appendix – Fig. 6).

We also tested if, when controlling for inter-individual similarity in the Big Five personality traits, social network proximity would remain significantly positively related to neural similarity when using linear mixed-effects models to characterize similarity in functional connectivity within and between functional brain networks. As in our main analyses using this

approach, social network proximity was associated with similarity in functional connectivity between several pairs of brain networks after accounting for personality similarity. Again, all significant relationships were positive (i.e., greater social network proximity was associated with greater neural similarity in all cases). As in the main results, when accounting for both demographic and personality similarity, the DMN appeared most frequently in the models in which social network proximity was associated with similarity in functional connectivity within and between brain networks (Appendix – Table 5).

For both sets of analyses (i.e., both for predictive modeling analyses and for analyses measuring relationships between social network proximity and similarity in functional connectivity within and between brain networks using linear mixed-effects models), when controlling for similarity in the Big Five personality traits, convergent results were obtained when defining the social network in different ways. For example, similar results were obtained when excluding dyads comprised of members who live in the same residences both when using predictive modeling ($p_{permutation}$ = .026; Appendix – Fig. 7) and linear mixed-effects models (Appendix – Table 6), and when social ties were weighted by inter-individual communication frequency (see Appendix – Fig. 8 for predictive modeling results, $p_{permutation}$ = .039; Appendix – Table 7 for results using linear mixed-effects models) or by meeting frequency (Appendix – Fig. 9, $p_{permutation}$ = .011, and Appendix – Table 8), rather than by emotional closeness. Using a social network in which edges were unweighted (i.e., in which emotional closeness and frequency of communication or meeting were not considered), neural similarity was not predictive of social network proximity using our predictive modeling approach (as in the main results; Appendix – Fig. 10); however, neural similarity remained positively associated with proximity in the social network using linear mixed-effects models based on similarity in connectivity within and

between functional brain networks (as in the main results; Appendix – Table 9). Taken together, these results suggest that inter-subject similarity in functional connectomes is associated with social network proximity, particularly when taking into account information about the relative interpersonal closeness of directly connected dyads (e.g., emotional closeness, communication frequency, meeting frequency). Furthermore, these relationships are not due to interpersonal similarity in terms of the personality traits measured here (i.e., the Big Five personality traits).

Connectome similarity is most strongly related to social network proximity among individuals who live close to one another

The results of our primary analyses demonstrate that similarity in individuals' functional connectomes is associated with proximity in their real-world social network. Prior work has also established a relationship between geographic proximity and social network proximity (Mossong et al., 2008; Nahemow & Lawton, 1975; Stopczynski et al., 2018). We explored if and how geographic proximity might impact the relationship between neural similarity and social network proximity.

Very similar people who live far from one another may be less likely to become friends (compared to very similar people who live close to one another), as greater physical distance could lead to fewer encounters. Living closeby may provide opportunities for people to befriend those with whom they are especially compatible (including, for example, similar others). In the same vein, social network proximity may also be particularly pronounced among people who live close to one another if associations between neural similarity and social network proximity reflect social influence (i.e., social network proximity causing similarity), rather than, or in addition to, assortativity (i.e., similarity causing social network proximity). For example, there

may be more opportunities for interpersonal influence effects to unfold among people who are close to one another in both social ties and their physical location. Both of the possibilities described above would predict that the relationship between neural similarity and social network proximity would be strongest among people in close geographic proximity to one another. It is also possible that neural similarity would be most strongly related to social network proximity among people who live relatively far from one another–for example, people may only maintain friendships with those who live far from themselves if they are exceptionally compatible with one another.

To begin to arbitrate between these possibilities, we conducted an additional exploratory analysis to test whether geographic distance moderates the relationship between connectome similarity and social network proximity. To calculate a single variable measuring inter-subject similarity in functional connectomes that approximated the neural similarity data used in the predictive modeling analysis, we used the aforementioned PLSR-based algorithm and extracted the primary PLS component (see Methods). A linear mixed-effects model with crossed random effects for both participants was used to test for an interaction between the effects of connectome similarity and geographic distance on social network proximity; the main effects of geographic distance and neural similarity were also included in the model (see Methods). We note that the results of the analyses reported in the preceding sections should be used to assess relationships between neural similarity and social network proximity; the purpose of this analysis was specifically to test if and how geographic distance moderates the relationships between connectome similarity and social network proximity reported above.

We observed a significant interaction between geographic distance and neural similarity ($ß$ = -0.163, SE = 0.044, $p < 0.0001$); significant main effects of neural similarity ($ß$ = 0.840, SE

= 0.071, $p < 0.0001$) and geographic distance ($ß = -0.322$, $SE = 0.066$, $p < 0.0001$) were also observed. The main effect of geographic distance suggests that people who lived closer to one another in the village tended to be closer to one another in the social network. To better understand the interaction between neural similarity and geographic distance, we conducted a simple slopes analysis. This revealed significant associations between neural similarity and social network proximity among people who lived close to one another in the village (i.e., for whom the walking distance between dyad members' residences was approximately one standard deviation below the mean; see Methods), $ß = 0.994$, 95% CI [0.835, 1.154], $SE = 0.081$, $t = 17.280$, $p < 0.0001$, as well as among people who lived an average distance from one another in the village, $ß = 0.839$, 95% CI [0.702, 0.976], $SE = 0.070$, $t = 16.963$, $p < 0.0001$, and among people who lived far from one another in the village (i.e., walking distance one standard deviation above the mean), $ß = 0.677$, 95% CI [0.513, 0.839], $SE = 0.083$, $t = 11.480$, $p < 0.0001$. Thus, the relationship between neural similarity and social network proximity appeared to be most pronounced among those who lived closest to one another in the village (Fig. 4).

We also observed a significant interaction between the effects of neural similarity and geographic distance on social network proximity in four of the nine models in which similarity in functional connectivity within and between brain networks was associated with social network proximity. This is consistent with the notion that the relationship between connectome similarity and social network proximity is contingent on geographic proximity (Appendix – Fig. 11). As in the moderation analysis using the primary PLS component described above, in three of these four models, the most positive relationship between neural similarity and social network proximity was observed among participants who lived closest to one another – specifically, this was the case in models characterizing similarity in connectivity (1) between the DMN and the

dorsal attention network, (2) between the DMN and the fronto-parietal task control network, and (3) within the cingulo-opercular task control network. That said, there was some heterogeneity in the nature of this interaction across models. For example, in the remaining model that evinced a significant interaction, the strongest relationship between neural similarity and social network proximity was observed among people whose homes were relatively far apart (Appendix – Fig. 11). As such, we hesitate to draw strong conclusions from these exploratory moderation analyses. In order to move towards a more systematic understanding of these phenomena, we suggest that future work continue to investigate how interpersonal similarity and geographic proximity interact to predict social network proximity.

Discussion

The current results demonstrate that similarity in individuals' patterns of neural connectivity at rest is related to closeness in their real-world social network, above and beyond effects of demographic variables or the Big Five personality traits. These findings are in line with past research showing that friends exhibit similar neural responses when perceiving naturalistic stimuli (e.g., movies), which have been attributed to similarities in how people close together in social ties interpret and respond to their environment (Hyon, Kleinbaum, et al., 2020; Parkinson et al., 2018). The current findings demonstrate that friendship and social network proximity are related not only to individuals' neural responses to exogenous stimuli, but also to their intrinsically organized neural activity at rest. Prior work has demonstrated that an individual's whole-brain resting-state functional connectome can function as a "fingerprint," in that it is both uniquely identifying and stable across disparate points in time (Finn et al., 2015; Horien et al., 2019). Here, we show that inter-subject similarity in a distributed pattern of functional

connectivity is associated with social network proximity. Similarity in individuals' connectomes was overwhelmingly positively associated with their social closeness in the real world, suggesting that friends share similar resting-state activity. Moreover, we find that the relationship between connectome similarity and social network proximity is moderated by physical proximity, such that the link between neural similarity and social network proximity tends to be most pronounced among people who live close to one another. Integrating the current findings into the extant literature on resting-state functional connectivity can shed light on the types of individual difference variables that may be exceptionally similar among friends and inform hypotheses to test in future research, as described in more detail below.

We found that similarity in functional connectivity at rest was associated with social network proximity while controlling for demographic similarities. We also observed remarkably similar results while controlling for inter-subject similarity not only in demographic variables, but also in the Big Five personality traits. Despite recent evidence demonstrating that similarity in functional connectomes is associated with similarity in the Big Five personality traits (W. Liu et al., 2019), personality data does not account for the current results, in which similarity in functional connectomes was associated with friendship above and beyond the effects of similarity in the Big Five personality traits. Rather, the aspects of functional connectome similarity that predicted friendship in the current study may be related to similarities in latent cognitive, emotional and/or behavioral traits that are exceptionally similar among friends but that are not sufficiently captured by the self-report personality measure used here. When considered in tandem with the current results, the large body of research linking cognitive, emotional, and behavioral variables to functional brain connectivity (Vaidya & Gordon, 2013) provides preliminary clues regarding what kinds of interpersonal similarities might underlie the observed

relationship between neural similarity and social network proximity. For example, patterns of resting-state connectivity associated with the fronto-parietal task control and somatomotor networks have recently been shown to be predictive of individual differences in trait empathic concern (Christov-Moore et al., 2020). Similarly, functional connectivity of the DMN is predictive of a component of empathy reflecting the extent to which an individual feels another's pain (Otti et al., 2010). Variables that are not traditionally considered social may also underlie relationships between neural similarity and social network proximity. For example, past work demonstrates that people close together in a social network have particularly similar neural responses in regions associated with attentional allocation, such as the superior parietal lobule, while viewing movies (Hyon, Kleinbaum, et al., 2020; Parkinson et al., 2018). Inter-individual similarity in attentional allocation, and in other processes that are not inherently social, could facilitate the development of a sense of "generalized shared reality" (i.e., the sense of sharing similar thoughts, feelings or beliefs with someone else, including about the world outside of one's social relationships or interactions), which has recently been shown to predict social connection between individuals (Rossignac-Milon et al., 2020). Thus, past work linking resting-state connectivity within and between the brain networks implicated in the current study to individual difference variables that are not typically considered "social" may also be relevant. For example, functional connectivity of the DMN has been linked to individual differences in creativity (Beaty et al., 2018), memory (Meskaldji et al., 2016), fluid intelligence (Cole et al., 2012), and attentional skills (Pagnoni, 2012). In the current study's predictive modeling analysis, of the functional connectivity-based predictors that best predicted social network proximity, 45% were associated with the DMN; moreover, in the analyses linking connectivity within and between specific brain networks to social network proximity, the DMN was the most frequently

implicated network. Thus, the current results point to testable hypotheses about the kinds of interpersonal similarities that may be particularly pronounced among people close to one another in social ties. These interpersonal similarities may include similarities in social characteristics (e.g., different facets of empathy) and in qualities that are typically not considered social but that might have implications for social connection to the extent that they are similar or dissimilar across individuals.

While the current study was primarily concerned with testing if individuals' social network proximity was linked to the similarity of their functional connectomes, we also conducted an exploratory analysis testing if geographic distance moderates this relationship, given the well-established link between individuals' physical closeness and social closeness in the real-world (Apicella et al., 2012; Lambiotte et al., 2008; Liben-Nowell et al., 2005; Onnela et al., 2011). Associations between similarity in functional connectivity and social network proximity appeared to be strongest among people who lived close to each other in the village (Fig. 4). This could plausibly be caused by the constraints that geographic distance can impose on both assortativity and social influence processes. For example, assortativity may unfold more readily among people who live close to one another than among people who live far apart, given that similar people who live far from one another may be less likely to meet and befriend one another than similar people who live close to each other. On the other hand, social influence processes may unfold most readily among people who are close to one another in both social ties and physical space.

More generally, the current results alone are unable to inform claims about the causal relationship between functional connectome similarity and social network proximity. As noted above, the moderating role of geographic distance could plausibly stem from assortativity or

social influence processes. Future longitudinal studies should test if pre-existing similarities in resting-state activity causally predict social network proximity or if social network proximity facilitates the convergence of individuals' functional connectomes over time. For example, pre-existing similarities in functional connectomes that reflect latent trait similarities may foster friendship formation due to interpersonal similarities facilitating communication and affiliative tie formation (Berger & Calabrese, 1975; Clore & Byrne, 1974). This would be consistent with suggestions that misattunement between individuals disrupts the smoothness of social interactions (Redcay & Schilbach, 2019) and may account for some instances of social disconnection, including, but not limited to, the social disconnection that characterizes some forms of psychopathology–i.e., with the "social interaction mismatch hypothesis" (Bolis et al., 2017; Redcay & Schilbach, 2019). Future work could test this possibility by combining the forms of data collected in the current study with unobtrusive behavioral measures of interpersonal coordination and orienting during social interactions (Lahnakoski et al., 2020).

Alternatively, the current findings could stem from well-established social influence processes that unfold within dyads (Cialdini & Goldstein, 2004; de Waal, 2007) and percolate outward in social networks, causing people to influence and be influenced by others to whom they are connected only indirectly (Apicella et al., 2012). Future work could use unobtrusive methods to track interaction patterns between individuals (Cattuto et al., 2010) and how people approach and attend to one another during interactions (Lahnakoski et al., 2020) to enrich understanding of how social influence effects unfold over time in the real-world. The repeated, intensive, and sustained interactions that characterize friendships may lead friends to develop similarities in how they tend to think, feel, and behave, which become entrenched over time and reflected in patterns of brain connectivity. In other words, in the same way that sustained and

intensive practice on complex cognitive tasks involves particular patterns of engagement of specific brain networks that impact future characteristics of functional connectivity at rest (Mackey et al., 2013), sustained and intensive interactions between friends could lead to convergence in styles of thinking, feeling, and behaving that are reflected in similarity in functional brain connectivity at rest. Living near one's friends may make it easier to have intensive and frequent interactions with them, which in turn, could foster greater interpersonal similarity over time. This would be consistent with the findings that connectome similarity was most strongly associated with social network proximity among people who lived close to one another (Fig. 4) and that connectome similarity was particularly predictive of social network proximity when weighting edges in the social network by in-person meeting frequency (Appendix – Fig. 4). It is also possible that assortativity and social influence processes interact; for example, social network proximity may increase interpersonal similarity through social influence, and the resultant interpersonal similarities may further promote friendship formation (e.g., because interpersonal similarity increases the predictability of social interactions, leading to more fluid and enjoyable interactions, and thus increasing the likelihood of friendship formation (Berger & Calabrese, 1975)). Future work using longitudinal designs will be important to elucidate the relative contributions of these mechanisms to the correspondence between similarity in patterns of neural responding at rest and social network proximity.

The unique characteristics of our sample should be taken into consideration when interpreting the current results. Given that our sample consists of older adults living in a remote, rural village on an island in South Korea, future work should test whether functional connectomes are predictive of social network proximity in additional samples. Similarly, future work should investigate whether the neural variables important for predicting social network

proximity in the current study are also important for predicting social network structure in other communities. The kinds of interpersonal similarities that engender or result from social network proximity likely vary across contexts, and thus, investigations involving different communities (e.g., communities in different cultural settings, different age groups) may yield different results (McNabb et al., 2020). In a similar vein, the magnitude of the relationship between geographic distance and social network proximity, as well as the interaction between geographic distance and interpersonal similarity in predicting social network proximity, likely differs across contexts (e.g., depending on an area's population density and the extent to which geographic and functional distance are associated in a given community). Furthermore, given prior work demonstrating that similarity in neural responses to naturalistic stimuli is also predictive of social network proximity (Hyon, Kleinbaum, et al., 2020; Parkinson et al., 2018) and that tasks can emphasize individual differences in functional connectivity (Finn et al., 2017), future work should test if and how interpersonal similarity in functional connectivity during tasks, including naturalistic stimulation, is associated with social network proximity. Relatedly, future work could examine how social network proximity relates to similarity in neural responding in social contexts, given recent evidence that social network variables relate to differential patterns of neural responding in social contexts, such as when making recommendations to others (O'Donnell et al., 2017) or experiencing social exclusion (Schmälzle et al., 2017). Similarly, in light of past work demonstrating that neural synchrony is associated with successful communication (Stephens et al., 2010), future work could benefit from considering how functional connectivity during social interactions relates to the quality of those interactions, and more generally, from adopting a "second-person neuroscience" approach to examine neural processes during real-time social interactions (Schilbach, 2016). Additionally, given that some

forms of interpersonal misattunement (e.g., diverging prediction and interaction styles) may disrupt social interactions and the formation of social connections in several psychiatric conditions (Bolis et al., 2017; Redcay & Schilbach, 2019; Schilbach, 2016), future work could examine how idiosyncratic patterns of functional connectivity relate to social impairments that characterize many forms of psychopathology (Bolis et al., 2017) and social disconnection more generally (Green et al., 2018).

Taken together, the current results suggest the possibility of homophily based on similarities in neural responding at rest. More specifically, we find that similar patterns of resting-state functional connectivity distributed across the brain are associated with friendship and social network proximity. Past research on homophily has often focused on relatively coarse variables, such as demographic characteristics; prior work testing the relationship between friendship and similarities in personality has tended to yield null or inconsistent patterns of findings. Thus, much remains unknown regarding how friendship and social network proximity relate to inter-individual similarities in psychologically meaningful variables. However, the current study suggests that similarities in functional connectomes may capture similarities in meaningful latent variables that are distinct from demographic characteristics and the Big Five personality traits, and that are associated with individuals' social closeness in their real-world social network. Thus, functional connectomes could serve as neural signatures that identify individuals who are likely to form social ties, and more generally, as powerful tools for studying how individuals' brains influence, and are influenced by, the organizational structure of real-world social networks.

Methods

Part 1: Social network characterization

Subjects

Individuals in Part 1 of the study were subjects from the third wave of the Korean Social Life, Health, and Aging Project (KSHAP (Joo et al., 2017; J. J.-M. Lee et al., 2014)). KSHAP is a study on the health and social networks of older adults in rural communities in South Korea. The current sample of subjects reside in Township K, Ganghwa-gun in Incheon, South Korea, and the size of the township is 26.43 km^2. The total township population was 860 individuals, and 591 individuals (349 females, mean age = 72.79, SD = 7.18) participated in the social network survey, resulting in a response rate of 68.7%. The study was approved by and performed in accordance with the standards of the Institutional Review Board of Yonsei University, and all subjects provided written informed consent for the experiment. See J.-M. Lee et al. 2014 for a comprehensive overview of measures included in Wave 1 of KSHAP data collection. In addition to the measures listed in J.-M. Lee et al. 2014, the third wave of KSHAP data included resting state fMRI data on a subset of participants, as well as additional measures of general cognitive functioning (used for screening fMRI participants as described in the Subjects section of "Part 2: Neuroimaging methods") and a measure of personality (the Big Five 44-item Inventory (Kim et al., 2016)).

Social network characterization

The social network survey was administered in the subjects' homes and in community centers. Subjects responded to a survey asking them to enumerate their social network members ("alters"), including a spouse (if any) and up to five people with whom they most often discussed

important concerns in the past 12 months. This first prompt read, "*People often discuss important things with others. For example, this could be something good or bad that happened to you, or it could be your usual worry. When you look back over the past year, how many people do you talk to often about important things, and who are those people?*" In a second prompt, subjects were also asked to enumerate a "very important" seventh individual. This second prompt read, "*Is there any person who seems very important to you, other than your spouse or the discussion partners whom you mentioned? This person would be someone with whom you have not been in frequent discussions over the past year, but with whom you are still feeling friendly.*" These "very important" alters were not included in subsequent data analysis given that the nature of these alters are qualitatively different from those enumerated in response to the first prompt. Subjects provided information about each alter's name, gender, and residence. Subjects were also asked to rate the extent to which they were emotionally close with each of their alters (1: Not very close; 2: Somewhat close; 3: Very close; 4: Extremely close). Alters who were not married to the subjects and living outside of Township K were excluded. Alters who were enumerated by more than one subject were identified based on the following criteria: (1) at least two out of three Korean characters in their names matched, (2) their gender matched, (3) their age difference was less than five years, and (4) their addresses belonged to the same village.

Social network analysis was performed using the Python package igraph (Csárdi & Nepusz, 2014). We constructed a weighted, undirected graph, in which at least one social tie between two nodes (i.e., nomination) was sufficient to constitute an undirected edge. For example, an undirected edge would connect two nodes, $person_i$ and $person_j$, if (1) $person_i$ nominated $person_j$ as an alter, (2) $person_i$ nominated $person_i$ as an alter, or (3) $person_i$ and $person_j$ each nominated the other as an alter. For reciprocated edges (n = 270), each edge was weighted

by the mean of emotional closeness ratings provided by each member of the dyad. For unreciprocated (i.e., not mutually reported) ties (n = 745), if both dyad members had completed the survey, the corresponding single emotional closeness rating was averaged with zero (i.e., divided by two) in order to account for the unreciprocated nature of non-mutual social ties. The resultant penalized emotional closeness value was used to weight the undirected edge. However, in cases where the nominated alter would have been incapable of reciprocating the nomination (i.e., in cases where the alter did not participate in the survey; n = 320 edges), the corresponding single emotional closeness rating was used to weight the undirected edge. The resulting social network graph consisted of a total of 799 nodes and 1,015 edges and was used to estimate social distances between individuals.

Our main analyses involved weighting edges by ratings of emotional closeness. As mentioned in the Results section (see Appendix for further details), we repeated our main analyses using networks in which edges were (1) weighted by communication frequency, (2) weighted by meeting frequency, and (3) unweighted. While communication and meeting frequencies were highly correlated with one another (r = 0.90), correlations between emotional closeness ratings and meeting frequency (r = 0.28) and between emotional closeness ratings and communication frequency (r = 0.32) were comparatively modest.

Social distances were computed between fMRI participants within each connected component of the social network (Fig. 1); data from dyads within all connected components of the social network was concatenated for subsequent statistical analyses. For our main analyses, and for additional analyses using alternative edge weightings, Dijkstra's algorithm (Dijkstra, 1959) was used to calculate the social distance between members of dyads within each connected component. Dijkstra's algorithm finds the path of "least resistance" between each pair of nodes,

where “resistance” is defined as the cost of traversing a path between those nodes; here, cost was defined as the inverse of an edge’s weight. Thus, weighted social distance was defined as the smallest sum of inverted edge weights across intermediary edges between two individuals. Alternatively, social distance can be operationalized as the smallest number of intermediary edges required to connect two individuals in the network (i.e., geodesic distance), where all edges are weighted equally. As noted above, social distances based on edges weighted by emotional closeness, which were highly correlated with unweighted social distances (r = 0.88), were used for our main analyses so that emotional closeness could be taken into account. We then negated the weighted social distance values to convert them into social network proximity values (i.e., higher values reflect greater closeness in the social network) in subsequent analyses.

Part 2: Neuroimaging study

Subjects

Of the 591 individuals that participated in Part 1, 195 individuals underwent further screening for preclinical neurocognitive disorders in one year later. Individuals were excluded if they (1) scored 1.5 SD below the mean on the Mini-Mental State Examination for Dementia Screening (MMSE-DS (Han et al., 2010)), (2) were in the fifth percentile on the Long-term Memory Recall Index or Working Memory Index in the Elderly Memory Scale (Chey, 2007), or (3) had significant cognitive or behavioral changes in the preceding year, as assessed using the Clinical Dementia Rating (CDR (Morris, 1993)). Sixty-eight subjects passed the screening process and participated in the fMRI session, in which they were instructed to rest quietly with their eyes open and not to fall asleep. Three subjects were excluded due to excessive movement,

neurological abnormality, and diffuse signal confounds. One subject did not complete the social network survey and was also excluded.

Of the remaining 64 fMRI subjects, there were 2,016 unique potential fMRI dyads. Of the 2,016 unique fMRI dyads, 737 dyads had undefined distances between them (i.e., nodes were in separate components of the network) and were excluded from analysis. Of the 1,279 remaining dyads, 1,038 dyads were characterized by a geodesic distance greater than four and were excluded from analyses given prior work demonstrating that similarities in neural responses in people four or more "degrees of separation" apart are highly variable and not significantly different from that of social dyads two or three "degrees of separation" from one another (Parkinson et al., 2018). More generally, a large body of research demonstrates that relationships between interpersonal similarities in a variety of cognitive, emotional, and behavioral phenomena (e.g., risk perception, cooperation, smoking, depression, loneliness, happiness) and social network proximity disappear beyond three to four "degrees of separation" (Cacioppo et al., 2009; Christakis & Fowler, 2007, 2008; Fowler & Christakis, 2010; Moussaïd et al., 2015, 2017; J. N. Rosenquist et al., 2011). This widely documented phenomenon may result from social influence effects decaying with social distance (Christakis & Fowler, 2013), the relative instability of long chains of social ties (Christakis & Fowler, 2013), assortativity (i.e., attraction to similar others) only being possible when opportunities to encounter similar others exist (which becomes less likely as individuals become further removed from one another in social ties), or some combination of these factors. While the current work does not attempt to arbitrate between these possibilities, we limited our analyses to dyads four or fewer "degrees of separation" from one another in light of these findings.

We note that recoding very large social distances to a common value (e.g., ~4) would have minimal impact when analyzing networks with smaller diameters and fewer dyads at remote social distances from one another (e.g., when analyzing the social network of a classroom rather than a village, city, or province). However, in networks with larger diameters (here, the diameter of the largest connected component in the network is 18) and where the vast majority of dyads have a social distance greater than four (here, 1,038 out of 1279, or 81% of fMRI dyads), recoding high social distance dyads would result in the vast majority of dyads being assigned the same social distance value (e.g., of four). Moreover, because we hypothesize that this very large set of dyads would be extremely heterogeneous with respect to their level of similarity, as described above, this would introduce noise that would likely obfuscate the effects that we hypothesized *a priori* to exist at more proximal social distances. That said, we note that although we constrained our main analyses to dyads four or fewer "degrees of separation" from one another, given our *a priori* hypotheses, when analyses were repeated without excluding dyads five or more "degrees of separation" from one another, neural similarity was still significantly related to social network proximity across several brain networks. In all cases where connectivity similarity was related to social network proximity, this relationship was positive. This held true when using social distances weighted by emotional closeness, as in our main analyses (Appendix – Table 12) and when basing social distance on unweighted "degrees of separation" (Appendix – Table 13).

Subjects indicated whether their alters were their parent, child, grandchild, sibling or "other" relative (e.g., cousin, aunt, etc.). Of the 241 resulting dyads, three dyads consisted of genetically related subjects and were excluded from analyses (two genetically related dyads consisted of siblings and one consisted of "other" relatives). In sum, these 1,778 dyads were

excluded from analysis, resulting in 238 unique fMRI dyads, which consisted of 57 fMRI subjects. Ultimately, we analyzed data from these 57 fMRI subjects (35 females, mean age = 70.66, SD = 6.28). The fMRI study was approved by and performed in accordance with the relevant guidelines and regulations by the Institutional Review Board of Yonsei University, and all subjects provided written informed consent for the research procedure.

Image acquisition

Subjects were scanned at the Seoul National University Brain Imaging Center using a 3T Siemens Trio scanner. An echo-planar sequence (2,000 ms TR; 30 ms TE; resolution 3.0 mm x 3.0 mm x 3.0 mm; gap = 1 mm; field of view 240 x 240 mm) was used to acquire resting-state fMRI data. For each subject, two 5-minute runs were acquired, totaling 10 minutes of data. A high-resolution T1-weighted magnetic prepared rapid gradient echo (MPRAGE) scan was acquired or each subject (2,300 ms TR; 30 ms TE; field of view 256 x 256 mm; resolution 1 mm x 1 mm x 1 mm) at the end of the scanning session.

fMRI data preprocessing

fMRIPrep version 1.1.8 was used for anatomical and functional data preprocessing (Esteban et al., 2019). Each subject's T1-weighted (T1w) image was corrected for intensity non-uniformity with N4BiasFieldCorrection, distributed with ANTs 2.1.0, and used as T1w-reference throughout the workflow. The T1w-reference was then skull-stripped with a Nipype implementation of the antsBrainExtraction.sh workflow (from ANTs), using OASIS30ANTs as target template. Spatial normalization to the ICBM 152 Nonlinear Asymmetrical template version 2009c (MNI152NLin2009cAsym) was performed through nonlinear registration with

antsRegistration (implemented in ANTs 2.1.0), using brain-extracted versions of both T1w volume and template. Brain tissue segmentation of cerebrospinal fluid (CSF), white-matter (WM), and gray-matter (GM) was performed on the brain-extracted T1w using FSL FAST.

For each of the two BOLD runs per subject, the following preprocessing was performed. First, a reference volume and its skull-stripped version were generated using a custom methodology of fMRIPrep. The BOLD reference was then co-registered to the T1w reference using FSL FLIRT with the boundary-based registration cost-function (BBR). Co-registration was configured with nine degrees of freedom to account for distortions remaining in the BOLD reference. Head-motion parameters with respect to the BOLD reference (transformation matrices, and six corresponding rotation and translation parameters) were estimated before any spatiotemporal filtering using FSL MCFLIRT. Automatic removal of motion artifacts using independent component analysis (ICA-AROMA) was performed on the preprocessed BOLD in MNI space time-series after removal of non-steady state volumes and spatial smoothing with an isotropic, Gaussian kernel of 6mm full-width at half-maximum. The BOLD time-series were then resampled to MNI152NLin2009cAsym standard space, generating a preprocessed BOLD run in MNI152NLin2009cAsym space.

The confounding variables generated by fMRIPrep that were used as nuisance variables in the current study included global signals extracted from within the CSF, WM, and whole-brain masks, framewise displacement, three translational motion parameters, three rotational motion parameters, a basis set of cosine functions up to a cutoff of 128s, and a set of physiological noise regressors that were extracted to perform component-based noise correction (anatomical CompCor, aCompCor). More specifically, aCompCor variables were calculated within the intersection of a subcortical mask (created by heavily eroding the brain mask) and the union of

the CSF and WM masks. These confounds were regressed out of the data for each preprocessed run. Temporal filtering was performed with a band-pass filter between 0.009 and 0.08 Hz.

Functional parcellation and whole-brain connectome construction

To delineate the brain into regions of interest (ROIs), we used the Power et al. 2011 atlas with 264 brain regions, 236 of which are associated with one of 13 functionally defined brain networks - visual, auditory, cingulo-opercular task control, cerebellar, dorsal attention, default mode, fronto-parietal control, memory retrieval, salience, somatosensory motor-hand, somatosensory motor-mouth, subcortical, and ventral attention networks. Here, only the 236 ROIs associated with the abovementioned brain networks were used for analysis.

For each subject, in each of the 236 ROIs, the fMRI signal was spatially averaged within a spherical mask (radius = 5 voxels) and extracted at each timepoint to characterize the neural time series at each brain region. We then calculated the pairwise Pearson correlations between all ROIs' time series in order to construct a symmetric 236 x 236 functional connectivity matrix. This was conducted separately for each of the two resting-state fMRI runs. The two functional connectivity matrices from each run were then Fisher z-transformed and averaged to characterize each subject's whole-brain resting-state functional connectome.

Calculating dyadic similarities in whole-brain connectomes

For each subject, the off-diagonal half of the whole-brain functional connectivity matrix was flattened into a vector containing 27,730 functional connectivity values. For each of the unique pairs of fMRI subjects, we calculated pairwise Euclidean distances (i.e., absolute value of numerical differences) between the corresponding functional connectivity values in subjects'

connectome vectors. We then negated these Euclidean distance values to convert them into similarity values (i.e., higher values reflected higher neural similarity). This resulted in a vector of 27,730 similarity values that characterized whole-brain connectome similarity for each unique pair of fMRI subjects. To account for demographic similarities that may be related to social network proximity and/or similarity in resting-state functional connectivity, prior to all subsequent analyses, we regressed out the effects of inter-subject similarities in age (i.e., negated Euclidean distance between each pair of individuals' ages) and in gender (i.e., 1: same gender; 0: dissimilar gender) from social network proximity. Significant associations between demographic similarity (as well as personality similarity) and similarity in connectivity within and between functional brain networks are reported in Appendix – Table 10; significant associations between demographic similarity (as well as personality similarity) and social network proximity are reported in Appendix – Table 11.

Whole-brain connectome-based predictive modeling of social distance

As described in the main text, we tested if similarities in individuals' distributed patterns of whole-brain resting-state functional connectivity would be predictive of their proximity in their real-world social network, after having controlled for the effects of demographic variables in the previous data analytic step. We used Scikit-learn to implement PLSR (Pedregosa et al., 2011), a multivariate data-driven regression model that implements dimension reduction by maximizing the covariance between predictors and the response variable to yield latent variables, which are subsequently used as predictors. As such, PLSR is well-suited for datasets whose predictors are characterized by high dimensionality and multicollinearity and is thus a powerful

tool to predict response variables using multivariate fMRI data (Krishnan et al., 2011; McIntosh & Mišić, 2013).

Scikit-learn's KFold function was used to divide the data into ten training and test folds (Pedregosa et al., 2011). Using Scikit-learn's Pipeline function, we created an algorithm that performed three steps in sequence on the training data for each fold (models fit to each fold's training data were used to predict social network proximity based on neural similarities in the corresponding testing data): (1) normalize the predictors using Scikit-learn's RobustScaler function, (2) identify the 1,000 predictors that were mostly strongly associated with social network proximity (as measured using F-scores calculated by univariate linear regression between each predictor and social distance), and (3) implement PLSR using these 1,000 predictors. Although PLSR is a robust solution to problems of high dimensionality, performing dimension reduction prior to implementing PLSR improves model performance (Mehmood et al., 2012). We used a nested cross-validation scheme to perform hyperparameter tuning using a grid search procedure (i.e., optimizing the n_components hyperparameter from a grid/range of integers ranging from 1 to 10), such that the training data of each of the 10 outer data folds was further subdivided into 10 inner folds consisting of sub-training and validation datasets. Within each of these inner folds, for each hyperparameter value provided in the hyperparameter grid (i.e., n_components values ranging from one to ten), the algorithm was trained on the sub-training data and tested on the validation data. The hyperparameter value used in the model with the best performance across all validation sets was identified as the optimal hyperparameter for the corresponding outer training fold. Using this optimal hyperparameter, the algorithm was trained on the outer fold's training data and tested on the outer fold's testing data. This process was repeated for each of the ten outer data folds. Because each dyad was included in the testing

data for one of the outer data folds, this procedure yielded a predicted social network proximity value for each dyad in the sample. Out-of-sample performance was evaluated by calculating the Pearson *r*-value between predicted and actual social distance values. To account for the dependency structure of the data, this *r*-value was then tested against a null distribution of *r*-values generated by permutation testing. Neuroimaging data was randomly shuffled across fMRI participants 5,000 times while holding all else in the dataset constant. In each permuted dataset, the entire data analytic procedure described above (including calculation of dyadic similarities in functional connectomes) was repeated to generate a null distribution of 5,000 *r*-values. *P*-values were determined by calculating the frequency with which the true model's *r*-value exceeded the *r*-values in the null distribution.

To test whether inter-subject similarities in functional connectomes would be predictive of social network proximity above and beyond the effects of similarities not only in demographic variables but also in personality traits, we repeated the primary analysis described above while also controlling for inter-individual similarities in personality. Personality was assessed using the Big Five 44-item Inventory (Kim et al., 2016), and dyadic similarities in personality were calculated by computing (and negating) the Euclidean distance between individuals' set of five personality traits (i.e., Extraversion, Agreeableness, Consciousness, Neuroticism, and Openness).

Modeling social network proximity as a function of similarity in functional connectivity at the level of brain networks

To complement our data-driven predictive modeling framework and inform interpretations of these results, we tested the relationships between social network proximity and inter-subject similarity in functional connectivity within brain networks and between each

possible unique pair of brain networks. To calculate similarity in functional connectivity within each of the 13 functional brain networks defined in the Power et al. 2011 atlas, the following procedure was performed for each subject. For each brain network, functional connectivity edges between nodes associated with the brain network were averaged, yielding a single value reflecting the average level of functional connectivity within that brain network. To calculate similarity in functional connectivity between brain networks for each of the 78 possible unique pairs of brain networks, the following procedure was performed for each subject. For each pair of brain networks, functional connectivity values corresponding to edges between nodes associated with each of the two brain networks were averaged, yielding a single value reflecting the average level of functional connectivity between those two brain networks. In total, 91 aggregate functional connectivity values (13 characterizing connectivity within each brain network and 78 characterizing connectivity between each of the unique pairs of brain networks) were calculated for each subject. For each aggregate functional connectivity value, inter-subject similarity was computed using Euclidean distance. These values were then negated to convert them to similarity values.

For each brain network and for each unique pair of brain networks (i.e., 91 models total), the relationship between inter-subject similarity in functional connectivity and social network proximity was assessed using linear mixed-effects models with crossed random effects (i.e., random intercepts) for both participants to account for dependencies in the data introduced by having repeated observations for each participant. We adopted the method suggested by Chen et al. 2017 for analyses of inter-subject similarities of fMRI data, which was implemented using lme4 and lmerTest in R (Bates et al., 2015; Kuznetsova et al., 2017). The inter-subject similarity data was doubled to allow for crossed random effects, as suggested by Chen et al. 2017. For

statistical inference, to avoid inflating degrees of freedom due to the resultant data redundancy, degrees of freedom were then corrected as suggested and validated by Chen et al. 2017–e.g., the degrees of freedom for the standard error were adjusted from ($2N - k - 1$) to ($N - k - 1$), where k is the number of fixed effects in the model and N is the number of observations (dyads). Standard errors were adjusted with a scaling factor of $\sqrt{2N-1}/\sqrt{N-1}$, where N is the number of participants. All reported findings reflect results using the corrected degrees of freedom and standard error estimates. FDR correction was then implemented to correct for multiple comparisons across all 91 statistical tests.

Exploratory moderation analysis

Exploratory analyses tested whether geographic distance moderated the relationship between connectome similarity and social network proximity. For a given pair of subjects, geographic distance was calculated by computing the walking distance in meters between the geographic coordinates encoding the location of residence for each individual. The significance of the main effect of geographic distance on social network proximity, as well as the interaction between geographic distance and neural similarity on social network proximity, was assessed using linear mixed-effects models (using the approach described in the preceding section) that contained fixed effects for neural similarity (described in more detail below), geographic distance, and their interaction, and crossed random effects for both participants in each dyad. We carried out this procedure using two approaches to characterize neural similarity: (1) using the primary PLS component (to approximate the neural similarity data used in the predictive modeling analyses) and (2) using the aggregate neural similarity measures from the nine models

in which similarity in functional connectivity within and between brain networks was associated with social network proximity (see Table 1).

In the first approach, we implemented a PLSR-based algorithm to characterize the connectome similarity variable. We first identified the modal *n_components* value across all 10 data folds in the main analysis. In a separate implementation of the PLSR-based algorithm, we then set the *n_components* value equal to the aforementioned modal value. This algorithm then used connectome similarity across the entire sample to predict social network proximity across the entire sample, and the primary PLS component was extracted to be used as the neural similarity variable in the moderation analysis. A cross-validation scheme was not used here, as it would have produced multiple sets of different PLS components. Therefore, this analysis is not used to assess the significance of the relationship between neural similarity and social network proximity and is used only to assess how this relationship differs as a function of geographic distance for the aspects of neural connectivity that are associated with social network proximity.

This process yielded latent variables that maximized the covariance between all of the functional connectivity-based predictors and social network proximity. We extracted the latent variable that best maximized this covariance, and we then used this single variable as the connectome similarity variable in approach (1) of the moderation analysis. This procedure was used to obtain a single variable that approximated the overall characterization of functional connectome similarity obtained in the predictive modeling analysis (as this variable necessarily varied across data folds in the predictive modeling analysis), so that the impact of geographic distance on the relationship between this aggregate variable and social network proximity could be explored. Given this procedure for deriving this aggregate connectome similarity measure, inferences regarding the relationship between neural similarity and social network proximity,

should be based on the analyses described in the preceding sections (rather than the main effect of neural similarity in this analysis or the extent to which each simple slope differs from 0). This exploratory analysis is specifically focused on examining how, for neural variables that are related to social network proximity, the relationship between functional connectivity similarity and social network proximity varies as a function of geographic distance.

We followed the common convention (Aiken & West, 1991; Cohen et al., 2003) of visualizing slopes at three levels of the moderator (the mean +/- 1 SD). However, given that the smallest geographic proximity values in this dataset were 0.958 SD below the mean, this is the precise value of geographic proximity used for characterizing and visualizing the simple slope for participants who lived particularly close to one another (rounded down to -1 SD below mean in the legend of Fig. 4 for simplicity).

Appendix

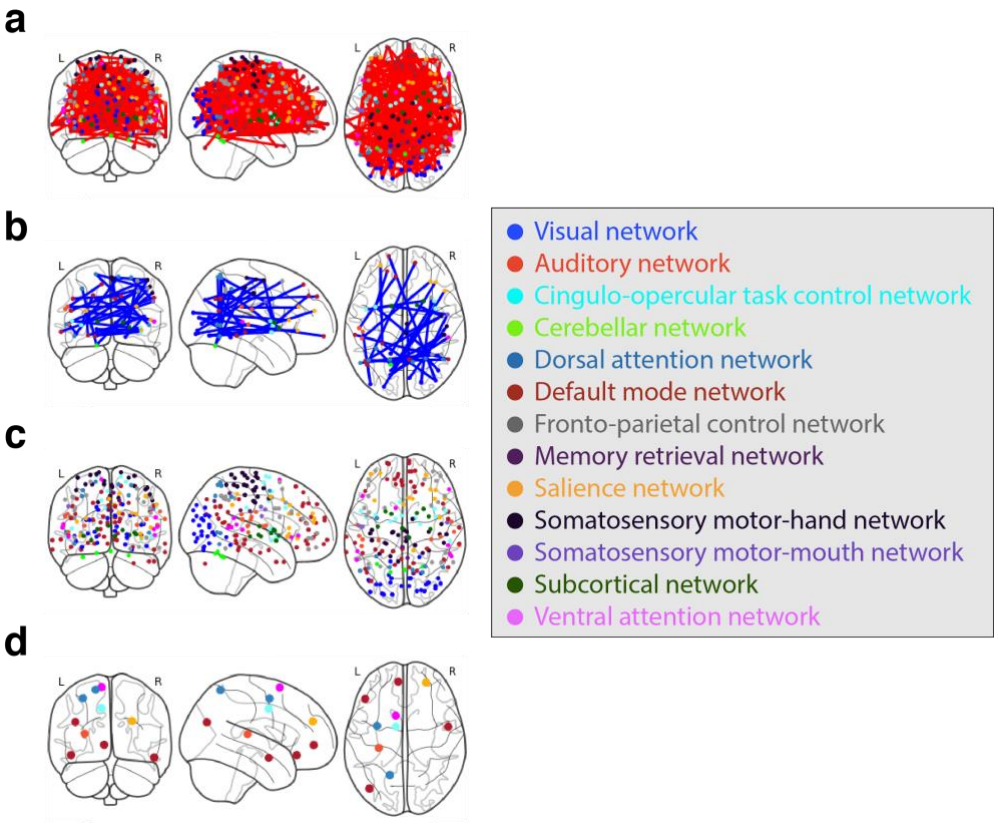

Appendix - Figure 1. Consistently-selected predictors of social network proximity were widely distributed across the brain. In the main predictive modeling analysis, the PLSR-based algorithm predicted social network proximity from left-out data while controlling for inter-subject similarities in demographic variables. There were 293 neural similarity predictors that were consistently selected across all ten data folds for predicting social network proximity, and these predictors spanned all thirteen function brain networks defined in the Power et al. 2011 atlas. **(a)** Of these 293 predictors, 261 predictors were positively associated with social network proximity (this information can be seen more clearly in Fig. 3d). **(b)** In contrast, only 32 predictors were negatively associated with social network proximity (also see Fig. 3e). **(c)** These 293 predictors characterized functional connectivity between 192 different nodes, each of which was associated with one of the aforementioned thirteen brain networks. Given the large number of nodes and edges between them that were selected by the algorithm, chord diagrams, rather than brain images, are provided in the main text (Fig. 3) to convey information about the implicated brain networks. **(d)** The proportion of edges in which each node was involved was calculated, and the nodes that ranked in the top 50% of involvement are visualized here (node color signifies brain network).

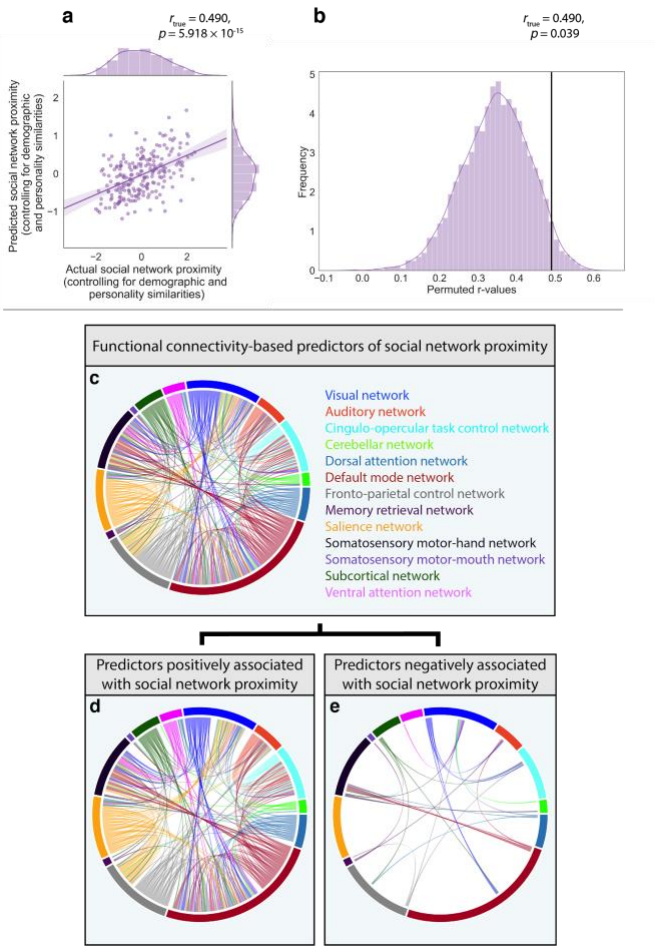

Appendix - Figure 2. Similarity in functional connectomes predicts social network proximity when excluding cohabitating dyads. (a) The primary predictive modeling analysis was repeated when excluding 12 dyads living in the same residences, and we observed a pattern of results similar to those from the primary analysis (Fig. 3). In this subset of 222 dyads, inter-subject similarity in functional connectomes was significantly predictive of social network proximity while controlling for inter-subject similarities in demographic variables. **(b)** This relationship was significant after conducting permutation testing to account for the dependency structure of the data (see Methods for further details). **(c)** The algorithm consistently selected a multivariate pattern of 267 neural similarity predictors across all ten cross-validation data folds for predicting social network proximity. These predictors spanned all thirteen functional brain networks defined in the Power et al. 2011 atlas. **(d)** A positive relationship between 239 of these 267 predictors and social network proximity was observed. **(e)** In contrast, only 28 predictors were negatively associated with social network proximity. Note: Colors used for connections between two different brain networks were arbitrarily assigned to one of the two implicated networks.

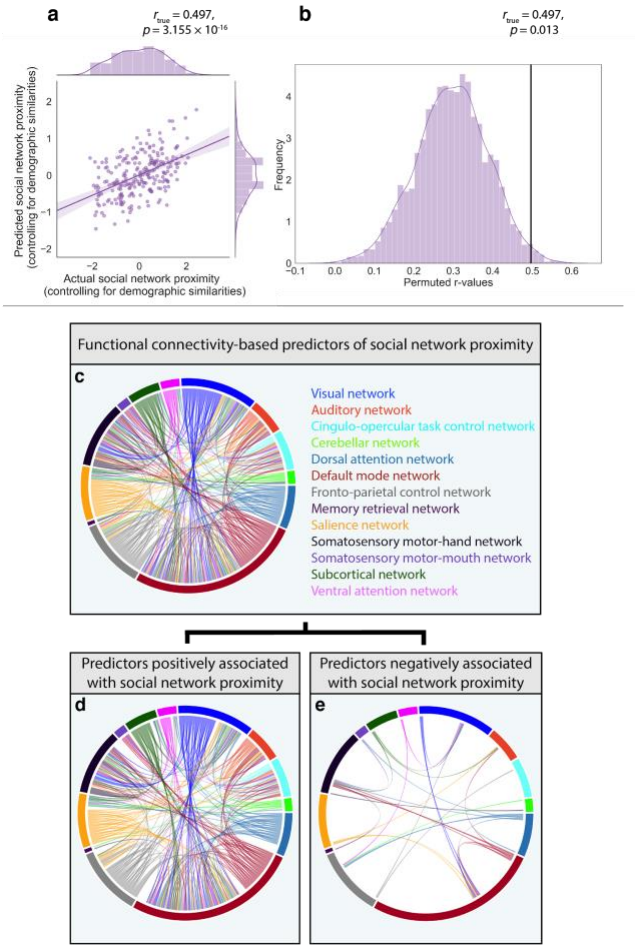

Appendix – Figure 3. Similarity in functional connectomes predicts social network proximity when weighting edges by communication frequency. (a) The primary predictive modeling analysis was repeated when weighting edges by inter-individual communication frequency, and we observed a pattern of results similar to those from the primary analysis (Fig. 3). Inter-subject similarity in functional connectomes was significantly predictive of social network proximity while controlling for inter-subject similarities in demographic variables. **(b)** This relationship was significant after conducting permutation testing to account for the dependency structure of the data (see Methods for further details). **(c)** The algorithm consistently selected a multivariate pattern of 265 neural similarity predictors across all ten cross-validation data folds for predicting social network proximity. These predictors spanned all thirteen functional brain networks defined in the Power et al. 2011 atlas. **(d)** A positive relationship between 235 of these 265 predictors and social network proximity was observed. **(e)** In contrast, only 30 predictors were negatively associated with social network proximity. Note: Colors used for connections between two different brain networks were arbitrarily assigned to one of the two implicated networks.

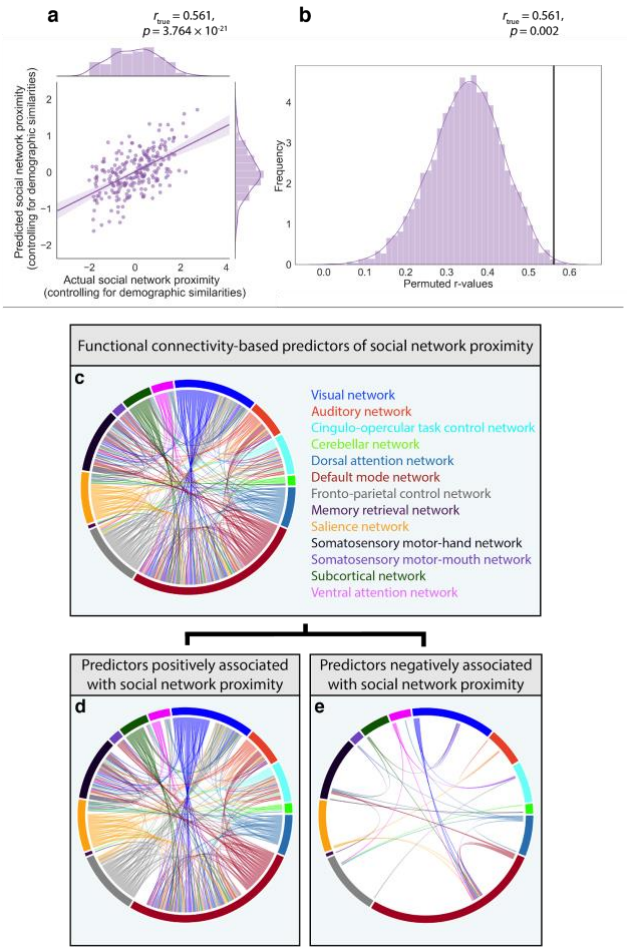

Appendix - 4. Similarity in functional connectomes predicts social network proximity when weighting edges by meeting frequency. (a) The primary predictive modeling analysis was repeated when weighting edges by inter-individual meeting frequency, and we observed a pattern of results similar to those from the primary analysis (Fig. 3). Inter-subject similarity in functional connectomes was significantly predictive of social network proximity when controlling for inter-subject similarities in demographic variables. **(b)** This relationship was significant after conducting permutation testing to account for the dependency structure of the data (see Methods for further details). **(c)** The algorithm consistently selected a multivariate pattern of 256 neural similarity predictors across all ten cross-validation data folds for predicting social network proximity. These predictors spanned all thirteen functional brain networks defined in the Power et al. 2011 atlas. **(d)** A positive relationship between 235 of these 256 predictors and social network proximity was observed. **(e)** In contrast, only 34 predictors were negatively associated with social network proximity. Note: Colors used for connections between two different brain networks were arbitrarily assigned to one of the two implicated networks.

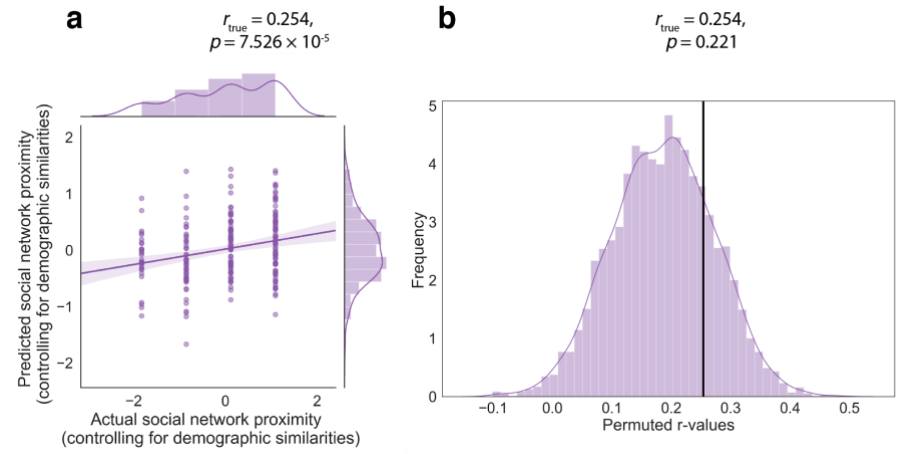

Appendix - 5. Similarity in functional connectomes is not predictive of social network proximity when using unweighted edges. (a) The primary analysis was repeated when using unweighted edges. **(b)** Inter-subject similarity in functional connectomes was not predictive of social network proximity when controlling for inter-subject similarities in demographics, unlike in analyses using edges that encode emotional closeness (Fig. 3), communication frequency (Appendix - Fig. 3), or meeting frequency (Appendix - Fig. 4).

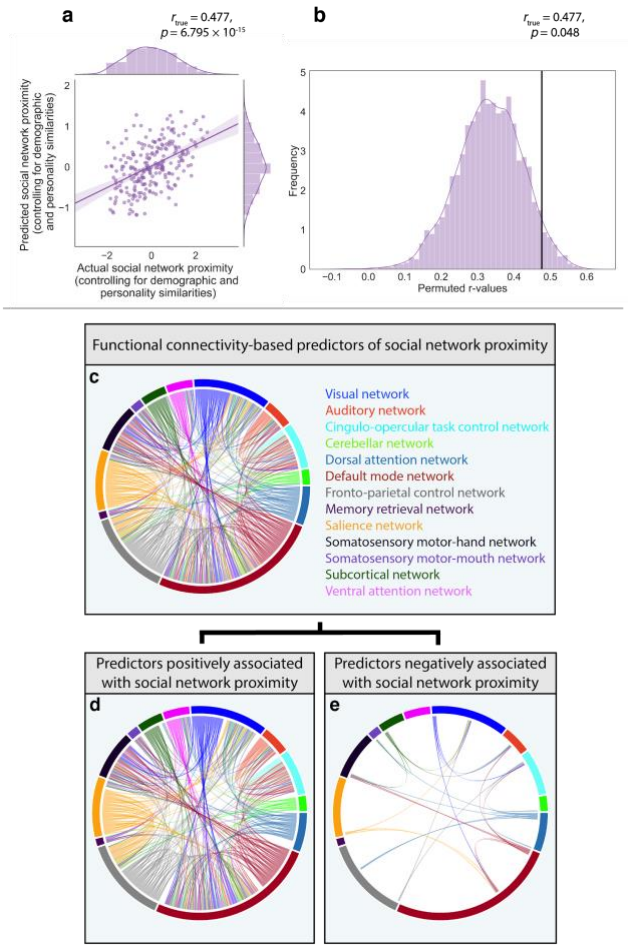

Appendix – Figure 6. Similarity in functional connectomes predicts social network proximity when controlling for similarities in personality. (a) The primary predictive modeling analysis was repeated when controlling for similarities in personality, and we observed a pattern of results similar to those from the primary analysis (Fig. 3). Inter-subject similarity in functional connectomes was significantly predictive of social network proximity when controlling for inter-subject similarities in demographics and the Big Five personality traits. **(b)** This relationship was significant after conducting permutation testing to account for the dependency structure of the data (see Methods for further details). **(c)** The algorithm consistently selected a multivariate pattern of 312 neural similarity predictors across all ten cross-validation data folds for predicting social network proximity. These predictors spanned all thirteen functional brain networks defined in the Power et al. 2011 atlas. **(d)** A positive relationship between 286 of these 312 predictors and social network proximity was observed. **(e)** In contrast, only 26 predictors were negatively associated with social network proximity. Note: Colors used for connections between two different brain networks were arbitrarily assigned to one of the two implicated networks.

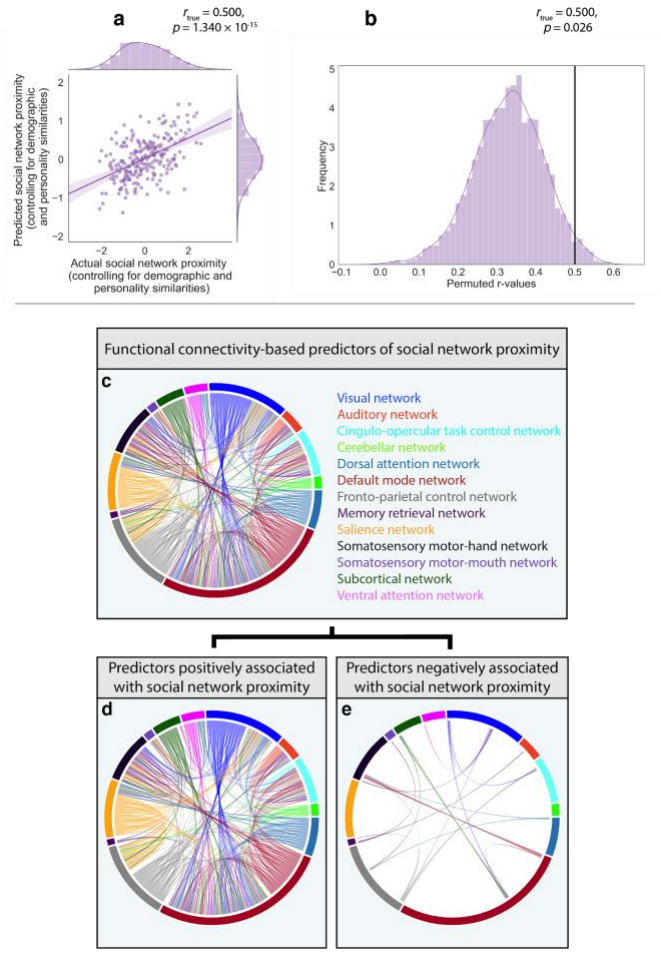

Appendix – Figure 7. Similarity in functional connectomes predicts social network proximity when controlling for similarities in personality and excluding cohabitating dyads. (a) The primary predictive modeling analysis was repeated when controlling for similarities in personality, and we observed a pattern of results similar to those from the primary analysis (Fig. 3). Inter-subject similarity in functional connectomes was significantly predictive of social network proximity when controlling for inter-subject similarities in demographics and the Big Five personality traits. **(b)** This relationship was significant after conducting permutation testing to account for the dependency structure of the data (see Methods for further details). **(c)** The algorithm consistently selected a multivariate pattern of 312 neural similarity predictors across all ten cross-validation data folds for predicting social network proximity. These predictors spanned all thirteen functional brain networks defined in the Power et al. 2011 atlas. **(d)** A positive relationship between 286 of these 312 predictors and social network proximity was observed. **(e)** In contrast, only 26 predictors were negatively associated with social network proximity. Note: Colors used for connections between two different brain networks were arbitrarily assigned to one of the two implicated networks.

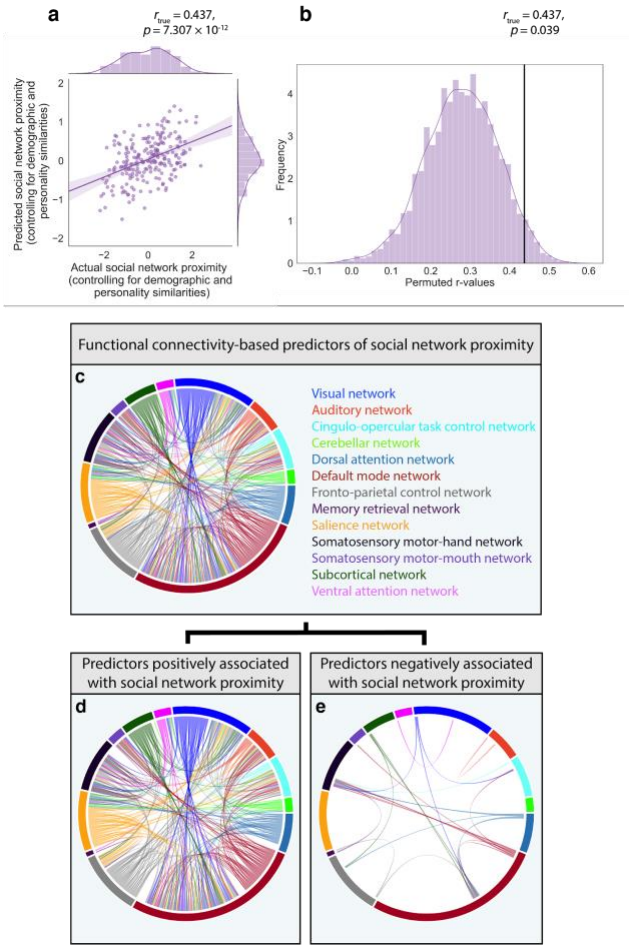

Appendix – Figure 8. Similarity in functional connectomes predicts social network proximity when weighting edges by communication frequency while also controlling for similarities personality and excluding cohabitating dyads. (a) We observed a pattern of results similar to those from the primary predictive modeling analysis (Fig. 3) when weighting edges by communication frequency while also controlling for similarities in personality and excluding cohabitating dyads, such that inter-subject similarity in functional connectomes was significantly predictive of social network proximity. **(b)** This relationship was significant after conducting permutation testing to account for the dependency structure of the data (see Methods for further details). **(c)** The algorithm consistently selected a multivariate pattern of 293 neural similarity predictors across all ten cross-validation data folds for predicting social network proximity. These predictors spanned all thirteen functional brain networks defined in the Power et al. 2011 atlas. **(d)** A positive relationship between 268 of these 293 predictors and social network proximity was observed. **(e)** In contrast, only 25 predictors were negatively associated with social network proximity. Note: Colors used for connections between two different brain networks were arbitrarily assigned to one of the two implicated networks.

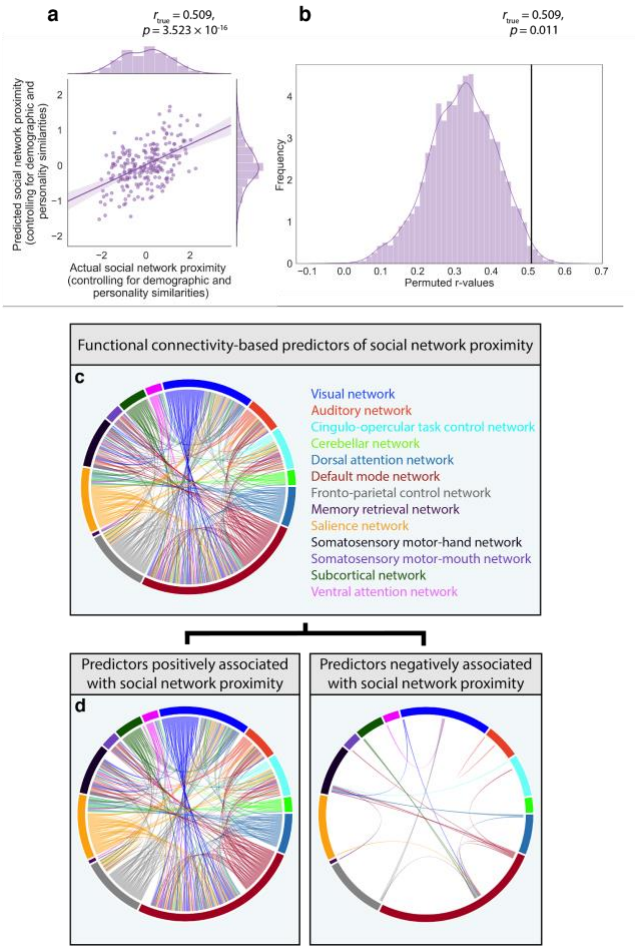

Appendix – Figure 9. Similarity in functional connectomes predicts social network proximity when weighting edges by meeting frequency while also controlling for similarities in personality and excluding cohabitating dyads. (a) We observed a pattern of results similar to those from the primary predictive modeling analysis (Fig. 3) when weighting edges by meeting frequency while also controlling for inter-subject similarities in the Big Five personality traits and excluding cohabitating dyads, such that inter-subject similarity in functional connectomes was significantly predictive of social network proximity. **(b)** This relationship was significant after conducting permutation testing to account for the dependency structure of the data (see Methods for further details). **(c)** The algorithm consistently selected a multivariate pattern of 295 neural similarity predictors across all ten cross-validation data folds for predicting social network proximity. These predictors spanned all thirteen functional brain networks defined in the Power et al. 2011 atlas. **(d)** A positive relationship between 273 of these 295 predictors and social network proximity was observed. **(e)** In contrast, only 22 predictors were negatively associated with social network proximity. Note: Colors used for connections between two different brain networks were arbitrarily assigned to one of the two implicated networks.

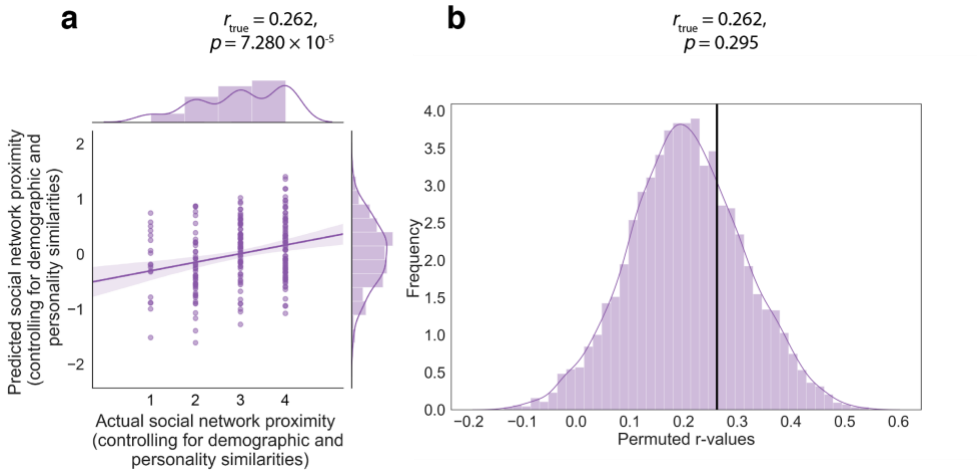

Appendix - Figure 10. Similarity in functional connectomes is not predictive of social network proximity when using unweighted edges while also controlling for similarities in personality and excluding cohabitating dyads. (a) The primary predictive modeling analysis was repeated when using unweighted edges while also controlling for similarities in the Big Five personality traits and excluding cohabitating dyads. **(b)** Inter-subject similarity in functional connectomes was not predictive of social network proximity, unlike in analyses that also control for interpersonal similarities in personality but use edges that encode emotional closeness (Appendix – Fig. 6-7), communication frequency (Appendix – Fig. 8), or meeting frequency (Appendix – Fig. 9).

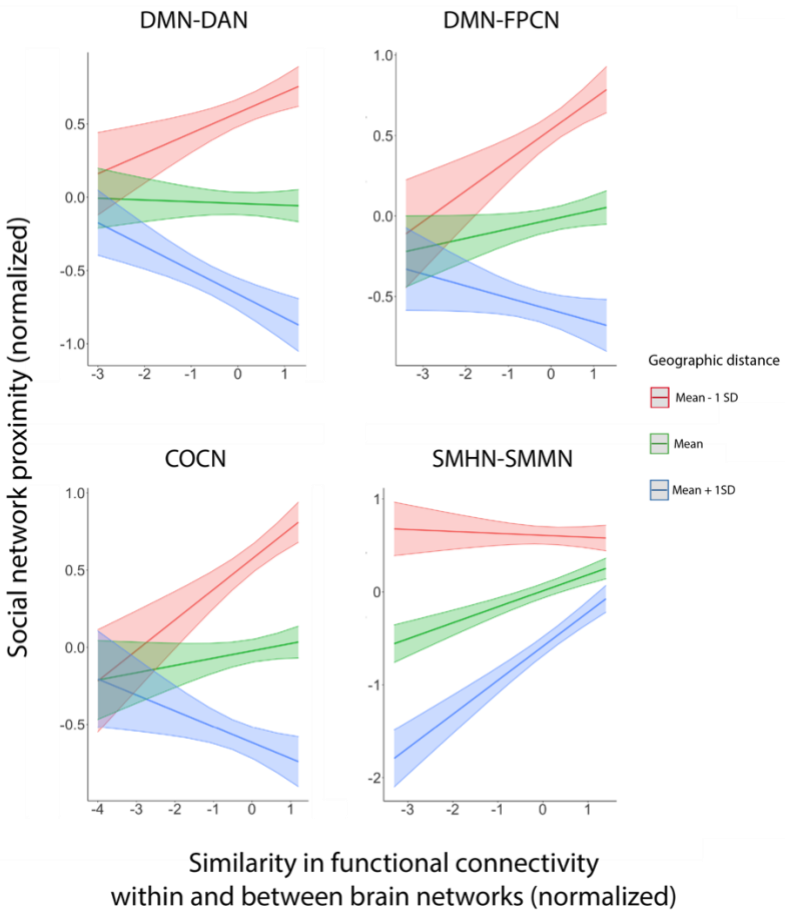

Appendix – Figure 11. Geographic proximity moderates the relationship between social network proximity and similarity in functional connectivity within and between brain networks. Linear mixed-effects models were used to test for an interaction between the effects of similarity in functional connectivity within and between specific brain networks and geographic proximity on social network proximity (see Methods). This was performed for each of the nine models in which similarity in functional connectivity within and between brain networks was associated with social network proximity (Table 1). In four of these nine models, significant interaction effects were observed, such that similarity in functional connectivity within the cingulo-opercular task control network (β = -0.150, SE = 0.052, p = 7.231 x 10^{-5}), between the default mode and dorsal attention networks (β = -0.150, SE = 0.055, p = 1.363 x 10^{-4}), and between the default mode and fronto-parietal task control networks (β = -0.133, SE = 0.061, p = 2.440 x 10^{-3}) was particularly pronounced among participants who lived closest to one another. A fourth significant interaction was also observed such that similarity in functional connectivity between the somatosensory motor-hand and somatosensory-hand networks (β = 0.193, SE = 0.059, p = 5.891 x 10^{-6}) was particularly pronounced among participants who lived relatively far apart. COCN, Cingulo-opercular task control network; DMN, Default mode network; DAN, Dorsal attention network; FPCN, Fronto-parietal task control network; SMHN, Somatosensory motor-hand network; SMMN, Somatosensory motor-hand network. Shaded areas represent 95% confidence intervals.

Appendix – Table 1. Results of linear mixed-effects models testing for associations between functional connectivity within and between brain networks and social network proximity when excluding cohabitating dyads.

Brain network(s)	***ß***	***SE***	***p***	***p* (FDR-corrected)**
DMN-CN	0.160	0.068	0.001	0.040
DMN-VAN	0.168	0.070	0.001	0.040
FPCN-SAN	0.159	0.071	0.002	0.040
SMHN-SMMN	0.156	0.068	0.001	0.040
COCN	0.151	0.070	0.003	0.049

Each model included crossed random effects for participants and a fixed effect for neural similarity, with social network proximity as the outcome variable. *P*-values and standard errors were adjusted to account for data redundancy (see Methods). Only significant associations are shown. CN, Cerebellar network; COCN, Cingulo-opercular task control network; DMN, Default mode network; FPCN, Fronto-parietal task control network; SAN, Salience network; SMHN, Somatosensory motor-hand network; SMMN, Somatosensory motor-mouth network; VAN, Ventral attention network.

Appendix – Table 2. Results of linear mixed-effects models testing for associations between functional connectivity within and between brain networks and social network proximity when weighting edges by communication frequency.

Brain network(s)	***ß***	***SE***	***p***	***p* (FDR-corrected)**
AN-SMHN	0.183	0.068	1.734×10^{-4}	0.008
DMN-VAN	0.189	0.069	1.411×10^{-4}	0.008
COCN	0.181	0.071	3.759×10^{-4}	0.011
SMHN-SMMN	0.164	0.066	0.001	0.014
DMN-DAN	0.164	0.069	0.001	0.016
COCN-AN	0.164	0.075	0.002	0.029
SAN-CN	0.147	0.068	0.003	0.029
DMN-FPCN	0.151	0.068	0.002	0.029
DMN-CN	0.137	0.067	0.004	0.038
SMHN-SUN	0.140	0.069	0.005	0.038
SMHN-VN	0.140	0.068	0.004	0.038

Each model included crossed random effects for participants and a fixed effect for neural similarity, with social network proximity as the outcome variable. *P*-values and standard errors were adjusted to account for data redundancy (see Methods). Only significant associations are shown. AN, Auditory network; CN, Cerebellar network; COCN, Cingulo-opercular task control network; DMN, Default mode network; DAN, Dorsal attention network; FPCN, Fronto-parietal task control network; SAN, Salience network; SMHN, Somatosensory motor-hand network; SMMN, Somatosensory motor-mouth network; SUN, Subcortical network; VAN, Ventral attention network; VN, Visual network.

Appendix – Table 3. Results of linear mixed-effects models testing for associations between functional connectivity within and between brain networks and social network proximity when weighting edges by meeting frequency.

Brain network(s)	***ß***	***SE***	***p***	***p* (FDR-corrected)**
AN-SMHN	0.193	0.068	7.439×10^{-5}	0.005
DMN-VAN	0.194	0.069	9.903×10^{-5}	0.005
COCN	0.193	0.071	1.538×10^{-4}	0.005
DMN-DAN	0.183	0.069	2.240×10^{-4}	0.005
SMHN-SMMN	0.161	0.067	0.001	0.013
SNA-CN	0.159	0.068	0.001	0.014
DMN-FPCN	0.160	0.068	0.001	0.014
SMHN-SUN	0.157	0.069	0.002	0.018
COCN-AN	0.168	0.076	0.002	0.019
DMN-CN	0.143	0.067	0.003	0.026
SMHN-VN	0.142	0.069	0.004	0.030
COCN-SMMN	0.145	0.072	0.005	0.036
DMN-SMHN	0.136	0.069	0.006	0.039

Each model included crossed random effects for participants and a fixed effect for neural similarity, with social network proximity as the outcome variable. *P*-values and standard errors were adjusted to account for data redundancy (see Methods). Only significant associations are shown. AN, Auditory network; CN, Cerebellar network; COCN, Cingulo-opercular task control network; DMN, Default mode network; DAN, Dorsal attention network; FPCN, Fronto-parietal task control network; Salience network; SMHN, Somatosensory motor-hand network; SMMN, Somatosensory motor-mouth network; SUN, Subcortical network; VAN, Ventral attention network; VN, Visual network.

Appendix – Table 4. Results of linear mixed-effects models testing for associations between functional connectivity within and between brain networks and social network proximity when using unweighted edges.

Brain network(s)	***ß***	***SE***	***p***	***p* (FDR-corrected)**
DMN-FPCN	0.191	0.064	3.247×10^{-5}	0.003
DMN-VAN	0.162	0.065	4.879×10^{-4}	0.022
AN-SMHN	0.150	0.064	0.001	0.025
SMHN-SMMN	0.150	0.064	0.001	0.025

Each model included crossed random effects for participants and a fixed effect for neural similarity, with social network proximity as the outcome variable. *P*-values and standard errors were adjusted to account for data redundancy (see Methods). Only significant associations are shown. AN, Auditory network; DMN, Default mode network; FPCN, Fronto-parietal task control network; SMHN, Somatosensory motor-hand network; SMMN, Somatosensory motor-mouth network; VAN, Ventral attention network.

Appendix – Table 5. Results of linear mixed-effects models testing for associations between functional connectivity within and between brain networks and social network proximity when controlling for similarities in personality.

Brain network(s)	***ß***	***SE***	***p***	***p* (FDR-corrected)**
DMN-VAN	0.191	0.068	8.312×10^{-5}	0.008
DMN-CN	0.172	0.066	3.056×10^{-4}	0.008
DMN-DAN	0.170	0.067	4.490×10^{-4}	0.008
FPCN-SAN	0.179	0.068	2.423×10^{-4}	0.008
SMHN-SMMN	0.167	0.066	4.127×10^{-4}	0.008
AN-SMHN	0.153	0.067	0.001	0.021
DMN-FPCN	0.150	0.067	0.002	0.023
COCN	0.149	0.069	0.002	0.027

Each model included crossed random effects for participants and a fixed effect for neural similarity, with social network proximity as the outcome variable. *P*-values and standard errors were adjusted to account for data redundancy (see Methods). Only significant associations are shown. AN, Auditory network; CN, Cerebellar network; COCN, Cingulo-opercular task control network; DMN, Default mode network; DAN, Dorsal attention network; FPCN, Fronto-parietal task control network; SAN, Salience network; SMHN, Somatosensory motor-hand network; SMMN, Somatosensory motor-mouth network; VAN, Ventral attention network.

Appendix – Table 6. Results of linear mixed-effects models testing for associations between functional connectivity within and between brain networks and social network proximity when controlling for similarities in personality and excluding cohabitating dyads.

Brain network(s)	***ß***	***SE***	***p***	***p* (FDR-corrected)**
DMN-VAN	0.176	0.069	4.131×10^{-4}	0.019
FPCN-SAN	0.176	0.068	3.300×10^{-4}	0.019
DMN-CN	0.167	0.068	0.001	0.019
SMHN-SMMN	0.155	0.068	0.001	0.031

Each model included crossed random effects for participants and a fixed effect for neural similarity, with social network proximity as the outcome variable. *P*-values and standard errors were adjusted to account for data redundancy (see Methods). Only significant associations are shown. CN, Cerebellar network; DMN, Default mode network; FPCN, Fronto-parietal task control network; SAN, Salience network; SMHN, Somatosensory motor-hand network; SMMN, Somatosensory motor-mouth network; VAN, Ventral attention network.

Appendix – Table 7. Results of linear mixed-effects models testing for associations between functional connectivity within and between brain networks and social network proximity when weighting edges by communication frequency while also controlling for similarities in personality and excluding cohabitating dyads.

Brain network(s)	***ß***	***SE***	***p***	***p* (FDR-corrected)**
SAN-SN	0.199	0.070	8.554×10^{-5}	0.004
DMN-VAN	0.209	0.072	5.890×10^{-5}	0.004
AN-SMHN	0.182	0.071	3.449×10^{-4}	0.009
COCN	0.191	0.075	$3.87\ 7x\ 10^{-4}$	0.009
SMHN-SMMN	0.172	0.069	0.001	0.010
COCN-AN	0.182	0.081	0.002	0.020
DMN-CN	0.160	0.070	0.001	0.020
SMHN-SUN	0.163	0.073	0.002	0.020
DMN-DAN	0.152	0.072	0.003	0.033
DMN-FPCN	0.145	0.071	0.005	0.041

Each model included crossed random effects for participants and a fixed effect for neural similarity, with social network proximity as the outcome variable. *P*-values and standard errors were adjusted to account for data redundancy (see Methods). Only significant associations are shown. AN, Auditory network; CN, Cerebellar network; COCN, Cingulo-opercular task control network; DMN, Default mode network; DAN, Dorsal attention network; FPCN, Fronto-parietal task control network; SMHN, Somatosensory motor-hand network; SMMN, Somatosensory motor-mouth network; SUN, Subcortical network; VAN, Ventral attention network.

Appendix – Table 8. Results of linear mixed-effects models testing for associations between functional connectivity within and between brain networks and social network proximity when weighting edges by meeting frequency while also controlling for similarities in personality and excluding cohabitating dyads.

Brain network(s)	***ß***	***SE***	***p***	***p* (FDR-corrected)**
SAN-SN	0.212	0.07	3.098×10^{-5}	0.002
DMN-VAN	0.211	0.072	5.160×10^{-5}	0.002
AN-SMHN	0.193	0.071	1.593×10^{-4}	0.004
COCN	0.206	0.075	1.445×10^{-4}	0.004
SMHN-SUN	0.184	0.073	4.693×10^{-4}	0.009
SMHN-SMMN	0.169	0.069	0.001	0.011
COCN-AN	0.195	0.082	0.001	0.011
DMN-CN	0.163	0.070	0.001	0.011
DMN-DAN	0.169	0.072	0.001	0.011
CN-SMHN	0.165	0.072	0.001	0.013
DMN-FPCN	0.151	0.071	0.003	0.026
MRN	0.144	0.073	0.005	0.038
SAN-VAN	0.146	0.073	0.005	0.038
FPCN-SAN	0.148	0.077	0.007	0.042
SMHN-VAN	0.144	0.074	0.007	0.042

Each model included crossed random effects for participants and a fixed effect for neural similarity, with social network proximity as the outcome variable. *P*-values and standard errors were adjusted to account for data redundancy (see Methods). Only significant associations are shown. AN, Auditory network; CN, Cerebellar network; COCN, Cingulo-opercular task control network; DMN, Default mode network; DAN, Dorsal attention network; FPCN, Fronto-parietal task control network; MRN, Memory retrieval network; SAN, Salience network;

SMHN, Somatosensory motor-hand network; SMMN, Somatosensory motor-mouth network; SUN, Subcortical network; VAN, Ventral attention network.

Appendix – Table 9. Results of linear mixed-effects models testing for associations between functional connectivity within and between brain networks and social network proximity when using unweighted edges while also controlling for similarities in personality and excluding cohabitating dyads.

Brain network(s)	***ß***	***SE***	***p***	***p* (FDR-corrected)**
DMN-FPCN	0.176	0.067	2.721×10^{-4}	0.012
DMN-VAN	0.187	0.069	1.747×10^{-4}	0.012
SAN-CN	0.171	0.068	4.708×10^{-4}	0.014
SMHN-SMMN	0.164	0.067	0.001	0.015
AN-SMHN	0.150	0.067	0.002	0.027
DMN-SN	0.150	0.067	0.002	0.027
VAN-SUN	0.147	0.067	0.002	0.027

Each model included crossed random effects for participants and a fixed effect for neural similarity, with social network proximity as the outcome variable. *P*-values and standard errors were adjusted to account for data redundancy (see Methods). Only significant associations are shown. AN, Auditory network; CN, Cerebellar network; DMN, Default mode network; FPCN, Fronto-parietal task control network; SAN, Salience network; SMHN, Somatosensory motor-hand network; SMMN, Somatosensory motor-mouth network; SUN, Subcortical network; VAN, Ventral attention network.

Appendix – Table 10. Results of mixed-effects models testing for associations between social network proximity and similarities in demographics and personality.

Variable	***ß***	***SE***	***p***	***p* (FDR-corrected)**
Personality	-0.019	0.068	0.688	0.688
Age	0.089	0.065	0.055	0.166
Gender	-0.120	0.130	0.195	0.292

A set of linear mixed-effects models included fixed effects for similarity in each demographic variable (age, gender) and in overall personality (based on the Big Five personality traits), with social network proximity as the outcome variable. All models included crossed random effects for participants. *P*-values and standard errors were adjusted to account for data redundancy (see Methods). FDR correction was used to correct for multiple comparisons across all three models.

Appendix – Table 11. Results of mixed-effects models testing for associations between neural similarity and similarities in demographics and personality.

Variable	**Brain network(s)**	***ß***	***SE***	***P***	***p* (FDR-corrected)**
Age	FPCN-AN	0.165	0.054	2.163×10^{-5}	0.006
Age	CN	0.140	0.051	1.435×10^{-4}	0.020
Personality	DMN-SMHN	-0.147	0.059	0.001	0.048
Personality	SAN-SUN	-0.108	0.044	0.001	0.048

The relationship between similarity in functional connectivity and each of the three variables of interest (i.e., age similarity, gender similarity, and personality similarity) was assessed using a set of linear mixed-effects models with demographic and personality similarity variables as fixed effects, neural similarity as the outcome variable, and crossed random effects for participants (see Methods). Models used similarity in functional connectivity within and between brain networks as the neural similarity variables (i.e., 91 different neural similarity variables), yielding a total of 273 models. *P*-values and standard errors were adjusted to account for data redundancy (see Methods). FDR correction was used to correct for multiple comparisons across all 273 models. Only significant associations are shown. AN, Auditory network; CN, Cerebellar network; DMN, Default mode network; FPCN, Fronto-parietal task control network; SAN, Salience network; SMHN, Somatosensory motor-hand network; SUN, Subcortical network.

Appendix – Table 12. Results of linear mixed-effects models testing for associations between functional connectivity within and between brain networks and social network proximity when including all dyads.

Brain network(s)	***ß***	***SE***	***p***	***p* (FDR-corrected)**
FPCN-VAN	0.177	0.037	1.364×10^{-10}	1.241×10^{-8}
FPCN-CN	0.138	0.036	1.592×10^{-7}	7.245×10^{-6}
FPCN-DAN	0.103	0.035	5.422×10^{-5}	0.002

Models included crossed random effects for participants and a fixed effect for neural similarity, and social network proximity as the outcome variable. *P*-values and standard errors were adjusted to account for data redundancy (see Methods). FDR correction was used to correct for multiple comparisons across all 91 models. Only significant associations are shown. CN, Cerebellar network; DAN, Dorsal attention network; FPCN, Fronto-parietal task control network; VAN, Ventral attention network.

Appendix – Table 13. Results of linear mixed-effects models testing for associations between functional connectivity within and between brain networks and social network proximity when using unweighted edges and including all dyads.

Brain network(s)	***ß***	***SE***	***p***	***p* (FDR-corrected)**
FPCN-VAN	0.140	0.034	1.157×10^{-8}	1.053×10^{-6}
FPCN-CN	0.115	0.031	3.655×10^{-7}	1.663×10^{-5}
FPCN-DAN	0.087	0.033	2.060×10^{-4}	0.006

Models included crossed random effects for participants and a fixed effect for neural similarity, and social network proximity as the outcome variable. *P*-values and standard errors were adjusted to account for data redundancy (see Methods). FDR correction was used to correct for multiple comparisons across all 91 models. Only significant associations are shown. CN, Cerebellar network; DAN, Dorsal attention network; FPCN, Fronto-parietal task control network; VAN, Ventral attention network.

Chapter 3: Pre-existing neural similarity predicts future increases in social closeness

Introduction

What determines who becomes and stays friends? Many factors are linked to friendship, including physical proximity and interpersonal similarities (Festinger et al., 1950; Marmaros & Sacerdote, 2006). Recent work has leveraged neuroimaging to detect similarities among friend (Hyon, Kleinbaum, et al., 2020; Parkinson et al., 2018) by capturing how people process the world around them (Nguyen et al., 2019; Yeshurun et al., 2017). However, given the cross-sectional nature of past research, it is unknown if neural similarity causes friendship, or simply results from it. Here, we show that pre-existing similarities in neural responses to audiovisual movies–acquired before participants met one another–predicted proximity in a friendship network (i.e., being friends rather than multiple "degrees of separation" apart) eight months later. We also examined changes in distance in participants' shared social network over time, which result from the formation, persistence, and dissolution of friendships. Compared to people who drifted farther apart, people who grew closer in social ties showed greater neural similarity before meeting one another. Thus, whereas some friendships may initially form due to circumstance and dissolve over time, later-emerging and longer-lasting friendships may be rooted in "deeper" interpersonal compatibilities that are indexed by pre-existing neural similarities. The localization of these results suggests that pre-existing similarities in how people interpret, attend to, and emotionally respond to their surroundings facilitate future friendship. These results provide evidence for neural homophily, such that pre-existing neural similarities foster friendship and increased social closeness.

Humans tend to cluster in their real-world social networks based on similarities in their demographic characteristics, such as age, gender, and ethnicity, as well as in their behaviors and preferences (Kandel, 1978; Knoke, 1990; Mark, 1998; Marsden, 1988; McPherson et al., 2001). This tendency to surround oneself with similar others, a phenomenon known as homophily, is a ubiquitous property of human social networks that has been observed across wide-ranging contexts, from modern industrialized societies to hunter-gatherer communities and online communities (Apicella et al., 2012; Fu et al., 2012; K. Lewis et al., 2012; McPherson et al., 2001). Such inter-individual similarities in demographic characteristics, behaviors, and preferences may reflect similarities in how friends think about and respond to the world around them.

To investigate this possibility, prior work has attempted to relate inter-individual similarities in self-reported personality traits (e.g., Big Five personality traits) to how close people are in their social network. However, this approach has yielded null or inconsistent results (Asendorpf & Wilpers, 1998; Casciaro, 1998; Feiler & Kleinbaum, 2015; Klein et al., 2004; Y. H. Lee et al., 2010; Y. Liu & Ipe, 2010; Pollet et al., 2011; Selfhout et al., 2009; Totterdell et al., 2008; Venkataramani et al., 2010), suggesting that traditional approaches using personality surveys or questionnaires may not be sensitive to the types of inter-individual similarities that characterize friends. More recent work has demonstrated that inter-individual similarity in thoughts, feelings, and beliefs about the world (a "generalized shared reality") is predictive of social connection between individuals (Rossignac-Milon et al., 2020). Consistent this notion, a growing body of research has demonstrated that people closer together in their real-world social networks (i.e., who are fewer "degrees of separation" from one another) are characterized by similarities in neuroanatomy, neural responses to watching naturalistic stimuli (i.e., audiovisual

movies), and patterns of neural activity at rest (D'Onofrio et al., 2021; Hyon, Kleinbaum, et al., 2020; Hyon, Youm, et al., 2020; Parkinson et al., 2018). Although this handful of studies demonstrates the utility of neuroimaging in probing the types of similarities that are shared among friends, their cross-sectional nature limits the types of inferences that can be made about the causal relationship between neural similarity and social network proximity. Here, we leveraged a longitudinal study design to test if pre-existing similarities in neural responses to naturalistic stimuli predict future proximity in a real-world friendship network eight months later, and if pre-existing neural similarity was also associated with increases in social closeness over time.

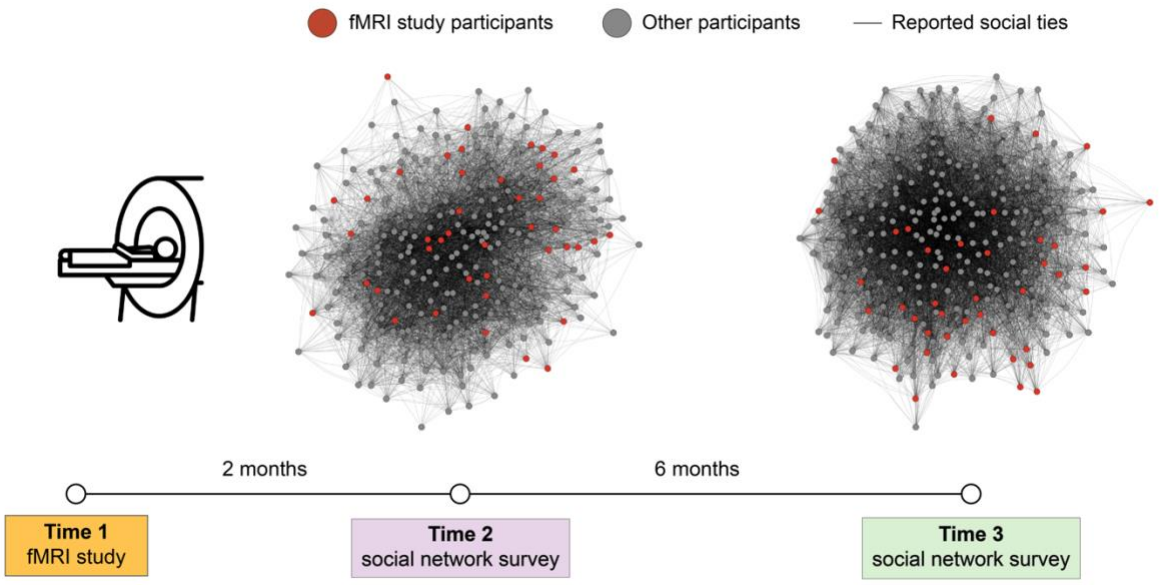

Figure 1. Data collection timeline and social network characterization. A subset of students in a graduate program (red nodes; $N = 41$) participated in the fMRI study before the start of their first year of the program (Time 1). The majority of participants were scanned shortly after arriving on the campus ($\text{Median}_{\text{days between arrival and fMRI scan}} = 3$; $\text{Mode}_{\text{days between arrival and fMRI scan}} = 1$; see Methods for details). Two months later (Time 2), every student in the program participated in a social network survey ($N = 288$; 100% response rate). The majority of these students ($N = 287$; 99.6% response rate) completed the social network survey again six months after Time 2 (Time 3). Their social networks at Time 2 and at Time 3 were reconstructed using these data.

Results

A subset of individuals in a graduate student cohort participated in the fMRI study (N_{fMRI} = 41) before the beginning of their program (Time 1). The majority of fMRI participants were scanned shortly after their arrival on campus (see Fig. 1 and Appendix – Fig. 1). During the fMRI study, participants watched a series of naturalistic audiovisual stimuli (i.e., film clips). We then characterized the complete social network of this cohort two months later (after the beginning of their academic program, Time 2) and again six months later (Time 3). For each unique pair of fMRI participants, pre-existing neural similarities were characterized at Time 1, and social distance was characterized at Times 2 and 3 (Fig. 2).

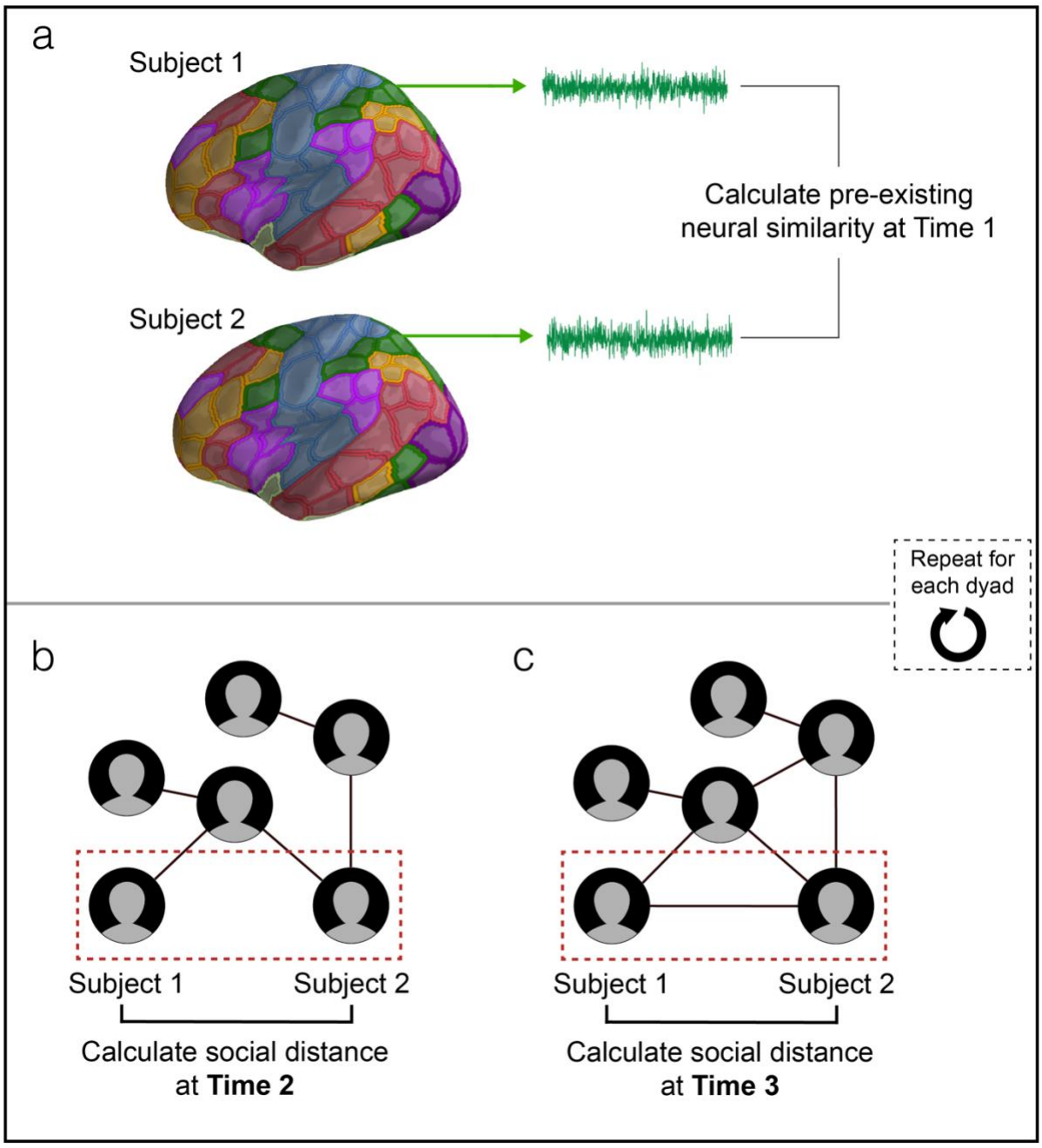

Figure 2. Calculation of neural similarity and social distance. (a) Participants' data were resampled to standard space and parcellated into 200 brain regions using the Schaefer et al. (2018) parcellation scheme. Each region is associated with a brain network from the Yeo et al. (2011) seven-network parcellation, signified by different colors. For each region, the mean neural response was extracted at each time point during the fMRI scan, yielding a mean neural response time series. This was repeated for each participant. For a given pair of fMRI participants, the similarity of their neural response time series in each brain region at Time 2 was calculated using Pearson's *r*. For each pair of fMRI participants, the geodesic distance between them in the social network of their academic cohort was calculated at **(b)** Time 2 and at **(c)** Time 3.

If pre-existing neural similarities truly reflect "deep" interpersonal compatibilities, we reasoned that such similarities may be particularly predictive of friendships after students have ample time to get to know one another and sort out with whom they are compatible. As such, our primary analyses involve testing if Time 1 neural similarities predict (1) greater future proximity in the friendship network at our latest time point (Time 3; 8 months later) and (2) increases in social closeness over time (i.e., in the 6 months between Times 2 and 3). For completeness, we also visualized mean neural similarities for dyads within each of the three social distance levels at Time 2 in Appendix – Fig. 2 and the links between pre-existing neural similarities and social network proximity two months into the academic program in Appendix – Fig. 3.

More specifically, in each brain region, we tested if individuals who came to be characterized by a social distance of 1 (i.e., friends) 8 months into the academic program had greater neural similarity before meeting one another than individuals characterized by greater social distances. Additionally, for each pair of fMRI participants, we calculated their change in social distance over time (i.e., from Time 2 to Time 3) and tested if (and in which brain region(s)) individuals who grew closer in social ties over time had exhibited greater initial neural similarity before meeting one another relative to individuals who did not grow closer over time (see Methods).

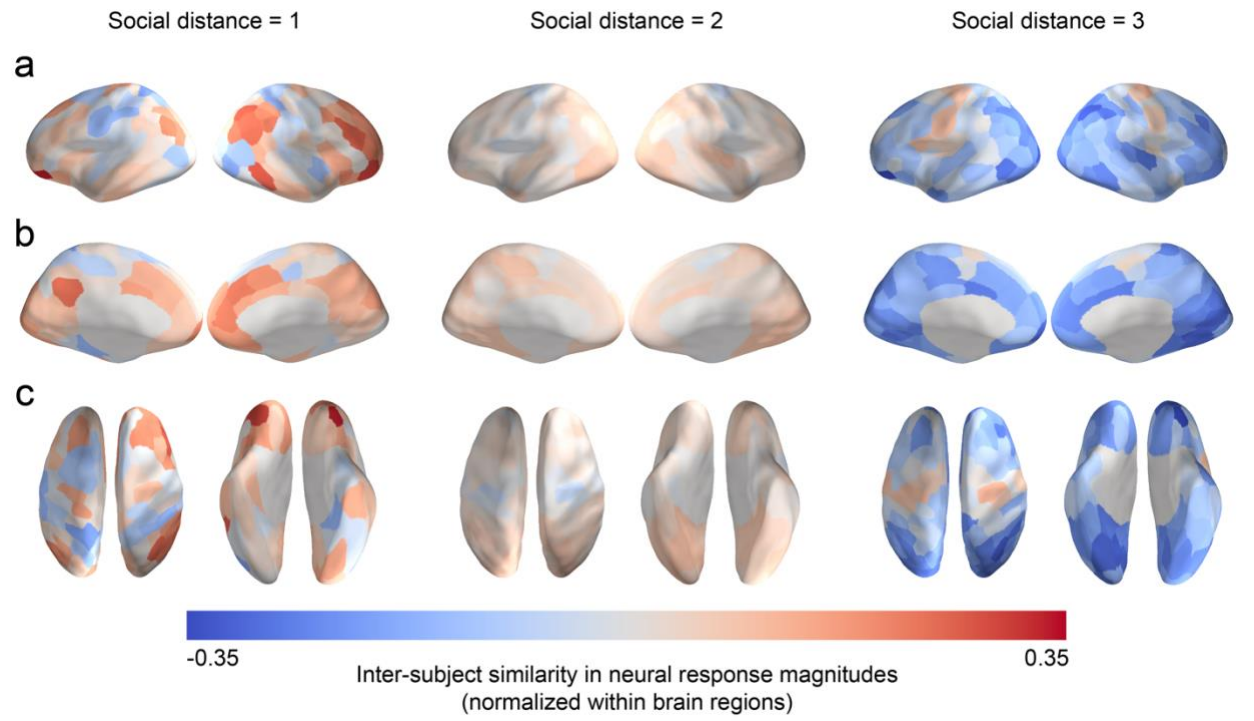

Figure 3. Pre-existing neural similarities averaged within levels of social distance measured 8 months later. Data are overlaid on a cortical surface model and are shown in **(a)** lateral, **(b)** medial, and **(c)** dorsal and ventral views. Inter-participant neural similarities were normalized (i.e., z-scored across dyads for each region), averaged within social distance level, then projected onto an inflated model of the cortical surface. Warmer colors correspond to relatively similar neural responses for a given region, and cooler colors correspond to relatively dissimilar neural responses for a given region.

Pre-existing neural similarity predicted friendship 8 months later.

Mean neural similarities for dyads within each of the three social distance levels are visualized in Fig. 3. We tested if pre-existing neural similarities among individuals who came to be characterized by a social distance of 1 (i.e., friends) 8 months later were greater than pre-existing neural similarities among individuals who did not. Statistical significance was determined using permutation testing (see Methods). Relative to people who did not become friends, people who became friends 8 months after the fMRI study did not exhibit significantly higher pre-existing neural similarity (Fig. 4a).

We followed up on these analyses, in which all non-friends had been collapsed into a single category, with analogous analyses comparing pre-existing neural similarities among friends to those among individuals characterized by a social distance of 2 (i.e., friends-of-friends) or 3 (i.e., friends-of-friends-of-friends). Whereas no significant differences were observed between friends and friends-of-friends, friends exhibited significantly higher pre-existing neural similarity in a portion of the left orbitofrontal cortex (OFC; Fig. 4c) relative to pairs of individuals characterized by a social distance of 3 ($p < 0.001$, FDR-corrected). A similar pattern of results was observed when controlling for inter-individual similarities in handedness and demographic characteristics (Appendix – Fig. 4) and when excluding the pairs of individuals who reported having interacted with each other (e.g., briefly met at a happy hour) prior to the neuroimaging session (i.e., excluding 18 dyads of the total 820 dyads; Appendix – Fig. 5).

In exploratory analyses, we investigated if accounting for inter-individual similarities in ratings of enjoyment and interest in the stimuli would fully account for and/or significantly diminish the difference in neural similarity between friends and pairs of individuals characterized by a social distance of 3 (see Methods). First, we found that the effect in the OFC remained significant when controlling for inter-individual similarities in ratings of enjoyment and interest (Appendix – Fig. 6), suggesting that similarity in neural responding in this brain region captured similarities in friends' responses to the stimuli that the interest and enjoyment ratings did not. Next, to inform our interpretation of the psychological meaning of the OFC result, we tested if controlling for inter-individual similarities in ratings of enjoyment and/or interest would significantly diminish the difference in neural similarity between friends and pairs of individuals characterized by a social distance of 3. Neither controlling for inter-individual similarity in interest ratings nor controlling for inter-individual similarity in enjoyment ratings significantly

decreased the difference in neural similarity between friends and individuals characterized by a social distance of 3.

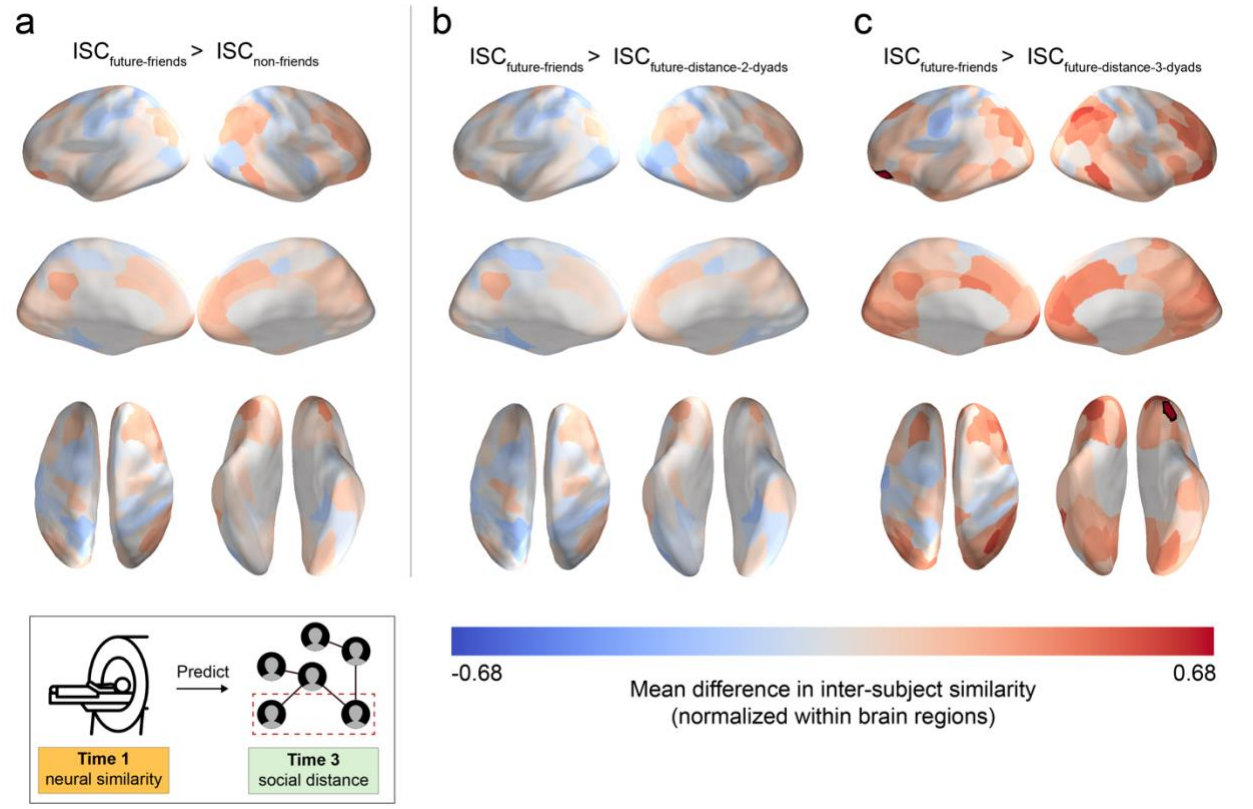

Figure 4. People who became friends with each other showed greater pre-existing neural similarity than those who ended up 3 "degrees of separation" from each other 8 months later. Data are overlaid on a cortical surface model. Warmer colors correspond to relatively greater neural similarity for future friends compared to other pairs of participants, and cooler colors correspond to relatively less neural similarity for future friends compared to other pairs of participants. Null results were observed when testing if individuals who became friends exhibited greater pre-existing neural similarity relative to **(a)** individuals who did not become friends and **(b)** individuals who ended up 2 degrees of separation from each other. **(c)** Individuals who became friends with each other showed greater pre-existing neural similarity in a portion of the left OFC ($p < 0.001$, FDR-corrected) relative to individuals who ended up 3 degrees of separation from each other in the social network 8 months after Time 1. Regions with significant differences for each contrast are outlined in black.

Individuals who grew closer over time had higher pre-existing neural similarity.

For each dyad, we calculated their change in social distance between Time 2 (two months into their academic program) and Time 3 (8 months in). Dyads were divided into three categories depending on if they grew closer over time (i.e., decrease in social distance), grew apart over

time (i.e., increase in social distance), or remained at the same social distance. Mean neural similarities across dyads within each of the three change-in-social-distance categories are visualized in Fig. 5. We tested if pre-existing neural similarities among individuals who grew closer over time were greater than among individuals who did not grow closer over time (i.e., who grew apart or whose social distance did not change). Statistical significance was determined using permutation testing (see Methods). Relative to individuals who did not grow closer over the course of 6 months, people who grew closer did not exhibit significantly greater pre-existing neural similarity (Fig. 6a).

We followed up on these analyses, in which all pairs of participants that did not grow closer to each other over time had been collapsed into a single category, with analogous analyses comparing pre-existing similarities among pairs of individuals who grew closer over time (i.e., between Times 2 and 3) to those among pairs of individuals whose social distance did not change or who grew apart over time. Pairs of individuals who grew closer over time did not exhibit significantly higher pre-existing neural similarity relative to individuals whose social distance did not change over time (Fig. 6b). However, relative to individuals that grew apart over time, individuals who grew closer over time exhibited significantly higher pre-existing neural similarity in bilateral thalamus, left amygdala, and 40 cortical regions spanning visual cortex, occipitotemporal cortex, superior parietal cortex, angular gyrus, medial frontal cortex, and lateral prefrontal cortex ($p < 0.05$, FDR-corrected; Fig. 6c). A similar pattern of results was observed when controlling for inter-individual similarities in handedness and demographic characteristics (Appendix – Fig. 7), when excluding pairs of individuals who reported having interacted with each other in any way prior to the neuroimaging session (Appendix – Fig. 8), and when controlling for enjoyment and interest ratings (Appendix – Fig. 9).

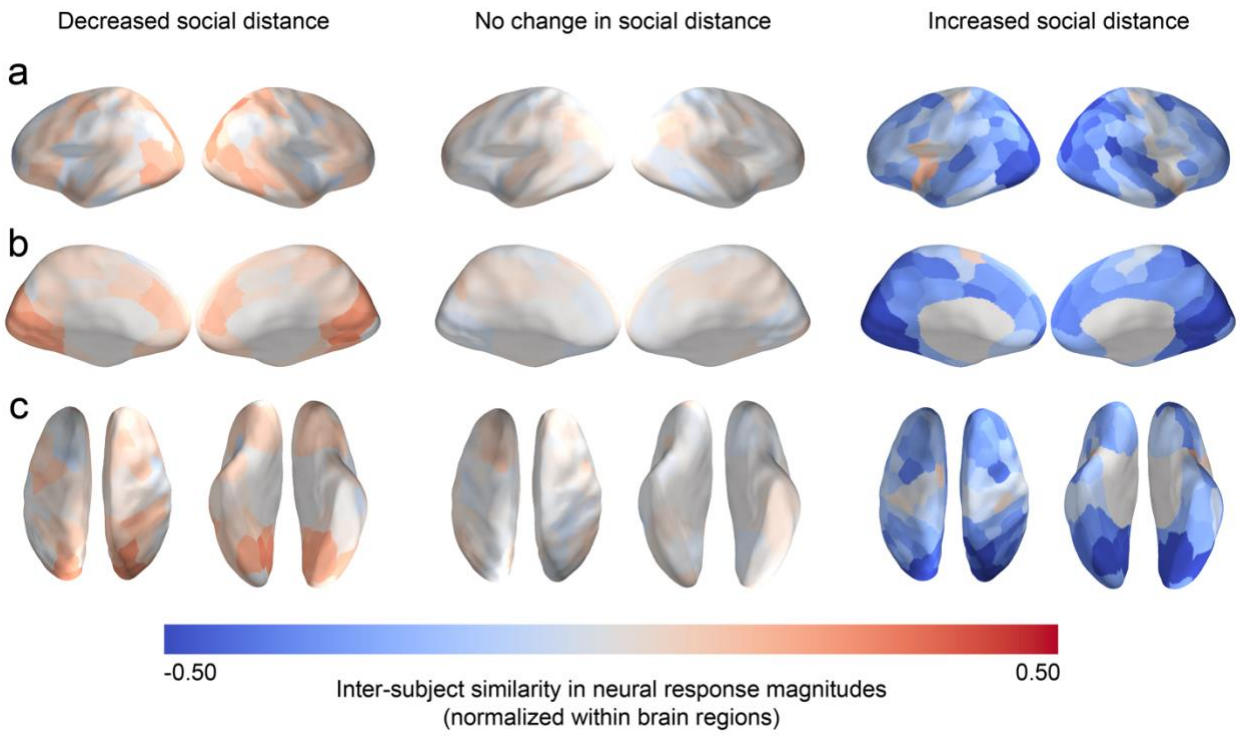

Figure 5. Pre-existing inter-participant similarities in mean neural response time series, averaged within levels of change in social distance over time. Data are overlaid on a cortical surface model and are shown in **(a)** lateral, **(b)** medial, and **(c)** dorsal and ventral views. Inter-participant neural similarities were normalized (i.e., z-scored across dyads for each region), averaged within levels of change in social distance, then projected onto an inflated model of the cortical surface. Warmer colors correspond to relatively similar neural responses for a given region, and cooler colors correspond to relatively dissimilar neural responses for a given region.

To further investigate why individuals who grew closer over time exhibited significantly higher pre-existing neural similarity relative to individuals who grew apart over time, we tested if accounting for inter-individual similarities in ratings of enjoyment and interest in the stimuli would significantly diminish the difference in neural similarity between these two groups (see Methods). This analysis was repeated for each of the brain regions in which we observed a significant difference in mean neural similarity (i.e., regions outlined in black in Fig. 6c). Controlling for inter-individual similarities in ratings of enjoyment of the stimuli significantly decreased the extent to which individuals who grew closer over time exhibited higher neural similarity in a portion of right superior parietal cortex (Difference in mean normalized neural

similarity = 0.015; $p < 0.05$) relative to individuals who grew apart over time. However, this effect was not observed when controlling for inter-individual similarities in ratings of interest in the stimuli or in other brain regions.

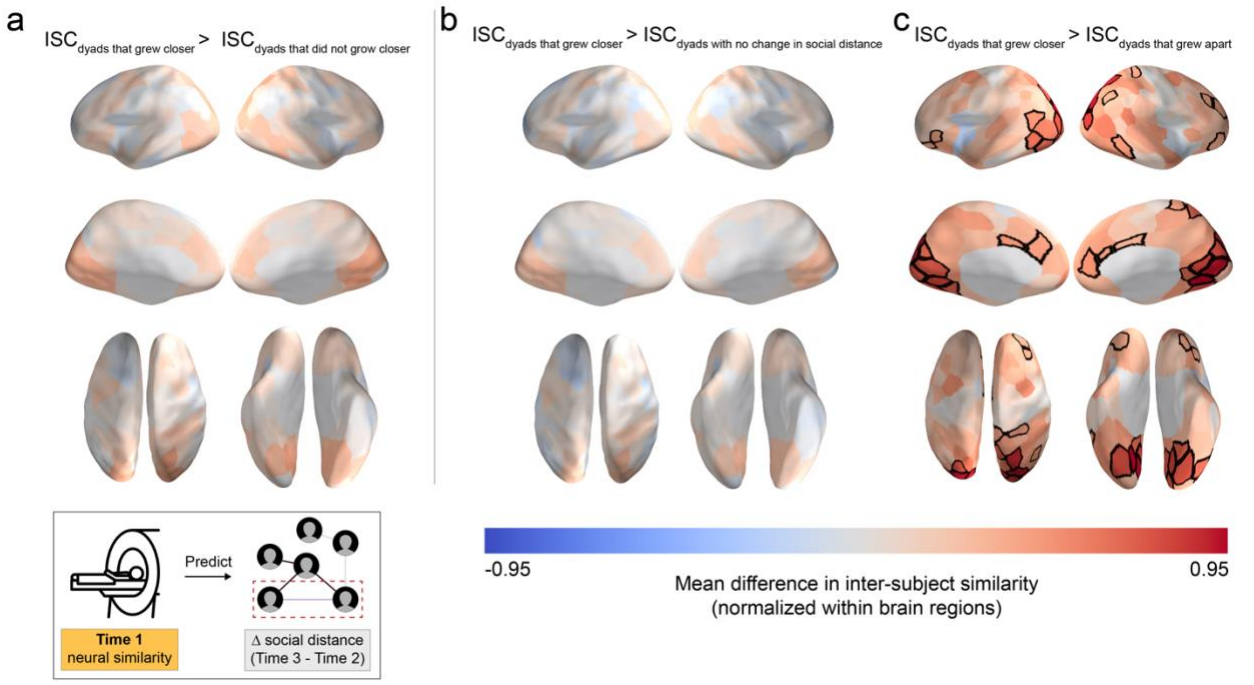

Figure 6. Pairs of individuals who grew closer to each other over time showed greater pre-existing neural similarity than individuals who grew farther apart over time. Data are overlaid on a cortical surface model. Warmer colors correspond to relatively greater mean neural similarity for a given brain region, and cooler colors correspond to relatively less mean neural similarity. For a given dyad, change in social distance over time was calculated by subtracting their social distance at Time 2 from their social distance at Time 3. Dyads were then placed into three categories depending on if their social distance increased, decreased, or remained the same. In the first set of analyses visualized here **(a)**, dyads whose social distance either increased over time or did not change were treated as a single category (i.e., dyads who did not grow closer). Individuals who grew closer to each other over time (i.e., characterized by a decrease in social distance over time) did not exhibit greater pre-existing neural similarity relative to individuals who did not grow closer to each other. **(b)** Individuals who grew closer to each other over time did not exhibit greater pre-existing neural similarity relative to individuals whose social distance did not change. **(c)** Pairs of individuals who grew closer to each other over time exhibited greater pre-existing neural similarity in 40 cortical regions spanning portions of visual cortex, occipitotemporal cortex, superior parietal cortex, angular gyrus, medial frontal cortex, and lateral prefrontal cortex relative to pairs of individuals who grew apart over time. Regions with significant differences ($p < 0.05$, FDR-corrected) for each contrast are outlined in black.

Discussion

Do pre-existing neural similarities predict future friendship? The current results provide evidence for neural homophily, such that relative to people who end up relatively far from one

another in social ties, people who end up becoming friends with one another demonstrated greater pre-existing neural similarity before meeting one another. Additionally, pre-existing neural similarity was particularly strongly linked to changes in inter-individual social distance between two and eight months after entering a new community. Such changes reflect the formation, persistence, and dissolution of friendships in the community's social network.

Relative to individuals that were characterized by a social distance of 3 after having lived in a new community for eight months, individuals who became friends exhibited greater pre-existing neural similarity in a portion of left OFC. Given the role of OFC in processing of subjective value (Padoa-Schioppa & Cai, 2011), neural similarity in this brain region may reflect similarities in tastes and preferences (e.g., similarities in what individuals find funny). Controlling for inter-individual similarity in the extent to which individuals were interested in the stimuli did not significantly diminish the difference in pre-existing neural similarity between friends and individuals characterized by a social distance of 3. Although neural similarity in this brain region may reflect similarity in the processing of subjective value, inter-individual similarity in self-reported ratings of preferences may not sufficiently account for the subjective value processing that may be particularly aligned among friends.

A similar pattern of results was observed when examining the relationship between pre-existing neural similarities and changes in inter-individual social distance over the course of 6 months. Relative to dyads who drifted apart over time, dyads who grew closer in social ties over time were characterized by exceptionally similar neural responses in portions of bilateral OFC, and this difference in neural similarity was not significantly diminished when controlling for similarities in individuals' self-reported enjoyment of or interest in the stimuli. Furthermore, dyads who grew closer in social ties over time also exhibited exceptionally similar neural

responses in many brain regions spanning default mode network (DMN), the frontoparietal control network (FPCN), and the dorsal attention network (DAN), suggesting that pre-existing neural similarities are particularly predictive of whether friendships form, persist, or dissolve over time.

In particular, this relationship was observed in canonical DMN regions (Raichle, 2015), such as the angular gyrus and medial prefrontal cortex, which have a well-established role in social cognitive functions such as mentalizing and perspective-taking (Dufour et al., 2013; Schurz et al., 2014; Spunt et al., 2015). Similarities in neural responding in these DMN regions are associated with convergent interpretations and affective responses to complex narratives (P. H. A. Chen et al., 2020; Finn et al., 2018; Nguyen et al., 2019; Saalasti et al., 2019; Smirnov et al., 2019; Yeshurun et al., 2017). Thus, similar responding in these regions among people who later became friends may reflect pre-existing similarities in how such individuals deployed socio-cognitive processing to interpret the stimuli. Indeed, a recent framework has suggested that the DMN serves as an active "sense-making" network that integrates prior beliefs and long-term memories (e.g., intrinsic information) with processing of extrinsic information to create models of real-life situations as they unfold in real-time (Yeshurun et al., 2021). However, this relationship was not observed in all DMN regions (e.g., temporal poles, precuneus) but was observed in portions of ventral temporal cortex and occipitotemporal cortex. Together with angular gyrus, these regions, in part, have been suggested to comprise "gestalt cortex," in which inter-individual similarity in seemingly effortless subjective construals of complex narratives is associated with neural similarity (Lieberman, 2022). Thus, neural similarities in these regions may capture the creation of high-level meaning across individuals as they watch naturalistic stimuli.

People who grew closer over time also exhibited greater pre-existing neural similarities in several regions of the FPCN, such as the lateral prefrontal cortex, cingulate cortex, and a portion of the inferior temporal gyrus. Recent work has shown that a subsystem of the FPCN couples with the DMN across a multitude of tasks, such as those involving mentalizing, emotional processing, metacognitive awareness, prospective memory, stimulus-independent and abstract thinking, and future planning (Dixon et al., 2018). Given the well-established role of the FPCN in executive control (Vincent et al., 2008), the FPCN may support top-down management of thought by constraining one's focus on contextually relevant material while simultaneously allowing for introspective thought (Christoff et al., 2016; Dixon et al., 2018), such as the processing of personally salient information or internally-focused autobiographical planning (Smallwood et al., 2012; Spreng et al., 2010). In the context of watching naturalistic stimuli, the integration of internal trains of thought (e.g., prior beliefs and memories) and processing of extrinsic stimuli is crucial for understanding complex narratives (Yeshurun et al., 2021), suggesting that the FPCN may work in concert with the DMN to engage in "sense-making" of complex narratives. This is in line with prior work demonstrating that similarity in neural responding in both the DMN and FPCN is associated with similarity in subjective understanding of a complex narrative (Nguyen et al., 2019). Such similarities in subjective construals of narratives may be particularly conducive to friendship formation, as they may reflect, more generally, alignment in how individuals make sense of the world around them.

We also observed pre-existing neural similarities in the superior parietal lobule and occipitotemporal cortex among friends that were significantly greater than that of people more distant from each other in their social network. Given that both of these regions are associated with the DAN (Schaefer et al., 2018; Yeo et al., 2011), these neural similarities may reflect

similarities in attentional allocation and in level of engagement. A growing body of research has demonstrated that attention modulates DMN activity during the processing of complex narratives (Ki et al., 2016; Regev et al., 2019; Yeshurun et al., 2021). In the context of viewing naturalistic stimuli, pre-existing neural similarities in the DAN may reflect inter-individual similarities in how people allocate their attention and what people find particularly engaging, which may lead to convergent interpretations of complex stimuli.

Controlling for inter-individual similarities in ratings of enjoyment of and interest in the stimuli did not significantly diminish the exceptionally large difference in pre-existing neural similarity between individuals that grew closer over time and those that drifted apart in nearly every brain region in which individuals that grew closer over time exhibited exceptionally higher pre-existing neural similarity. This suggests that pre-existing neural similarities largely capture similarities that are linked to whether people grow closer or drift apart over time, but that go beyond what is captured by self-reported ratings of interest and enjoyment. At the same time, accounting for inter-individual similarity in patterns of enjoyment ratings did significantly decrease the difference in neural similarity between pairs of people who grew closer and those who drifted farther apart in a portion of the right superior parietal cortex. This suggests that pre-existing similarities in neural responding in this region among people who grow closer to one another over time partially reflect similarities in such individuals' patterns of enjoyment of the stimuli and/or similarities in neural processing (e.g., in how people allocate their attention) that are impacted by similarities in what they find enjoyable.

Taken together, the current results suggest that inter-individual similarities in neural responses in individuals who interpret, attend to, and emotionally respond to audiovisual movies in a similar fashion are exceptionally likely to become friends in the future and remain friends or

grow closer over time. Viewing naturalistic stimuli demands continuous integration of dynamic information streams as they unfold in real-time, thereby evoking a wide range of socio-cognitive and emotional processes that characterize everyday mental life (Bottenhorn et al., 2019; Nastase et al., 2020; Vanderwal et al., 2019). Thus, similarities in how people think about and respond to naturalistic stimuli may reflect, more generally, similarities in how people think about and respond to the world around them. Taken together with the current results, this growing body of research continues to demonstrate that these inter-individual similarities may facilitate social connection and the formation of social ties. Indeed, separate work has shown that a sense of "generalized shared reality" (i.e., similarities in feelings, beliefs, and concerns about the world in general) is linked to social connection and interpersonal liking (Rossignac-Milon et al., 2020) and thus may be conducive to friendship formation. The pre-existing neural similarities observed in the current study may also underpin similarities in sociobehavioral tendencies, which can lead individuals to participate in similar activities and frequent similar social spaces. Such sociobehavioral similarities can also foster the formation of affiliative ties by facilitating interpersonal communication and predictability (Berger & Calabrese, 1975; Clore & Byrne, 1974; Redcay & Schilbach, 2019).

Additionally, variability in these pre-existing neural similarities may have also facilitated the formation, persistence, and dissolution of direct social ties between the two-month mark and the eight-month mark after individuals entered their new community. It is possible that some initial friendships at the two-month mark may have been formed based on circumstance (e.g., befriending others who conveniently sit nearby in class), rather than based on "deep" interpersonal compatibility (e.g., a sense of generalized shared reality; Rossignac-Milon et al., 2020). However, between the two-month mark and the eight-month mark, neural homophily

processes may have had more time to unfold. As a result, given sufficient time, pairs of individuals may have formed and/or maintained friendships due to interpersonal compatibilities reflected in pre-existing neural similarity. On the other hand, friendships born out of mere circumstance may have dissolved due to interpersonal incompatibilities, reflected in pre-existing neural dissimilarities, which only became apparent with the extended passage of time.

The current results are consistent with the possibility of neural homophily, such that future friends share pre-existing neural similarity before meeting one another. Future work would benefit from investigating the role of social influence, as it is likely that homophily and social influences processes interact in human social networks. For example, pre-existing similarities in how individuals think about and respond to the world around them may, in part, cause individuals to become friends, as suggested by the current results. Over time, these individuals may undergo repeated, sustained social interactions that lead to further convergence in how they tend to speak, think, feel, and behave (Cialdini & Goldstein, 2004; de Waal, 2007; Kovacs & Kleinbaum, 2020), which may further convergence in neural processing. This effect of social influence can percolate outward to more distal social ties, which allows for even indirectly individuals to influence and be influenced by each other (Christakis & Fowler, 2009). Although the current study attempted to test for both neural homophily and social influence, planned collection of fMRI data two years after the participants entered their new community was prohibited by the COVID-19 pandemic. Future work can leverage longitudinal fMRI to further examine such phenomena.

A growing body of cross-sectional research integrating neuroimaging and social network analysis has demonstrated that individuals closer together in their real-world social network tend to share similarities in neuroanatomy (D'Onofrio et al., 2021), (resting-state functional

connectomes (Hyon, Youm, et al., 2020), and neural responses to watching naturalistic stimuli (Hyon, Kleinbaum, et al., 2020; Parkinson et al., 2018). However, the cross-sectional nature of this work has limited the types of inferences that can be made about the causal relationship between neural similarity and social distance. The current research expands upon this work and sheds light on the causal role of neural homophily in shaping human social structures.

Although the current sample included participants from a wide range of nationalities (see Methods), the current results are reflective of a single context, and results may vary across cultures and contexts. Past cross-sectional work has linked neural (Hyon, Youm, et al., 2020) and behavioral (Apicella et al., 2012) similarities to social network proximity across markedly different cultural contexts. However, it is important to note that the current evidence for neural homophily is constrained within a single cultural context. Additionally, although the general phenomenon of neural homophily may be consistently observed across cultures and contexts, the types of interpersonal similarities that predict future friendship may vary. Thus, future work examining these effects across diverse cultures will yield a more comprehensive understanding of how this phenomenon may differentially unfold across different social networks.

Methods

Participants

fMRI participants. All data collection procedures were completed in accordance with the standards of the local ethical review board. A subset of 43 individuals from an incoming graduate student cohort (N_{cohort} = 288) at a private university in the United States participated in the neuroimaging study. Participants were scanned as soon as possible after their arrival on campus. The majority of fMRI participants were scanned shortly after arriving on campus (Appendix – Fig. 1). The modal number of days between participants' arrival on campus and their participation in the fMRI study was 1 day and the median number of days was 3 days. Two of the fMRI participants were scanned more than 1 month after their arrival on campus; these participants had been enrolled in two different prior graduate programs at the university but had not met one another at the time of the fMRI scan. Participants provided informed consent in accordance with the policies of the institution's ethical review board. Of the 43 participants, one participant did not complete the scan and was excluded from analysis and one participant did not participate in the social network survey administered at Time 3 (see *Social network survey participants*) and thus was excluded from analysis. Data from the resulting 41 participants (14 female) aged 25-34 (M = 28.63, SD = 2.15) were used for analysis. Of these participants, two participants had excess movement in only one of the four fMRI runs; thus, these scans were excluded from the analyses involving these two participants. Of these 41 participants, 38 were right-handed and three were left-handed. Twenty-four participants self-identified their nationality as that of the United States, with five participants from India, two participants from Australia, two participants from Peru, and one participant each from Argentina, Iran, Russia, Kyrgyzstan, the United Kingdom, China, Brazil, and Canada. Fifteen participants identified as White/Non-

Hispanic, two identified as Hispanic/Latino, one identified as Black/Non-Hispanic, one identified as Asian/Asian-American/Pacific-Islander, one identified as multi-racial, and 21 chose to not indicate their ethnicity. The neuroimaging study was advertised to all students in each cohort via email. All students who were interested in participating and who passed a standard MRI safety screening participated in the scan.

Social network survey participants. Approximately two months (Time 2) and 8 months (Time 3) after the fMRI scan, the social network of the academic cohort was characterized (Fig. 1). Participants were from the same cohort of 288 (129 females) first-year graduate students who had been recruited for the fMRI study at Time 1 and participated as part of their coursework on leadership. At Time 2, all students in the cohort completed an online social network survey (i.e., 100% response rate). At Time 3, all students except one individual completed the survey (i.e., 99.6% response rate).

Experimental procedures

fMRI acquisition. Participants were scanned using a Siemens Prisma 3T scanner. Six functional runs were acquired using an echo-planar sequence (25 ms echo time (TE); 2000 ms repetition time (TR); 3.0 mm x 3.0 mm 3.0 mm resolution; 240 mm FOV; 40 interleaved transverse slices with no gap. A high-resolution T1-weighted anatomical scan was also acquired for each participant (2.32 ms TE; 2300 ms TR; 240 mm FOV; 0.9 mm x 0.9 mm x 0.9 mm resolution)

fMRI paradigm and stimuli. Before the fMRI study began, participants were told that they would be watching a set of videos while being scanned, which would vary in content, and that their experience in the study would be akin to watching television while someone else

"channel surfed." All participants saw the same clips in the same order (as if the clips comprised different scenes of a continuous movie), to avoid inducing response variability between participants related to differences in how clips were presented. Stimuli consisted of 14 videos presented with sound over the course of six fMRI runs. Videos ranged in duration from 88 to 305 s (see Table S1 for brief descriptions of stimuli). Criteria used to select stimuli are described in more detail elsewhere (Parkinson et al., 2018). Briefly, efforts were made to select stimuli that (1) most participants would not have seen before, (2) would be engaging for participants, and (3) would evoke diverging inferences and patterns of attentional allocation across viewers, and thus, psychologically meaningful variability in neural responding (e.g., because different people might attend to, emotionally react to, and/or interpret them differently). After the fMRI session, participants filled out an online survey and provided ratings of the extent to which they enjoyed and were interested in each of the stimuli shown during the fMRI session. For each stimulus, a screenshot was shown and participants answered, "How interesting did you find this video?" and "How much did you enjoy this video?" on a Likert scale from 1 to 5.

Social network survey. Participants followed an e-mailed link to the study website where they responded to a survey designed to assess their position in the social network of students in their cohort of the academic program. The survey question was adapted from Burt (1992) and has been previously used in the modified form used here (Feiler & Kleinbaum, 2015; Kleinbaum et al., 2015; Parkinson et al., 2018). It read, *"Consider the people with whom you like to spend your free time. Since you arrived at [institution name], who are the classmates you have been with most often for informal social activities, such as going out to lunch, dinner, drinks, films, visiting one another's homes, and so on?"* A roster-based name generator was used to avoid inadequate or biased recall. Participants indicated the presence of a social tie with an

individual by placing a checkmark next to his or her name. Participants could indicate any number of social ties, and had no time limit for responding to this question.

We note that in this particular graduate program, students lived in close proximity to each other in an isolated, rural area. Furthermore, they took classes together and frequently ate meals and socialized together. Taken together, these characteristics of this graduate program engendered an intense and immersive social experience.

Data analysis

fMRI preprocessing and parcellation. fMRIPrep version 1.4.0 was used for anatomical and functional data preprocessing (Esteban et al., 2019). The T1-weighted (T1w) image was corrected for intensity non-uniformity (INU) with N4BiasFieldCorrection, distributed with ANTs 2.1.0, and used as T1w-reference throughout the workflow. The T1w-reference was then skull-stripped with a Nipype implementation of the antsBrainExtraction.sh workflow (from ANTs), using OASIS30ANT as target template. Brain tissue segmentation of cerebrospinal fluid (CSF), white-matter (WM) and gray-matter (GM) was performed on the brain-extracted T1w using FSL FAST. Volume-based spatial normalization to MNI152NLin2009cAsym standard space was performed through nonlinear registration with antsRegistration (ANTs 2.1.0), using brain-extracted versions of both T1w reference and the T1w template.

For each of the 6 BOLD runs per participant (across all tasks and sessions), the following preprocessing was performed. First, a reference volume and its skull-stripped version were generated using a custom methodology of fMRIPrep. The BOLD reference was then co-registered to the T1w reference using FSL FLIRT with the boundary-based registration cost-function. Co-registration was configured with nine degrees of freedom to account for distortions

remaining in the BOLD reference. Head-motion parameters with respect to the BOLD reference (transformation matrices, and six corresponding rotation and translation parameters) were estimated before any spatiotemporal filtering using FSL MCFLIRT. Automatic removal of motion artifacts using independent component analysis (ICA-AROMA) was performed on the preprocessed BOLD on MNI space time-series after removal of non-steady state volumes and spatial smoothing with an isotropic, Gaussian kernel of 6mm FWHM (full-width half-maximum). The confounding variables generated by fMRIPrep that were used as nuisance variables in the current study included global signals extracted from the CSF, WM, and whole-brain masks, framewise displacement, three translational motion parameters, and three rotational motion parameters. These confounds were regressed out of the data for each preprocessed run. Temporal filtering was performed with a band-pass filter between 0.009 and 0.08 Hz.

The Schaefer et al. (2018) parcellation scheme (resampled to MNI152NLin2009cAsym standard space) with 200 parcels was used in the current study to define the 200 cortical ROIs. Each parcel is associated with one of seven brain networks from the Yeo et al. (2011) seven-network parcellation - the visual, somatomotor, dorsal attention, ventral attention, limbic, frontoparietal task control, and default mode networks. The Harvard-Oxford subcortical atlas (Desikan et al., 2006) was used to define 14 subcortical ROIs - bilateral nucleus accumbens, amygdala, putamen, caudate, thalamus, hippocampus, and pallidum.

Social network analysis. The following steps were taken to characterize the social networks at Time 2 and at Time 3. Social network data were analyzed using igraph in R (Csárdi & Nepusz, 2014). An unweighted graph consisting of mutually reported social ties was used to estimate social distances between individuals. In other words, an undirected edge would connect two actors only if they had both nominated one another as friends. Social distance was defined as

the geodesic distance between people in the social network – i.e., as the smallest number of intermediary social ties required to connect them in the network. Pairs of individuals who both named one another as friends were assigned a social distance of one. Individuals would be assigned a distance of two from one another if they had a mutually reported friendship with a shared friend, but were not friends with one another, and so on.

At Time 2, of the 820 dyads of fMRI participants, 63 (7.68%) were characterized by a social distance of one (i.e., they were friends), 436 (53.17%) were characterized by a social distance of two (i.e., they were friends of one another's friends), 280 (34.15%) were characterized by a social distance of three, and 41 (5.00%) were characterized by a social distance of four. Dyads characterized by a social distance of four were recoded as dyads characterized by a social distance of three given that similarities in neural responses in people four or more degrees of separation apart have previously been found to be highly variable and not significantly different from that of social dyads two or three degrees of separation from one another (Parkinson et al., 2018). More generally, a large body of research demonstrates that relationships between interpersonal similarities in a variety of cognitive, emotional, and behavioral phenomena (e.g., risk perception, cooperation, smoking, depression, loneliness, and happiness) and social network proximity disappear beyond three to four "degrees of separation" (Cacioppo et al., 2009; Christakis & Fowler, 2007, 2008; Fowler & Christakis, 2010; Moussaïd et al., 2015, 2017; J. N. Rosenquist et al., 2011; J. Niels Rosenquist et al., 2010). At Time 3, of the 820 dyads of fMRI participants, 93 (11.34%) were characterized by a social distance of one, 544 (66.34%) were characterized by a social distance of two, and 183 (22.32%) were characterized by a social distance of three. For each social network, for descriptive purposes, we then calculated the average number of social ties across individuals, the median number of social

ties, and the reciprocity of the graph, which refers to the probability that person *i* nominated person *j* as a friend if person *j* nominated person *i* as a friend (mean social ties$_{\text{Time 2}}$ = 72, median social ties$_{\text{Time 2}}$ = 65, reciprocity$_{\text{Time 2}}$ = 0.53; mean social ties$_{\text{Time 3}}$ = 100, median social ties$_{\text{Time 3}}$ = 91, reciprocity$_{\text{Time 3}}$ = 0.56). Here, the number of social ties refers to degree centrality, where incoming and outgoing ties are summed.

Testing if pre-existing neural similarity differed between levels of social distance at Time 3

The following analysis was performed in each of the 200 cortical and 14 subcortical brain regions. For each fMRI participant, all six fMRI scans were concatenated into a single time series (with the exception of two participants who only had three scans that were concatenated due to excess movement in the excluded scan). For each fMRI participant, the neural response time series was spatially averaged across all voxels within a given region. For each unique pair of fMRI participants, we then calculated the Pearson *r* between their neural response time series, yielding a value reflecting neural similarity for a given region. For a given region, these neural similarity values were then Fisher-*z* transformed and normalized across fMRI dyads using scikit-learn's StandardScaler() function (Pedregosa et al., 2011).

To test if individuals characterized by a social distance of 1 (i.e., friends) initially exhibited significantly higher neural similarity in a given brain region than did individuals characterized by a social distance of 2 or 3 (i.e., non-friends), we first bucketed all individuals characterized by a social distance of 2 or 3 into a single category of social distance (i.e., non-friends). The mean neural similarity was then calculated for each of the two resulting levels of social distance (i.e., friends and non-friends). We then subtracted the mean neural similarity among pairs of individuals who did not become friends from the mean neural similarity among

pairs of individuals who did become friends. To assess the statistical significance of this difference, we implemented the following permutation testing procedure. Neuroimaging data were randomly shuffled across fMRI participants 1,000 times while holding all else in the dataset constant. In each permuted dataset, the mean neural similarity among individuals characterized by a social distance of 2 or 3 (shuffled) was again subtracted from the mean neural similarity among individuals characterized by a social distance of 1 (shuffled). This procedure yielded a null distribution of 1,000 permuted difference values. We then calculated the extent to which the true difference value was greater than the null distribution in order to generate a p-value. These p-values were then corrected for false discovery rates (FDR) across all 214 regions.

This analytical procedure was repeated to test if individuals characterized by a social distance of 1 exhibited significantly higher neural similarity in a given region than did individuals characterized by a social distance of 2. It was also repeated to test if individuals characterized by a social distance of 1 exhibited significantly higher neural similarity in a given region than did individuals characterized by a social distance of 3.

In each brain region in which a significant difference in neural similarity between groups was observed, we then tested if inter-individual similarity in self-reported ratings of enjoyment of the stimuli accounted for a significant portion of this difference. Even when a similar pattern of results is observed with and without controlling for similarities in behavioral ratings, it is possible that the magnitude of the neural similarity difference between groups would significantly decrease when controlling for such behavioral similarities if the neural similarities are partially driven by them. These exploratory analyses thus aim to inform the psychological interpretation of the significant findings. First, for a given dyad, inter-individual similarity in enjoyment or interest ratings was measured by calculating the Euclidean distance between

individuals' vectorized series of enjoyment ratings across the stimuli to yield a single similarity value. We then calculated the between-group difference in mean normalized neural similarity, and we separately calculated the between-group difference in mean normalized neural similarity after controlling for inter-individual similarities in enjoyment ratings. We then subtracted the latter difference value from the former difference value to yield a value capturing the extent to which between-group difference in neural similarity was diminished when controlling for inter-individual enjoyment similarity. To test whether this decrease in between-group difference in neural similarity was statistically significant, we implemented the following permutation testing procedure. Enjoyment ratings were randomly shuffled across fMRI participants 1,000 times while holding all else in the dataset constant. In each permuted dataset, the above-mentioned analytic procedure was repeated to generate a value capturing the decrease in between-group difference in neural similarity when controlling for enjoyment similarity. This procedure yielded a null distribution of 1,000 values capturing the decrease in between-group difference in neural similarity when controlling for enjoyment similarity. We then calculated the extent to which the true value was greater than this null distribution in order to generate a p-value.

This analytical procedure was repeated using self-reported ratings of interest in the stimuli to test if inter-individual similarity in self-reported ratings of interest in the stimuli accounted for significant portions of the differences in neural similarity between groups.

Testing if neural similarity significantly differed between levels of change in social distance between Time 2 and Time 3

For each pair of fMRI participants, change in social distance between Time 2 and Time 3 was calculated by subtracting their Time 3 social distance from their Time 2 social distance. To

test if individuals characterized by a decrease in social distance (i.e. individuals who grew closer over time) between Time 2 and 3 exhibited greater pre-existing neural similarity in a given brain region than did individuals characterized by no change in social distance between Time 2 and 3 or an increase in social distance (i.e., individuals who grew apart over time) between Time 2 and 3, we first bucketed all individuals characterized by no change or an increase in social distance into a single category of individuals who did not grow closer over time. In total, of the 820 dyads of fMRI participants, 279 dyads were characterized by a decrease in social distance, 445 dyads were characterized by no change in social distance, and 96 dyads were characterized by an increase in social distance. The following analysis was performed in each of the 200 cortical and 14 subcortical brain regions. The mean neural similarity was calculated for individuals who grew closer over time and separately for individuals who did not grow closer over time. We then subtracted the mean neural similarity among individuals who did not grow closer over time from the mean neural similarity among individuals who did grow closer over time. To assess the statistical significance of this difference, we implemented the following permutation testing procedure. Neuroimaging data were randomly shuffled across fMRI participants 1,000 times while holding all else in the dataset constant. In each permuted dataset, the mean neural similarity among individuals who did not grow closer over time was again subtracted from the mean neural similarity among individuals who did grow closer over time. This procedure yielded a null distribution of 1,000 permuted difference values. We then calculated the extent to which the true difference value was greater than the null distribution in order to generate a p-value. These p-values were then corrected for false discovery rates (FDR) across all 214 regions.

This analytical procedure was repeated to test if individuals who grew closer over time exhibited greater pre-existing neural similarity in a given region than did individuals whose social distance did not change over time individuals who grew apart over time.

In each brain region in which a significant difference in neural similarity between groups was observed, we then tested if inter-individual similarity in self-reported ratings of enjoyment of or interest in the stimuli accounted for this significant difference using the same data analytic and permutation-testing approaches described in the preceding section ("Testing if pre-existing neural similarity differed between levels of social distance at Time 3").

Appendix

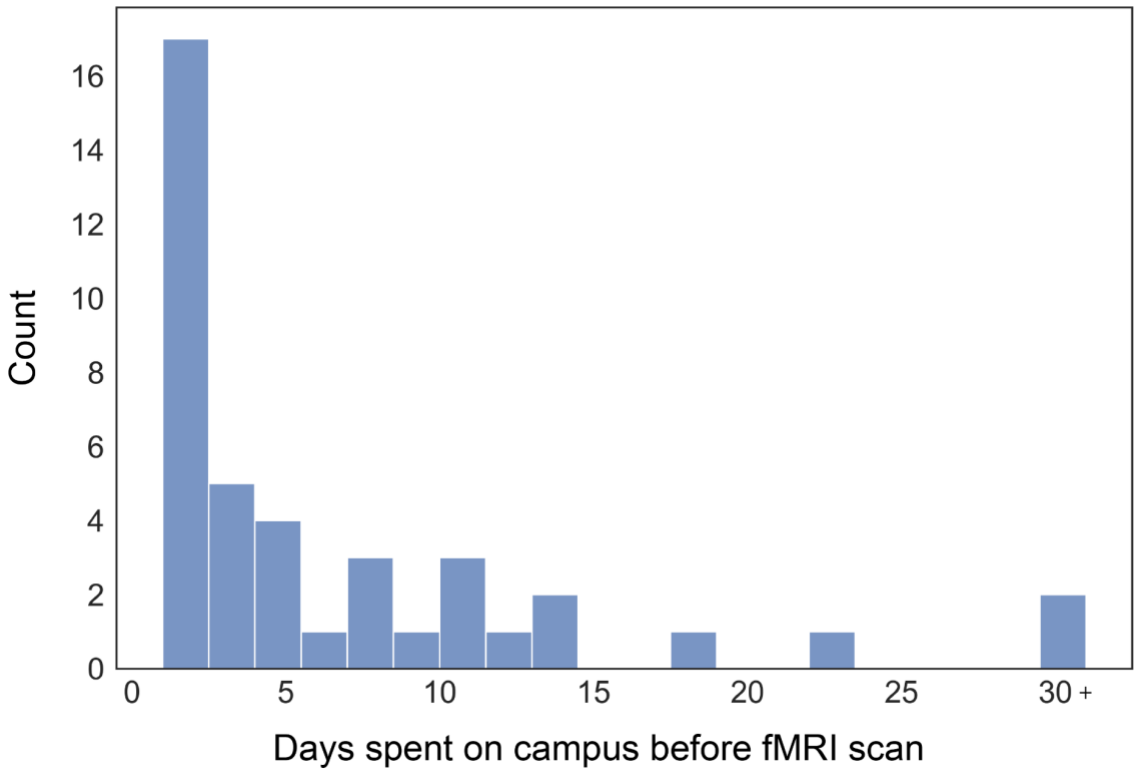

Appendix – Figure 1. Distribution of days between participants' arrival on campus and the fMRI study. The majority of fMRI participants were scanned shortly after their arrival on campus (Mode = 1 day; Median = 3 days). Only two participants were on campus for more than 30 days before the fMRI study; one participant was on campus for 400 days due to being enrolled in a prior graduate program at the same university, and the other participant was on campus for 1095 days due to being enrolled in a different prior graduate program at the same university. Thus, it was highly unlikely that participants formed meaningful relationships prior to the fMRI study. Additionally, we observed a similar pattern of results in the current study when excluding fMRI dyads who had encountered each other prior to the fMRI study (Appendix – Figures 4 and 7).

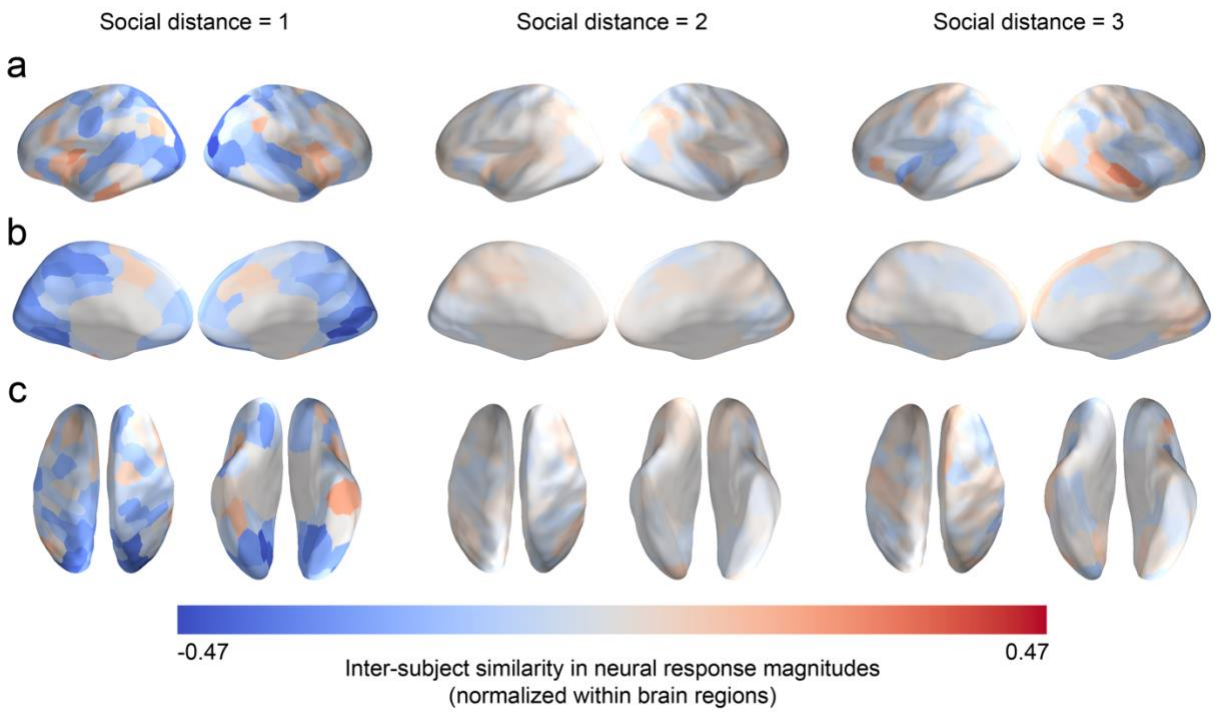

Appendix – Figure 2. Pre-existing neural similarities averaged within levels of social distance measured 2 months later at Time 2. Data are overlaid on a cortical surface model and are shown in **(a)** lateral, **(b)** medial, and **(c)** dorsal and ventral views. Inter-participant neural similarities were normalized (i.e., z-scored across dyads for each region), averaged within social distance level, then projected onto an inflated model of the cortical surface. Warmer colors correspond to relatively similar neural responses for a given region, and cooler colors correspond to relatively dissimilar neural responses for a given region.

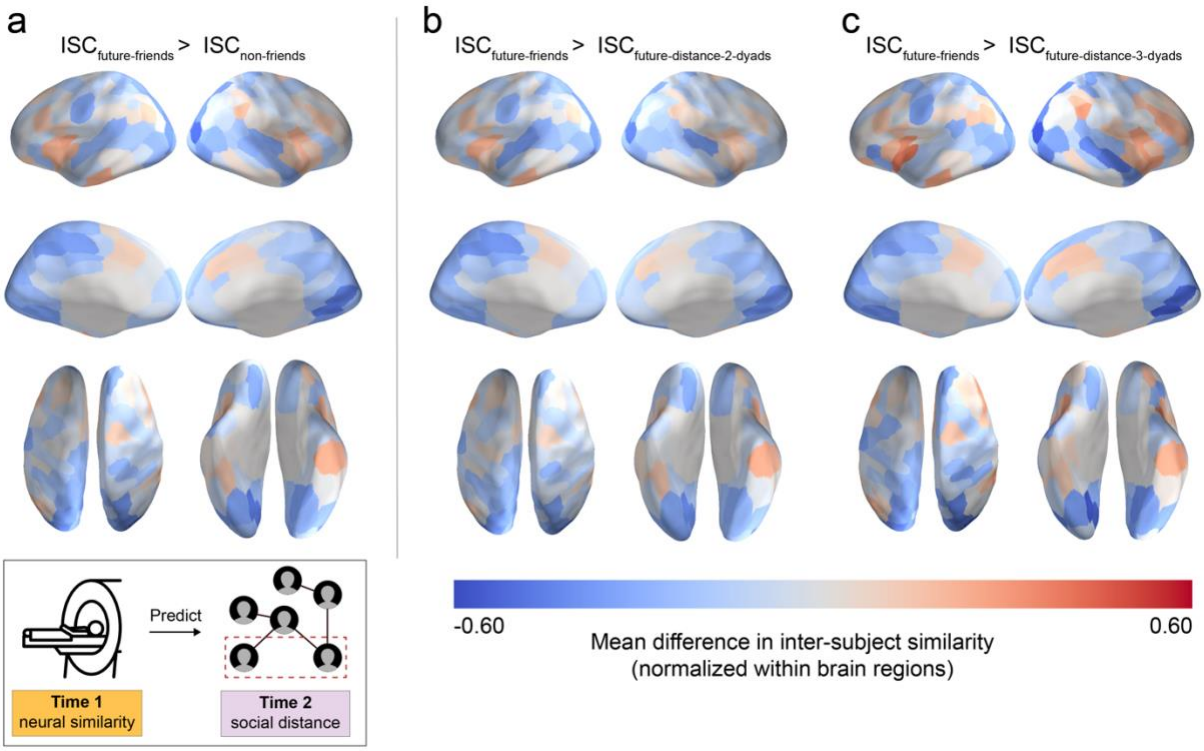

Appendix – Figure 3. Early in the school year, pre-existing neural similarities were not yet associated with friendship. Data are overlaid on a cortical surface model. Warmer colors correspond to relatively greater mean neural similarity, and cooler colors correspond to relatively less mean neural similarity. Early in the school year (two months in, at Time 2), null results were observed when testing **(a)** if individuals who became friends exhibited greater pre-existing neural similarity relative to individuals who did not become friends and if individuals who became friends exhibited greater pre-existing neural similarity relative to **(b)** individuals who ended up in 2 degrees of separation from each other and **(c)** individuals who ended up in 3 degrees of separation from each other.

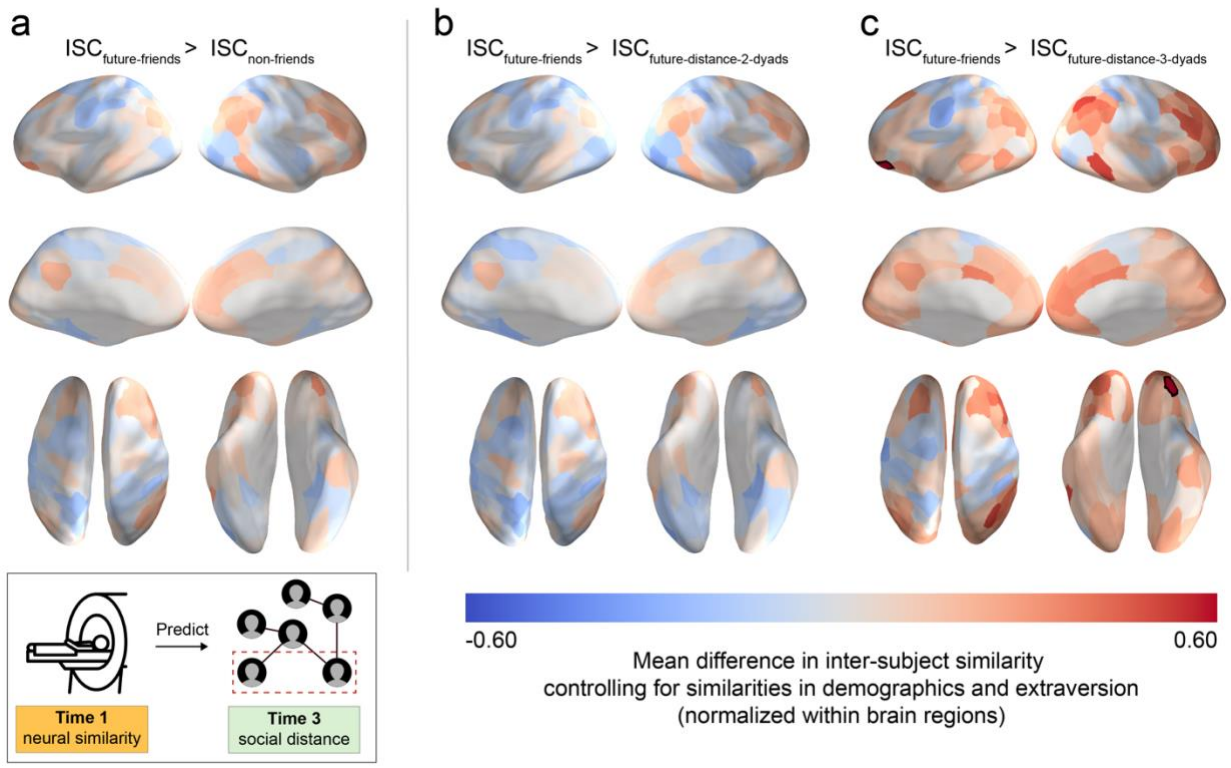

Appendix – Figure 4. People who became friends showed greater pre-existing neural similarity than those who ended up 3 "degrees of separation" from each other 8 months later when controlling for similarities in demographics. Data are overlaid on a cortical surface model. Warmer colors correspond to relatively greater mean neural similarity, and cooler colors correspond to relatively less mean neural similarity. **(a)** Null results were observed when testing if individuals who became friends exhibited greater pre-existing neural similarity relative to **(b)** individuals who did not become friends and **(b)** individuals who ended up 2 degrees of separation from each other. **(c)** Relative to individuals who ended up 3 degrees of separation from each other in the social network, individuals who became friends with each other showed greater pre-existing neural similarity in a portion of the left OFC ($p < 0.001$, FDR-corrected). Regions with significant differences for each contrast are outlined in black.

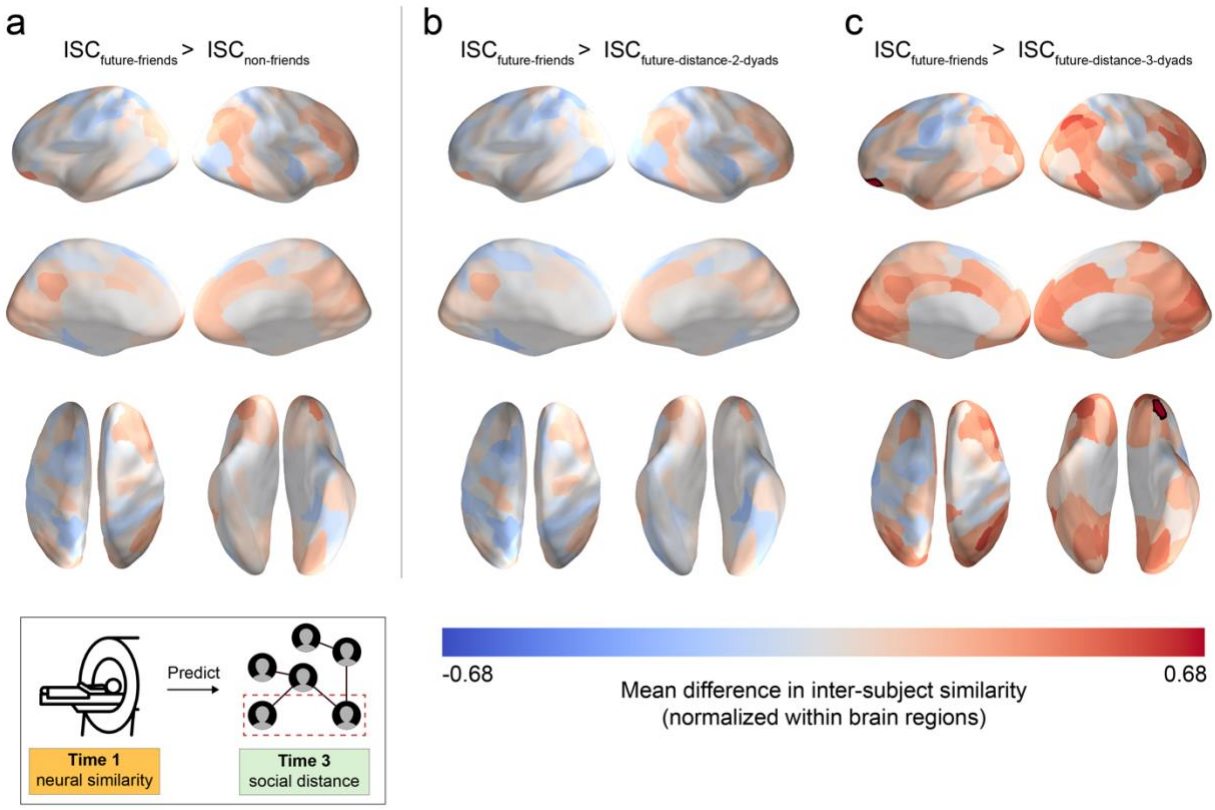

Appendix – Figure 5. People who became friends showed greater pre-existing neural similarity than those who ended up 3 "degrees of separation" from each other 8 months later when excluding dyads who met each other prior to the neuroimaging session. Data are overlaid on a cortical surface model. Warmer colors correspond to relatively greater mean neural similarity, and cooler colors correspond to relatively less mean neural similarity. Null results were observed when testing if individuals who became friends exhibited greater pre-existing neural similarity relative to **(a)** individuals who did not become friends and **(b)** individuals who ended up 2 degrees of separation from each other. **(c)** Individuals who became friends with each other showed greater pre-existing neural similarity in a portion of the left OFC ($p < 0.001$, FDR-corrected) relative to individuals who ended up 3 degrees of separation from each other in the social network. Regions with significant differences for each contrast are outlined in black.

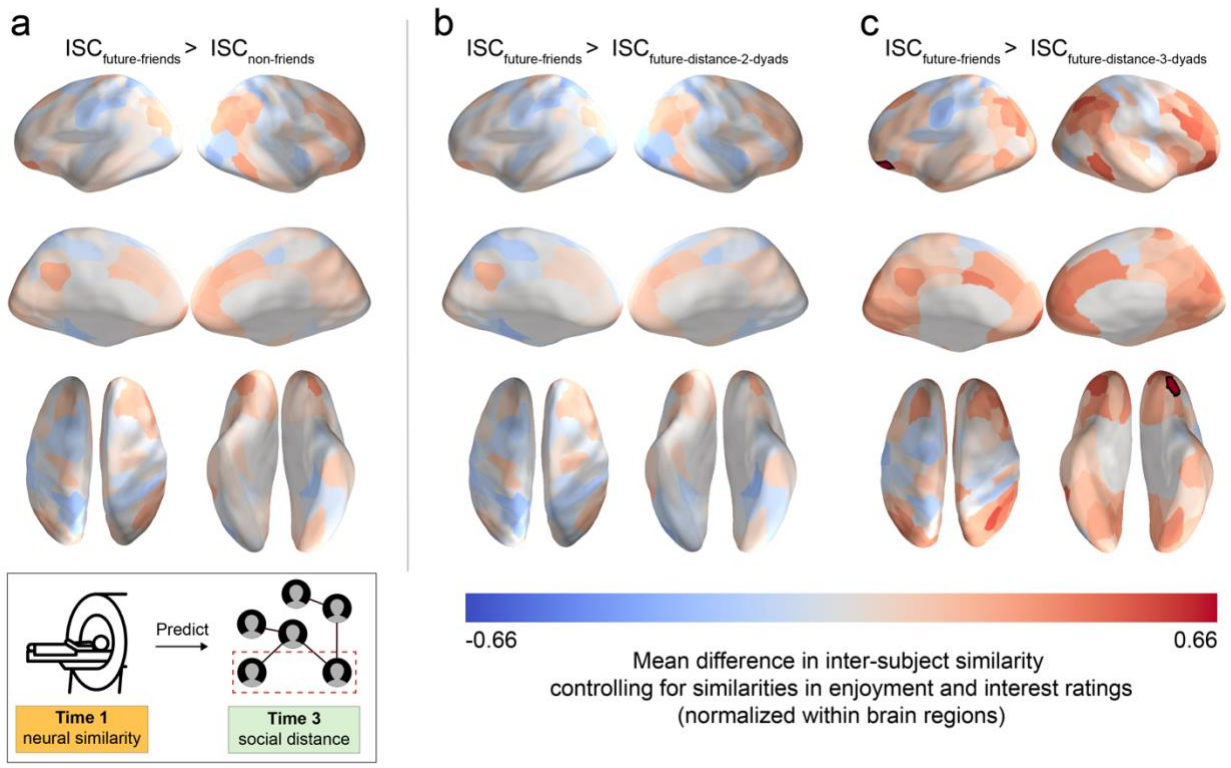

Appendix – Figure 6. People who became friends showed greater pre-existing neural similarity than those who ended up 3 "degrees of separation" from each other 8 months later when controlling for similarities in enjoyment and interest ratings. Data are overlaid on a cortical surface model. Warmer colors correspond to relatively greater mean neural similarity, and cooler colors correspond to relatively less mean neural similarity. (a) Null results were observed when testing if individuals who became friends exhibited greater pre-existing neural similarity relative to (b) individuals who did not become friends and (b) individuals who ended up 2 degrees of separation from each other. (c) Relative to individuals who ended up 3 degrees of separation from each other in the social network, individuals who became friends with each other showed greater pre-existing neural similarity in a portion of the left OFC ($p < 0.001$, FDR-corrected). Regions with significant differences for each contrast are outlined in black.

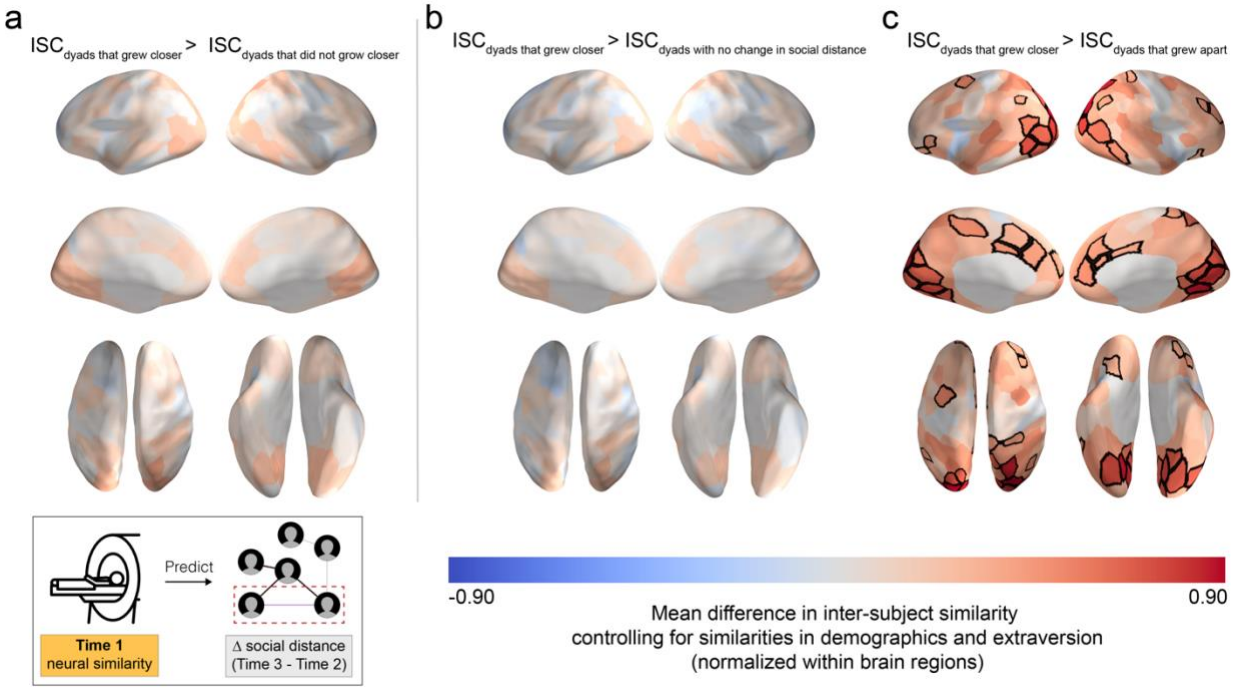

Appendix – Figure 7. Individuals who grew closer over time showed greater pre-existing similarity than individuals who grew farther apart over time when controlling for similarities in demographics. Data are overlaid on a cortical surface model. Warmer colors correspond to relatively greater mean neural similarity, and cooler colors correspond to relatively less mean neural similarity. For a given dyad, change in social distance over time was calculated by subtracting their social distance at Time 2 from their social distance at Time 3. Depending on these values, dyads were then placed into three categories depending on if their social distance increased, decreased, or remained the same (see Methods). Dyads whose social distance either increased over time or did not change were treated as a single category (i.e., dyads who did not grow closer). Individuals who grew closer over time (i.e., characterized by a decrease in social distance over time) did not exhibit significantly greater pre-existing neural similarity relative to **(a)** individuals that did not grow closer over time or **(b)** individuals whose social distance did not change. **(c)** Individuals who grew closer over time exhibited greater pre-existing neural similarity in regions spanning visual cortex, occipitotemporal cortex, superior parietal cortex, angular gyrus, medial frontal cortex, and lateral prefrontal cortex ($p < 0.05$, FDR-corrected) relative to individuals who grew apart over time. Regions with significant differences for each contrast are outlined in black.

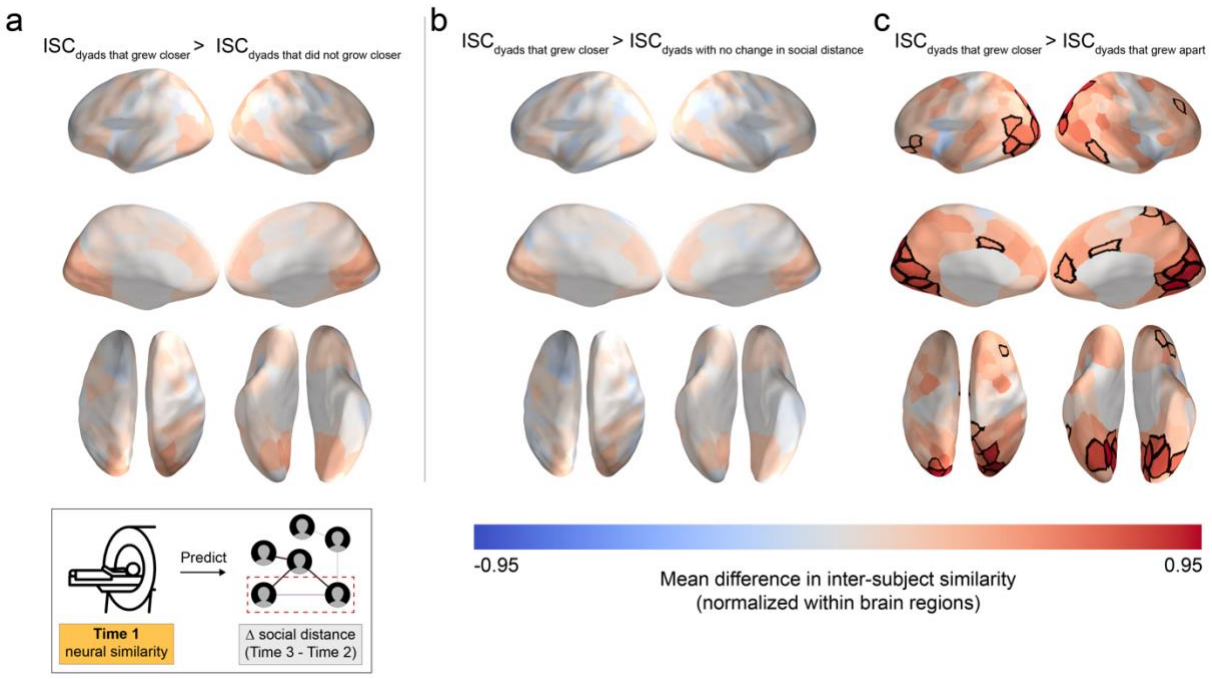

Appendix – Figure 8. Individuals who grew closer over time showed greater pre-existing similarity than individuals who grew farther apart over time when excluding dyads who knew each other prior to the neuroimaging session. Data are overlaid on a cortical surface model. Warmer colors correspond to relatively greater mean neural similarity, and cooler colors correspond to relatively less mean neural similarity. For a given dyad, change in social distance over time was calculated by subtracting their social distance at Time 2 from their social distance at Time 3. Depending on these values, dyads were then placed into three categories depending on if their social distance increased, decreased, or remained the same (see Methods). Dyads whose social distance either increased over time or did not change were treated as a single category (i.e., dyads who did not grow closer). Individuals who grew closer over time (i.e., characterized by a decrease in social distance over time) did not exhibit significantly greater pre-existing neural similarity relative to individuals **(a)** who did not grow closer over time or **(b)** whose social distance did not change. **(c)** Individuals who grew closer over time exhibited greater pre-existing neural similarity in regions spanning visual cortex, occipitotemporal cortex, superior parietal cortex, angular gyrus, medial frontal cortex, and lateral prefrontal cortex ($p < 0.05$, FDR-corrected) relative to individuals who grew apart over time. Regions with significant differences for each contrast are outlined in black.

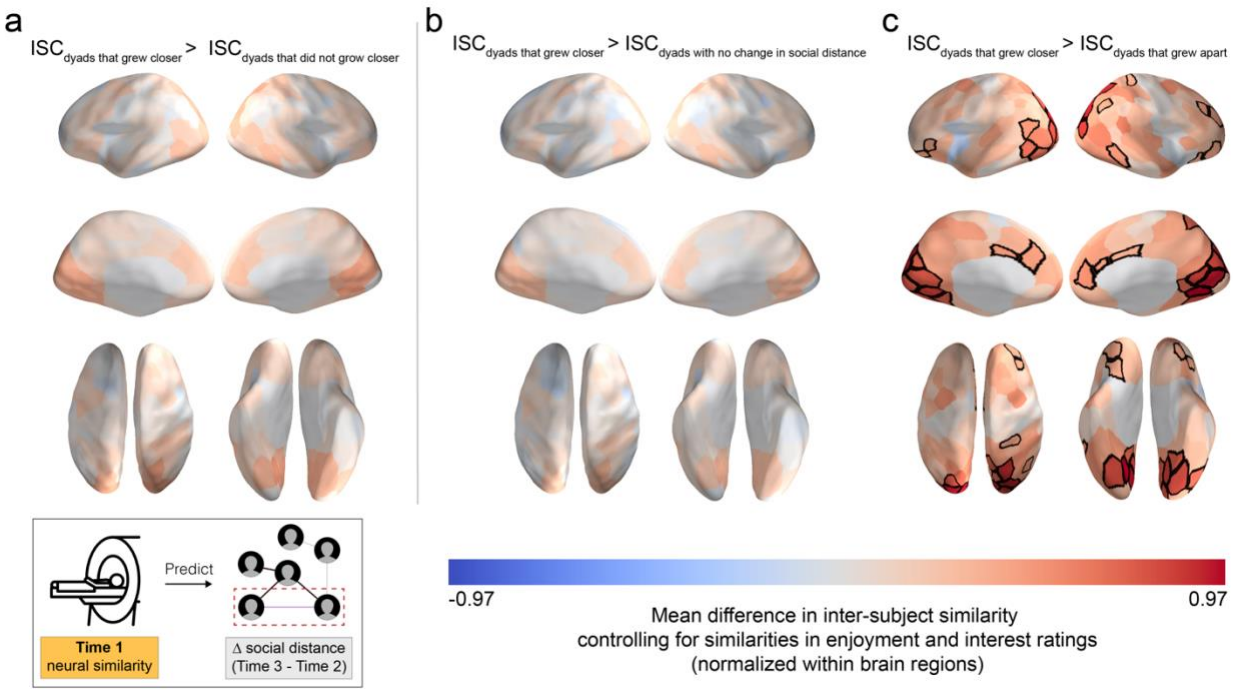

Appendix – Figure 9. Individuals who grew closer over time showed greater pre-existing similarity than individuals who grew farther apart over time when controlling for similarities in enjoyment and interest ratings. Data are overlaid on a cortical surface model. Warmer colors correspond to relatively greater mean neural similarity, and cooler colors correspond to relatively less mean neural similarity. For a given dyad, change in social distance over time was calculated by subtracting their social distance at Time 2 from their social distance at Time 3. Depending on these values, dyads were then placed into three categories depending on if their social distance increased, decreased, or remained the same (see Methods). Dyads whose social distance either increased over time or did not change were treated as a single category (i.e., dyads who did not grow closer). Individuals who grew closer over time (i.e., characterized by a decrease in social distance over time) did not exhibit significantly greater pre-existing neural similarity relative to **(a)** individuals that did not grow closer over time or **(b)** individuals whose social distance did not change. **(c)** Individuals who grew closer over time exhibited greater pre-existing neural similarity in regions spanning visual cortex, occipitotemporal cortex, superior parietal cortex, angular gyrus, medial frontal cortex, and lateral prefrontal cortex ($p < 0.05$, FDR-corrected) relative to individuals who grew apart over time. Regions with significant differences for each contrast are outlined in black.

Appendix – Table 1. Summary of video clips shown in the fMRI study

Clip		Description	Duration (s)
1	'An Astronaut's View of Earth'	An astronaut discusses viewing Earth from space, and in particular, witnessing the effects of climate change from space. He then urges viewers to mobilize to address this issue.	223
2	Google Glass review	A journalist wears a Google Glass headset for a day and weighs the pros and cons of being an 'early adopter' of this technology.	88
3	'Crossfire'	Two journalists debate the appropriateness of President Obama's use of humor in a speech; excerpts from the speech are shown.	89
4	'All I Want'	A sentimental music video depicting a social outcast with a facial deformity seeking companionship.	305
5	Wedding film	A homemade film depicting scenes from two men's wedding ceremony and subsequent celebration with family and friends.	120
6	Scientific demonstration	An astronaut at the International Space Station demonstrates and explains what happens when one wrings out a waterlogged washcloth in space.	118
7	'Food Inc.'	An excerpt from a documentary discussing how the fast food industry influences food production and farming practices in the United States.	178
8	'We Can Be Heroes'	An excerpt from a mockumentary-style series in which a man discusses why he nominated himself for the title of Australian of the Year.	202
9	'Ban College Football'	Journalists and athletes debate whether or not football should be banned as a college sport.	195
10	Soccer match	Highlights from a soccer match.	91
11	Baby sloth sanctuary	A documentary about caring for baby sloths at a sanctuary in Costa Rica.	200
12	'Ew!'	A comedy skit in which grown men play teenage girls disgusted by things around them.	169
13	'Life's Too Short'	An example of 'cringe comedy' in which a dramatic actor is depicted unsuccessfully trying his hand at improvisational comedy.	106
14	'America's Funniest Home Videos'	A series of homemade video clips depicting examples of unintentional physical comedy arising from accidents.	101

Table adapted from Parkinson et al. (2018).

General Discussion

Summary

The research in this dissertation integrates methods from multimodal neuroimaging, social network analysis, and machine learning to investigate how the brain shapes and is shaped by real-world social networks. The current results shed light on the types of neurocognitive functioning that may be unique to individuals that occupy positions of centrality and brokerage in their social network. Furthermore, this research demonstrates that inter-individual similarities in patterns of whole-brain resting-state functional connectivity are predictive of how close people are in their social network. Finally, these results suggest that pre-existing similarities in individuals' neural responses to naturalistic stimuli are predictive of not only future friendship formation but also whether friendship persists or dissolves over time.

The first study, presented in Chapter 1, leveraged structural neuroimaging to characterize multivariate patterns of white matter microstructural integrity within four key brain networks supporting socio-affective functioning. Using machine learning, we demonstrated that patterns of white matter microstructural integrity distributed across brain networks implicated in affective and mirroring processes were predictive of individuals' eigenvector centrality and brokerage in their social network. These results suggest that neurocognitive processes supporting the perception and processing of emotions and those that underpin the self-regulation of behavior to adapt to social circumstances may be particularly unique to individuals that are highly popular and to individuals that serve as social brokers, connecting otherwise unconnected individuals. These results provide novel insight into the socio-affective functioning that may particularly characteristic of individuals that occupy social network positions associated with social prestige, popularity, and leverage.

The second study, presented in Chapter 2, investigated whether people closer together in their social network were characterized by more similar resting-state brain activity. Using machine learning, we demonstrated that inter-individual similarities in whole-brain resting-state functional connectomes were predictive of inter-individual social network proximity in their social network. Our machine learning algorithm successfully used inter-individual similarity in functional connectomes to predict inter-individual social network proximity, whether social network proximity was weighted by emotional closeness ratings, communication frequency, or in-person meeting frequency. Furthermore, the positive relationship between inter-individual neural similarity and social network proximity was moderated by inter-individual geographic proximity, suggesting that the relationship between neural similarity and social network proximity was particularly robust among individuals that lived closer to each other. Taken together, these results demonstrate that people closer together in their social network share exceptionally similar resting-state brain activity and that this relationship varies as a function of inter-individual geographic distance.

The third study, presented in Chapter 3, demonstrates that pre-existing inter-individual similarities in neural responses to watching naturalistic stimuli was predictive of friendship formation eight months later. These pre-existing neural similarities were predominantly localized to brain networks in which neural similarity has previously been shown to be linked to shared understanding and interpretation of complex narratives. Thus, the current results suggest that pre-existing similarities in how individuals more generally think about the world around them may, in part, determine whether they become friends in the future. Furthermore, we also examined how inter-individual social distance changed over time due to the formation, persistence, and dissolution of friendships. Individuals that grew closer in social ties over time were characterized

by greater pre-existing neural similarity relative to individuals that grew apart, suggesting that pre-existing neural similarity may capture "deeper" interpersonal compatibilities that give rise to longer-lasting friendships and friendships that may form over longer periods of time, in contrast to friendships that may initially form out of mere circumstance. Taken together, these results provide shed light on the role of neural homophily in shaping social networks, whereby pre-existing neural similarities causally predict friendship and whether friendships form, persist, or dissolve over time.

Future directions

Although the study presented in Chapter 3 provides evidence that pre-existing neural similarities predict future friendship, further research is needed to investigate the role of social influence in shaping social networks, whereby inter-individual neural similarity may increase over the course of friendship. As discussed in Chapter 3, this study attempted to collect fMRI data at two timepoints to investigate whether friendship predicts increased neural similarity over time. However, due to limitations imposed by the COVID-19 pandemic, we were unable to collect a second round of fMRI data to test this hypothesis. Future studies leveraging longitudinal fMRI data collection can further shed light on the role of neural homophily and social influence and on the extent to which these mechanisms interact to shape social networks.

Furthermore, similar longitudinal designs can be leveraged to test whether pre-existing individual differences in white matter microstructural integrity are predictive of individuals' future social network position characteristics (e.g., eigenvector centrality, brokerage) and whether the occupation of particular social network positions is predictive of future changes in neural structure and function. Although the study presented in Chapter 1 demonstrated that

patterns of white matter microstructural integrity distributed across brain systems supporting socio-affective functioning were predictive of individuals' social network position characteristics, this finding was derived from cross-sectional data. Longitudinal research would make significant contributions to our understanding of how neurocognitive processes and associated sociobehavioral tendencies may be particularly advantageous for attaining various positions of centrality and brokerage. Such work would also advance our understanding of how the brain's neural structure and function may change in order to meet the heightened socio-cognitive demands of occupying positions of centrality and brokerage.

Future work may also benefit from incorporating multimodal neuroimaging data into models used to predict individual differences in social network position characteristics. Although the study presented in Chapter 1 provides a proof-of-concept for using structurally-derived neuroimaging features to predict social network position characteristics, including functionally-derived neuroimaging features (e.g., features extracted from fMRI responses to highly controlled tasks or naturalistic stimuli) in addition to structurally-derived neuroimaging features (i.e., multimodal feature fusion; Zhu et al. 2015; Calhoun and Sui 2016) can boost the accuracy of models used to predict individuals social network position characteristics. Moreover, the inclusion of features derived from fMRI neural responses may also facilitate the interpretation of such models, particularly in cases where these neural responses are evoked by highly controlled paradigms designed to elicit particular neurocognitive functions (e.g., mentalizing). Furthermore, a similar multimodal fusion approach can be used to improve the performance and interpretation of models used to predict inter-individual social network proximity (e.g., friendship) based on unimodal features alone, such as the model used in the study described in Chapter 2 of this dissertation.

The studies described in this dissertation shed light on the individual differences in brain structure and associated neurocognitive processes that are linked to particular social network position characteristics and on the types of inter-individual neural similarities that are associated with and predict friendship in the real world. Taken together, this work provides proof-of-concept for the utility of using a multi-method approach (e.g., social network analysis, structural and functional neuroimaging) to examine the complex relationship between individual differences in the brain and social network structure and the utility of longitudinal study design to investigate how individual differences in the brain relate to changes in social network structure over time. However, the current research constitutes only a small portion of the nascent but rapidly growing field that has continued to integrate tools from social psychology, cognitive neuroscience, and social network analysis to examine how an individual's brain is remarkably influenced by direct and indirect social relationships and how an individual can also exert influence that propagates throughout a social network to effect change in the brains of others. Future work should strive to conduct further longitudinal studies and multimodal neuroimaging to advance our understanding of how the brain shapes is shaped by real-world social networks.

References

Aiken, L. S., & West, S. G. (1991). *Multiple regression: Testing and interpreting interactions.* SAGE Publications Inc.

Alt, N. P., Parkinson, C., Kleinbaum, A. M., & Johnson, K. L. (2021). The face of social networks: Naive observers' accurate assessment of others' social network positions from faces. *Social Psychological and Personality Science*. http://journals.sagepub.com/doi/10.1177/19485506211003723

Anderson, C., Keltner, D., & John, O. P. (2003). Emotional convergence between people over time. *Journal of Personality and Social Psychology*, *84*(5), 1054–1068. https://doi.org/10.1037/0022-3514.84.5.1054

Apicella, C. L., Marlowe, F. W., Fowler, J. H., & Christakis, N. A. (2012). Social networks and cooperation in hunter-gatherers. *Nature*, *481*(7382), 497–501. https://doi.org/10.1038/nature10736

Apps, M. A. J., Rushworth, M. F. S., & Chang, S. W. C. (2016). The anterior cingulate gyrus and social cognition: Tracking the motivation of others. *Neuron*, *90*(4), 692. https://doi.org/10.1016/J.NEURON.2016.04.018

Asendorpf, J. B., & Wilpers, S. (1998). Personality effects on social relationships. *Journal of Personality and Social Psychology*, *74*(6), 1531–1544. https://doi.org/10.1037/0022-3514.74.6.1531

Baek, E. C., Hyon, R., López, K., Finn, E. S., Porter, M. A., & Parkinson, C. (2022). In-degree centrality in a social network is linked to coordinated neural activity. *Nature Communications 2022 13:1*, *13*(1), 1–13. https://doi.org/10.1038/s41467-022-28432-3

Baek, E. C., Porter, M. A., & Parkinson, C. (2021). Social network analysis for social

neuroscientists. *Social Cognitive and Affective Neuroscience*, *16*(8). https://academic.oup.com/scan/article/16/8/883/5838123

Báez-Mendoza, R., Vázquez, Y., Mastrobattista, E. P., & Williams, Z. M. (2021). Neuronal circuits for social decision-making and their clinical implications. *Frontiers in Neuroscience*, *15*, 1291. https://doi.org/10.3389/FNINS.2021.720294/BIBTEX

Ballinger, G. A., Cross, R., & Holtom, B. C. (2016). The right friends in the right places: Understanding network structure as a predictor of voluntary turnover. *The Journal of Applied Psychology*, *101*(4), 535–548. https://doi.org/10.1037/APL0000061

Banissy, M. J., Kanai, R., Walsh, V., & Rees, G. (2012). Inter-individual differences in empathy are reflected in human brain structure. *NeuroImage*, *62*(3), 2034–2039. https://doi.org/10.1016/J.NEUROIMAGE.2012.05.081

Barrett, L. F., Lewis, M., & Haviland-Jones, J. M. (2016). *Handbook of Emotions*. Guilford Publications.

Basyouni, R., & Parkinson, C. (2022). Mapping the social landscape: tracking patterns of interpersonal relationships. *Trends in Cognitive Sciences*, *26*(3), 204–221. https://doi.org/10.1016/J.TICS.2021.12.006

Bates, D., Mächler, M., Bolker, B. M., & Walker, S. C. (2015). Fitting linear mixed-effects models using lme4. *Journal of Statistical Software*, *67*(1), 1–48. https://doi.org/10.18637/jss.v067.i01

Baumgartner, T., Nash, K., Hill, C., & Knoch, D. (2015). Neuroanatomy of intergroup bias: A white matter microstructure study of individual differences. *NeuroImage*, *122*, 345–354. https://doi.org/10.1016/j.neuroimage.2015.08.011

Beaty, R. E., Kenett, Y. N., Christensen, A. P., Rosenberg, M. D., Benedek, M., Chen, Q., Fink,

A., Qiu, J., Kwapil, T. R., Kane, M. J., & Silvia, P. J. (2018). Robust prediction of individual creative ability from brain functional connectivity. *Proceedings of the National Academy of Sciences of the United States of America*, *115*(5), 1087–1092. https://pubmed.ncbi.nlm.nih.gov/29339474/

Beaulieu, C. (2002). The basis of anisotropic water diffusion in the nervous system - A technical review. *NMR in Biomedicine*, *15*, 435–455. https://doi.org/10.1002/nbm.782

Behrens, T., Berg, H. J., Jbabdi, S., Rushworth, M. F. S., & Woolrich, M. W. (2007). Probabilistic diffusion tractography with multiple fibre orientations: What can we gain? *NeuroImage*, *34*(1), 144–155. https://doi.org/10.1016/j.neuroimage.2006.09.018

Behrens, T., Hunt, L., Woolrich, M., & Rushworth, M. (2008). Associative learning of social value. *Nature*, *456*(7219), 245–249. https://doi.org/10.1038/nature07538

Behrens, T., Woolrich, M. W., Jenkinson, M., Johansen-Berg, H., Nunes, R. G., Clare, S., Matthews, P. M., Brady, J. M., & Smith, S. M. (2003). Characterization and propagation of uncertainty in diffusion-weighted MR imaging. *Magnetic Resonance in Medicine*, *50*(5), 1077–1088. https://pubmed.ncbi.nlm.nih.gov/14587019/

Berger, C. R., & Calabrese, R. J. (1975). Some explorations in initial interaction and beyond: Toward a developmental theory of interpersonal communication. *Human Communication Research*, *1*(2), 99–112. https://doi.org/10.1111/j.1468-2958.1975.tb00258.x

Bickart, K. C., Hollenbeck, M. C., Barrett, L. F., & Dickerson, B. C. (2012). Intrinsic amygdala–cortical functional connectivity predicts social network size in humans. *The Journal of Neuroscience*, *32*(42), 14729. https://doi.org/10.1523/JNEUROSCI.1599-12.2012

Bickart, K. C., Wright, C. I., Dautoff, R. J., Dickerson, B. C., & Barrett, L. F. (2011). Amygdala volume and social network size in humans. *Nature Neuroscience*, *14*(2), 163.

https://doi.org/10.1038/NN.2724

Bolis, D., Balsters, J., Wenderoth, N., Becchio, C., & Schilbach, L. (2017). Beyond autism: Introducing the Dialectical Misattunement Hypothesis and a Bayesian account of intersubjectivity. In *Psychopathology* (Vol. 50, Issue 6, pp. 355–372). S. Karger AG. https://doi.org/10.1159/000484353

Bonacich, P. (1972). Factoring and weighting approaches to status scores and clique identification. *The Journal of Mathematical Sociology*, *2*(1), 113–120. https://doi.org/10.1080/0022250X.1972.9989806

Bonacich, P. (1987). Power and centrality: A family of measures. *American Journal of Sociology*, *92*(5), 1170–1182. https://doi.org/10.1086/228631

Bond, R. M., Fariss, C. J., Jones, J. J., Kramer, A. D. I., Marlow, C., Settle, J. E., & Fowler, J. H. (2012). A 61-million-person experiment in social influence and political mobilization. *Nature*, *489*(7415), 295–298. https://doi.org/10.1038/nature11421

Bottenhorn, K. L., Flannery, J. S., Boeving, E. R., Riedel, M. C., Eickhoff, S. B., Sutherland, M. T., & Laird, A. R. (2019). Cooperating yet distinct brain networks engaged during naturalistic paradigms: A meta-analysis of functional MRI results. *Network Neuroscience*, *3*(1), 27. https://doi.org/10.1162/NETN_A_00050

Brakefield, T. A., Mednick, S. C., Wilson, H. W., De Neve, J. E., Christakis, N. A., & Fowler, J. H. (2014). Same-sex sexual attraction does not spread in adolescent social networks. *Archives of Sexual Behavior*, *43*(2), 335–344. https://doi.org/10.1007/S10508-013-0142-9

Brass, D. J. (1984). Being in the right place: A structural analysis of individual influence in an organization. *Administrative Science Quarterly*, *29*(4), 518. https://doi.org/10.2307/2392937

Brent, L. J. N. (2015). Friends of friends: are indirect connections in social networks important to

animal behaviour? *Animal Behaviour*, *103*, 211–222. https://doi.org/10.1016/J.ANBEHAV.2015.01.020

Brent, L. J. N., Heilbronner, S. R., Horvath, J. E., Gonzalez-Martinez, J., Ruiz-Lambides, A., Robinson, A. G., Pate Skene, J. H., & Platt, M. L. (2013). Genetic origins of social networks in rhesus macaques. *Scientific Reports*, *3*(1), 1–8. https://doi.org/10.1038/srep01042

Brewer, D. D. (2000). Forgetting in the recall-based elicitation of personal and social networks. *Social Networks*, *22*(1), 29–43. https://doi.org/10.1016/S0378-8733(99)00017-9

Brewer, D. D., & Garrett, S. B. (2001). Evaluation of interviewing techniques to enhance recall of sexual and drug injection partners. *Sexually Transmitted Diseases*, *28*(11), 666–677. https://doi.org/10.1097/00007435-200111000-00010

Bukowski, H., Tik, M., Silani, G., Ruff, C. C., Windischberger, C., & Lamm, C. (2020). When differences matter: rTMS/fMRI reveals how differences in dispositional empathy translate to distinct neural underpinnings of self-other distinction in empathy. *Cortex*, *128*, 143–161. https://doi.org/10.1016/J.CORTEX.2020.03.009

Burt, R. (1984). Network items and the general social survey. *Social Networks*, *6*(4), 293–339. https://doi.org/10.1016/0378-8733(84)90007-8

Burt, R. (1994). Structural holes: The social structure of competition. In *Networks and Organizations: Structure, Form, and Action*. Harvard University Press. https://doi.org/10.1177/0265407512465997

Burt, R. (1997). The contingent value of social capital. *Administrative Science Quarterly*, *42*(2), 339–365. https://doi.org/10.2307/2393923

Burt, R. (2004). Structural holes and good ideas. *American Journal of Sociology*, *110*(2), 349–

399. https://doi.org/10.1086/421787

Burt, R. (2012). Network-related personality and the agency question: Multirole evidence from a virtual world. *American Journal of Sociology*, *118*(3), 543–591. https://doi.org/10.1086/667856

Burt, R. (2015). Reinforced structural holes. *Social Networks*, *43*, 149–161. https://doi.org/10.1016/J.SOCNET.2015.04.008

Burt, R., Kilduff, M., & Tasselli, S. (2013). Social network analysis: Foundations and frontiers on advantage. *Annual Review of Psychology*, *64*(1), 527–547. https://doi.org/10.1146/annurev-psych-113011-143828

Butler, E. A. (2015). Interpersonal affect dynamics: It takes two (and time) to tango. *Emotion Review*, *7*(4), 336–341. https://doi.org/10.1177/1754073915590622

Cabeza, R., Ciaramelli, E., Olson, I. R., & Moscovitch, M. (2008). The parietal cortex and episodic memory: an attentional account. *Nature Reviews Neuroscience 2008 9:8*, *9*(8), 613–625. https://doi.org/10.1038/nrn2459

Cacioppo, J. T., Fowler, J. H., & Christakis, N. A. (2009). Alone in the crowd: The structure and spread of loneliness in a large social network. *Journal of Personality and Social Psychology*, *97*(6), 977–991. https://doi.org/10.1037/a0016076

Cantlon, J. F., & Li, R. (2013). Neural activity during natural viewing of sesame street statistically predicts test scores in early childhood. *PLoS Biology*, *11*(1), e1001462. https://doi.org/10.1371/journal.pbio.1001462

Casciaro, T. (1998). Seeing things clearly: social structure, personality, and accuracy in social network perception. *Social Networks*, *20*(4), 331–351. https://doi.org/10.1016/S0378-8733(98)00008-2

Cattuto, C., Van den Broeck, W., Barrat, A., Colizza, V., Pinton, J.-F., & Vespignani, A. (2010). Dynamics of person-to-person interactions from distributed RFID sensor networks. *PLoS ONE*, *5*(7), e11596. https://doi.org/10.1371/journal.pone.0011596

Cetron, J. S., Connolly, A. C., Diamond, S. G., May, V. V., Haxby, J. V., & Kraemer, D. J. M. (2019). Decoding individual differences in STEM learning from functional MRI data. *Nature Communications 2019 10:1*, *10*(1), 1–10. https://doi.org/10.1038/s41467-019-10053-y

Chavez, R. S., & Heatherton, T. F. (2015). Multimodal frontostriatal connectivity underlies individual differences in self-esteem. *Social Cognitive and Affective Neuroscience*, *10*(3), 364–370. https://doi.org/10.1093/scan/nsu063

Chen, G., Taylor, P. A., Shin, Y. W., Reynolds, R. C., & Cox, R. W. (2017). Untangling the relatedness among correlations, Part II: Inter-subject correlation group analysis through linear mixed-effects modeling. *NeuroImage*, *147*, 825–840. https://doi.org/10.1016/j.neuroimage.2016.08.029

Chen, P. H. A., Jolly, E., Cheong, J. H., & Chang, L. J. (2020). Intersubject representational similarity analysis reveals individual variations in affective experience when watching erotic movies. *NeuroImage*, *216*. https://doi.org/10.1016/J.NEUROIMAGE.2020.116851

Chey, J. (2007). Elderly memory disorder scale. *Seoul: Hakjisa*.

Christakis, N. A., & Fowler, J. H. (2007). The spread of obesity in a large social network over 32 years. *New England Journal of Medicine*, *357*(4), 370–379. https://doi.org/10.1056/NEJMsa066082

Christakis, N. A., & Fowler, J. H. (2008). The collective dynamics of smoking in a large social network. *New England Journal of Medicine*, *358*(21), 2249–2258.

https://doi.org/10.1056/NEJMsa0706154

Christakis, N. A., & Fowler, J. H. (2009). *Connected: The Surprising Power of Our Social Networks and How They Shape Our Lives*. Little, Brown and Co.

Christakis, N. A., & Fowler, J. H. (2013). Social contagion theory: Examining dynamic social networks and human behavior. *Statistics in Medicine*, *32*(4), 556–577. https://pubmed.ncbi.nlm.nih.gov/22711416/

Christoff, K., Irving, Z. C., Fox, K. C. R., Spreng, R. N., & Andrews-Hanna, J. R. (2016). Mind-wandering as spontaneous thought: a dynamic framework. *Nature Reviews Neuroscience 2016 17:11*, *17*(11), 718–731. https://doi.org/10.1038/nrn.2016.113

Christov-Moore, L., Reggente, N., Douglas, P. K., Feusner, J. D., & Iacoboni, M. (2020). Predicting empathy from resting state brain connectivity: A multivariate approach. *Frontiers in Integrative Neuroscience*, *14*, 3.

Cialdini, R. B., & Goldstein, N. J. (2004). Social influence: Compliance and conformity. *Annual Review of Psychology*, *55*(1), 591–621. https://doi.org/10.1146/annurev.psych.55.090902.142015

Clore, G. L., & Byrne, D. A. (1974). A reinforcement-affect model of attraction. In *Foundations of Interpersonal Attraction* (pp. 143–165). Academic Press.

Cohen, J., Cohen, P., West, S. G., & Aiken, L. S. (2003). *Applied multiple regression/correlation analysis for the behavioral sciences* (3rd ed.). Lawrence Erlbaum Associates Pulbishers.

Cole, M. W., Yarkoni, T., Repovš, G., Anticevic, A., & Braver, T. S. (2012). Global connectivity of prefrontal cortex predicts cognitive control and intelligence. *Journal of Neuroscience*, *32*(26), 8988–8999. https://doi.org/10.1523/JNEUROSCI.0536-12.2012

Corbetta, M., & Shulman, G. L. (2002). Control of goal-directed and stimulus-driven attention in

the brain. *Nature Reviews Neuroscience 2002 3:3*, *3*(3), 201–215. https://doi.org/10.1038/nrn755

Corr, P. J., & Mobbs, D. (2018). From epiphenomenon to biologically important phenomena. *Personality Neuroscience*, *1*. https://doi.org/10.1017/PEN.2017.1

Courtney, A., Baltiansky, D., Fang, W., Roshanaei, M., Aybas, Y., Samuels, N., Wetchler, E., Wu, Z., Jackson, M. O., & Zaki, J. (2021). Social microclimates and well-being. *PsyArXiv*. https://doi.org/10.31234/OSF.IO/PHA3J

Courtney, A. L., Rapuano, K. M., Sargent, J. D., Heatherton, T. F., & Kelley, W. M. (2018). Reward system activation in response to alcohol advertisements predicts college drinking. *Journal of Studies on Alcohol and Drugs*, *79*(1), 29. https://doi.org/10.15288/JSAD.2018.79.29

Csárdi, G., & Nepusz, T. (2014). The igraph software package for complex network research. *InterJournal Complex Systems*, 1695. https://doi.org/10.3724/SP.J.1087.2009.02191

Cutting, A. L., & Dunn, J. (1999). Theory of mind, emotion understanding, language, and family background: Individual differences and interrelations. *Child Development*, *70*(4), 853–865. https://doi.org/10.1111/1467-8624.00061

Cvitanovic, C., Cunningham, R., Dowd, A. M., Howden, S. M., & van Putten, E. I. (2017). Using social network analysis to monitor and assess the effectiveness of knowledge brokers at connecting scientists and decision-makers: An australian case study. *Environmental Policy and Governance*, *27*(3), 256–269. https://doi.org/10.1002/eet.1752

D'Onofrio, P., Norman, L. J., Sudre, G., White, T., & Shaw, P. (2021). The anatomy of friendship: Neuroanatomic homophily of the social brain among classroom friends. *Cerebral Cortex*. https://doi.org/10.1093/CERCOR/BHAB398

Davis, J. L., & Rusbult, C. E. (2001). Attitude alignment in close relationships. *Journal of Personality and Social Psychology*, *81*(1), 65–84. https://doi.org/10.1037//0022-3514.81.1.65

de Waal, F. B. M. (2007). *On Being Moved: From Mirror Neurons to Empathy* (Braten, S.). John Benjamins.

Decety, J. (2011). Dissecting the neural mechanisms mediating empathy. *Emotion Review*, *3*(1), 92–108. https://doi.org/10.1177/1754073910374662

Decety, J., & Jackson, P. L. (2004). The functional architecture of human empathy. *Behavioral and Cognitive Neuroscience Reviews*, *3*(2), 71–100. https://doi.org/10.1177/1534582304267187

Decety, J., & Lamm, C. (2007). The role of the right temporoparietal junction in social interaction: How low-level computational processes contribute to meta-cognition. *Neuroscientist*, *13*(6), 580–593. https://doi.org/10.1177/1073858407304654

Desikan, R. S., Ségonne, F., Fischl, B., Quinn, B. T., Dickerson, B. C., Blacker, D., Buckner, R. L., Dale, A. M., Maguire, R. P., Hyman, B. T., Albert, M. S., & Killiany, R. J. (2006). An automated labeling system for subdividing the human cerebral cortex on MRI scans into gyral based regions of interest. *NeuroImage*, *31*(3), 968–980. https://doi.org/10.1016/j.neuroimage.2006.01.021

DeYoung, C. G., Hirsh, J. B., Shane, M. S., Papademetris, X., Rajeevan, N., & Gray, J. R. (2010). Testing predictions from personality neuroscience: Brain structure and the big five. *Psychological Science*, *21*(6). https://doi.org/10.1177/0956797610370159

Dietvorst, R. C., Verbeke, W. J. M. I., Bagozzi, R. P., Yoon, C., Smits, M., & Van Der, L. (2009). A sales force-specific theory-of-mind scale: Tests of its validity by classical

methods and functional magnetic resonance imaging. *Journal of Marketing Research*, *46*(5), 653–668. https://doi.org/10.1509/jmkr.46.5.653

Dijksterhuis, A. (2004). Think different: The merits of unconscious thought in preference development and decision making. *Journal of Personality and Social Psychology*, *87*(5), 586–598. https://doi.org/10.1037/0022-3514.87.5.586

Dijkstra, E. W. (1959). A note on two problems in connexion with graphs. *Numerische Mathematik*, *1*(1), 269–271. https://doi.org/10.1007/BF01386390

Dixon, M. L., De La Vega, A., Mills, C., Andrews-Hanna, J., Spreng, R. N., Cole, M. W., & Christoff, K. (2018). Heterogeneity within the frontoparietal control network and its relationship to the default and dorsal attention networks. *Proceedings of the National Academy of Sciences of the United States of America*. https://doi.org/10.1073/pnas.1715766115

Dubois, J., & Adolphs, R. (2016). Building a science of individual differences from fMRI. *Trends in Cognitive Sciences*, *20*(6), 425–443. https://doi.org/10.1016/J.TICS.2016.03.014

Dubois, J., Galdi, P., Han, Y., Paul, L. K., & Adolphs, R. (2018). Resting-state functional brain connectivity best predicts the personality dimension of openness to experience. *Personality Neuroscience*, *1*. https://pubmed.ncbi.nlm.nih.gov/30225394/

Dufour, N., Redcay, E., Young, L., Mavros, P. L., Moran, J. M., Triantafyllou, C., Gabrieli, J. D. E., & Saxe, R. (2013). Similar Brain Activation during False Belief Tasks in a Large Sample of Adults with and without Autism. *PLOS ONE*, *8*(9), e75468. https://doi.org/10.1371/JOURNAL.PONE.0075468

Dunbar, R. I. M. (1993). Coevolution of neocortical size, group size and language in humans. *Behavioral and Brain Sciences*, *16*(4), 681–694.

https://doi.org/10.1017/S0140525X00032325

Dunbar, R. I. M. (2003). The social brain: Mind, language, and society in evolutionary perspective. *Annual Review of Anthropology*, *32*, 163–181. https://doi.org/10.1146/ANNUREV.ANTHRO.32.061002.093158

Dunbar, R. I. M. (2021). *Friends: Understanding the Power of our Most Important Relationships*. Little, Brown and Co.

Ellwardt, L., Labianca, G. J., & Wittek, R. (2012). Who are the objects of positive and negative gossip at work? A social network perspective on workplace gossip. *Social Networks*, *34*(2), 193–205. https://doi.org/10.1016/j.socnet.2011.11.003

Erdley, C. A., & Day, H. J. (2017). Friendship in childhood and adolescence. In *The Psychology of Friendship* (pp. 3–19). Oxford University Press.

Eres, R., Decety, J., Louis, W. R., & Molenberghs, P. (2015). Individual differences in local gray matter density are associated with differences in affective and cognitive empathy. *NeuroImage*, *117*, 305–310. https://doi.org/10.1016/J.NEUROIMAGE.2015.05.038

Esteban, O., Markiewicz, C. J., Blair, R. W., Moodie, C. A., Isik, A. I., Erramuzpe, A., Kent, J. D., Goncalves, M., DuPre, E., Snyder, M., Oya, H., Ghosh, S. S., Wright, J., Durnez, J., Poldrack, R. A., & Gorgolewski, K. J. (2019). fMRIPrep: a robust preprocessing pipeline for functional MRI. *Nature Methods*, *16*, 111–116. https://doi.org/10.1038/s41592-018-0235-4

Everett, M. G., & Valente, T. W. (2016). Bridging, brokerage and betweenness. *Social Networks*, *44*, 202–208. https://doi.org/10.1016/J.SOCNET.2015.09.001

Falk, E. B., & Bassett, D. S. (2017). Brain and social networks: Fundamental building blocks of human experience. In *Trends in Cognitive Sciences* (Vol. 21, Issue 9, pp. 674–690).

Elsevier Ltd. https://doi.org/10.1016/j.tics.2017.06.009

Falk, E. B., Berkman, E. T., Mann, T., Harrison, B., & Lieberman, M. D. (2010). Predicting persuasion-induced behavior change from the brain. *Journal of Neuroscience*, *30*(25), 8421–8424. https://doi.org/10.1523/JNEUROSCI.0063-10.2010

Falk, E. B., Berkman, E. T., Whalen, D., & Lieberman, M. D. (2011). Neural activity during health messaging predicts reductions in smoking above and beyond self-report. *Health Psychology : Official Journal of the Division of Health Psychology, American Psychological Association*, *30*(2), 177. https://doi.org/10.1037/A0022259

Falk, E. B., Morelli, S. A., Welborn, B. L., Dambacher, K., & Lieberman, M. D. (2013). Creating buzz: the neural correlates of effective message propagation. *Psychological Science*, *24*(7), 1234–1242. https://doi.org/10.1177/0956797612474670

Fang, R., Landis, B., Zhang, Z., Anderson, M. H., Shaw, J. D., & Kilduff, M. (2015). Integrating personality and social networks: A meta-analysis of personality, network position, and work outcomes in organizations. *Organization Science*, *26*(4), 1243–1260. https://pubsonline.informs.org/doi/abs/10.1287/orsc.2015.0972

Fedorenko, E., Hsieh, P. J., Nieto-Castañón, A., Whitfield-Gabrieli, S., & Kanwisher, N. (2010). New method for fMRI investigations of language: defining ROIs functionally in individual subjects. *Journal of Neurophysiology*, *104*(2), 1177–1194. https://doi.org/10.1152/JN.00032.2010

Feiler, D. C., & Kleinbaum, A. M. (2015). Popularity, similarity, and the network extraversion bias. *Psychological Science*, *26*(5), 593–603. https://doi.org/10.1177/0956797615569580

Festinger, L., Schachter, S., & Back, K. (1950). *Social Pressures in Informal Groups*. Harper & Bros.

Finn, E. S., Corlett, P. R., Chen, G., Bandettini, P. A., & Constable, R. T. (2018). Trait paranoia shapes inter-subject synchrony in brain activity during an ambiguous social narrative. *Nature Communications*, *9*(1). https://doi.org/10.1038/s41467-018-04387-2

Finn, E. S., Scheinost, D., Finn, D. M., Shen, X., Papademetris, X., & Constable, R. T. (2017). Can brain state be manipulated to emphasize individual differences in functional connectivity? *NeuroImage*, *160*, 140–151. https://doi.org/10.1016/j.neuroimage.2017.03.064

Finn, E. S., Shen, X., Scheinost, D., Rosenberg, M. D., Huang, J., Chun, M. M., Papademetris, X., & Constable, R. T. (2015). Functional connectome fingerprinting: Identifying individuals using patterns of brain connectivity. *Nature Neuroscience*, *18*(11), 1664–1671. https://doi.org/10.1038/nn.4135

Fischl, B. (2012). FreeSurfer. *NeuroImage*, *62*(2), 774–781. https://doi.org/10.1016/J.NEUROIMAGE.2012.01.021

Fischl, B., Salat, D. H., Busa, E., Albert, M., Dieterich, M., Haselgrove, C., Van Der Kouwe, A., Killiany, R., Kennedy, D., Klaveness, S., Montillo, A., Makris, N., Rosen, B., & Dale, A. M. (2002). Whole brain segmentation: automated labeling of neuroanatomical structures in the human brain. *Neuron*, *33*(3), 341–355. https://doi.org/10.1016/S0896-6273(02)00569-X

Flynn, F. J., Reagans, R. E., Amanatullah, E. T., & Ames, D. R. (2006). Helping one's way to the top: Self-monitors achieve status by helping others and knowing who helps whom. *Journal of Personality and Social Psychology*, *91*(6), 1123–1137. https://doi.org/10.1037/0022-3514.91.6.1123

Fowler, J. H., & Christakis, N. A. (2009). Dynamic spread of happiness in a large social network: Longitudinal analysis over 20 years in the Framingham Heart Study. *BMJ*,

338(7685), 23–26. http://www.bmj.com/

Fowler, J. H., & Christakis, N. A. (2010). Cooperative behavior cascades in human social networks. *Proceedings of the National Academy of Sciences of the United States of America*, *107*(12), 5334–5338. https://doi.org/10.1073/pnas.0913149107

Fowler, J. H., Dawes, C. T., & Christakis, N. A. (2009). Model of genetic variation in human social networks. *Proceedings of the National Academy of Sciences of the United States of America*, *106*(6), 1720–1724. https://doi.org/10.1073/pnas.0806746106

Freeman, J. B., & Johnson, K. L. (2016). More than meets the eye: Split-second social perception. *Trends in Cognitive Sciences*, *20*(5), 362. https://doi.org/10.1016/j.tics.2016.03.003

Friston, K., Mattout, J., & Kilner, J. (2011). Action understanding and active inference. *Biological Cybernetics*, *104*(1–2), 137–160. https://doi.org/10.1007/s00422-011-0424-z

Fu, F., Nowak, M. A., Christakis, N. A., & Fowler, J. H. (2012). The evolution of homophily. *Scientific Reports*, *2*, 845. https://doi.org/10.1038/srep00845

Funder, D. C., & Harris, M. J. (1986). On the several facets of personality assessment: The case of social acuity. *Journal of Personality*, *54*(3), 528–550. https://doi.org/10.1111/j.1467-6494.1986.tb00411.x

Gonzaga, G. C., Campos, B., & Bradbury, T. (2007). Similarity, convergence, and relationship satisfaction in dating and married couples. *Journal of Personality and Social Psychology*, *93*(1), 34–48. https://doi.org/10.1037/0022-3514.93.1.34

Gould, R. V., & Fernandez, R. M. (1989). Structures of Mediation: A Formal Approach to Brokerage in Transaction Networks. *Sociological Methodology*, *19*, 89. https://doi.org/10.2307/270949

Green, M. F., Horan, W. P., Lee, J., McCleery, A., Reddy, L. F., & Wynn, J. K. (2018). Social disconnection in schizophrenia and the general community. *Schizophrenia Bulletin*, *44*(2), 242–249. https://doi.org/10.1093/schbul/sbx082

Gross, J. J. (2015). Emotion regulation: Current status and future prospects. *Psychological Inquiry*, *26*(1), 1–26. https://doi.org/10.1080/1047840X.2014.940781

Haberman, J., Brady, T. F., & Alvarez, G. A. (2015). Individual differences in ensemble perception reveal multiple, independent levels of ensemble representation. *Journal of Experimental Psychology. General*, *144*(2), 432–446. https://doi.org/10.1037/XGE0000053

Hahl, O., Kacperczyk, A., & Davis, J. P. (2016). Knowledge asymmetry and brokerage: Linking network perception to position in structural holes: *Strategic Organization*, *14*(2), 118–143. https://doi.org/10.1177/1476127015624274

Hampson, M., Driesen, N. R., Skudlarski, P., Gore, J. C., & Constable, R. T. (2006). Brain connectivity related to working memory performance. *The Journal of Neuroscience*, *26*(51), 13338–13343. https://doi.org/10.1523/JNEUROSCI.3408-06.2006

Hampton, W. H., Unger, A., Von Der Heide, R. J., & Olson, I. R. (2016). Neural connections foster social connections: A diffusion-weighted imaging study of social networks. *Social Cognitive and Affective Neuroscience*, *11*(5), 721–727.

Han, J., Kim, T., Jhoo, J., Park, J., Kim, K., Ryu, S., Moon, S., Choo, I., Lee, D., Yoon, J., Do, Y., Lee, S., & Kim, M. (2010). A normative study of the mini-mental state examination for dementia screening (MMSE-DS) and its short form (SMMSE-DS) in the korean elderly. *Journal of Korean Geriatric Psychiatry*, *14*(1), 27–37.

Hildebrandt, M. K., Jauk, E., Lehmann, K., Maliske, L., & Kanske, P. (2021). Brain activation during social cognition predicts everyday perspective-taking: A combined fMRI and

ecological momentary assessment study of the social brain. *NeuroImage*, *227*, 117624. https://doi.org/10.1016/J.NEUROIMAGE.2020.117624

Horien, C., Shen, X., Scheinost, D., & Constable, R. T. (2019). The individual functional connectome is unique and stable over months to years. *NeuroImage*, *189*, 676–687. https://doi.org/10.1016/j.neuroimage.2019.02.002

Hurlbert, J. S., Haines, V. A., & Beggs, J. J. (2000). Core networks and tie activation: What kinds of routine networks allocate resources in nonroutine situations? *American Sociological Review*, *65*(4), 598–618. https://doi.org/10.2307/2657385

Huxhold, O., Fiori, K. L., & Windsor, T. D. (2013). The dynamic interplay of social network characteristics, subjective well-being, and health: the costs and benefits of socio-emotional selectivity. *Psychology and Aging*, *28*(1), 3–16. https://doi.org/10.1037/A0030170

Hyon, R., Kleinbaum, A. M., & Parkinson, C. (2020). Social network proximity predicts similar trajectories of psychological states: Evidence from multi-voxel spatiotemporal dynamics. *NeuroImage*, *216*. https://doi.org/10.1016/j.neuroimage.2019.116492

Hyon, R., Youm, Y., Kim, J., Chey, J., Kwak, S., & Parkinson, C. (2020). Similarity in functional brain connectivity at rest predicts interpersonal closeness in the social network of an entire village. *Proceedings of the National Academy of Sciences*, *117*(52), 33149–33160. https://doi.org/10.1073/PNAS.2013606117

Iacoboni, M., Woods, R. P., Brass, M., Bekkering, H., Mazziotta, J. C., & Rizzolatti, G. (1999). Cortical mechanisms of human imitation. *Science*, *286*(5449), 2526–2528. https://doi.org/10.1126/science.286.5449.2526

Ickes, W., Stinson, L., Bissonnette, V., & Garcia, S. (1990). Naturalistic social cognition: Empathic accuracy in mixed-sex dyads. *Journal of Personality and Social Psychology*,

59(4), 730–742. https://doi.org/10.1037/0022-3514.59.4.730

Jackson, M. O. (2009). Genetic influences on social network characteristics. *Proceedings of the National Academy of Sciences*, *106*(6), 1687–1688. https://doi.org/10.1073/pnas.0813169106

Jackson, M. O., & Matthew O. Jackson. (2008). *Social and Economic Networks*. Princeton Univ Press.

John, O. P., Naumann, L. P., & Soto, C. J. (2008a). *Paradigm Shift to the Integrative Big-Five Trait Taxonomy: History, Measurement, and Conceptual Issues* (Oliver P. John, R. W. Robins, & L. A. Pervin (eds.)). Guilford Press.

John, O. P., Naumann, L. P., & Soto, C. J. (2008b). Paradigm Shift to the Integrative Big Five Trait Taxonomy: History, Measurement, and Conceptual Issues. In *Handbook of Personality: Theory and Research* (pp. 114–158). The Guilford Press.

Joo, W. T., Kwak, S., Youm, Y., & Chey, J. (2017). Brain functional connectivity difference in the complete network of an entire village: The role of social network size and embeddedness. *Scientific Reports*, *7*(1), 1–12. https://doi.org/10.1038/s41598-017-04904-1

Kable, J. W., & Levy, I. (2015). Neural markers of individual differences in decision-making. *Current Opinion in Behavioral Sciences*, *5*, 100. https://doi.org/10.1016/J.COBEHA.2015.08.004

Kanai, R., Bahrami, B., Roylance, R., & Rees, G. (2012). Online social network size is reflected in human brain structure. *Proceedings of the Royal Society B: Biological Sciences*, *279*(1732), 1327–1334. https://doi.org/10.1098/RSPB.2011.1959

Kandel, D. B. (1978). Similarity in real-life adolescent friendship pairs. *Journal of Personality and Social Psychology*, *36*(3), 306–312. https://doi.org/10.1037/0022-3514.36.3.306

Kastner, S., Ungerleider, L. G., Ungerleider, S. K. and L. G., Kastner, S., & Ungerleider, L. G. (2000). Mechanisms of visual attention in the human cortex. *Annual Review of Neuroscience*, *23*, 315–341. https://doi.org/10.1146/annurev.neuro.23.1.315

Ki, J. J., Kelly, S. P., & Parra, L. C. (2016). Attention strongly modulates reliability of neural responses to naturalistic narrative stimuli. *The Journal of Neuroscience*, *36*(10), 3092–3101. https://doi.org/10.1523/JNEUROSCI.2942-15.2016

Kim, S. W. S. Y., Kim, J. M., Yoo, J. A., Bae, K. Y., Kim, S. W. S. Y., Yang, S. J., Shin, I. S., & Yoon, J. S. (2016). Standardization and validation of Big Five Inventory-Korean version (BFI-K) in elders. *Korean Journal of Biological Psychiatry*, *17*(1), 15–25.

King, M. F., & Bruner, G. C. (2000). Social desirability bias: A neglected aspect of validity testing. *Psychology & Marketing*, *17*(2), 79–103. https://doi.org/10.1002/(SICI)1520-6793(200002)17:2<79::AID-MAR2>3.0.CO;2-0

Kleck, R. E., Richardson, S. A., & Ronald, L. (1974). Physical appearance cues and interpersonal attraction in children. *Child Development*, *45*(2), 305. https://doi.org/10.2307/1127949

Klein, K. J., Lim, B.-C., Saltz, J. L., & Mayer, D. M. (2004). How do they get there? An examination of the antecedents of centrality in team networks. *Academy of Management Journal*, *47*(6), 952–963. https://doi.org/10.5465/20159634

Kleinbaum, A. M., Jordan, A. H., & Audia, P. G. (2015). An altercentric perspective on the origins of brokerage in social networks: How perceived empathy moderates the self-monitoring effect. *Organization Science*, *26*(4), 1226–1242. https://doi.org/10.1287/orsc.2014.0961

Kliemann, D., Richardson, H., Anzellotti, S., Ayyash, D., Haskins, A. J., Gabrieli, J. D. E., &

Saxe, R. R. (2018). Cortical responses to dynamic emotional facial expressions generalize across stimuli, and are sensitive to task-relevance, in adults with and without Autism. *Cortex*, *103*, 24–43. https://doi.org/10.1016/J.CORTEX.2018.02.006

Knoke, D. (1990). Networks of political action: Toward theory construction. *Social Forces*, *68*(4), 1041. https://doi.org/10.2307/2579133

Kosslyn, S. M., Cacioppo, J. T., Davidson, R. J., Hugdahl, K., Lovallo, W. R., Spiegel, D., & Rose, R. (2002). Bridging psychology and biology: the analysis of individuals in groups. *American Psychologist*, *57*(5), 341–351. https://doi.org/10.1037//0003-066X.57.5.341

Kovacs, B., & Kleinbaum, A. M. (2020). Language-style similarity and social networks. *Psychological Science*, *31*(2), 202–213. https://doi.org/10.1177/0956797619894557

Krackhardt, D. (1990). Assessing the political landscape: Structure, cognition, and power in organizations. *Administrative Science Quarterly*, *35*(2), 342. https://doi.org/10.2307/2393394

Krishnan, A., Williams, L. J., McIntosh, A. R., & Abdi, H. (2011). Partial Least Squares (PLS) methods for neuroimaging: A tutorial and review. *NeuroImage*, *56*(2), 455–475. https://doi.org/10.1016/j.neuroimage.2010.07.034

Kuznetsova, A., Brockhoff, P. B., & Christensen, R. H. B. (2017). lmerTest package: Tests in linear mixed effects models. *Journal of Statistical Software*, *82*(13), 1–26. https://doi.org/10.18637/jss.v082.i13

Lahnakoski, J. M., Forbes, P. A. G., McCall, C., & Schilbach, L. (2020). Unobtrusive tracking of interpersonal orienting and distance predicts the subjective quality of social interactions. *Royal Society Open Science*, *7*(8), 191815. https://doi.org/10.1098/rsos.191815

Lahnakoski, J. M., Glerean, E., Jääskeläinen, I. P., Hyönä, J., Hari, R., Sams, M., &

Nummenmaa, L. (2014). Synchronous brain activity across individuals underlies shared psychological perspectives. *NeuroImage*, *100*, 316–324.

Lahnakoski, J. M., Glerean, E., Salmi, J., Jääskeläinen, I. P., Sams, M., Hari, R., & Nummenmaa, L. (2012). Naturalistic fMRI mapping reveals superior temporal sulcus as the hub for the distributed brain network for social perception. *Frontiers in Human Neuroscience*, *0*(AUGUST), 233. https://doi.org/10.3389/FNHUM.2012.00233/BIBTEX

Lakin, J. L., Jefferis, V. E., Cheng, C. M., & Chartrand, T. L. (2003). The chameleon effect as social glue: Evidence for the evolutionary significance of nonconscious mimicry. *Journal of Nonverbal Behavior*, *27*(3), 145–162. https://link.springer.com/article/10.1023/A:1025389814290

Lambiotte, R., Blondel, V. D., de Kerchove, C., Huens, E., Prieur, C., Smoreda, Z., & Van Dooren, P. (2008). Geographical dispersal of mobile communication networks. *Physica A: Statistical Mechanics and Its Applications*, *387*(21), 5317–5325. https://doi.org/10.1016/j.physa.2008.05.014

Landis, B. (2016). Personality and social networks in organizations: A review and future directions. *Journal of Organizational Behavior*, *37*, S107–S121. https://doi.org/10.1002/JOB.2004

Lee, H., Heller, A. S., van Reekum, C. M., Nelson, B., & Davidson, R. J. (2012). Amygdala-prefrontal coupling underlies individual differences in emotion regulation. *NeuroImage*, *62*(3), 1575–1581. https://doi.org/10.1016/J.NEUROIMAGE.2012.05.044

Lee, J. J.-M., Lee, W. J., Kim, H. C., Choi, W., Lee, J. J.-M., Sung, K., Chu, S. H., Park, Y.-R., & Youm, Y. (2014). The Korean social life, health and aging project-health examination cohort. *Epidemiology and Health*, *36*. https://doi.org/10.4178/EPIH/E2014003

Lee, Y. H., Yang, L. S., Wan, K. M., & Chen, G. H. (2010). Interactive effects of personality and friendship networks on contextual performance. *Social Behavior and Personality*, *38*(2), 197–208. https://doi.org/10.2224/SBP.2010.38.2.197

Lennox, R. D., & Wolfe, R. N. (1984). Revision of the self-monitoring scale. *Journal of Personality and Social Psychology*, *46*(6), 1349–1364. https://doi.org/10.1037//0022-3514.46.6.1349

Leonardi, P. M., & Bailey, D. E. (2016). Recognizing and selling good ideas: Network articulation and the making of an offshore innovation hub. *Academy of Management Discoveries*, *3*(2), 116–144. https://doi.org/10.5465/AMD.2015.0151

Lerner, R. M., & Lerner, J. V. (1977). Effects of age, sex, and physical attractiveness on child-peer relations, academic performance, and elementary school adjustment. *Developmental Psychology*, *13*(6), 585–590. https://doi.org/10.1037/0012-1649.13.6.585

Lewis, K., Gonzalez, M., & Kaufman, J. (2012). Social selection and peer influence in an online social network. *Proceedings of the National Academy of Sciences*, *109*(1), 68–72. https://doi.org/10.1073/pnas.1109739109

Lewis, P. A., Rezaie, R., Brown, R., Roberts, N., & Dunbar, R. I. M. (2011). Ventromedial prefrontal volume predicts understanding of others and social network size. *NeuroImage*, *57*(4), 1624–1629. https://doi.org/10.1016/J.NEUROIMAGE.2011.05.030

Liben-Nowell, D., Novak, J., Kumar, R., Raghavan, P., & Tomkins, A. (2005). Geographic routing in social networks. *Proceedings of the National Academy of Sciences of the United States of America*, *102*(33), 11623–11628. https://doi.org/10.1073/pnas.0503018102

Lieberman, M. D. (2022). Seeing minds, matter, and meaning: The CEEing model of pre-reflective subjective construal. *Psychological Review*.

https://doi.org/https://doi.org/10.1037/rev0000362

Ligneul, R., Obeso, I., Ruff, C. C., & Dreher, J. C. (2016). Dynamical representation of dominance relationships in the human rostromedial prefrontal cortex. *Current Biology*, *26*(23), 3107–3115. https://doi.org/10.1016/J.CUB.2016.09.015

Lin, S., Keysar, B., & Epley, N. (2010). Reflexively mindblind: Using theory of mind to interpret behavior requires effortful attention. *Journal of Experimental Social Psychology*, *46*(3), 551–556. https://doi.org/10.1016/j.jesp.2009.12.019

Liu, W., Kohn, N., & Fernández, G. (2019). Intersubject similarity of personality is associated with intersubject similarity of brain connectivity patterns. *NeuroImage*, *186*, 56–69. https://www.sciencedirect.com/science/article/pii/S1053811918320342

Liu, Y., & Ipe, M. (2010). How do they become nodes? revisiting team member network centrality. *Journal of Psychology: Interdisciplinary and Applied*, *144*(3), 243–258. https://doi.org/10.1080/00223981003648260

Ma, Y., Wang, C., & Han, S. (2011). Neural responses to perceived pain in others predict real-life monetary donations in different socioeconomic contexts. *NeuroImage*, *57*(3), 1273–1280. https://doi.org/10.1016/J.NEUROIMAGE.2011.05.003

Mackey, A. P., Singley, A. T. M., & Bunge, S. A. (2013). Intensive reasoning training alters patterns of brain connectivity at rest. *Journal of Neuroscience*, *33*(11), 4796–4803. https://doi.org/10.1523/JNEUROSCI.4141-12.2013

Mar, R. A. (2011). The neural bases of social cognition and story comprehension. *Annual Review of Psychology*, *62*, 103–134. https://doi.org/10.1146/ANNUREV-PSYCH-120709-145406

Mark, N. (1998). Birds of a feather sing together. *Social Forces*, *77*(2), 453. https://doi.org/10.2307/3005535

Marmaros, D., & Sacerdote, B. (2006). How do friendships form? *The Quarterly Journal of Economics*, *121*(1), 79–119. https://doi.org/10.1093/QJE/121.1.79

Marsden, P. V. (1988). Homogeneity in confiding relations. *Social Networks*, *10*(1), 57–76. https://doi.org/10.1016/0378-8733(88)90010-X

Marsden, P. V. (1990). Network data and measurement. *Annual Review of Sociology*, *16*(1), 435–463. https://doi.org/10.1146/annurev.so.16.080190.002251

Marsden, P. V. (2003). Interviewer effects in measuring network size using a single name generator. *Social Networks*, *25*(1), 1–16. https://doi.org/10.1016/S0378-8733(02)00009-6

Masuda, N., Porter, M. A., & Lambiotte, R. (2017). Random walks and diffusion on networks. *Physics Reports*, *716–717*, 1–58. https://doi.org/10.1016/J.PHYSREP.2017.07.007

McDermott, R., Fowler, J. H., & Christakis, N. A. (2009). Breaking up is hard to do, unless everyone else is doing it too: Social network effects on divorce in a longitudinal sample. *SSRN Electronic Journal*. https://doi.org/10.2139/SSRN.1490708

McIntosh, A. R., & Mišić, B. (2013). Multivariate statistical analyses for neuroimaging data. *Annual Review of Psychology*, *64*(1), 499–525. https://doi.org/10.1146/annurev-psych-113011-143804

McNabb, C. B., Burgess, L. G., Fancourt, A., Mulligan, N., FitzGibbon, L., Riddell, P., & Murayama, K. (2020). No evidence for a relationship between social closeness and similarity in resting-state functional brain connectivity in schoolchildren. *Scientific Reports*. https://doi.org/10.1038/s41598-020-67718-8

McPherson, M., Smith-Lovin, L., & Cook, J. M. (2001). Birds of a feather: Homophily in social networks. *Annual Review of Sociology*, *27*(1), 415–444. https://doi.org/10.1146/annurev.soc.27.1.415

Mednick, S. C., Christakis, N. A., & Fowler, J. H. (2010). The spread of sleep loss influences drug use in adolescent social networks. *PLOS ONE*, *5*(3), e9775. https://doi.org/10.1371/JOURNAL.PONE.0009775

Mehmood, T., Liland, K. H., Snipen, L., & Sæbø, S. (2012). A review of variable selection methods in Partial Least Squares Regression. In *Chemometrics and Intelligent Laboratory Systems* (Vol. 118, pp. 62–69). https://doi.org/10.1016/j.chemolab.2012.07.010

Mehra, A., Dixon, A. L., Brass, D. J., & Robertson, B. (2006). The social network ties of group leaders: Implications for group performance and leader reputation. *Organization Science*, *17*(1), 64–79. https://doi.org/10.1287/orsc.1050.0158

Mehra, A., Kilduff, M., & Brass, D. J. (2001). The social networks of high and low self-monitors: Implications for workplace performance. *Administrative Science Quarterly*, *46*(1). https://doi.org/10.2307/2667127

Meskaldji, D. E., Preti, M. G., Bolton, T. A., Montandon, M. L., Rodriguez, C., Morgenthaler, S., Giannakopoulos, P., Haller, S., & Van De Ville, D. (2016). Prediction of long-term memory scores in MCI based on resting-state fMRI. *NeuroImage: Clinical*, *12*, 785–795. http://www.ncbi.nlm.nih.gov/pubmed/27812505

Metoki, A., Alm, K. H., Wang, Y., Ngo, C. T., & Olson, I. R. (2017). Never forget a name: White matter connectivity predicts person memory. *Brain Structure and Function*, *222*(9), 4187–4201. https://doi.org/10.1007/s00429-017-1458-3

Miller, M. B., & Van Horn, J. D. (2007). Individual variability in brain activations associated with episodic retrieval: A role for large-scale databases. *International Journal of Psychophysiology*, *63*(2), 205–213. https://doi.org/10.1016/J.IJPSYCHO.2006.03.019

Miranda-Dominguez, O., Mills, B. D., Carpenter, S. D., Grant, K. A., Kroenke, C. D., Nigg, J.

T., & Fair, D. A. (2014). Connectotyping: Model based fingerprinting of the functional connectome. *PLoS ONE*, *9*(11), e111048. https://doi.org/10.1371/journal.pone.0111048

Mobasseri, S., Stein, D. H., & Carney, D. R. (2022). The accurate judgment of social network characteristics in the lab and field using thin slices of the behavioral stream. *Organizational Behavior and Human Decision Processes*, *168*, 104103. https://doi.org/10.1016/J.OBHDP.2021.09.002

Morelli, S. A., Leong, Y. C., Carlson, R. W., Kullar, M., & Zaki, J. (2018). Neural detection of socially valued community members. *Proceedings of the National Academy of Sciences of the United States of America*, *115*(32), 8149–8154. www.pnas.org/cgi/doi/10.1073/pnas.1712811115

Morelli, S. A., Ong, D. C., Makati, R., Jackson, M. O., & Zaki, J. (2017). Empathy and well-being correlate with centrality in different social networks. *Proceedings of the National Academy of Sciences of the United States of America*, *114*(37), 9843–9847. https://doi.org/10.1073/pnas.1702155114

Morris, J. C. (1993). The Clinical Dementia Rating (CDR): Current version and scoring rules. *Neurology*, *43*(11), 2412–2414. https://doi.org/10.1212/wnl.43.11.2412-a

Mossong, J., Hens, N., Jit, M., Beutels, P., Auranen, K., Mikolajczyk, R., Massari, M., Salmaso, S., Tomba, G. S., Wallinga, J., Heijne, J., Sadkowska-Todys, M., Rosinska, M., & Edmunds, W. J. (2008). Social contacts and mixing patterns relevant to the spread of infectious diseases. *PLoS Medicine*, *5*(3), e74. https://doi.org/10.1371/journal.pmed.0050074

Moussaïd, M., Brighton, H., & Gaissmaier, W. (2015). The amplification of risk in experimental diffusion chains. *Proceedings of the National Academy of Sciences of the United States of*

America, *112*(18), 5631–5636. https://doi.org/10.1073/pnas.1421883112

Moussaïd, M., Herzog, S. M., Kämmer, J. E., & Hertwig, R. (2017). Reach and speed of judgment propagation in the laboratory. *Proceedings of the National Academy of Sciences of the United States of America*, *114*(16), 4117–4122. https://doi.org/10.1073/pnas.1611998114

Nahemow, L., & Lawton, M. P. (1975). Similarity and propinquity in friendship formation. *Journal of Personality and Social Psychology*, *32*(2), 205–213. https://doi.org/10.1037/0022-3514.32.2.205

Nastase, S. A., Goldstein, A., & Hasson, U. (2020). Keep it real: Rethinking the primacy of experimental control in cognitive neuroscience. *NeuroImage*, *222*, 117254. https://doi.org/10.1016/J.NEUROIMAGE.2020.117254

Neubert, M. J., & Taggar, S. (2004). Pathways to informal leadership: The moderating role of gender on the relationship of individual differences and team member network centrality to informal leadership emergence. *Leadership Quarterly*, *15*(2), 175–194. https://doi.org/10.1016/J.LEAQUA.2004.02.006

Neumann, R., & Strack, F. (2000). "Mood contagion": The automatic transfer of mood between persons. *Journal of Personality and Social Psychology*, *79*(2), 211–223. https://doi.org/10.1037//0022-3514.79.2.211

Nguyen, M., Vanderwal, T., & Hasson, U. (2019). Shared understanding of narratives is correlated with shared neural responses. *NeuroImage*, *184*, 161–170. https://www.sciencedirect.com/science/article/pii/S1053811918307948

Noonan, M. P., Mars, R. B., Sallet, J., Dunbar, R. I. M., & Fellows, L. K. (2018). The structural and functional brain networks that support human social networks. *Behavioural Brain*

Research, *355*, 12–23. https://doi.org/10.1016/j.bbr.2018.02.019

O'Donnell, M. B., Bayer, J. B., Cascio, C. N., & Falk, E. B. (2017). Neural bases of recommendations differ according to social network structure. *Social Cognitive and Affective Neuroscience*, *12*(1), 61–69. https://doi.org/10.1093/scan/nsw158

O'Donnell, M. B., & Falk, E. B. (2015). Big data under the microscope and brains in social context: Integrating methods from computational social science and neuroscience. *Https://Doi.Org/10.1177/0002716215569446*, *659*(1), 274–289. https://doi.org/10.1177/0002716215569446

Obstfeld, D. (2005). Social Networks, the tertius Iungens orientation, and involvement in innovation. *Administrative Science Quarterly*, *50*(1), 100–130. https://doi.org/10.2189/ASQU.2005.50.1.100

Oh, H., & Kilduff, M. (2008). The ripple effect of personality on social structure: Self-monitoring origins of network brokerage. *Journal of Applied Psychology*, *93*(5), 1155–1164. https://doi.org/10.1037/0021-9010.93.5.1155

Onnela, J.-P., Arbesman, S., González, M. C., Barabási, A.-L., & Christakis, N. A. (2011). Geographic constraints on social network groups. *PLoS ONE*, *6*(4), e16939. https://doi.org/10.1371/journal.pone.0016939

Osgood, D. W., Ragan, D. T., Wallace, L., Gest, S. D., Feinberg, M. E., & Moody, J. (2013). Peers and the emergence of alcohol use: Influence and selection processes in adolescent friendship networks. *Journal of Research on Adolescence : The Official Journal of the Society for Research on Adolescence*, *23*(3), 500–512. https://doi.org/10.1111/JORA.12059

Otti, A., Guendel, H., Läer, L., Wohlschlaeger, A. M., Lane, R. D., Decety, J., Zimmer, C., Henningsen, P., & Noll-Hussong, M. (2010). I know the pain you feel-how the human

brain's default mode predicts our resonance to another's suffering. *Neuroscience*, *169*(1), 143–148. https://doi.org/10.1016/j.neuroscience.2010.04.072

Pachucki, M. A., Jacques, P. F., & Christakis, N. A. (2011). Social network concordance in food choice among spouses, friends, and siblings. *American Journal of Public Health*, *101*(11), 2170–2177. https://doi.org/10.2105/AJPH.2011.300282

Padoa-Schioppa, C., & Cai, X. (2011). Orbitofrontal cortex and the computation of subjective value: Consolidated concepts and new perspectives. *Annals of the New York Academy of Sciences*, *1239*(1), 130. https://doi.org/10.1111/J.1749-6632.2011.06262.X

Pagnoni, G. (2012). Dynamical properties of BOLD activity from the ventral posteromedial cortex associated with meditation and attentional skills. *Journal of Neuroscience*, *32*(15), 5242–5249. https://doi.org/10.1523/JNEUROSCI.4135-11.2012

Parkhurst, J. T., & Hopmeyer, A. (2016). Sociometric popularity and peer-perceived popularity: Two distinct dimensions of peer status. *The Journal of Early Adolescence*, *18*(2), 125–144. https://doi.org/10.1177/0272431698018002001

Parkinson, C., Kleinbaum, A. M., & Wheatley, T. (2017). Spontaneous neural encoding of social network position. *Nature Human Behaviour*, *1*, 72. https://doi.org/10.1038/s41562-017-0072

Parkinson, C., Kleinbaum, A. M., & Wheatley, T. (2018). Similar neural responses predict friendship. *Nature Communications*, *9*(1), 332. https://doi.org/10.1038/s41467-017-02722-7

Parkinson, C., & Wheatley, T. (2014). Relating anatomical and social connectivity: White matter microstructure predicts emotional empathy. *Cerebral Cortex*, *24*(3), 614–625. https://academic.oup.com/cercor/article/24/3/614/391313

Paschke, L. M., Dörfel, D., Steimke, R., Trempler, I., Magrabi, A., Ludwig, V. U., Schubert, T.,

Stelzel, C., & Walter, H. (2016). Individual differences in self-reported self-control predict successful emotion regulation. *Social Cognitive and Affective Neuroscience*, *11*(8), 1193–1204. https://doi.org/10.1093/SCAN/NSW036

Paunonen, S. V. (2003). *Big five factors of personality and replicated predictions of behavior*. https://doi.org/10.1037/0022-3514.84.2.411

Pedregosa, F., Michel, V., Grisel, O., Blondel, M., Prettenhofer, P., Weiss, R., Vanderplas, J., Cournapeau, D., Pedregosa, F., Varoquaux, G., Gramfort, A., Thirion, B., Grisel, O., Dubourg, V., Passos, A., Brucher, M., & Edoward, D. (2011). Scikit-learn: Machine learning in Python. *Journal of Machine Learning Research*, *12*, 2825–2830. http://scikit-learn.sourceforge.net.

Peer, M., Hayman, M., Tamir, B., & Arzy, S. (2021). Brain coding of social network structure. *Journal of Neuroscience*, *41*(22), 4897–4909. https://doi.org/10.1523/JNEUROSCI.2641-20.2021

Pinquart, M., & Sörensen, S. (2000). Influences of socioeconomic status, social network, and competence on subjective well-being in later life: a meta-analysis. *Psychology and Aging*, *15*(2), 187–224. https://doi.org/10.1037//0882-7974.15.2.187

Pollet, T. V., Roberts, S. G. B., & Dunbar, R. I. M. (2011). Extraverts have larger social network layers: But do not feel emotionally closer to individuals at any layer. *Journal of Individual Differences*, *32*(3), 161–169. https://doi.org/10.1027/1614-0001/A000048

Powell, J., Lewis, P. A., Roberts, N., García-Fiñana, M., & Dunbar, R. I. M. (2012). Orbital prefrontal cortex volume predicts social network size: an imaging study of individual differences in humans. *Proceedings of the Royal Society B: Biological Sciences*, *279*(1736), 2157–2162. https://doi.org/10.1098/RSPB.2011.2574

Power, J. D., Cohen, A. L., Nelson, S. M., Wig, G. S., Barnes, K. A., Church, J. A., Vogel, A. C., Laumann, T. O., Miezin, F. M., Schlaggar, B. L., & Petersen, S. E. (2011). Functional network organization of the human brain. *Neuron*, *72*(4), 665–678. https://doi.org/10.1016/j.neuron.2011.09.006

Rafnsson, S. B., Shankar, A., & Steptoe, A. (2015). Longitudinal influences of social network characteristics on subjective well-being of older adults: Findings from the ELSA study. *Journal of Aging and Health*, *27*(5), 919–934. https://doi.org/10.1177/0898264315572111

Raichle, M. E. (2015). The brain's default mode network. *Annual Review of Neuroscience*, *38*, 433–447. https://doi.org/10.1146/ANNUREV-NEURO-071013-014030

Rapuano, K. M., Laurent, J. S., Hagler, D. J., Hatton, S. N., Thompson, W. K., Jernigan, T. L., Dale, A. M., Casey, B. J., & Watts, R. (2020). Nucleus accumbens cytoarchitecture predicts weight gain in children. *Proceedings of the National Academy of Sciences of the United States of America*, *117*(43), 26977–26984. https://www.pnas.org/content/117/43/26977

Rapuano, K. M., Rosenberg, M. D., Maza, M. T., Dennis, N. J., Dorji, M., Greene, A. S., Horien, C., Scheinost, D., Todd Constable, R., & Casey, B. J. (2020). Behavioral and brain signatures of substance use vulnerability in childhood. *Developmental Cognitive Neuroscience*, *46*, 100878. https://doi.org/10.1016/J.DCN.2020.100878

Redcay, E., & Schilbach, L. (2019). Using second-person neuroscience to elucidate the mechanisms of social interaction. *Nature Reviews Neuroscience*, *20*(8), 495–505. https://doi.org/10.1038/s41583-019-0179-4

Reeder, R. R. (2017). Individual differences shape the content of visual representations. *Vision Research*, *141*, 266–281. https://doi.org/10.1016/J.VISRES.2016.08.008

Regev, M., Simony, E., Lee, K., Tan, K. M., Chen, J., & Hasson, U. (2019). Propagation of

information along the cortical hierarchy as a function of attention while reading and listening to stories. *Cerebral Cortex*, *29*(10), 4017–4034. https://doi.org/10.1093/CERCOR/BHY282

Rice, K., & Redcay, E. (2015). Spontaneous mentalizing captures variability in the cortical thickness of social brain regions. *Social Cognitive and Affective Neuroscience*, *10*(3), 327. https://doi.org/10.1093/SCAN/NSU081

Rice, K., Viscomi, B., Riggins, T., & Redcay, E. (2014). Amygdala volume linked to individual differences in mental state inference in early childhood and adulthood. *Developmental Cognitive Neuroscience*, *8*, 153–163. https://doi.org/10.1016/J.DCN.2013.09.003

Richardson, H., Lisandrelli, G., Riobueno-Naylor, A., & Saxe, R. (2018). Development of the social brain from age three to twelve years. *Nature Communications 2018 9:1*, *9*(1), 1–12. https://doi.org/10.1038/s41467-018-03399-2

Rizzolatti, G., & Craighero, L. (2004). The mirror-neuron system. *Annual Review of Neuroscience*, *27*, 169–192. https://pubmed.ncbi.nlm.nih.gov/15217330/

Roberts, S. G. B., Wilson, R., Fedurek, P., & Dunbar, R. I. M. (2008). Individual differences and personal social network size and structure. *Personality and Individual Differences*, *44*(4), 954–964. https://doi.org/10.1016/J.PAID.2007.10.033

Rosenberg, M. D., Finn, E. S., Scheinost, D., Papademetris, X., Shen, X., Constable, R. T., & Chun, M. M. (2015). A neuromarker of sustained attention from whole-brain functional connectivity. *Nature Neuroscience*, *19*(1), 165–171.

Rosenberg, M. D., Hsu, W. T., Scheinost, D., Constable, R. T., & Chun, M. M. (2018). Connectome-based models predict separable components of attention in novel individuals. *Journal of Cognitive Neuroscience*, *30*(2), 160–173.

https://doi.org/10.1162/JOCN_A_01197

Rosenquist, J. N., Fowler, J. H., & Christakis, N. A. (2011). Social network determinants of depression. *Molecular Psychiatry*, *16*(3), 273–281. https://doi.org/10.1038/mp.2010.13

Rosenquist, J. Niels, Murabito, J., Fowler, J. H., & Christakis, N. A. (2010). The spread of alcohol consumption behavior in a large social network. *Annals of Internal Medicine*, *152*(7), 426–433. https://doi.org/10.7326/0003-4819-152-7-201004060-00007

Rossignac-Milon, M., Bolger, N., Zee, K. S., Boothby, E. J., & Higgins, E. T. (2020). Merged minds: Generalized shared reality in dyadic relationships. *Journal of Personality and Social Psychology*. /record/2020-51514-001

Rouault, M., McWilliams, A., Allen, M. G., & Fleming, S. M. (2018). Human metacognition across domains: Insights from individual differences and neuroimaging. *Personality Neuroscience*, *1*, 1–13. https://doi.org/10.1017/PEN.2018.16

Rushworth, M. F. S., Mars, R. B., & Sallet, J. (2013). Are there specialized circuits for social cognition and are they unique to humans? *Current Opinion in Neurobiology*, *23*(3), 436–442. https://doi.org/10.1016/J.CONB.2012.11.013

Saalasti, S., Alho, J., Bar, M., Glerean, E., Honkela, T., Kauppila, M., Sams, M., & Jääskeläinen, I. P. (2019). Inferior parietal lobule and early visual areas support elicitation of individualized meanings during narrative listening. *Brain and Behavior*, *9*(5). https://doi.org/10.1002/BRB3.1288

Sallet, J., Mars, R. B., Noonan, M. P., Andersson, J. L., O'Reilly, J. X., Jbabdi, S., Croxson, P. L., Jenkinson, M., Miller, K. L., & Rushworth, M. F. S. (2011). Social network size affects neural circuits in macaques. *Science (New York, N.Y.)*, *334*(6056), 697–700. https://doi.org/10.1126/SCIENCE.1210027

Salmivalli, C., Lagerspetz, K., Bjorkqvist, K., Osterman, K., & Kaukiainen, A. (1996). Bullying as a group process: Participant roles and their relations to social status within the group. *Aggressive Behavior*, *22*(1), 1–15. https://doi.org/10.1002/AB.21438

Salvia, J., Sheare, J. B., & Algozzine, B. (1975). Facial attractiveness and personal-social development. *Journal of Abnormal Child Psychology*, *3*(3), 171–178. https://doi.org/10.1007/BF00916748

Sasovova, Z., Mehra, A., Borgatti, S. P., & Schippers, M. C. (2010). Network churn: The effects of self-monitoring personality on brokerage dynamics. *Administrative Science Quarterly*, *55*(4), 639–670. https://doi.org/10.2189/asqu.2010.55.4.639

Schaefer, A., Kong, R., Gordon, E. M., Laumann, T. O., Zuo, X.-N., Holmes, A. J., Eickhoff, S. B., & Yeo, B. T. T. (2018). Local-global parcellation of the human cerebral cortex from intrinsic functional connectivity MRI. *Cerebral Cortex*, *28*(9), 3095–3114. https://doi.org/10.1093/cercor/bhx179

Schilbach, L. (2016). Towards a second-person neuropsychiatry. In *Philosophical Transactions of the Royal Society B: Biological Sciences* (Vol. 371, Issue 1686, p. 20150081). Royal Society of London. https://doi.org/10.1098/rstb.2015.0081

Schmälzle, R., O'Donnell, M. B., Garcia, J. O., Cascio, C. N., Bayer, J., Bassett, D. S., Vettel, J. M., & Falk, E. B. (2017). Brain connectivity dynamics during social interaction reflect social network structure. *Proceedings of the National Academy of Sciences of the United States of America*, *114*(20), 5153–5158. https://doi.org/10.1073/PNAS.1616130114

Schneider, D., Regenbogen, C., Kellermann, T., Finkelmeyer, A., Kohn, N., Derntl, B., Schneider, F., & Habel, U. (2012). Empathic behavioral and physiological responses to dynamic stimuli in depression. *Psychiatry Research*, *200*(2–3), 294–305.

https://doi.org/10.1016/j.psychres.2012.03.054

Schurz, M., Radua, J., Aichhorn, M., Richlan, F., & Perner, J. (2014). *Fractionating theory of mind: A meta-analysis of functional brain imaging studies*. *42*, 9–34. https://doi.org/10.1016/J.NEUBIOREV.2014.01.009

Schwyck, M., Du, M., Li, Y., Chang, L. J., & Parkinson, C. (2022). Similarity among friends serves as a social prior: The assumption that "birds of a feather flock together" shapes social decisions and relationship beliefs. *PsyArXiv*. https://doi.org/10.31234/OSF.IO/D9BEM

Seibert, S. E., Kraimer, M. L., & Liden, R. C. (2001). A social capital theory of career success. *Academy of Management Journal*, *44*(2), 219–237. https://doi.org/10.2307/3069452

Selfhout, M., Burk, W., Branje, S., Denissen, J., van Aken, M., & Meeus, W. (2010). Emerging late adolescent friendship networks and big five personality traits: A social network approach. *Journal of Personality*, *78*(2), 509–538. https://doi.org/10.1111/j.1467-6494.2010.00625.x

Selfhout, M., Denissen, J., Branje, S., & Meeus, W. (2009). In the eye of the beholder: Perceived, actual, and peer-rated similarity in personality, communication, and friendship intensity during the acquaintanceship process. *Journal of Personality and Social Psychology*, *96*(6), 1152–1165. https://doi.org/10.1037/a0014468

Shamay-Tsoory, S. G. (2011). The neural bases for empathy. *Neuroscientist*, *17*(1), 18–24. https://doi.org/10.1177/1073858410379268

Shomstein, S. (2012). Cognitive functions of the posterior parietal cortex: top-down and bottom-up attentional control. *Frontiers in Integrative Neuroscience*, *6*(JULY 2012). https://doi.org/10.3389/FNINT.2012.00038

Smallwood, J., Brown, K., Baird, B., & Schooler, J. W. (2012). Cooperation between the default

mode network and the frontal–parietal network in the production of an internal train of thought. *Brain Research*, *1428*, 60–70. https://doi.org/10.1016/J.BRAINRES.2011.03.072

Smirnov, D., Saarimäki, H., Glerean, E., Hari, R., Sams, M., & Nummenmaa, L. (2019). Emotions amplify speaker-listener neural alignment. *Human Brain Mapping*, *40*(16), 4777–4788. https://doi.org/10.1002/HBM.24736

Smith, E. B., Brands, R. A., Brashears, M. E., & Kleinbaum, A. M. (2020). Social networks and cognition. *Annual Review of Sociology*, *46*(1), 159–174. https://doi.org/10.1146/annurev-soc-121919-054736

Snyder, M. (1974). Self-monitoring of expressive behavior. *Journal of Personality and Social Psychology*, *30*(4), 526–537. https://doi.org/10.1037/h0037039

Spreng, R. N., Stevens, W. D., Chamberlain, J. P., Gilmore, A. W., & Schacter, D. L. (2010). Default network activity, coupled with the frontoparietal control network, supports goal-directed cognition. *NeuroImage*, *53*(1), 303–317. https://doi.org/10.1016/J.NEUROIMAGE.2010.06.016

Spunt, R. P., Meyer, M. L., & Lieberman, M. D. (2015). *The default mode of human brain function primes the intentional stance*. *27*(6), 1116–1124. https://doi.org/10.1162/JOCN_A_00785

Stanton, M. A., & Mann, J. (2012). Early social networks predict survival in wild bottlenose dolphins. *PLoS ONE*, *7*(10), e47508. https://doi.org/10.1371/journal.pone.0047508

Stephens, G. J., Silbert, L. J., & Hasson, U. (2010). Speaker-listener neural coupling underlies successful communication. *Proceedings of the National Academy of Sciences of the United States of America*, *107*(32), 14425–14430. https://doi.org/10.1073/pnas.1008662107

Stopczynski, A., Pentland, A. 'Sandy,' & Lehmann, S. (2018). How physical proximity shapes

complex social networks. *Scientific Reports*, *8*(1), 1–10. https://doi.org/10.1038/s41598-018-36116-6

Talukdar, T., Román, F. J., Operskalski, J. T., Zwilling, C. E., & Barbey, A. K. (2018). Individual differences in decision making competence revealed by multivariate fMRI. *Human Brain Mapping*, *39*(6), 2664–2672. https://doi.org/10.1002/HBM.24032

Tan, L. H., Chen, L., Yip, V., Chan, A. H. D., Yang, J., Gao, J. H., & Siok, W. T. (2011). Activity levels in the left hemisphere caudate-fusiform circuit predict how well a second language will be learned. *Proceedings of the National Academy of Sciences of the United States of America*, *108*(6), 2540–2544. https://doi.org/10.1073/PNAS.0909623108

Todorov, A., Gobbini, M. I., Evans, K. K., & Haxby, J. V. (2007). Spontaneous retrieval of affective person knowledge in face perception. *Neuropsychologia*, *45*(1), 163–173. https://doi.org/10.1016/J.NEUROPSYCHOLOGIA.2006.04.018

Toegel, G., Anand, N., & Kilduff, M. (2007). Emotion helpers: The role of high positive affectivity and high self-monitoring managers. *Personnel Psychology*, *60*(2), 337–365. https://doi.org/10.1111/j.1744-6570.2007.00076.x

Totterdell, P., Holman, D., & Hukin, A. (2008). Social networkers: Measuring and examining individual differences in propensity to connect with others. *Social Networks*, *30*(4), 283–296. https://doi.org/10.1016/J.SOCNET.2008.04.003

Tusche, A., Bode, S., & Haynes, J. D. (2010). Neural responses to unattended products predict later consumer choices. *Journal of Neuroscience*, *30*(23), 8024–8031. https://doi.org/10.1523/JNEUROSCI.0064-10.2010

Underwood, B. J. (1975). Individual differences as a crucible in theory construction. *American Psychologist*, 128--134. http://citeseerx.ist.psu.edu/viewdoc/summary?doi=10.1.1.943.4495

Vaidya, C. J., & Gordon, E. M. (2013). Phenotypic variability in resting-state functional connectivity: Current status. In *Brain Connectivity* (Vol. 3, Issue 2, pp. 99–120). Brain Connect. https://doi.org/10.1089/brain.2012.0110

van Buuren, M., Lee, N. C., Vegting, I., Walsh, R. J., Sijtsma, H., Hollarek, M., & Krabbendam, L. (2021). Intrinsic network interactions explain individual differences in mentalizing ability in adolescents. *Neuropsychologia*, *151*, 107737. https://doi.org/10.1016/J.NEUROPSYCHOLOGIA.2020.107737

van den Brink, D., Van berkum, J. J. A., Bastiaansen, M. C. M., Tesink, C. M. J. Y., Kos, M., Buitelaar, J. K., & Hagoort, P. (2012). Empathy matters: ERP evidence for inter-individual differences in social language processing. *Social Cognitive and Affective Neuroscience*, *7*(2), 173–183. https://doi.org/10.1093/SCAN/NSQ094

Vanderwal, T., Eilbott, J., & Castellanos, F. X. (2019). Movies in the magnet: Naturalistic paradigms in developmental functional neuroimaging. *Developmental Cognitive Neuroscience*, *36*. https://doi.org/10.1016/J.DCN.2018.10.004

Venkataramani, V., Green, S. G., & Schleicher, D. J. (2010). Well-Connected Leaders: The Impact of Leaders' Social Network Ties on LMX and Members' Work Attitudes. *Journal of Applied Psychology*, *95*(6), 1071–1084. https://doi.org/10.1037/A0020214

Vincent, J. L., Kahn, I., Snyder, A. Z., Raichle, M. E., & Buckner, R. L. (2008). Evidence for a frontoparietal control system revealed by intrinsic functional connectivity. *Journal of Neurophysiology*, *100*(6), 3328. https://doi.org/10.1152/JN.90355.2008

Von der Heide, R., Vyas, G., & Olson, I. R. (2014). The social network-network: Size is predicted by brain structure and function in the amygdala and paralimbic regions. *Social Cognitive and Affective Neuroscience*, *9*(12), 1962–1972.

https://doi.org/10.1093/SCAN/NSU009

Wang, S. S., Wei, D. T., Li, W. F., Li, H. J., Wang, K. C., Xue, S., Zhang, Q., & Qiu, J. (2014). A voxel-based morphometry study of regional gray and white matter correlate of self-disclosure. *Social Neuroscience*, *9*(5), 495–503. https://doi.org/10.1080/17470919.2014.925502

Wang, X. (2016). Subjective well-being associated with size of social network and social support of elderly. *Journal of Health Psychology*, *21*(6), 1037–1042. https://doi.org/10.1177/1359105314544136

Wang, Y., Collins, J. A., Koski, J., Nugiel, T., Metoki, A., & Olson, I. R. (2017). Dynamic neural architecture for social knowledge retrieval. In *Proceedings of the National Academy of Sciences of the United States of America* (Vol. 114, Issue 16, pp. E3305–E3314). National Academy of Sciences. https://doi.org/10.1073/pnas.1621234114

Wang, Y., Metoki, A., Alm, K. H., & Olson, I. R. (2018). White matter pathways and social cognition. *Neuroscience and Biobehavioral Reviews*, *90*, 350–370.

Wang, Y., Metoki, A., Smith, D. V., Medaglia, J. D., Zang, Y., Benear, S., Popal, H., Lin, Y., & Olson, I. R. (2020). Multimodal mapping of the face connectome. *Nature Human Behaviour*, *4*(4), 397–411. https://doi.org/10.1038/s41562-019-0811-3

Wang, Y., Metoki, A., Xia, Y., Zang, Y., He, Y., & Olson, I. R. (2021). A large-scale structural and functional connectome of social mentalizing. *NeuroImage*, *236*. https://doi.org/10.1016/J.NEUROIMAGE.2021.118115

Wang, Y., & Olson, I. R. (2018). The Original Social Network: White Matter and Social Cognition. *Trends in Cognitive Sciences*, *22*(6), 504–516. https://doi.org/10.1016/j.tics.2018.03.005

Wasserman, S., & Faust, K. (1994). *Social Network Analysis: Methods and Applications*. Cambridge University Press. https://doi.org/10.1017/CBO9780511815478

Watanabe, N., & Yamamoto, M. (2015). Neural mechanisms of social dominance. *Frontiers in Neuroscience*, *9*(APR), 154. https://doi.org/10.3389/FNINS.2015.00154/BIBTEX

Weaverdyck, M. E., & Parkinson, C. (2018). The neural representation of social networks. *Current Opinion in Psychology*, *24*, 58–66. https://doi.org/10.1016/J.COPSYC.2018.05.009

Webster, M., & Driskell, J. E. (1983). Beauty as status. *American Journal of Sociology*, *89*(1), 140–165. https://doi.org/10.1086/227836

Wiesmann, C. G., Friederici, A. D., Singer, T., & Steinbeis, N. (2020). Two systems for thinking about others' thoughts in the developing brain. *Proceedings of the National Academy of Sciences of the United States of America*, *117*(12), 6928–6935. https://doi.org/10.1073/PNAS.1916725117/SUPPL_FILE/PNAS.1916725117.SAPP.PDF

Wilson, T. D. (2002). Strangers to Ourselves: Discovering the Adaptive Unconscious. In *Choice Reviews Online*. Belknap Press. https://doi.org/10.5860/choice.40-3712

Wilson, T. D., & Nisbett, R. E. (1978). The accuracy of verbal reports about the effects of stimuli on evaluations and behavior. *Social Psychology*, *41*(2), 118. https://doi.org/10.2307/3033572

Xu, J., & Potenza, M. N. (2012). White matter integrity and five-factor personality measures in healthy adults. *NeuroImage*, *59*(1), 800–807. https://doi.org/10.1016/j.neuroimage.2011.07.040

Yarkoni, T., Poldrack, R. A., Nichols, T. E., Van Essen, D. C., & Wager, T. D. (2011). Large-scale automated synthesis of human functional neuroimaging data. *Nature Methods*, *8*(8), 665–670. https://doi.org/10.1038/nmeth.1635

Yendiki, A., Panneck, P., Srinivasan, P., Stevens, A., Zöllei, L., Augustinack, J., Wang, R., Salat, D., Ehrlich, S., Behrens, T., Jbabdi, S., Gollub, R., & Fischl, B. (2011). Automated probabilistic reconstruction of white-matter pathways in health and disease using an atlas of the underlying anatomy. *Frontiers in Neuroinformatics*, *5*, 5–23. https://doi.org/10.3389/fninf.2011.00023

Yeo, B. T. T., Krienen, F. M., Sepulcre, J., Sabuncu, M. R., Lashkari, D., Hollinshead, M., Roffman, J. L., Smoller, J. W., Zöllei, L., Polimeni, J. R., Fischl, B., Liu, H., & Buckner, R. L. (2011). The organization of the human cerebral cortex estimated by intrinsic functional connectivity. *Journal of Neurophysiology*, *106*, 1125–1165. https://doi.org/10.1152/jn.00338.2011

Yeshurun, Y., Nguyen, M., & Hasson, U. (2021). The default mode network: Where the idiosyncratic self meets the shared social world. *Nature Reviews Neuroscience 2021 22:3*, *22*(3), 181–192. https://doi.org/10.1038/s41583-020-00420-w

Yeshurun, Y., Swanson, S., Simony, E., Chen, J., Lazaridi, C., Honey, C. J., & Hasson, U. (2017). Same story, different story: the neural representation of interpretive frameworks. *Psychological Science*, *28*(3), 307. https://doi.org/10.1177/0956797616682029

Youm, Y., Laumann, E. O., Ferraro, K. F., Waite, L. J., Kim, H. C., Park, Y. R., Chu, S. H., Joo, W. T., & Lee, J. A. (2014). Social network properties and self-rated health in later life: Comparisons from the Korean social life, health, and aging project and the national social life, health and aging project. *BMC Geriatrics*, *14*(1), 102. https://doi.org/10.1186/1471-2318-14-102

Yu, C. L., & Chou, T. L. (2018). A dual route model of empathy: A neurobiological prospective. *Frontiers in Psychology*, *9*, 2212. https://doi.org/10.3389/fpsyg.2018.02212

Zaki, J., & Ochsner, K. (2012). The neuroscience of empathy: Progress, pitfalls and promise. *Nature Neuroscience*, *15*(5), 675–680. https://doi.org/10.1038/nn.3085

Zaki, J., Weber, J., Bolger, N., & Ochsner, K. (2009). The neural bases of empathic accuracy. *Proceedings of the National Academy of Sciences of the United States of America*, *106*(27), 11382–11387. https://doi.org/10.1073/pnas.0902666106

Zerubavel, N., Bearman, P. S., Weber, J., & Ochsner, K. N. (2015). Neural mechanisms tracking popularity in real-world social networks. *Proceedings of the National Academy of Sciences of the United States of America*, *112*(49), 15072–15077. www.pnas.org/cgi/doi/10.1073/pnas.1511477112

Zingora, T., Stark, T. H., & Flache, A. (2020). Who is most influential? Adolescents' intergroup attitudes and peer influence within a social network. *Group Processes & Intergroup Relations*, *23*(5), 684–709. https://doi.org/10.1177/1368430219869460